

UNIVERSITÀ
DEGLI STUDI
DI PADOVA

Sede Amministrativa: Università degli Studi di Padova
Dipartimento di Medicina Molecolare

SCUOLA DI DOTTORATO DI RICERCA IN BIOMEDICINA
INDIRIZZO: MEDICINA RIGENERATIVA
CICLO XXVIII

Role of collagen VI in skeletal muscle regeneration and intestinal homeostasis

Direttore della Scuola: Ch.mo Prof. Stefano Piccolo
Coordinatore d'indirizzo: Ch.ma Prof.ssa Maria Teresa Conconi
Supervisore: Ch.ma Prof.ssa Luisa Dalla Valle
Co-tutore: Ch.mo Prof. Paolo Bonaldo

Dottoranda: Sibilla Molon

Abstract **I**

Riassunto **III**

Chapter I

1. Introduction **1**

1.1 Skeletal muscle and extracellular matrix 1

1.2 Collagen VI 4

1.3 Collagen VI-related muscle disorders 6

1.4 Collagen VI null mouse model and therapeutic approaches of collagen VI-related myopathies 7

1.5 Satellite cells and skeletal muscle regeneration 10

1.6 Role of collagen VI in skeletal muscle regeneration 14

1.7 Effect of cyclosporin A on muscle regeneration in collagen VI deficient mice 15

Collagen VI regulates satellite cell self-renewal and muscle regeneration 17

Cyclosporin A promotes in vivo myogenic response in collagen VI-deficient myophatic mice 31

References **39**

Chapter II

1. Introduction **45**

1.1 The gastrointestinal system 45

1.2 Inflammatory bowel diseases 47

1.3 Intestinal macrophages 49

1.3.1 Origins and functions of intestinal resident macrophages in intestine homeostasis 51

1.4 Mouse model of colitis 53

1.4.1 DSS-induced colitis mouse model 55

1.5 Role of macrophages in intestinal inflammation 58

1.6 Intestinal macrophages in human gut homeostasis and disease 60

1.7 The role of extracellular matrix in inflammation 61

2. Methods **65**

2.1 Animals 65

2.2 DSS experimental colitis 65
2.3 Histological analysis 66
2.4 Real time quantitative PCR (real time qPCR) 67
2.5 Immunofluorescence staining 68
2.6 Gastrointestinal functionality assays 69
2.7 Intestinal macrophage isolation 71
2.8 Myeloperoxidase activity assay 73
2.9 Statistical analysis 74

3. Results 75
3.1 Collagen VI is expressed in ileum and colon, and around longitudinal muscle myenteric plexus 75
3.2 Histological analysis does not reveal any gross abnormality in the intestine of collagen VI deficient mice 75
3.3 Myenteric plexus of collagen VI null distal ileum displays a normal pattern of peripherin organization and distribution 76
3.4 Collagen VI deficient mice display increased gastrointestinal motility 76
3.5 Ablation of collagen VI affects intestinal paracellular permeability 77
3.6 Lack of collagen VI influences the severity of DSS-induced colitis 78
3.7 Collagen VI deficiency are unable to efficiently turn off inflammation during recovery from acute DSS-induced colitis 79
3.8 Collagen VI expression is highly regulated during inflammation 80
3.9 During DSS-induced acute colitis, collagen VI deficient mice display a decreased expression of chemokine genes that is maintained during recovery 81
3.10 Collagen VI deficient mice display higher macrophage number, more polarized towards M1, and neutrophil activity during recovery from DSS-induced colitis 82
3.11 Collagen VI deficiency affects macrophage polarization and phagocytosis in physiological conditions and during mild inflammation 84
3.12 Collagen VI expression and the number of $CD163^{+}$ macrophages are increased in ileal mucosa and muscle layers of Crohn's disease patients 85

4. Discussion 87

5. Figures 103

References 127

ABSTRACT

During my PhD I focused on the role of collagen VI in skeletal muscle regeneration and in intestinal homeostasis. Collagen VI is a glycoprotein of the extracellular matrix (ECM) containing three genetically distinct chains and forming an extended microfilamentous network that interacts with the cells and with other ECM components. Mutations of collagen VI genes in humans cause several muscle diseases, including Bethlem myopathy and Ullrich congenital muscle dystrophy. The generation of a collagen VI knockout mouse model was fundamental for clarifying the pathomolecular defects caused by the absence of this protein and provided a valuable tool for developing novel therapeutic opportunities in patients. During the past decade, studies on collagen VI null mice revealed an increasingly important role for this ECM component in a plethora of different cell and tissue processes, including apoptosis and oxidative damage, autophagy, cell differentiation, maintenance of stemness, regulation of tissue regeneration and biomechanical properties.

In the first part of my PhD work, I was involved in a large project aimed at characterizing the role of collagen VI in muscle regeneration and in the regulation of the activities of satellite cells (SCs), the main adult stem cell population of skeletal muscles. Our studies revealed that collagen VI is a key component of the SC niche, and its lack affects muscle regeneration and impairs SC self-renewal in collagen VI null mice. Interestingly, we found that the absence of collagen VI affects the *in vivo* mechanical properties of skeletal muscles. Furthermore, *in vitro* studies revealed that SC stemness and regenerative capabilities are strongly compromised when SCs are cultured on biomimetic substrates with the abnormal stiffness displayed by collagen VI deficient muscles, compared to SCs cultured on biomimetic substrates with the normal muscle stiffness. Both the biomechanical properties value and the regenerative capability of collagen VI null muscle are improved after *in vivo* grafting with wild-type muscle fibroblasts, the main cell type producing collagen VI, thus pointing out that a key mechanism by which collagen VI regulates SC activity is via modulation of muscle mechanical properties. In a subsequent work, we found that pharmacological treatment of collagen VI null mice with cyclosporin A is able to stimulate myogenesis in physiological conditions by increasing the percentage of regenerating myofibers, and to improve muscle regeneration and SC homeostasis after cardiotoxin-induced injury.

In the second part of my PhD, I investigated the role of collagen VI in intestine. Despite

its broad distribution within the mucosa and the smooth muscle layers of the digestive tract, lack of collagen VI does not trigger any gross abnormality in the intestinal architecture of knockout mice. However, studies of the gastrointestinal functionality revealed that the lack of this ECM component lead to increased motility and decreased paracellular permeability. Induction of experimental acute colitis by administration of dextran sodium sulphate showed that collagen VI deficient mice have a decreased responsiveness and severity to acute colitis, with a lower body weight loss and decreased colonic inflammation when compared to wild-type subjected to the same treatment. Moreover, wild-type mice displayed an increased recruitment of inflammatory cells, in association with increased macrophage number and neutrophil activity, which decreased during 10 days of recovery subsequent to acute colitis, thus allowing proper tissue repair. Conversely, collagen VI deficient mice were unable to efficiently turn off inflammation during post-colitis recovery, displaying a high number of pro-inflammatory M1 colonic macrophages, an increased neutrophil activity and a higher body weight loss when compared to wild-type. Moreover, lack of collagen VI affected both macrophage polarization and activity in physiological conditions and during mild inflammation. Further studies allowed to reveal that lack of collagen VI affects the behavior of intestinal macrophages, both in physiological conditions and during mild inflammation, whose activity is essential to ensure intestinal mucosa homeostasis. These findings point at a role for collagen VI as a chemoattractant during acute inflammation and in tissue regeneration in the subsequent recovery phase. Immunofluorescence studies revealed an increased deposition of collagen VI in the colonic mucosa during acute colitis, and the protein was found in contact with macrophages. Interestingly, ileal biopsies of Crohn's disease patients displayed increased expression and deposition of collagen VI, in association with a high number of macrophages, suggesting that the dysregulation of this ECM component may play an active role in the onset and/or maintenance of inflammatory bowel diseases.

In conclusion, my PhD work provided novel information on the *in vivo* roles of collagen VI in cell and tissue homeostasis. In more general terms, these findings highlight the importance of a specific defined ECM microenvironment to ensure tissue homeostasis, and demonstrate that lack of one of the major ECM component may have a severe impact on cell behavior.

RIASSUNTO

Durante il mio percorso di dottorato mi sono occupata di studiare il ruolo del collagene VI nella rigenerazione del muscolo scheletrico e nell'omeostasi dell'intestino. Il collagene VI è una glicoproteina della matrice extracellulare (MEC) costituita da tre catene geneticamente distinte, le quali si organizzano in modo da formare un'estesa rete di microfilamenti in grado di connettere cellule e altri componenti della MEC. Mutazioni a carico dei geni codificanti le catene del collagene VI causano diverse patologie muscolari, principalmente la miopatia di Bethlem e la distrofia muscolare congenita di Ullrich. Gli studi condotti sul modello knockout murino privo di collagene VI hanno permesso di chiarire i difetti patomolecolari causati dall'assenza di questa proteina, dimostrandosi utile anche per l'identificazione di nuovi trattamenti farmacologici per le malattie umane. Nel coso degli anni, molteplici studi hanno messo in luce le diverse funzioni esercitate dal collagene VI nel regolare diversi eventi cellulari e tissutali, tra cui l'apoptosi e il danno ossidativo, l'autofagia, il differenziamento cellulare, il mantenimento della staminalità ai fini rigenerativi e le proprietà biomeccaniche.

Nel corso del mio dottorato ho partecipato inizialmente alla caratterizzazione del ruolo del collagene VI durante la rigenerazione del muscolo scheletrico e la sua influenza sull'attività delle cellule satelliti, la popolazione principale di cellule staminali adulte nei muscoli scheletrici. Da tali studi è emerso che il collagene VI è un componente essenziale della nicchia delle cellule satelliti. La mancanza di tale proteina determina una ridotta rigenerazione tissutale e una diminuita capacità delle cellule satelliti di compiere *self-renewal* in seguito a danni muscolari multipli. I muscoli dei topi privi di collagene VI sono caratterizzati da una minore *stiffness* e approfondite analisi condotte *in vitro* hanno rivelato che le proprietà staminali e rigenerative delle cellule satelliti sono fortemente compromesse quando coltivate su biomateriali con un modulo elastico che mima la condizione patologica. Le capacità rigenerative e le proprietà meccaniche dei muscoli di topi privi di collagen VI vengono ripristinate in seguito alla deposizione di collagene VI, ristabilita tramite *grafting* di fibroblasti muscolari isolati da topi wild-type. Complessivamente, questi studi hanno dimostrato che modulando le proprietà meccaniche del muscolo, il collagene VI è in grado di regolare l'attività delle cellule satelliti. Abbiamo inoltre dimostrato che la somministrazione di ciclosporina A è in grado di stimolare la miogenesi in condizioni fisiologiche, inducendo la formazione di

nuove fibre muscolari, e di migliorare la rigenerazione muscolare e l'omeostasi delle cellule satelliti in seguito a danni muscolari nei topi privi di collagene VI.

Successivamente mi sono dedicata ad indagare il ruolo del collagene VI nell'omeostasi dell'intestino. Sebbene questa proteina sia ampiamente distribuita nella mucosa e nello strato muscolare, la sua assenza sembra non comportare alterazioni macroscopiche sull'architettura intestinale. L'analisi della funzionalità del sistema gastrointestinale ha evidenziato un'aumentata motilità e una ridotta permeabilità paracellulare in assenza di collagene VI. Esperimenti di induzione di colite acuta mediante sodio solfato destano hanno rivelato che i topi privi di collagene VI presentano una ridotta risposta e severità, associate ad una minore perdita di peso corporeo e minore infiammazione della mucosa del colon rispetto ai topi wild-type. Inoltre, durante la fase di colite acuta il reclutamento di cellule infiammatorie è risultato essere aumentato nei topi wild-type, comportando un aumento del numero di macrofagi e di attività dei neutrofili, mentre si riduce durante la fase di recupero seguente la colite acuta, favorendo la rigenerazione tissutale. Di contro, nei topi privi di collagene VI l'infiammazione è risultata essere ancora attiva durante la fase di recupero, con un elevato numero di macrofagi pro-infiammatori M1, un'alta attività dei neutrofili e un peggioramento della perdita di peso. Inoltre l'assenza di collagene VI ha dimostrato influenzare il comportamento dei macrofagi della mucosa del colon, sia in condizioni fisiologiche sia durante i primi giorni di infiammazione acuta, la cui attività è essenziale per assicurare l'omeostasi della mucosa intestinale. Nel complesso, da questi studi è emerso che il collagene VI esercita un ruolo da chemoattrattore per le cellule infiammatorie durante la fase di colite acuta, mentre nella successiva fase di risoluzione la sua presenza è necessaria nell'indurre una corretta rigenerazione tissutale. Studi di immunofluorescenza hanno inoltre rivelato nei topi wild-type un'elevata espressione di collagene VI in stretto contatto con i macrofagi della mucosa del colon durante la fase di colite acuta. L'evidenza di un'aumentata espressione di collagene VI su biopsia di ileo di paziente affetto da morbo di Crohn, associata ad un elevato numero di macrofagi rispetto al controllo sano, suggerisce un coinvolgimento di questo componente della MEC nel decorso delle malattie infiammatorie intestinali.

In conclusione, le evidenze emerse in questo mio lavoro di tesi avvalorano l'importanza del ruolo della matrice extracellulare nell'omeostasi tissutale.

1. Introduction

1.1 Skeletal muscle and extracellular matrix

Skeletal muscle is one of the most dynamic and plastic tissues of the human body. In humans, skeletal muscle comprises approximately 40% of total body weight, contains 50–75% of all body proteins, and accounts for 30–50% of whole-body protein turnover. Muscle is mainly composed of water (75%), proteins (20%), and other substances including inorganic salts, minerals, fat, and carbohydrates (5%). In general, muscle mass depends on the balance between protein synthesis and degradation and both processes are sensitive to factors such as nutritional status, hormonal balance, physical activity/exercise, and injury or disease, among others (Frontera and Ochala, 2015).

All vertebrate skeletal muscles, apart from head muscles, are derived from mesodermal precursor cells originating from the somites, segments of paraxial mesoderm that form following an anterior-posterior progression on either side of the neural tube and notochord (Buckingham, 2001). Mammalian skeletal muscles consist of multinucleated post-mitotic cells called myofibers or "muscle fibers". Myofibers form during embryonic development through fusion of mononucleated muscle progenitors, some of which remain associated to adult myofibers as satellite cells, a specific type of myogenic stem cell present in adult muscles. Mature myofibers are plastic cells that can undergo changes in fiber size (atrophy/hyperthophy) or fiber type (fast-to-slow or slow-to-fast swich), and can also repair local damages to specific subcellular structures (Ciciliot and Schiaffino, 2010).

Each skeletal muscle is formed by thousands of muscle fibers surrounded by a connective tissue envelope, called epimysium, from which processes originate to form the perimysium that enwrap several myofibers. The perimysium divides the muscle into a series of compartments each containing a bundle of myofibers called fascicle. Each myofiber is further surrounded by the endomysium, a thin connective tissue layer containing a specialized extracellular matrix (ECM) in contact with basement membrane, capillaries and nerve terminals (Buckingham 2001). Muscle fibers are attached to tendons and bone through myotendinous junctions (Bentzinger et al., 2013). The basement membrane is composed by an inner basal lamina, in tight connection with the plasma membrane of myofibers, and by a fibroreticular lamina, bound to the

connective tissue (Sanes, 2003). The basal lamina is mainly constituted by two proteins, collagen IV and laminin, which interact each other through nidogen/entactin and perlecan (Timpl, 1996). The key role of these proteins is not only due to their anchoring role between endomysium and basal lamina, but also to their interaction with a number of cell receptors such as $\alpha_7\beta_1$ integrin (Campbell and Stull, 2003). The fibroreticular lamina is characterized by the presence of collagen I and III and by a microfilament network of collagen VI embedded in an amorphous proteoglycan-rich ground substance, which guarantees the connection between the basal lamina and the connective tissue (Kuo et al., 1997). The basement membrane not only provides mechanical support to myofibers, but also supplies a significant fraction of the tensile strength of the whole structure. Moreover, it plays crucial roles in myogenesis and muscle regeneration, in the integrity and function of neuromuscular junctions and in synaptogenesis (Sanes, 2003).

The primary functions of skeletal muscle are locomotor activity, postural behaviour and breathing (Chargé and Rudnicki, 2004). Each myofiber, with approximate sizes of 50-100 μm in diameter and 1 cm in length, is made of thousands of myofibrils, cylindrical structures with 1-2 μm diameters. Myofibers are organized in contractile unites, named sarcomeres, molecular machineries triggering muscle contraction through the relative movement of two interlocking macromolecular structures, the thin actin filaments and thick myosin filament. The sarcomere and sarcoplasm contain many other proteins that contribute to the structure of the cytoskeleton, coupling of the excitation and contraction processes, energy release, and the generation of force and power. These proteins include tropomyosin and the calcium-dependent troponin complex (troponins C, I, and T), which are associated with the actin filament and play very important roles in the activation process that leads to myofilament sliding and force generation. Further proteins contributing to the mechanical and physiological properties of muscle are titin and nebulin. Other cellular elements in the sarcoplasm of muscle fibers include: *i)* mitochondria, which form a three-dimensional network throughout the cell that generates the energy (ATP) needed for muscle contraction when oxygen is made available to the muscle fiber; *ii)* a transverse tubular system (T tubule), an invagination of the plasma membrane of myofibers whose important role is the conduction of the nerve action potential within the cell; and *iii)* the sarcoplasmic reticulum, a specialized form of endoplasmic reticulum responsible for the storage, release, and reuptake of calcium ions. The calcium is stored in the terminal cisternae (dilated regions of the

sarcoplasmic reticulum) that are in close contact with the transverse tubule system. The two cisternae on both sides of the T tubule, together with the T tubule itself, form a structure known as the triad (Frontera and Ochala, 2015).

Excitation–contraction (EC) coupling is the coordination of two processes that are needed for the generation of force: the transmission of the nerve stimulus to the triad followed by the release of calcium from the cisternae of the sarcoplasmic reticulum and the interaction between actin and myosin that forms cross-bridges. Axons of motor neurons, which transmit the synaptic signal to the myofibers, terminate into neuromuscular junctions (NMJ) in the proximity of triads. As soon as the action potential reaches the axon terminals, it induces the opening of the voltage-gated Ca^{2+} channels on the presynaptic nerve membrane. This allows a Ca^{2+} influx that induces synaptic vescicles to fuse with the presynaptic membrane and to release the neurotransmitter acetylcholine (ACh) in the synaptic cleft. From here, ACh diffuses and binds to acetylcoline receptors (AChRs) localized in the post-synaptic membrane of the muscle fiber. This binding leads to an increased permeability to both Na^{+} and K^{+} and opens the associated voltage-gated Na^{+} channels on the muscle membrane which, in turn, initiate an action potential causing Ca^{2+} release from the sarcoplasmic reticulum into the sarcoplasm. Ca^{2+} then binds to the regulatory protein troponin C on the actin thin myofilaments, resulting in conformational changes of other troponin subunits that expose the myosin-binding sites on the actin chain, leading to muscle contraction (Hopkins, 2006; Ferraro et al. 2012; Frontera and Ochala, 2015).

For long time ECM was considered as a mere mechanical support to tissues, but in the last years its roles in regulating growth factors availability and molecular pathways became increasingly evident. Nowadays, ECM is considered a highly dynamic structure whose components are bioactive macromolecules that modulate cellular events such as adhesion, migration, proliferation, differentiation, and survival (Daley et al., 2008). In skeletal muscle, the importance of ECM/cell contact and ECM integrity is underlined by a number of animal models and human diseases where defects in ECM proteins or in proteins connecting myofibers to ECM lead to muscle pathology (Sanes, 2003).

1.2 Collagen VI

Collagen VI is a glycoprotein of the ECM forming a microfilamentous network in various tissues, such as skin, brain, joints, tendons, peripheral nerve, heart, blood vessels, intestine and cornea, and particular abundant in skeletal muscles (Keene et al., 1988). It consists of three chains, α1(VI), α2(VI) and α3(VI), encoded by distinct genes (*COL6A1*, *COL6A2*, *COL6A3*, respectively) (Bonaldo et al., 1989; Bonaldo et al., 1990; Chu et al., 1990; Doliana et al., 1990). In humans, the *COL6A1* and *COL6A2* genes are organized in a head-to-tail fashion on chromosome 21q22.3, whereas the *COL6A3* gene maps on chromosome 2q37 (Weil et al., 1988). In mouse, *Col6a1* and *Col6a2* genes form a cluster located on chromosome 10C1, while *Col6a3* is located on chromosome 1D (Fitzgerald et al., 2008).

All collagen VI chains contain a relatively short central triple-helical region of 335-336 amino acid residues with repeated Gly-Xaa-Yaa sequences, which are flanked by large N- and C-terminal globular regions. The globular regions are mostly composed of repetitive domains of ~200 amino acids that share similarity with the von Willebrand factor type A (vWFA) domain. The α1(VI) and α2(VI) chains are approximately 140-150 kDa in size and contain one N-terminal and two C-terminal vWFA-A globular domains (namely N1, C1 and C2). On the other hand, the α3(VI) chain is ~260-300 kDa in size and displays ten N-terminal and two C-terminal vWF-A domains (N1-N10 and C1-C2), followed by three additional C-terminal modules (C3-C5) with different structures. C3 is a proline-rich domain, containing Ser and Thr repeats that may be utilized for *O*-glycosylation; C4 is a fibronectin type III domain, whereas C5 shows 40-50% identity to a variety of serine protease inhibitors of the Kunitz type and its cleaved immediately after the secretion of collagen VI in the ECM (Bonaldo and Colombatti, 1989, Chu et al., 1990; Zhang et al., 1993; Colombatti and Bonaldo, 1991) (Fig. 1). Alternative splicing of the *COL6A2* transcript was found to generate three different α2(VI) protein variants, referred to as α2C2, α2C2a and α2C2a' (Saitta, et al., 1990). Also the *COL6A3* transcript can undergo multiple alternative splicings, generating different α3(VI) variants characterized by a variable number of vWF-A modules (Zanussi et al., 1992; Dziadek et al., 2002) (Fig.1).

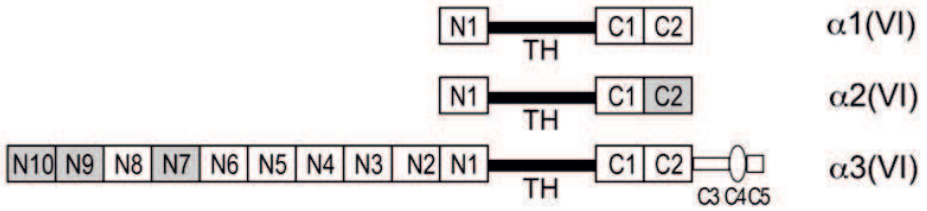


Figure 1. Primary structure of collagen VI. The three chains are made of different domains. N1-N10, N-terminal vWF-A globular domains; C1-C5, C-terminal domains; TH, triple helical region. Grey squares indicate domain undergoing alternative splicing (Bernardi and Bonaldo, 2008).

Collagen VI is synthesized and secreted by cells organizing an ECM, such as fibroblasts and smooth muscle cells, and transcriptional regulation is a key step in its production (Braghetta et al., 2008). In muscle, collagen VI is mainly produced by interstitial fibroblasts and it is a major component of the endomysium (Kuo et al., 1997; Zou et al., 2008). Secretion of collagen VI is a complex multistep process and requires the intracellular association of the three alpha chains in a 1:1:1 stoichiometric ratio to form triple-helical monomers (≈500 kDa). Monomers are assembled intracellularly into disulphide bonded antiparallel dimers (≈1000 kDa), which then align to form large tetramers (≈2000 kDa) that are also stabilized by disulfide bonds. Finally, tetramers are secreted in the extracellular space where they interact each other by end-to-end association through non-covalent bonds, forming characteristic microfilaments with beaded 105 nm-long repeats, as revealed by electron microscopy (Hessle and Engvall, 1984; Engvall et al., 1986; Colombatti et al., 1987; Colombatti and Bonaldo, 1987).

In 2008, three additional genes (named *Col6a4*, *Col6a5*, *Col6a6*) arranged in tandem on mouse chromosome 9 and coding for novel collagen VI chains [α4(VI), α5(VI) and α6(VI), respectively] were identified. The human orthologs of these genes (*COL6A4*, *COL6A5*, *COL6A6)* map to human chromosome 3q21, where the tandem orientation of the three genes is conserved. However, during primate evolution the *COL6A4* gene became broken into two pieces, thus becoming a non-functional pseudogene. The novel chains coded by these genes share domain organization and high sequence homology with α3(VI), suggesting that they may substitute for α3(VI) during collagen VI assembly likely forming α1α2α4, α1α2α5 or α1α2α6 triple helical monomers (Fitzgerald et al., 2008; Gara et al., 2008). Furthermore, these chains display distinct tissue distribution patterns, suggesting that they may have tissue-specific functions and allowing a modulation of collagen VI properties (Gara et al., 2011).

Given its complex structure and variety of domains, collagen VI has a wide range of interactions with other ECM components, such as fibronectin, hyaluronan, collagens I, II and IV, perlecan, biglycan and decorin. Moreover collagen VI is able to interact with different cell surface receptors, including $\alpha_1\beta_1$ and $\alpha_2\beta_1$ integrins and NG2 proteoglycan (Pfaff et al., 1993; Burg et al., 1996; Wiberg et al., 2002; Lampe and Bushby, 2005).

1.3 Collagen VI-related muscle disorders

Mutations of the genes encoding for collagen VI in humans are causative for a group of inherited muscle diseases showing a high degree of heterogeneity in clinical symptoms, collectively known as collagen VI-related myopathies. These comprise two major clinical forms, Bethlem myopathy [BM, (MIM 158810)] and Ullrich congenital muscular dystrophy [UCMD (MIM 254090)], but limb-girdle muscular dystrophy and congenital myosclerosis variants were also reported (Bönnemann, 2011).

BM was first described in 1976 by Bethlem and van Wijngaarden as an autosomal dominantly inherited mild proximal myopathy, characterized by slowly progressive axial and proximal muscle weakness with finger flexion contractures, proximal muscles being more involved than distal, and the extensors more than flexors (Lampe and Bushby, 2005; Merlini and Bernardi, 2008). Usually patients become symptomatic within the first and second decade. The classical phenotype is characterized by a variable clinical onset and intrafamilial variability (Bertini and Pepe, 2002). BM is a very heterogeneous disorder, and patients show a wide range of clinical features, from mild myopathy to more severe cases with early onset and features of slowly progressive muscular dystrophy (Bönnemann, 2011). BM inheritance is usually autosomal dominant, but recessive cases were also described (Gualandi et al., 2009). Immunohistochemistry shows apparently normal or mildly reduced levels of collagen VI in the endomysium of most BM patients, and quantitative or qualitative collagen VI defects can be detected in cultured fibroblasts derived from skin biopsies (Bernardi and Bonaldo, 2008).

UCMD was first described in 1930 by Ullrich and is an autosomal recessive severe congenital muscular dystrophy characterized by early onset, generalized and rapidly progressive muscle wasting and weakness with axial and proximal joint contractures and coexisting distal joint hypermobility (Lampe and Bushby, 2005; Bönnemann, 2011). The rapid progression of the clinical symptoms usually leads to early death, as a result of

respiratory failure. Usually, UCMD shows an autosomal recessive inheritance with homozygous or compound heterozygous mutations of the *COL6* genes, but several cases of UCMD with dominant mutation were also reported. Collagen VI appears to be strongly reduced or absent in muscle biopsies from UCMD patients, suggesting that UCMD mutations severely affect the synthesis and secretion of this protein in muscle (Bernardi and Bonaldo, 2008).

Congenital myosclerosis (MIM 255600) is a rare inherited disorder characterized by slender muscles with "woody" consistency, associated with early, diffuse and progressive muscle contractures that cause severe limitation of movement of axial, proximal, and distal joints. The disease is linked to a homozygous mutation of the *COL6A2* gene, which was originally found in affected sibs of an Italian family. Secreted collagen VI is quantitatively reduced and structurally abnormal in biopsies and cultures fibroblasts (Merlini et al., 2008a).

1.4 Collagen VI null mouse model and therapeutic approaches of collagen VI-related myopathies

To gain insight into the *in vivo* function of collagen VI, in 1996 the team of Prof. Bonaldo generated a collagen VI knockout (*Col6a1*$^{-/-}$) mouse model. This animal model provided valuable information on the pathomolecular defects underlying collagen VI deficiency, both for the biological point of view and for the prospective therapy of BM and UCMD. *Col6a1*$^{-/-}$ mice were obtained by targeted inactivation of the second exon of the *Col6a1* gene, thus leading to the complete absence of the α1(VI) chain. Ablation of α1(VI) chain does not affect the mRNAs levels for α2(VI) and α3(VI) chain, but the lack of α1(VI) in *Col6a1*$^{-/-}$ mice completely abolishes the assembly and secretion of collagen VI in the ECM (Bonaldo et al., 1998). *Col6a1*$^{-/-}$ mice are fertile, develop normally and do not display any overt sign of anatomical defect. The absence of collagen VI in *Col6a1*$^{-/-}$ mice leads to an early onset of myophatic disease, characterized by histological defects on different skeletal muscles, including muscle necrosis and phagocytosis, pronounced variation in myofiber diameter and increase in central nucleated myofibers, a finding which indicates muscle degeneration and regeneration. The myopathic phenotype triggered by collagen VI ablation suggests that the *Col6a1*$^{-/-}$ mouse could be considered an animal model of BM, based on the several features shared by *Col6a1*$^{-/-}$ mice and BM patients: both display a relatively mild myopathy, with an early onset appearing early in

life and showing slow progression with age. Further analysis revealed that *Col6a1*$^{-/-}$ muscles displays loss of the contractile strength in diaphragm, flexor digitorum brevis (FDB), tibialis anterior and gastrocnemius muscles, in association with spontaneous apoptosis and ultrastructural alterations of myofiber organelles (Irwin et al., 2003). In particular, mitochondria have abnormal cristae with tubular shape and altered matrix density associated with the presence of dense bodies. Marked dilations of sarcoplasmic reticulum were detected, especially at the level of triadic system, whereas sarcomeres, sarcolemma and basal lamina appear normal. In addition, myonuclei with the typical hallmarks of apoptosis are found in *Col6a1*$^{-/-}$ myofibers displaying organelle alterations, and the increased incidence of apoptosis in *Col6a1*$^{-/-}$ myofibers was confirmed by TUNEL assay. *Ex vivo* analysis on FDB myofibers treated with the selective F_1F_0 ATPase inhibitor oligomycin revealed the presence of a latent mitochondrial dysfunction that affects myofiber functionality in *Col6a1*$^{-/-}$ mice (Irwin et al., 2003). In particular, the latent mitochondrial dysfunction is related to an increased opening propensity of the permeability transition pore (PTP) of the inner mitochondrial membrane, thus leading to mitochondria depolarization, altered calcium handling by sarcoplasmic reticulum, cytochrome c release and finally to apoptosis (Bernardi and Bonaldo, 2008). Moreover, *in vivo* treatment with cyclosporin A, an inhibitor of cyclophilin D (Cyp-D, a peptidyl-prolyl cis-trans isomerase that is a component of the PTP), led to the rescue of the apoptotic and mitochondrial defects and more importantly attenuated the myopathic phenotype of *Col6a1*$^{-/-}$ muscles (Irwin et al., 2003). Additional evidence that pointed out a role of PTP in the pathogenesis of the myopathic phenotype was obtained by genetic ablation of Cyp-D on *Col6a1*$^{-/-}$ mice, leading to a marked attenuation of the phenotypic defects of collagen VI deficient mice (Palma et al., 2009).

In 2010, subsequent work from Bonaldo's team allowed to elucidate the molecular mechanisms causing the organelle defects in *Col6a1*$^{-/-}$ mice, revealing a link between defective regulation of autophagy and muscle wasting and weakness (Grumati et al., 2010). Autophagy is a highly conserved homeostatic mechanism used for the degradation and recycling of bulk cytoplasm, long-lived proteins and organelles through the lysosomal machinery (Mizushima et al., 2008). Interestingly, the autophagic machinery was found to be inefficient in the absence of collagen VI, due to abnormal signalling leading to defective regulation of Beclin 1 and Bnip3, two key factors needed for the activation of the autophagic process, with lower lipidation of the microtubule-associated protein-1 light chain 3 (LC3). In particular, lack of collagen VI leads to

persistent activation of the Akt/mTOR pathway in myofibers, with consequent blockade of the autophagic machinery (Grumati et al., 2010; Grumati et al., 2011). The formation of autophagosomes, *i.e.* the double-membrane vesicles that sequester cytoplasmic portions and deliver them to lysosomes for degradation, is strongly reduced in *Col6a1*$^{-/-}$ muscles, and following 24-hour starvation, a well-known stimulus for autophagy induction, autophagy activation is still impaired in collagen VI deficient muscles. As a consequence of the defective autophagy, dysfunctional and damaged organelles accumulate in *Col6a1*$^{-/-}$ muscles, leading to the onset of the myopathic phenotype (Grumati et al., 2010; Grumati et al., 2011). Interestingly, reactivation of autophagy in *Col6a1*$^{-/-}$ mice by genetic, dietary and pharmacological approaches restored myofiber survival and rescued the myopathic phenotype, leading to normalization of muscle homeostasis and strength. Therefore, these diverse *in vivo* approaches were not only able to successfully reactivate autophagy, but also to ameliorate muscle histology and myofiber defects, with a significant increase of muscle strength (Grumati et al., 2010; Grumati et al., 2011).

Studies on muscle biopsies and muscle cell cultures from BM and UCMD patients allowed to reveal similar pathomolecular defects in human collagen VI-related myopathies. As for *Col6a1*$^{-/-}$ mice, the latent mitochondrial dysfunction and spontaneous apoptosis of patients' muscle cultures were rescued by cyclosporin A treatment, as well as by adhesion onto purified collagen VI (Angelin et al., 2007). Moreover, further studies revealed that Beclin 1 and Bnip3 protein levels are reduced in muscle biopsies from BM and UCMD patients, thus revealing that defective regulation of autophagy is a shared feature of mice and men with collagen VI deficiency (Grumati et al., 2010).

The beneficial effects displayed by cyclosporin A treatment in *Col6a1*$^{-/-}$ mice, allowed to perform a first pilot clinical trial in four UCMD and one BM patients in 2008. Interestingly, oral administration of cyclosporine A for one month not only was able to recover apoptosis and mitochondrial dysfunction, but was also associated with muscle regeneration in pediatric UCMD patients (Merlini et al., 2008b). A subsequent long-term clinical study in UCMD/BM patients by oral administration of CsA for one month followed by a maintenance therapy for 1 to 3 years, revealed amelioration of muscle strength, rescue of mitochondrial dysfunction and increased muscle regeneration (Merlini et al., 2011).

During the past few years, several studies in *Col6a1*$^{-/-}$ mice helped to shed further light on the role that collagen VI exerts in tissues where it is expressed, revealing that this ECM protein is involved in the regulation of a number of cellular pathways, spanning from biomechanical properties, which are typical of collagen components of the ECM, to more specific cytoprotective functions. These include counteracting apoptosis and oxidative damage, favoring tumor growth and progression, regulation of the autophagic machinery and of cell differentiation and recruitment, and even contributing to the maintenance of stemness and regulation of tissue regeneration. Furthermore, other human disorders were recently linked to altered expression or mutations of the genes encoding collagen VI, thus emphasizing the importance of this protein for tissue homeostasis (Cescon et al., 2015).
Despite its network of interactions with several ECM and cell membrane components and the plethora of emerging findings about its functions in tissue homeostasis, the specific nature of the cell receptor(s) that mediate the surprisingly broad range of signals elicited by collagen VI remains unknown.

1.5 Satellite cells and skeletal muscle regeneration

Mammalian skeletal muscle has an impressive ability to regenerate itself in physiological conditions or upon injuries that may occur as a result of disease, such as muscular dystrophy, exposure to myotoxic agents, ischemia, sharp or blunt trauma or muscle's own contraction (Karalaki et al., 2009).

The main players in muscle regeneration are the so-called satellite cells (SCs), a specific population of muscle cells located between the basal lamina and the plasma membrane of myofibers (Mauro et al., 1961). SCs are necessary for post-natal muscle growth, and are responsible for maintenance, hypertrophy and repair of adult skeletal muscle (Musarò, 2014). SCs comprise 30–35% of all myofiber nuclei in postnatal mouse muscles, whereas the number decreases to 2.5–6% in adult muscles (Motohashi and Asakura, 2014). In resting muscle, SCs exist in a dormant state, known as quiescence or the reversible G0 state, tightly regulated by Notch signals and maintained by miRNA, essential for the long-term conservation of the satellite cell pool (Dumont et al., 2015). Quiescent SCs express several markers, among which Pax7, a paired box transcription factor, is thought to be exclusively expressed in SCs of mature muscle and has been

proposed to be the most reliable marker for both mouse and human SCs. Upon stimulation, SCs activate and re-enter the cell cycle, undergoing proliferation and differentiation. The progression of SCs through the myogenic program is orchestrated by the up- or down-regulation of Pax7 and of myogenic regulatory factors (MRFs), which include Myf5, MyoD and myogenin (Snijeder et al., 2015). SCs are activated to generate a committed population of myoblasts that can either fuse with existing myofibers, repairing damaged muscle fibers, or alternatively fuse to each other to form new myofibers. A small minority of myoblasts return to quiescent state, replenishing the resident pool of SCs through self-renewal (Musarò, 2014).

Quiescent SCs ($Pax7^{+}Myf5^{-}MyoD^{-}$) are activated in response to both physiological processes (such as exercise) and pathological conditions (such as injury and degenerative diseases), and can undergo symmetric divisions to expand the satellite stem cell population, or asymmetric divisions which generate one stem cell and one committed daughter cell that will progress through the myogenic process. Committed myogenic progenitors ($Pax7^{+}Myf5^{+}$ and/or $MyoD^{+}$), also called myoblasts, proliferate and are able to asymmetrically divide or directly differentiate into myocytes ($MyoG^{+}$), which fuse and form new myofibers (Dumont et al., 2015). Despite the presence of many differentiating cells in adult muscle, the total number of SCs remains constant through multiple rounds of regeneration and this equilibrium is due to the ability of SCs to self-renew, which provides progeny for differentiation while uncommitted mother cells are retained (Bentzinger et al., 2013).

SC activity is strictly regulated by the niche, a microenvironment composed by extracellular factors and cells which provide biochemical, mechanical and structural cues. The SC niche is exceptionally complex and the sources of environmental influences are diverse. The composition of SC niche can change based on the homeostasis and necessity of skeletal muscle, dynamically regulating SC quiescence, activation/proliferation, differentiation and self-renewal. Notably, the niche can change its composition based on the homeostasis and needs of skeletal muscle. In particular, several cell types, including immune cells, fibrogenic cells, vessel-associated cells and committed and differentiated cells of the myogenic lineage, have emerged as important constituents of the SC niche during the regenerative process. Furthermore, a plethora of different cell signals, including Notch signaling, Wnt signaling, and various growth factors, such as hepatocyte growth factor (HGF), insulin-like growth factor-1 (IGF-1), vascular endothelial growth factor (VEGF), fibroblast growth factor-2 (FGF-2), platelet-

derived growth factor (PDGF), and transforming growth factor (TGF-β), take part to SC regulation (Broek et al., 2010; Bentzinger et al. 2013).

A growing body of evidence supports ECM components as essential signal mediators in the niche, both for maintaining stem cell identity and regulating activation. One of the major roles of this ECM is to provide structural integrity to the niche. However, it also plays a role in localizing molecules such as growth factors and glycoproteins that regulate the balance between activation and quiescence. During regeneration, post-injury muscle basal lamina undergoes substantially remodelling, subsequent to the activation of proteases, such as matrix metalloproteinases, that allows SCs to leave the niche and migrate to the site of injury (Thomas et al., 2015). Besides its role in providing biochemical signals, ECM modulates the stiffness, *i.e.* the mechanical properties of the microenvironment, by regulating the so-called elastic modulus (*E*, also called Young's modulus), which is known to influence the stemness and regenerative capability of SCs (Cosgrove et al. 2009; Guilak et al. 2009; Gilbert et al. 2010). Indeed, small alterations to the niche ECM can have profound effects on SC localization, activation, self-renewal, proliferation and differentiation.

The cellular dynamics during muscle regeneration are highly complex and occur with distinct temporal and spatial kinetics. Several experimental models of muscle injuries are used to study the events of muscle regeneration and SC behaviour. Among these, one of the most commonly used is cardiotoxin damage, a snake venom that induces myofiber degeneration but preserves basal lamina, thus sparing SCs, vessels and nerves (Couteaux et al., 1988). Indeed, after injury muscle regeneration can be divided into two distinct phases: *i) degeneration* and *ii) regeneration*. Starting events of *degeneration* are characterized by a rapid necrosis of the injured myofibers and the disruption of the sarcolemma (cell membrane of myofibers), with subsequent release of cytosolic proteins, like creatine kinase, and the infiltration of the damage muscle by inflammatory cells (Karalaki et al., 2009). The first inflammatory cells that invade the injured tissue are neutrophils, peaking in concentration between 6 and 24 h, followed by inflammatory $CD68^{+}CD163^{-}$ M1 macrophages, whose number rapidly increase within 24 h after injury (Tidball and Villalta, 2010). After infiltration, macrophages not only phagocytose cellular debris and remove the disrupted myofilaments, other cytosolic structures and the damage sarcolemma, but also release pro-inflammatory cytokines, such as TNFα, IL-6 and IL-1β, which activate myogenic cells. A second population of macrophages, called $CD68^{-}CD163^{+}$ anti-inflammatory (M2), apparently derived from M1 macrophages by

phenotypic switch, reach their peak at 2 to 4 days after injury and secrete the anti-inflammatory cytokine IL-10, contributing to the termination of inflammation and stimulating myogenic cell differentiation, thus enhancing in this way the *regenerative* phase (Tidball and Villalta, 2010). Moreover, macrophages, especially M2 subset, also secrete different ECM proteins according to the stage of macrophage differentiation, such as fibronectin and collagen VI, important components of the muscle stem cell niche that promote SC self-renewal (Bentzinger et al., 2013). SC activation, that occurs within the second and fourth days after injury, concerns not only the cells associated with degenerated fibers, but also those present in undamaged fibers and in the neighbouring intact muscles (Kuang et al., 2008). After the activation, myogenic cells start to proliferate and migrate to the damaged site, differentiate into myoblasts and fuse to existing damaged fibers for repair or alternatively to each other to form new myofibers. New myofibers appear during the following day and, by 7–10 days after cardiotoxin injection, the overall architecture of the muscle is restored, although most regenerated myofibers are smaller and display centrally located myonuclei. Only when fusion is completed, myofibers start to increase their size and myonuclei, located on the centre of the fiber, begin move to the periphery; in humans myonuclei movement happens quickly, but in mouse centrally myonuclei persist for months (Karalaki et al., 2009). Growth and maturation of newly formed myofibers requires the presence of nerve. If neuromuscular connections are not established, regenerating myofibers remain atrophic (Tedesco et al., 2010). Indeed, nerve activity can directly influence protein turnover and gene expression within multinucleated regenerating myotubes and indirectly influence the proliferation and differentiation of satellite cells. The progressive maturation of regenerating myofibers occurs by 15 days. The last stage of the regenerative phase is characterize by ECM remodelling and angiogenesis. The activation of the ECM results in the overproduction of several types of collagens, fibronectin, elastin, proteoglycans, and laminin, which serve to stabilize the tissue, to act as a scaffold for the new fibers, and to guide the formation of neuromuscular junctions (Musarò, 2014).

Even if myogenic cells plays a central role in muscle regeneration, several studies demonstrated the existence of myogenic precursor originating from tissues other than skeletal muscle that are recruited in response to homing signals emanating from injured skeletal muscle, including mesenchymal stem cells, mesangioblasts, muscular stem cells

called “side-population”, endothelial progenitor cells, hematopoietic cells and adipose-derived stem cells (Broek et al., 2010).

The regenerative of skeletal muscle declines significantly with age. Reduced myofiber size is observed in combination with the accumulation of intramuscular fat, fibrosis and chronic inflammation, suggesting that aged muscles exhibit impaired regeneration potential and reduced muscle mass and strength. In fact, several studies pointed out that SC self-renewal and the ability of SCs to maintain/return to quiescence are impaired in aged muscles (Dumont et al., 2015). Moreover, studies examining the basal lamina of aged muscle and other tissues have demonstrated a pronounced thickening with a loss of laminated structure, becoming irregular and amorphous, a change which could affect the ability of the basal lamina to store and release growth factors and other signalling molecules involved in maintaining the SC niche (Thomas et al., 2015).

Muscle regeneration is also affected in several muscle disorders, many of which are caused by defects in proteins that bind components of the basal lamina. The most common and well-studied are the muscular dystrophies, a heterogeneous group of inherited progressive disorders characterized by pronounced muscle weakness, fibrosis and fatty infiltration, and resulting from mutations of dystrophin (Duchenne muscular dystrophy), laminin (congenital muscular dystrophy type 1A), collagen IV (Walker-Warburg syndrome), collagen VI (Ulrich congenital muscular dystrophy and Bethlem myopathy), and components of the dystroglycan complex (dystroglycanopathies) (Thomas et al., 2015).

1.6 Role of collagen VI in skeletal muscle regeneration

During the first year of my PhD, I was involved in a project aimed at investigating the role of collagen VI in skeletal muscle regeneration. We demonstrated that collagen VI is a major component of SC niche, being required for the proper self-renewal and maintenance of SCs, and it plays a key role during skeletal muscle regeneration induced by cardiotoxin (Urciuolo et al., 2013). By investigating *Col6a1*$^{-/-}$ mice, we found that the SC pool is increased in collagen VI deficient muscles when compared to wild-type muscles. Moreover, ablation of collagen VI leads to impaired muscle regeneration and reduced SC self-renewal capability in *Col6a1*$^{-/-}$ mice after multiple injuries. In addition, by performing *in vitro* studies on sorted SCs and isolated myofibers, we found that collagen VI exerts a direct effect on SC activation and self-renewal. We demonstrated

that these defects are associated with a significantly decreased stiffness in *Col6a1*$^{-/-}$ tibialis anterior muscles. When we grafted in wild-type tibialis anterior muscles SCs cultured on biomimetic structures with this lower stiffness value (7 kPa), we found that their stemness and regenerative capabilities were compromised when compared to those displayed by wild-type tibialis anterior muscles grafted with SCs cultured on the proper stiffness (12 kPa). When local collagen VI *in vivo* deposition in *Col6a1*$^{-/-}$ muscles was restored by grafting with wild-type fibroblasts, the biomechanical properties of *Col6a1*$^{-/-}$ muscles were ameliorated and SCs defects rescued (Urciuolo et al., 2013).

I contributed to this work by performing the histological and morphological characterization of wild-type and *Col6a1*$^{-/-}$ muscles in physiological condition and after injury, and by carrying out *in vivo* muscle grafting with fibroblasts and SCs. I also contributed to the analysis of wild-type and *Col6a1*$^{-/-}$ SCs, both *in vivo* and *in vitro*.

1.7 Effect of cyclosporin A on muscle regeneration in collagen VI deficient mice

During the first and in the second year of my PhD, I was involved in another project aimed at throwing light on the mechanisms underlying the increased muscle regenerative potential seen in UCMD pediatric patients that underwent the clinical trial with cyclosporin A (§ 1.3). Towards this aim, we investigated in detail the effects of cyclosporin A in ameliorating muscle regeneration and SC activity in *Col6a1*$^{-/-}$ mice, both under physiological condition and after SC depletion by cardiotoxin-induced injury (Gattazzo et al., 2014).

Our findings showed that cyclosporin A treatment for 10 days in physiological condition leads to a significant increase of the percentage of regenerating myofibers and of the SCs pool in *Col6a1*$^{-/-}$ tibialis anterior muscles, when compared to vehicle-treated *Col6a1*$^{-/-}$ animals. Moreover, data obtained on injured muscles showed that cyclosporin A is able to stimulate myogenesis in *Col6a1*$^{-/-}$ mice by significantly increasing the number of myogenin (MyoG)-positive cells and of regenerating myofibers at the early stages of muscle regeneration, thus indicating that cyclosporin A administration is able to improve muscle differentiation upon damage in the *Col6a1*$^{-/-}$ myopathic mouse model (Gattazzo et al., 2014). To assess the effects of cyclosporin A on counteracting the defective muscle regeneration and the depletion of SC triggered by multiple injuries, we

performed triple injury experiment and treated mice with the drug for 10 days during the third injury. After 30 days from the last injury, cyclosporin A treatment increased muscle mass in *Col6a1*$^{-/-}$ mice, in addition to the increase of myofiber cross-sectional area. Interestingly, cyclosporin A treatment was also able to significantly reduce muscle fibrosis when compared to vehicle-treated mice. Importantly, cyclosporin A was able to increase SC number following repeated injuries in *Col6a1*$^{-/-}$ mice, thus confirming the ability of cyclosporin A to improve muscle regeneration and SC homeostasis (Gattazzo et al., 2014). Altogether, these finding indicate that cyclosporin A is able to stimulate muscle regeneration and preserve the SC pool in the collagen VI disease mouse model, supporting and strengthening the increased muscle regeneration observed in UCMD patients undergoing clinical trial.

I contributed to this work by performing the histological and morphological characterization of wild-type and *Col6a1*$^{-/-}$ muscles in physiological condition and after injury. I also contributed to the analysis of SCs and I performed cardiotoxin damage.

nature COMMUNICATIONS

ARTICLE

Received 4 Feb 2013 | Accepted 2 May 2013 | Published 7 Jun 2013

DOI: 10.1038/ncomms2964

Collagen VI regulates satellite cell self-renewal and muscle regeneration

Anna Urciuolo[1], Marco Quarta[2,*], Valeria Morbidoni[1,*], Francesca Gattazzo[1,*], Sibilla Molon[1], Paolo Grumati[1], Francesca Montemurro[3], Francesco Saverio Tedesco[4], Bert Blaauw[1], Giulio Cossu[4], Giovanni Vozzi[3], Thomas A. Rando[2] & Paolo Bonaldo[1]

Adult muscle stem cells, or satellite cells have essential roles in homeostasis and regeneration of skeletal muscles. Satellite cells are located within a niche that includes myofibers and extracellular matrix. The function of specific extracellular matrix molecules in regulating SCs is poorly understood. Here, we show that the extracellular matrix protein collagen VI is a key component of the satellite cell niche. Lack of collagen VI in *Col6a1*$^{-/-}$ mice causes impaired muscle regeneration and reduced satellite cell self-renewal capability after injury. Collagen VI null muscles display significant decrease of stiffness, which is able to compromise the *in vitro* and *in vivo* activity of wild-type satellite cells. When collagen VI is reinstated *in vivo* by grafting wild-type fibroblasts, the biomechanical properties of *Col6a1*$^{-/-}$ muscles are ameliorated and satellite cell defects rescued. Our findings establish a critical role for an extracellular matrix molecule in satellite cell self-renewal and open new venues for therapies of collagen VI-related muscle diseases.

[1] Department of Biomedical Sciences, University of Padova, Padova 35131, Italy. [2] Department of Neurology and Neurological Sciences, Glenn Laboratories for the Biology of Aging, Stanford University School of Medicine, Stanford, California 94305, USA. [3] Interdepartmental Research Center E. Piaggio, University of Pisa, Pisa 56126, Italy. [4] Department of Cell and Developmental Biology, University College London, London WC1E 6DE, UK. * These authors contributed equally to this work. Correspondence and requests for materials should be addressed to P.B. (email: bonaldo@bio.unipd.it) or to T.A.R. (email: rando@stanford.edu).

© 2013 Macmillan Publishers Limited. All rights reserved.

Interactions between cells and extracellular matrix (ECM) have key roles in tissues undergoing extensive mechanical stress, such as skeletal muscles[1]. A major component of the ECM of skeletal muscles is collagen VI, a protein composed by three genetically distinct chains and forming a discrete network of beaded microfilaments in the basement membrane of muscle endomysium[2,3]. Collagen VI deposition in skeletal muscles is mainly provided by interstitial muscular fibroblasts[4]. Moreover, expression of collagen VI genes is regulated by myogenic cells, whose presence is a prerequisite for inducing the deposition of collagen VI by fibroblasts[5]. The critical role of collagen VI in skeletal muscles is supported by the fact that mutations of *COL6* genes in humans cause various muscle disorders, including Bethlem myopathy and Ullrich congenital muscular dystrophy[2,3]. Collagen VI null (*Col6a1*$^{-/-}$) mice display a mild myopathic phenotype associated with mitochondrial dysfunction, defective autophagy and spontaneous apoptosis of muscle fibers[6–8].

Satellite cells (SCs) are located between the basal lamina and the plasma membrane of muscle fibers[9], and this anatomic localization represents their niche. This niche is characterized by an asymmetric distribution of muscle components, where SCs contact myofibers through the apical surface whereas the ECM lies on their basal surface[9,10]. The myogenic commitment and differentiation of SCs is under the control of key transcription factors, such as the paired box protein 7 (Pax7) and the myogenic regulatory factors MyoD and Myogenin (MyoG)[11–15]. During muscle regeneration, SCs undergo proliferation, generating both a stem cell population by self-renewal and more differentiated cells that give rise to myoblasts that undergo terminal differentiation and fusion[16]. A growing body of evidence indicates that the niche serves as an instructive environment by which SCs respond to extrinsic stimuli associated with muscle growth and repair[17–23]. Changes in the ECM composition provide regulatory cues to SCs, thus influencing their quiescence, activation, differentiation and/or self-renewal[24]. On the other hand, ECM composition affects the mechanical properties of tissue microenvironment, which in turn influence the activity of various stem cells, including SCs[25,26].

Here, we demonstrate that collagen VI is a critical component of SC niche that is required for preserving SC self-renewal and muscle regeneration. *In vitro* and *in vivo* data indicate that one key mechanism through which collagen VI regulates SC activity is the modulation of muscle stiffness. Grafting with wild-type fibroblasts elicits extensive deposition of collagen VI and rescues SC self-renewal and muscle stiffness in *Col6a1*$^{-/-}$ mice. Our findings provide novel insights into the relevance of collagen VI for skeletal muscles and reveal an unforeseen role for this ECM molecule in the regulation of SC homeostasis.

Results

Collagen VI is an extracellular component of SC niche. We first evaluated collagen VI synthesis and localization with respect to SCs in murine extensor digitorum longus (EDL) and tibialis anterior (TA) muscles. Collagen VI was abundant in the endomysium of both muscles, and the protein was adjacent to the surface of SCs (Fig. 1a and Supplementary Fig. S1a). The localization was also confirmed *ex vivo* on freshly isolated myofibers and on sorted SCs (Fig. 1b; Supplementary Fig. S1b,c and Supplementary Movies). Interestingly, collagen VI was expressed by sorted SCs, and *Col6a1* transcripts were regulated during SC activation. Differently from collagen I (the major collagen of muscle interstitial ECM), *Col6a1* transcripts were abundant in quiescent SCs and their amount decreased in activated SCs (Fig. 1c and Supplementary Table S1). When TA muscles were subjected to injury with cardiotoxin[27], collagen VI deposition was markedly increased during the initial phases of regeneration and the protein was found nearby all Pax7^{+} cells 4 days after injury (Fig. 1d,e and Supplementary Figs. S1d and S2). These data indicate that collagen VI is expressed by SCs in a regulated manner and is an ECM component of the niche whose deposition is markedly increased upon muscle regeneration.

Lack of collagen VI affects SCs and muscle regeneration. Based on the above findings, we used collagen VI null (*Col6a1*$^{-/-}$) mice to explore the role of collagen VI in regulating SC function. In addition to abnormalities of muscle fibers in *Col6a1*$^{-/-}$ mice (a higher incidence of centrally nucleated fibers and a lower mean myofiber cross-sectional area), there was an increased number of SCs, with a corresponding increase of SC proliferation and apoptosis, when compared with wild-type muscles (Supplementary Figs. S3 and S4).

We next subjected wild-type and *Col6a1*$^{-/-}$ muscles to cardiotoxin injury. Despite the higher number of SCs before injury, *Col6a1*$^{-/-}$ TA muscles displayed smaller newly forming myofibers 7 days after injury and the number of SCs between *Col6a1*$^{-/-}$ and wild-type TA muscles was markedly reduced when compared with untreated animals (Fig. 2a and Supplementary Fig. S5a). To assess whether the observed alterations were simply due to delayed regeneration in *Col6a1*$^{-/-}$ muscles, we analyzed TA 30 days after injury, when the late myogenic differentiation program was completed. Despite an increase of myofiber cross-sectional area, regenerated *Col6a1*$^{-/-}$ muscles displayed a decreased number of SCs compared with untreated muscles (Fig. 2b and Supplementary Fig. S5b). These results indicate that lack of collagen VI leads to a decreased ability to properly maintain the SC pool after muscle damage, without any overt impairment of the differentiation and fusion of the SC progeny. To ascertain whether this phenotype was caused by a defective self-renewal ability of SCs, we performed multiple injury experiments and analyzed muscles 7 and 30 days after the last injury (Supplementary Fig. S5c). The inability of collagen VI-deficient muscles to regenerate properly after multiple rounds of injury was very evident. Following double injury, *Col6a1*$^{-/-}$ TA muscles displayed a significantly lower number of newly forming myofibers 7 days after injury and a decrease of both myofiber cross-sectional area and muscle mass after 30 days (Fig. 2c,d and Supplementary Fig. S5d,e). This was even more striking in triple injury experiments, where muscle regeneration was dramatically impaired in *Col6a1*$^{-/-}$ TA muscles, with extensive fibrotic lesions and significant decrease of muscle mass, while wild-type TA muscles were still able to regenerate properly (Fig. 2c,d and Supplementary Fig. S5d,f). Notably, following repeated injuries, *Col6a1*$^{-/-}$ TA muscles showed a progressive decline in SC number (Fig. 2e). The progressive depletion of the SC pool in *Col6a1*$^{-/-}$ muscles after injury indicates that collagen VI is strictly needed for the correct function of the niche and the maintenance of SC pool during muscle regeneration.

Collagen VI regulates SC activity *in vitro*. Based on these results, we used different *in vitro* approaches to analyze the effects elicited by collagen VI on SCs. Sorted SCs were prepared from wild-type and *Col6a1*$^{-/-}$ hindlimb muscles and cultured for 48 h on matrigel-coated dishes in the presence or absence of purified native collagen VI. To analyze the differentiation program, we divided cultured SCs into different populations. Early differentiation was evaluated on the basis of Pax7 and MyoD expression, by classifying cells in Pax7^{+}MyoD^{-}, Pax7^{+}MyoD^{+} and Pax7^{-}MyoD^{+} populations[28], whereas the onset of terminal differentiation was evaluated based on MyoG expression and by dividing cells into Pax7^{+}MyoG^{-} and Pax7^{-}MyoG^{+}

© 2013 Macmillan Publishers Limited. All rights reserved.

NATURE COMMUNICATIONS | DOI: 10.1038/ncomms2964 ARTICLE

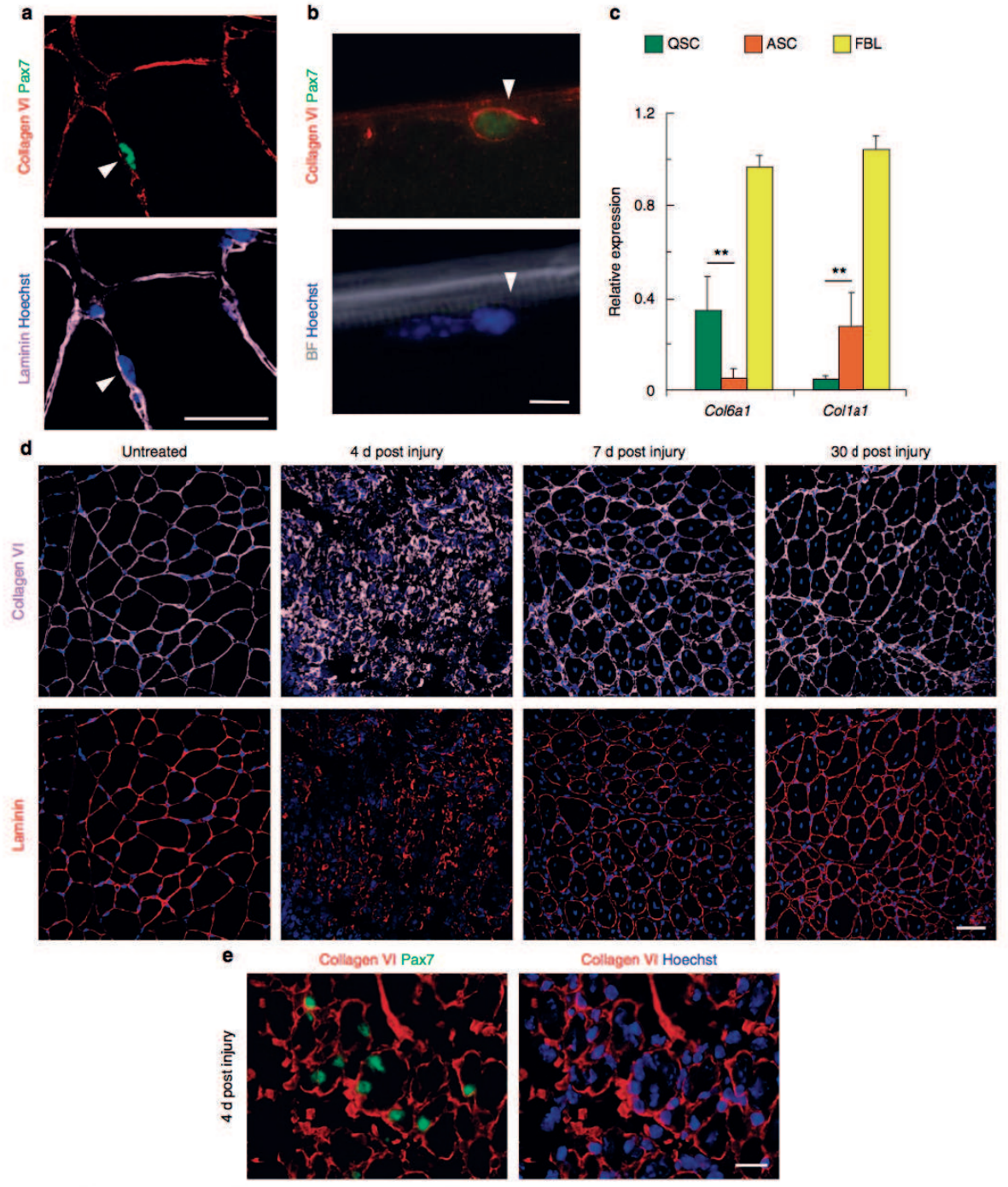


Figure 1 | Collagen VI is an extracellular component of SC niche. (**a**) Representative confocal image of immunofluorescence analysis for collagen VI (red), Pax7 (green) and laminin (light pink) in TA cross-sections from wild-type mice. The arrowhead points at one SC. Scale bar, 25 µm. (**b**) Representative confocal image of a freshly isolated wild-type EDL fiber, showing the immunolocalization of collagen VI (red) with respect to SC (green, arrowhead). BF, bright field. Scale bar, 10 µm. (**c**) Expression levels of *Col6a1* and *Col1a1* transcripts in quiescent (QSC) and activated (ASC) wild-type SCs and in wild-type muscle fibroblasts (FBL). *Gapdh* expression was used to calculate the relative expression of *Col6a1* and *Col1a1* transcripts. Data are shown as mean ± s.e.m. of three independent replicates (**$P<0.01$; unequal variance Student's *t*-test; $n=8$, each group). (**d**) Representative confocal z-stack images of immunofluorescence for collagen VI (light pink) and laminin (red) in TA cross-sections from wild-type mice under untreated conditions or 4 days, 7 days and 30 days after single cardiotoxin injury. Scale bar, 50 µm. (**e**) Representative views of immunofluorescence for collagen VI (red) and Pax7 (green) in wild-type TA 4 days after cardiotoxin injection. Nuclei were stained with Hoechst (blue). Scale bar, 50 µm.

© 2013 Macmillan Publishers Limited. All rights reserved.

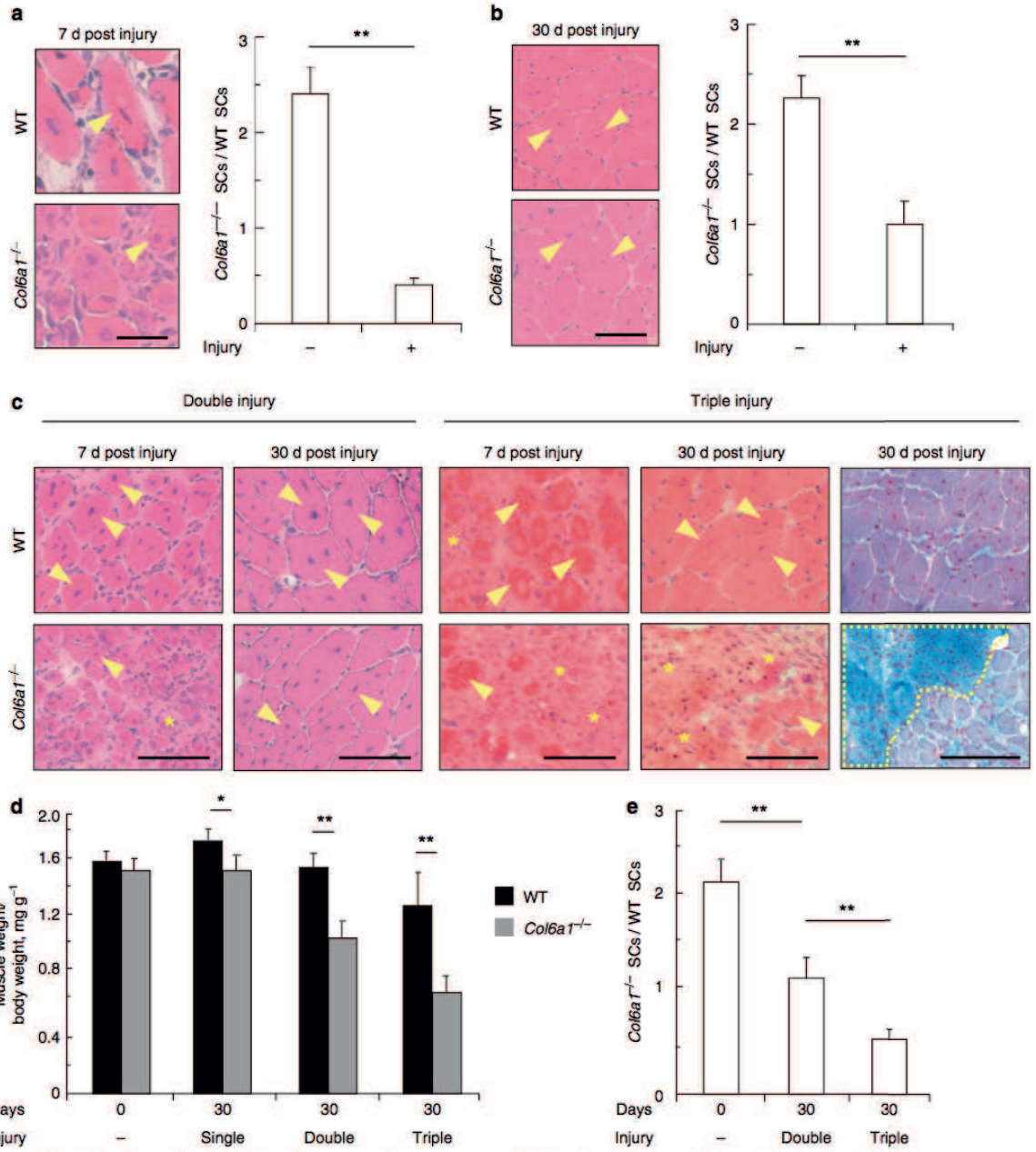


Figure 2 | Lack of collagen VI affects SC maintenance and muscle regeneration *in vivo*. (**a**) Left panel, haematoxylin-eosin staining of TA cross-sections from wild-type and *Col6a1*$^{-/-}$ mice 7 days after cardiotoxin injury. The arrowheads point at some newly forming myofibers. Scale bar, 25 μm. Right panel, ratio of SCs between *Col6a1*$^{-/-}$ and wild-type TA in untreated conditions (−) and 7 days after single injury (+). Data are shown as mean ± s.e.m of three independent replicates (**$P<0.01$; unequal variance Student's *t*-test; $n=6$ animals, each group). (**b**) Left panel, haematoxylin-eosin staining of TA cross-sections from wild-type and *Col6a1*$^{-/-}$ mice 30 days after cardiotoxin injury. The arrowheads point at some newly forming myofibers. Scale bar, 50 μm. Right panel, ratio of SCs between *Col6a1*$^{-/-}$ and wild-type TA in untreated conditions (−) and 30 days after single injury (+). Data are shown as mean ± s.e.m. of three independent replicates (**$P<0.01$; unequal variance Student's *t*-test; $n=6$ animals, each group). (**c**) Haematoxylin-eosin and Azan staining of TA cross-sections from wild-type and *Col6a1*$^{-/-}$ mice 7 days and 30 days after double and triple injury. Arrowheads point at some newly forming myofibers, asterisks label some areas still in the degeneration phase, and the dotted region in the lower right panel show fibrotic tissue substitution stained by Azan. Scale bar, 50 μm. (**d**) Quantification of TA weight/body weight of wild type and *Col6a1*$^{-/-}$ mice in untreated conditions (−) and 30 days after single, double or triple injury. Data are shown as mean ± s.e.m. of three independent replicates (*$P<0.05$; **$P<0.01$; unequal variance Student's *t*-test; $n=6$–8 animals, each group). (**e**) Ratio of SCs between *Col6a1*$^{-/-}$ and wild-type TA in untreated conditions (−) and 30 days after double or triple injury. Data are shown as mean ± s.e.m. of three independent replicates (**$P<0.01$; unequal variance Student's *t*-test; $n=6$ animals, each group). WT, wild-type.

© 2013 Macmillan Publishers Limited. All rights reserved.

populations[13–15]. When grown on matrigel, *Col6a1*$^{-/-}$ cultures displayed lower percentages of Pax7-expressing cells and corresponding higher percentages of cells expressing MyoD or MyoG. By contrast, growth on collagen VI led to a significant increase of Pax7-expressing cells and decrease of differentiating cells in both wild-type and *Col6a1*$^{-/-}$ cultures (Supplementary Fig. S6a–c and Supplementary Tables S2 and S3).

With the aim to reconstitute the ECM components found in the wild-type SC niche, we analyzed *Col6a1*$^{-/-}$ single fibers cultured for 72 h on matrigel in the absence or presence of collagen VI. *Col6a1*$^{-/-}$ SCs displayed a lower ability to preserve the Pax7^{+}MyoD^{-} population in single fiber culture, as observed in SC-derived culture (Fig. 3a,b and Table 1). When grown on dishes coated with purified collagen VI, *Col6a1*$^{-/-}$ fibers contacted the collagen VI network, which also localized nearby SCs (Fig. 3c and Supplementary Fig. S6d). Remarkably, *Col6a1*$^{-/-}$ SCs showed a higher ability to maintain the Pax7^{+}MyoD^{-} population when fibers were grown on purified collagen VI, with decreased apoptosis and increased proliferation when compared with cultures grown on matrigel alone (Fig. 3a,d,e). Taken together, these *in vitro* data indicate that collagen VI improves the maintenance and survival of cells expressing Pax7, a transcription factor critical for SC self-renewal after damage[11–14].

Collagen VI regulates SC activity *in vivo*. To assess whether the SC defects of collagen VI-deficient muscles may be secondary to the myopathic phenotype, we performed additional *in vivo* studies on *Col6a1*$^{-/-}$ mice. Our previous work established that the myopathic phenotype of *Col6a1*$^{-/-}$ mice is caused by a failure of the autophagic machinery in myofibers, a process that can be reinstated by feeding mice with a low-protein diet or treating them with rapamycin[8]. Based on this, we investigated whether the abnormal activity displayed by SC in *Col6a1*$^{-/-}$ mice is secondary to the myopathic phenotype. Toward this aim, we assessed whether reactivation of autophagy in myofibers, and the consequent rescue of the myopathy, may influence the activity of *Col6a1*$^{-/-}$ SCs. Interestingly, recovery of the autophagy-dependent myofiber defects did not exert any effect on SC activity of *Col6a1*$^{-/-}$ mice, neither in undamaged muscles nor after cardiotoxin injury (Supplementary Fig. S7).

To definitely uncouple the *Col6a1*$^{-/-}$ SC defects from the myopathy, we transplanted wild-type or *Col6a1*$^{-/-}$ SCs into regenerating *Col6a1*$^{-/-}$ muscle and analyzed their function in the host tissue. Indeed, if collagen VI has a direct effect on SCs *in vivo*, the protein expressed by transplanted wild-type cells should enable SCs to function normally in the host tissue and muscle regeneration should be significantly improved. Towards this aim, we sorted GFP^{+} SCs derived from wild-type (WTSCs) and *Col6a1*$^{-/-}$ (KOSCs) mice and injected them into cardiotoxin-injured *Col6a1*$^{-/-}$ muscles (Fig. 4a). Real-time PCR confirmed the presence of donor WTSCs and KOSCs in host muscles and revealed expression of collagen VI in *Col6a1*$^{-/-}$ muscles transplanted with WTSCs (Fig. 4b,c). Notably, the number of SCs in *Col6a1*$^{-/-}$ muscles transplanted with WTSCs was significantly higher than *Col6a1*$^{-/-}$ muscles transplanted with KOSCs (Fig. 4d). Concurrently, muscle regeneration was noticeably improved when *Col6a1*$^{-/-}$ muscles were transplanted with WTSCs, compared with *Col6a1*$^{-/-}$ muscles transplanted with KOSCs (Fig. 4e). These data confirm that the alterations displayed by SCs in *Col6a1*$^{-/-}$ mice are strictly dependent on the lack of collagen VI and indicate that the production of this protein by SCs is required for their proper activity during muscle regeneration.

Collagen VI affects SCs by regulating muscle stiffness. Having established a role for collagen VI in regulating SC activity and muscle regeneration, we investigated the mechanism involved in this process. Although regulation of autophagy is a major mechanism through which collagen VI regulates myofiber homeostasis[8], the results discussed above exclude this mechanism as a determinant for collagen VI regulation of SC activity (Supplementary Fig. S7).

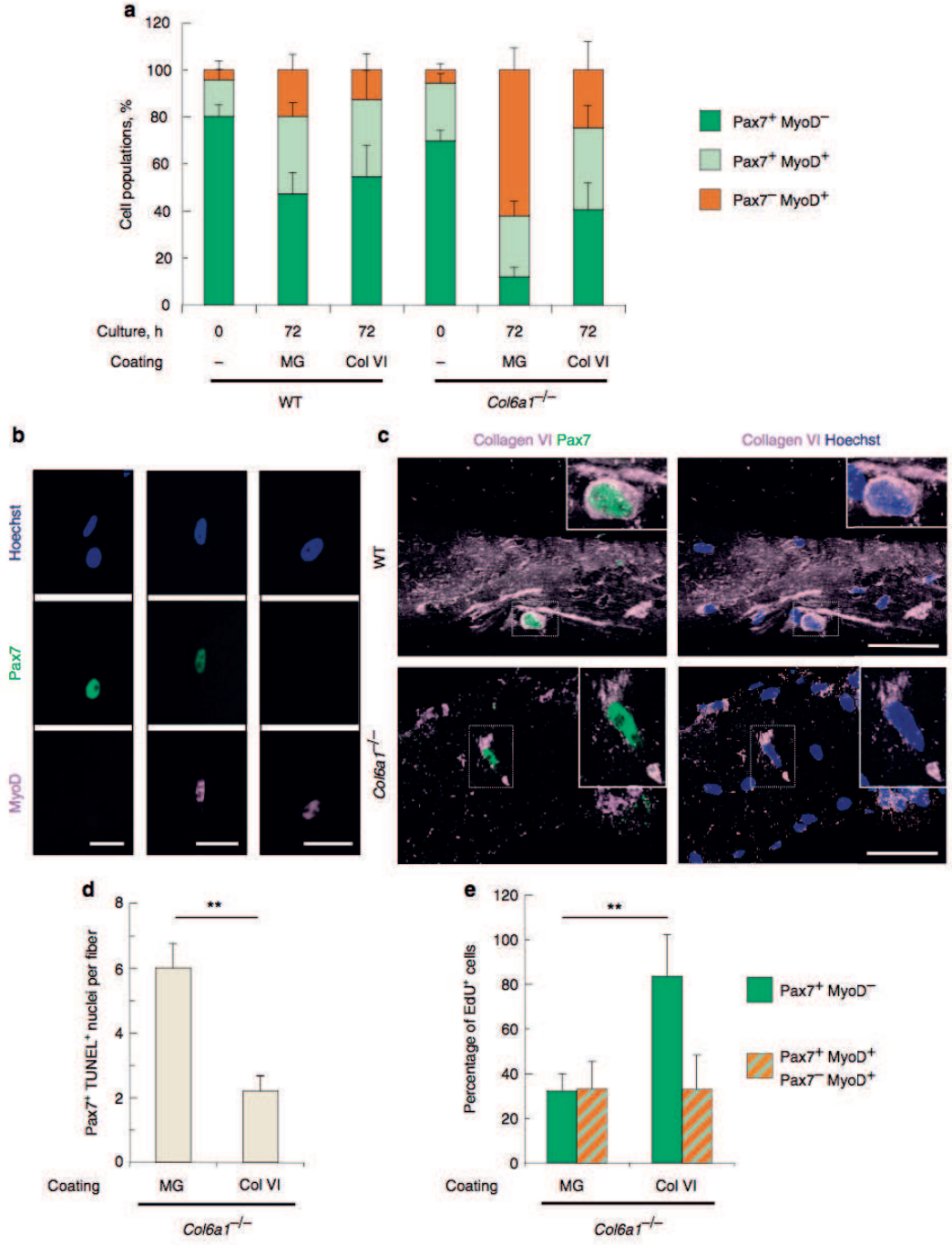
Given the abundance of collagen VI beaded microfilaments in endomysial basement membrane[29], we investigated whether collagen VI may be engaged in the regulation of muscle mechanical properties. Previous work demonstrated that differentiation of stem cells into myoblasts requires optimal tissue elasticity, closely matching the physiological stiffness of skeletal muscle[30]. Moreover, recent studies showed that SCs cultured on bioengineered structures mimicking muscle physiological elasticity display higher *in vitro* self-renewal and *in vivo* regeneration capabilities, when compared with cells grown on plastic[25]. To assess the contribution of collagen VI to muscle mechanical properties, we compared the stiffness of wild-type and *Col6a1*$^{-/-}$ TA muscles using a stress–strain test. Quantification of the Young modulus, an index of elasticity, revealed that *Col6a1*$^{-/-}$ muscles are more elastic ($E \sim 7$ kPa) than their wild-type counterparts ($E \sim 12$ kPa) (Fig. 5a and Supplementary Fig. S8a). *Col6a1*$^{-/-}$ muscles also maintained lower stiffness 4 days after cardiotoxin injury, when there is massive ECM production, indicating that the abnormal elasticity elicited by the lack of collagen VI cannot be compensated by the increased global deposition of other ECM proteins (Fig. 5a and Supplementary Fig. S8a). To investigate whether the observed changes in the mechanical properties of *Col6a1*$^{-/-}$ muscles have any major influence on *in vitro* SC activity, we isolated SCs from wild-type and *Col6a1*$^{-/-}$ GFP^{+} muscles and used them to obtain SC cultures grown on biomimetic structures with a stiffness of either ~ 7 kPa or ~ 12 kPa (Supplementary Fig. S8b). Wild-type SCs grown on structures of physiological (12 kPa) stiffness maintained a large proportion of Pax7^{+}MyoD^{-} cells ($\sim$70% of total myogenic cells), while this proportion was dramatically decreased ($<$8% of total myogenic cells) when SCs were grown on structures of 7-kPa stiffness, with a corresponding increase of Pax7^{+}MyoD^{+} and Pax7^{-}MyoD^{+} cells (Fig. 5b). Notably, the total cell numbers for both wild-type and *Col6a1*$^{-/-}$ genotypes were also markedly lower when SCs were cultured on the 7-kPa structures compared with the 12-kPa structures (Supplementary Fig. S8c). Altogether, this set of findings reveals that collagen VI is necessary to maintain muscle mechanical properties *in vivo* and that the altered stiffness displayed by *Col6a1*$^{-/-}$ muscles affects the maintenance of Pax7^{+} cells *in vitro*.

We next assessed the *in vivo* fate of SCs cultured on 7-kPa or 12-kPa biomimetic structures by injecting them into *Col6a1*$^{-/-}$ TA muscles (Fig. 5c). The presence of donor cells in host muscles led to the induction of muscle regeneration as expected, with no significant differences between cells cultured on structures of different stiffness (Fig. 5d,e). Conversely, the number of SCs was significantly increased in muscles transplanted with SCs grown on the 12-kPa structures, but not in those transplanted with SCs grown on the 7-kPa structures (Fig. 5f). Interestingly, several Pax7^{+} cells were found in the interstitium of muscles transplanted with SCs cultured on the less stiff structures (Supplementary Fig. S8d), suggesting that these myogenic cells are less able to adopt a SC localization compared with SCs cultured on structures of physiological stiffness. To get a more precise evaluation of the *in vivo* fate of SCs, we quantified the number of SCs associated with centrally nucleated fibers and found that it was significantly higher in regenerating fibers in muscles transplanted with SCs grown on the 12-kPa structures

© 2013 Macmillan Publishers Limited. All rights reserved.

(Fig. 5g). Altogether, these data indicate that SCs grown on structures mimicking the stiffness of wild-type muscle have a higher ability to preserve their stem cell function compared with SCs grown on structures mimicking the stiffness of collagen VI-deficient muscles, supporting the idea that matrix stiffness may be a key mechanism through which collagen VI exerts its effects on SCs.

Collagen VI restoration rescues SC self-renewal and muscle stiffness. Previous studies established that fibroblasts are the main producers of collagen VI in skeletal muscles[5]. Based on this, and with the aim to test the effect on SCs and muscle stiffness when collagen VI deposition is reinstated in *Col6a1*$^{-/-}$ mice, we performed grafting experiments with muscle fibroblasts in TA muscles. Fibroblasts were isolated from hindlimb muscles of



© 2013 Macmillan Publishers Limited. All rights reserved.

either wild-type (WTFB), GFP transgenic (GFPFB) or *Col6a1*$^{-/-}$ (KOFB) mice, characterized by immunofluorescence (Supplementary Fig. S9a) and injected into TA muscles of *Col6a1*$^{-/-}$ mice. Fibroblasts were found in the connective tissue of *Col6a1*$^{-/-}$ muscles, and WTFBs, but not KOFBs, produced and secreted collagen VI (Fig. 6a and Supplementary Fig. S9b,c). By 4 days after injection, fibroblasts were more diffuse and collagen VI was largely localized in the endomysium nearby Pax7^{+} cells (Fig. 6a,b and Supplementary Fig. S9b,c). To improve collagen VI deposition and overcome the potential loss of fibroblasts by an immune reaction against GFP[31], WTFBs or KOFBs were used and wild-type and *Col6a1*$^{-/-}$ mice were subjected to a second graft 6 days after the initial cell injection. Collagen VI was extensively produced and deposited around myofibers of *Col6a1*$^{-/-}$ muscles subjected to double grafting with WTFBs (Supplementary Fig. S9d).

We next investigated the effects of collagen VI deposition, by comparing wild-type and *Col6a1*$^{-/-}$ TA muscles subjected to injection with either WTFBs or KOFBs. Notably, *Col6a1*$^{-/-}$ TA muscles showed a significant increase of the Young modulus 12 days after grafting with WTFBs, while this physical parameter remained unchanged after grafting with KOFBs (Fig. 6c and Supplementary Fig. S9e). Independently from the genotype of grafted cells, injection of fibroblasts generated a response of SCs in wild-type muscles, as displayed by the local increase of centrally nucleated fibers and by the higher number of SCs (Supplementary Fig. S10a). Differently, the local number of SCs in *Col6a1*$^{-/-}$ TA was increased after grafting with WTFBs, with the concurrent increase of centrally nucleated fibers, but was unaffected by grafting with KOFBs (Fig. 6d and Supplementary Fig. S10b). Of note, we did not observe any rescue of the SC number in areas located nearby the engraftment, but lacking collagen VI deposition, suggesting that the effects on SC activity observed in *Col6a1*$^{-/-}$ muscles were elicited by engrafted WTFBs and collagen VI deposition, with no obvious involvement of additional cell types and/or independent paracrine mechanisms (Supplementary Fig. S10b). To assess whether fibroblast grafting and collagen VI deposition could also improve the maintenance of myogenic cells in *Col6a1*$^{-/-}$ muscles after injury, WTFBs were grafted 4 h after a single cardiotoxin injection and mice were killed 30 days later. Interestingly, collagen VI was still present around *Col6a1*$^{-/-}$ myofibers 30 days after injury (Fig. 6e and Supplementary Fig. S10c) and the SC ratio was significantly higher than that of the controlaterally injured non-grafted muscle, whereas no significant changes were observed in muscle weight and myofiber cross-sectional area (Fig. 6f and Supplementary Fig. S10d,e). Altogether, these data support a role for collagen VI in the regulation of *in vivo* muscle mechanical properties, which in turn can affect SC activity.

Discussion

The correct regulation of stem cell activity is crucial for maintaining tissue homeostasis in physiological and pathological conditions, such as after injury and during wound healing. A number of studies support the notion that the niche, a varied set of cells and extracellular factors nearby stem cells or in contact with them, has key roles in maintaining the quiescence and supporting the self-renewal of stem cells, including SCs. Our findings indicate that collagen VI, an ECM protein forming a distinctive microfibrillar system in several organs, is an essential component of muscle SC niche.

A wealth of observations indicates that the ECM undergoes extensive remodeling in the course of muscle regeneration[24]. Muscle substitution by fibrotic connective tissue is a common feature of several conditions, such as aging and Duchenne muscular dystrophy, pointing at a negative effect for excessive production of fibrillar collagens and interstitial ECM components[32]. Despite this, changes of niche composition are essential for proper SC activity during muscle regeneration[19,24]. We found that collagen VI deposition is markedly increased during the initial phases of muscle regeneration, when the protein forms a thick network enclosing myogenic cells. Previous *in vitro* and *in vivo* studies showed that collagen VI in muscle is produced

Table 1 | Quantification of Pax7^{+}MyoD^{-}, Pax7^{+}MyoD^{+} and Pax7^{-}MyoD^{+} cell populations on single wild type and *Col6a1*$^{-/-}$ myofibers.

	Pax7^{+} (*P-value*)	*Pax7*$^{+}$*MyoD*$^{+}$ (*P-value*)	*Pax7*$^{-}$*MyoD*$^{+}$ (*P-value*)
WT, t0 versus MG	<0.01	<0.05	<0.05
KO, t0 versus MG	<0.01	n.s.	<0.01
t0, WT versus KO	n.s.	n.s.	n.s.
MG, WT versus KO	<0.01	n.s.	<0.01
KO, MG versus Col VI	<0.01	n.s.	<0.01
Col VI, WT versus KO	n.s.	n.s.	n.s.

The table reports the statistical analysis of the data shown in Fig. 3a. Unequal variance Student's *t*-test was used and a *P*-value<0.05 was considered statistically significant (n.s., not significant). Col VI, purified collagen VI; KO, *Col6a1*$^{-/-}$; MG, matrigel; t0, freshly isolated fibers; WT, wild type.

Figure 3 | Collagen VI regulates SC activity *in vitro*. (**a**) Quantification of Pax7^{+}MyoD^{-}, Pax7^{+}MyoD^{+} and Pax7^{-}MyoD^{+} cell populations on single wild-type and *Col6a1*$^{-/-}$ myofibers fixed upon isolation (0 h) or following 72 h culture on matrigel-coated dishes in the presence or absence of purified native collagen VI. Data are shown as mean ± s.e.m. of three independent replicates. The statistical analysis is provided in Table 1 (unequal variance Student's *t*-test; $n=10$–22 myofibers, each group). (**b**) Three representative confocal images of cultured single myofibers and labeled with antibodies for Pax7 (green) and MyoD (light pink). Nuclei were stained with Hoechst (blue). Scale bar, 20 μm. (**c**) Confocal z-stack images of wild-type and *Col6a1*$^{-/-}$ fibers grown on purified collagen VI and analyzed by immunofluorescence for collagen VI (light pink) and Pax7 (green). The insets show higher magnifications of the squared areas. Scale bar, 50 μm. (**d**) Quantification of apoptotic Pax7^{+} cells by TUNEL test in *Col6a1*$^{-/-}$ single myofibers following 72 h culture on matrigel-coated dishes in the presence or absence of purified native collagen VI. Data are shown as mean ± s.e.m. of two independent replicates (**$P<0.01$; unequal variance Student's *t*-test; $n=10$ myofibers, each group). (**e**) Quantification of EdU^{+} cells, calculated as the percentage on Pax7^{+}MyoD^{-}, Pax7^{+}MyoD^{+} and Pax7^{-}MyoD^{+} cell populations, in *Col6a1*$^{-/-}$ single myofibers after 72 h culture on matrigel-coated dishes in the presence or absence of purified native collagen VI. Data are shown as mean ± s.e.m. of three independent replicates (**$P<0.01$; unequal variance Student's *t*-test; $n=10$ myofibers, each group). Col VI, collagen VI; KO, *Col6a1*$^{-/-}$; MG, matrigel; WT, wild-type.

© 2013 Macmillan Publishers Limited. All rights reserved.

ARTICLE NATURE COMMUNICATIONS | DOI: 10.1038/ncomms2964

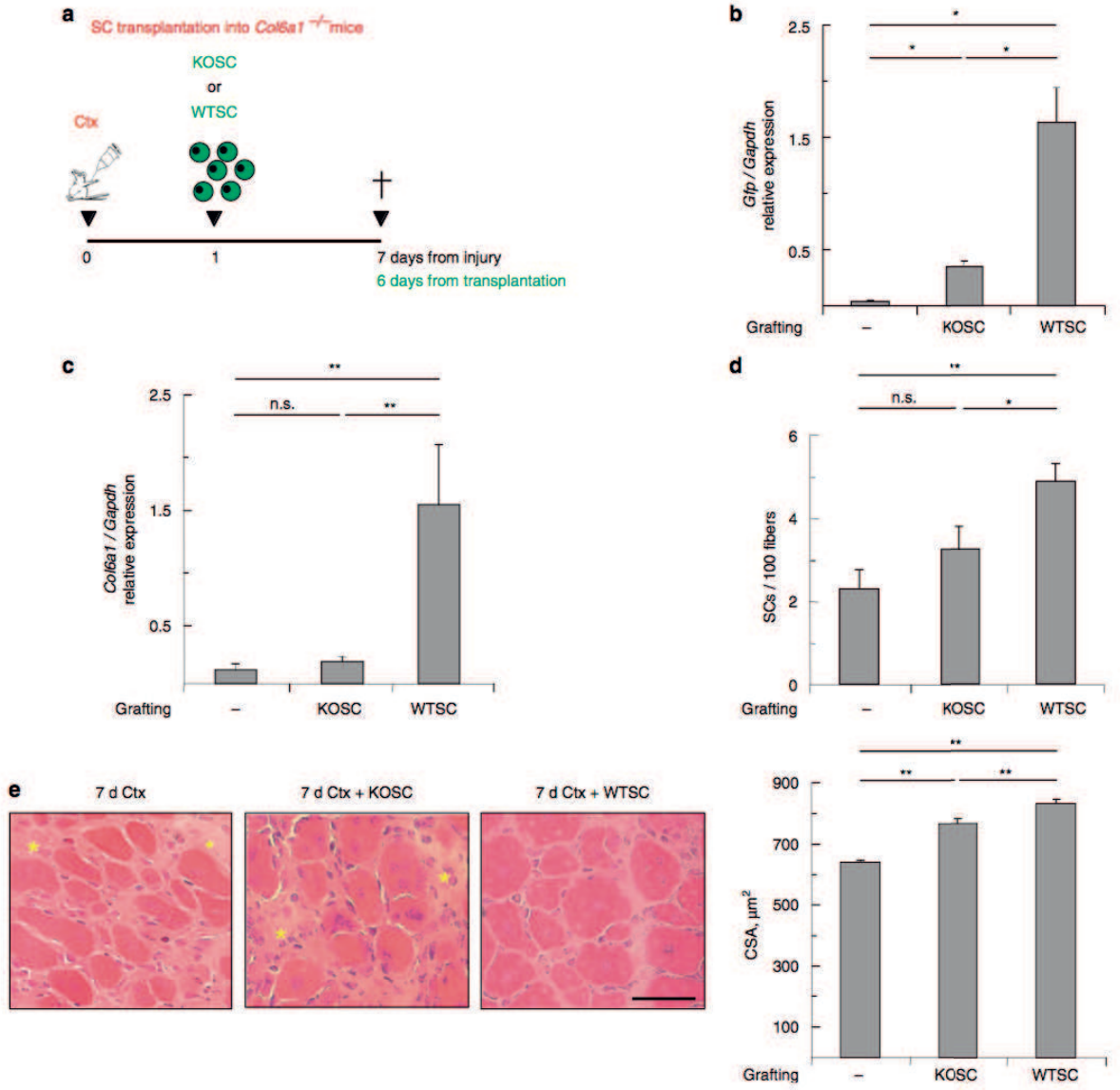


Figure 4 | Collagen VI has a direct effect on SC *in vivo*. (**a**) Schematic diagram of the experimental approach for grafting SCs in *Col6a1*$^{-/-}$ regenerating muscles. One day after cardiotoxin injury, 3,000 freshly isolated wild-type SCs or *Col6a1*$^{-/-}$ SCs expressing the GFP-LC3 fusion protein were injected in regenerating *Col6a1*$^{-/-}$ TA. Muscles were analyzed after 7 days from cardiotoxin injury. (**b**) Real-time PCR analysis of GFP expression in *Col6a1*$^{-/-}$ muscles derived from 7-day cardiotoxin-injured mice without grafting (−) or grafted with wild-type or *Col6a1*$^{-/-}$ SCs expressing GFP-LC3. Data are shown as mean ± s.e.m. of three independent replicates (*$P<0.01$; unequal variance Student's *t*-test; $n=5$ animals, each group). (**c**) Real-time PCR analysis of *Col6a1* expression in *Col6a1*$^{-/-}$ muscles derived from 7-day cardiotoxin-injured mice without grafting (−) or grafted with wild-type SCs or *Col6a1*$^{-/-}$ SCs. Data are shown as mean ± s.e.m. of three independent replicates (**$P<0.01$; n.s., not significant; unequal variance Student's *t*-test; $n=5$ animals, each group). (**d**) Quantification of SCs, calculated as the number of SCs on 100 fibers, in *Col6a1*$^{-/-}$ muscles derived from 7-day cardiotoxin-injured mice without grafting (−) or grafted with 3,000 wild-type SCs or *Col6a1*$^{-/-}$ SCs. Data are shown as mean ± s.e.m. of three independent replicates (**$P<0.01$; * $P<0.05$; n.s., not significant; unequal variance Student's *t*-test; $n=5$–6 animals, each group). (**e**) Left panel, representative images of haematoxylin-eosin staining of TA cross-sections from *Col6a1*$^{-/-}$ mice 7 days after cardiotoxin injury without grafting or grafted with wild-type SCs or *Col6a1*$^{-/-}$ SCs. The asterisks label some areas still in the degeneration phase. Scale bar, 50 µm. Right panel, quantification of myofiber mean cross-sectional area (CSA) in *Col6a1*$^{-/-}$ TA 7 days after cardiotoxin injury without grafting (−) or grafted with wild-type SCs or *Col6a1*$^{-/-}$ SCs. Data are shown as mean ± s.e.m. of three independent replicates (**$P<0.01$; unequal variance Student's *t*-test; $n=5$–6 animals, each group). Ctx, cardiotoxin; KOSC, *Col6a1*$^{-/-}$ SCs expressing GFP-LC3 protein; WTSC, wild-type SCs expressing GFP-LC3.

by endomysial fibroblasts, whereas neither myofibers nor myoblasts produce the protein[4,5]. Here, we found that collagen VI is also expressed by SCs and this expression is differently regulated during quiescence and activation. Our findings suggest that SCs are able to autoregulate the microenvironment of their niche on the basis of their behavior. Indeed, after damage,

© 2013 Macmillan Publishers Limited. All rights reserved.

NATURE COMMUNICATIONS | DOI: 10.1038/ncomms2964 ARTICLE

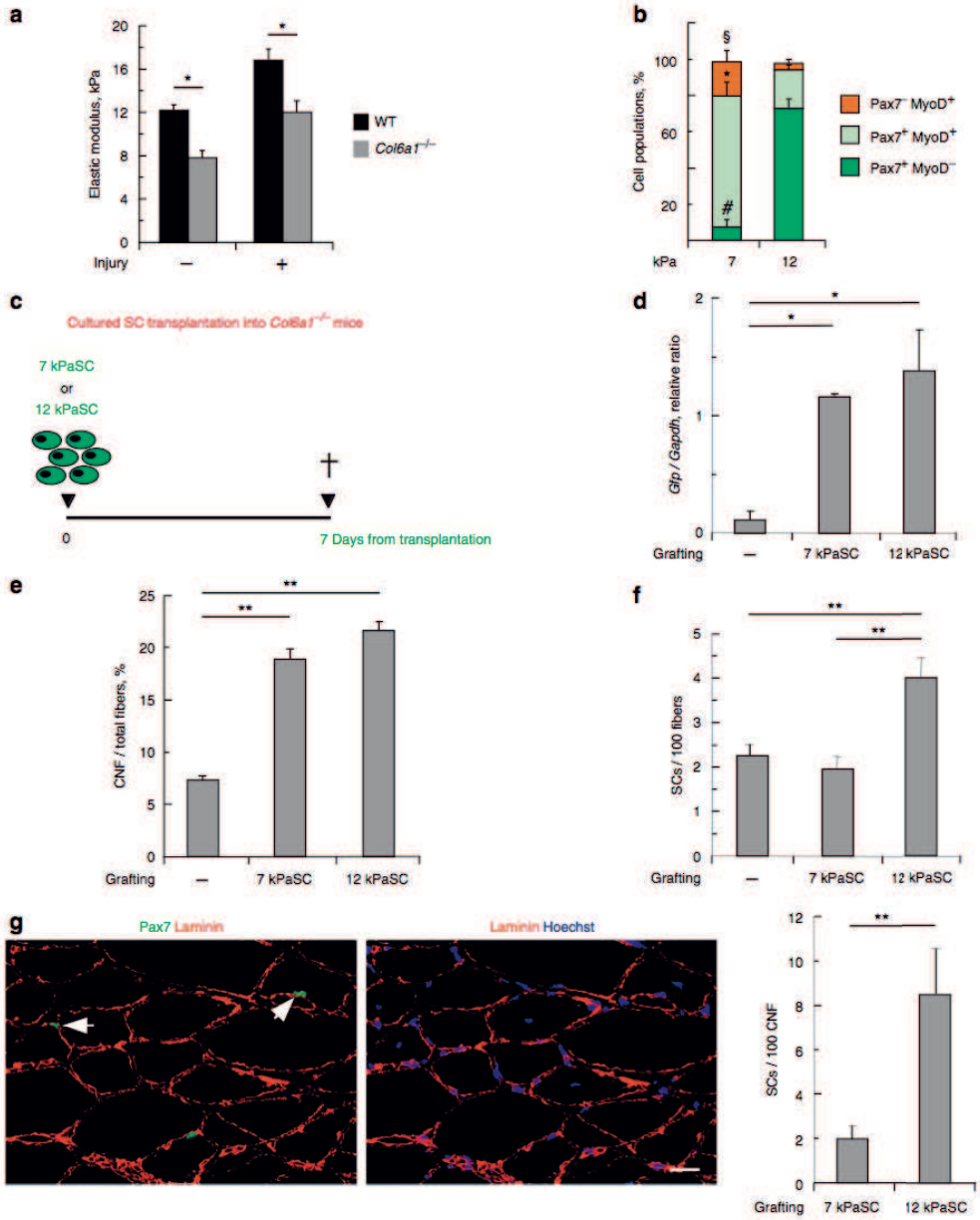


Figure 5 | Collagen VI affects SC self-renewal by regulating muscle stiffness *in vivo*. (**a**) Measurement of elastic modulus of wild-type and *Col6a1*$^{-/-}$ TA muscles under standard conditions (−) and 4 days after injury (+). Data are shown as mean ± s.e.m. of three independent replicates (*$P<0.05$; unequal variance Student's *t*-test; $n=10$ animals, each group). Error bars indicate s.d. (**b**) Quantification of Pax7$^+$MyoD$^-$, Pax7$^+$MyoD$^+$, and Pax7$^-$MyoD$^+$ cell populations in sorted wild-type SCs, following 7 days culture on biomimetic structures. Data are shown as mean ± s.e.m of two independent replicates ($^{\#}P<0.01$ for the Pax7$^+$MyoD$^-$ population; *$P<0.01$ for the Pax7$^+$MyoD$^+$ population; $^{\S}P<0.01$ for the Pax7$^-$MyoD$^+$ population; unequal variance Student's *t*-test; $n=8$ wells, each group). (**c**) Schematic diagram of the experimental approach for grafting cultured SCs grown on 7 kPa or 12 kPa in *Col6a1*$^{-/-}$ TA muscles. (**d**) Real-time PCR analysis of GFP DNA content in *Col6a1*$^{-/-}$ TA under untreated condition (−) or after grafting. Data are shown as mean ± s.e.m of three independent replicates (*$P<0.05$; unequal variance Student's *t*-test; $n=6$ animals, each group). (**e**) Analysis of centrally nucleated fibers (CNF) in *Col6a1*$^{-/-}$ TA under untreated condition (−) or 7 days after grafting. Data are shown as mean ± s.e.m. of three independent replicates (**$P<0.01$; unequal variance Student's *t*-test; $n=6$ animals, each group). (**f**) Quantification of SCs in *Col6a1*$^{-/-}$ TA under untreated condition (−) or 7 days after grafting. Data are shown as mean ± s.e.m. of three independent replicates (**$P<0.01$; unequal variance Student's *t*-test; $n=6$ animals, each group). (**g**) Left panel, representative images of *Col6a1*$^{-/-}$ TA grafted with cultured SCs, showing SCs localized in centrally nucleated fibers (CNFs, arrows). Scale bar, 25 μm. Right panel, quantification of SCs in CNFs of *Col6a1*$^{-/-}$ TA under untreated condition (−) or 7 days after grafting. Data are shown as mean ± s.e.m. of three independent replicates (**$P<0.01$; unequal variance Student's *t*-test; $n=6$ animals, each group) 7 kPaSC, wild-type SCs cultured on 7 kPa; 12 kPaSC, wild-type SCs cultured on 12 kPa; Col VI, collagen VI; MG, matrigel; WT, wild-type.

© 2013 Macmillan Publishers Limited. All rights reserved.

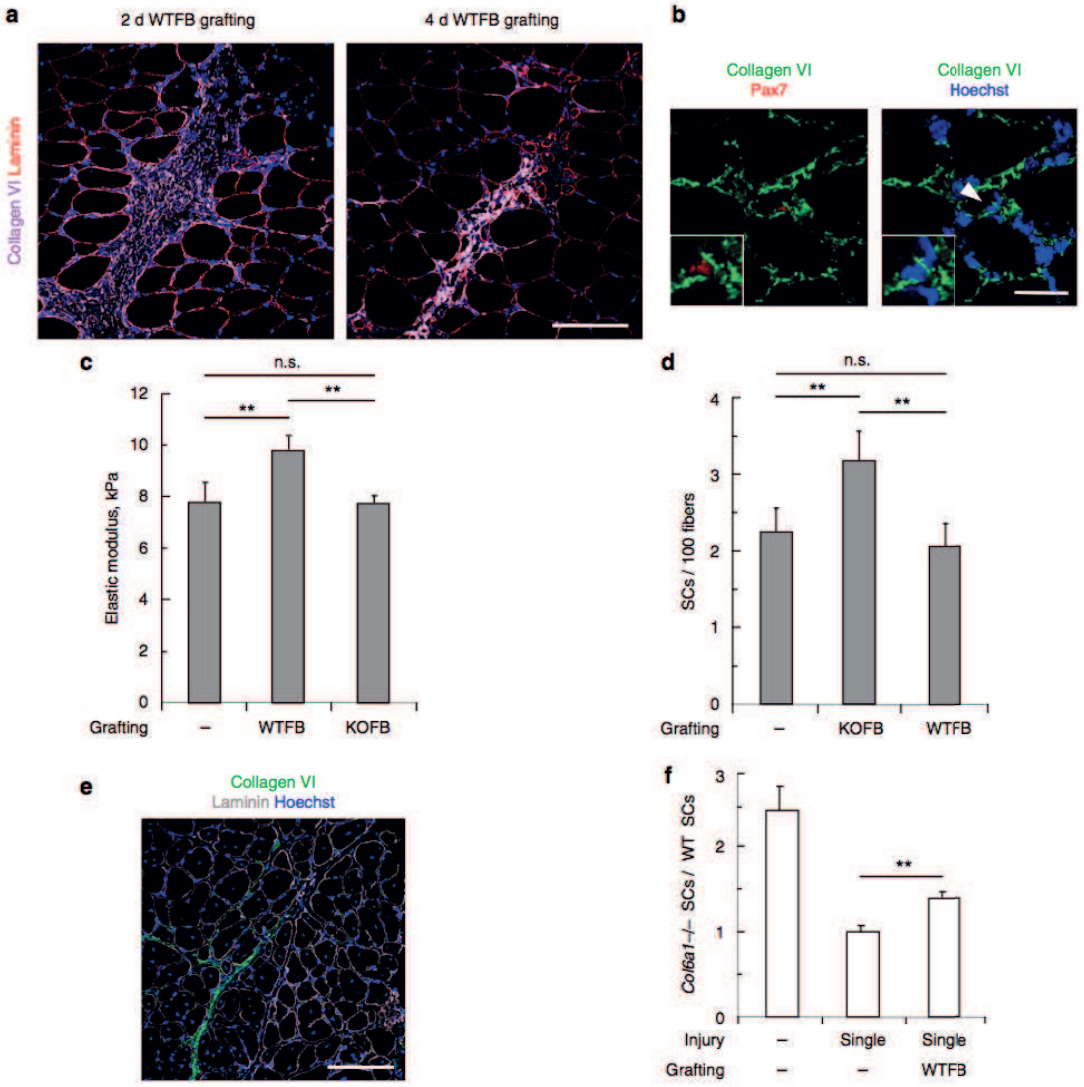


Figure 6 | Wild-type fibroblast grafting rescues SC self-renewal and muscle stiffness in *Col6a1*$^{-/-}$ muscles. (**a**) Representative confocal z-stack image of immunofluorescence analysis of *Col6a1*$^{-/-}$ TA muscles 2 and 4 days after transplantation with wild-type fibroblasts. Sections were labeled with antibodies against collagen VI (light pink) and laminin (red). Scale bar, 100 µm. (**b**) Representative confocal z-stack images of immunofluorescence for collagen VI (green) and Pax7 (red) in *Col6a1*$^{-/-}$ TA sections 4 days after grafting with wild-type fibroblasts. The arrowhead points at one Pax7^{+} cell, shown at higher magnification in the inset. Scale bar, 25 µm. (**c**) Quantification of the elastic modulus of *Col6a1*$^{-/-}$ TA under untreated conditions (–) and 12 days after grafting with wild-type fibroblasts or *Col6a1*$^{-/-}$ fibroblasts. Data are shown as mean ± s.d. of two independent replicates (**$P<0.01$; n.s., not significant; unequal variance Student's *t*-test; $n=10$ animals, each group). (**d**) Quantification of SCs in *Col6a1*$^{-/-}$ TA in untreated conditions (–) and in the graft region 12 days after grafting with wild-type fibroblasts or *Col6a1*$^{-/-}$ fibroblasts. Data are shown as mean ± s.e.m. of three independent replicates (**$P<0.01$; unequal variance Student's *t*-test; n.s., not significant; $n=6$ animals, each group). (**e**) Representative confocal z-stack image of immunofluorescence for collagen VI (green) and laminin (gray) in *Col6a1*$^{-/-}$ TA cross-sections 30 days after injury and grafting with wild-type fibroblasts. Scale bar, 100 µm. (**f**) Ratio of SCs between *Col6a1*$^{-/-}$ and wild-type mice under untreated conditions (–) or 30 days after cardiotoxin injury either in the absence or in the presence of a single grafting with wild-type fibroblasts. Data are shown as mean ± s.e.m. of three independent replicates (**$P<0.01$; unequal variance Student's *t*-test; $n=6$ animals, each group). Nuclei were stained with Hoechst (blue). KOFB, *Col6a1*$^{-/-}$ fibroblasts; WTFB, wild-type fibroblasts.

activated SCs leave their original niche for seeding in a 'new niche' enriched in ECM components, including collagen VI, which are mainly provided by interstitial fibroblasts. In this context, it is plausible that SCs need to change their intrinsic expression of ECM proteins, reducing the synthesis of collagen VI. Interestingly, recent literature studies support this concept by showing that SCs contribute to their own environment through the synthesis of ECM components such as collagens[33,34].

Moreover, it also became evident that the niche not only provides a number of molecular signals for SCs[17–23], but also

© 2013 Macmillan Publishers Limited. All rights reserved.

establishes a three-dimensional support with specific mechanical properties[10]. Healthy skeletal muscle tissue displays a definite elastic modulus ($E \sim 12$ kPa). These biomechanical properties of muscles are altered during disease, aging and injury, as demonstrated by the stiffer elastic modulus ($E > 18$ kPa) of muscles of dystrophin-deficient *mdx* mice and of aged mice, where SC activity is compromised[10]. Our findings indicate that (i) *Col6a1*$^{-/-}$ muscles display a distinct increase of elasticity, and that (ii) this lower stiffness is associated with a significant loss of *in vitro* and *in vivo* self-renewal capability of wild-type SCs, pointing to altered stiffness as one key mechanism underlying *in vivo* SC defects in collagen VI-deficient muscles.

Independent evidence points to collagen VI as an ECM molecule involved in the regulation of the mechanical properties of the cell microenvironment. For instance, the pericellular matrix of articular cartilage of *Col6a1*$^{-/-}$ mice was found to have a significantly reduced stiffness[35], suggesting a more general biomechanical role for collagen VI in different tissues. Moreover, collagen VI null mice were shown to be resistant to genetically induced mammary tumorigenesis[36], a process known to be particularly sensitive to the mechanical properties of the microenvironment[37,38]. Our findings support the concept of a strict relationship between SC homeostasis and regulation of muscle biomechanical properties (Supplementary Fig. 11)[10,25]. Future studies, aimed at dissecting the molecular factors involved in the transduction of the mechanical signals generated by collagen VI microfilaments in muscle endomysium, will allow a more thorough understanding of the pathways through which collagen VI exerts its effects within the SC niche. Moreover, we cannot exclude possible biochemical benefits of collagen VI on SCs that might also contribute to the observed changes. Actually, such biochemical benefits are also suggested by the *in vitro* effects exerted by collagen VI on wild-type SCs. This scenario, together with the results obtained by transplantation experiments with different cells (freshly isolated SCs, cultured SCs and fibroblasts), suggests that collagen VI is not only important in the regulation of muscle mechanical properties, but may also provide biochemical signals to SCs. Although further studies are needed in this direction, it is intriguing to hypothesize that collagen VI could have a dual function: on one hand it is critical for the regulation of the mechanical properties of skeletal muscle, and on the other hand it may interact with some SC receptors, including those that can modulate the physical perception of the microenvironment surrounding the cells.

Our study also provides new perspectives for human collagen VI diseases, as they represent non-cell-autonomous disorders of muscle[2]. The finding that cultured fibroblasts are able to secrete and deposit collagen VI in host *Col6a1*$^{-/-}$ muscle, with beneficial effects on SCs and muscle stiffness, opens novel therapeutic venues for collagen VI-related muscular dystrophies. In various tissues, fibroblasts represent a source for collagen VI, and dermal fibroblasts derived from skin biopsies have been largely used as a diagnostic tool in patients with collagen VI mutations[3]. The possibility that fibroblasts obtained from minimally invasive biopsies may be grown in culture and used for the production and deposition of collagen VI in muscle *in vivo* is an attractive therapeutic option that remains to be explored in the future.

Methods

Mice. We performed experiments in wild-type mice of the inbred C57BL/6J strain and in *Col6a1*$^{-/-}$ mice that we previously backcrossed in the C57BL/6J strain for eight generations[7]. We obtained data in 6-month-old mice by comparing sex-matched wild-type and *Col6a1*$^{-/-}$ animals. We used C57BL/6J, C57BL/6-Tg(ACTB-EGFP)1Osb/J (Jackson Laboratories) and *Col6a1*$^{-/-}$ mice to isolate muscle fibroblasts for grafting experiments. We used *Col6a1*$^{+/+}$;GFP-LC3 and *Col6a1*$^{-/-}$;GFP-LC3 mice (generated in our laboratory by crossing *Col6a1*$^{-/-}$ mice with GFP-LC3 mice[39]) to isolate SCs for transplantation experiments. Mice were housed in individual cages in an environmentally controlled room (23 °C, 12 h light/12 h dark cycle) and provided food and water *ad libitum*. Native collagen VI was purified from newborn mice as previously described[7]. Mouse procedures were approved by the Ethics Committee of the University of Padova and authorized by the Italian Ministry of Health.

***In vivo* treatments.** For cardiotoxin injury[27], we anesthetized mice with isoflurane (Merial) and injected TA muscles with 30 µl cardiotoxin (*Naja mossambica mossambica*, 10 µM; Sigma). Analgesia (Rimadyl) was administered for 3 days. For multiple injury experiments, TA muscles were injected with cardiotoxin 1 month after the previous injection (see also Supplementary Fig. S4C). For cell proliferation analysis, EdU (Invitrogen) was administered for 7 days by i.p. injection at 50 mg per kg body weight every 12 h. We carried out induction of autophagy by i.p. injection with rapamycin (2 mg per kg body weight; LC Laboratories) every 24 hr for 15 days or by feeding mice with LPD (TestDiet) for 1 month[8]. For SC transplantation, we resuspended 3,000 sorted SCs in 15 µl phosphate buffered saline (PBS) and injected them into TA muscle 24 h after cardiotoxin injury. For transplantation of cultured SCs, sorted SCs were grown in culture for 1 week on biomimetic structures, then 10^4 cells were resuspended in 15 µl PBS and injected into undamaged TA muscle. For grafting with muscle fibroblasts, we resuspended 10^5 cells in 15 µl PBS and injected them into each TA muscle. For double-grafting experiments, we used the same primary culture preparation for both injections and performed the second injection 6 days after the first one.

Isolation and culture of single EDL muscle fibers. We carefully dissected EDL muscles from 6-month-old mice and subjected them to enzymatic digestion with collagenase I (2 mg ml^{-1}, Gibco) for 80 min at 37 °C. We blocked the digestion with Dulbecco's Modified Eagle Medium (DMEM, Sigma) supplemented with 0.2 M L-glutamine (Invitrogen), 1:100 penicillin–streptomycin (Invitrogen), 1:100 fungizone (Invitrogen) and 10% horse serum (Gibco), and gently released single myofibers from muscles. With the aim to remove debris and interstitial cells, every 15–25 min, undamaged and non-contracted fibers were transferred in a new dish containing fresh medium for five times. Single selected fibers were maintained at 37 °C in a cell incubator between each wash cycle. Freshly isolated fibers were finally fixed in 4% paraformaldehyde in PBS for 15 min and maintained at 4 °C in PBS until use. For culture experiments, selected fibers were individually grown in adhesion, by placing them into chamber slides coated for at least 2 h with matrigel alone (ECM gel, Sigma) or with matrigel supplemented with purified collagen VI (5 µg cm^{-2}). We cultured fibers for 72 h at 37 °C in cell incubator, using DMEM supplemented with 20% horse serum, 10% fetal bovine serum (Gibco), 1% chicken embryo extract (Sera Laboratories International) and, where indicated, 10 nM EdU (Invitrogen).

Isolation and culture of SCs. We dissected hindlimb muscles from mice and gently dissociated them with a MACS dissociator (Miltenyi Biotec) to yield fragmented muscle suspensions. We digested muscle suspensions for 90 min in 37 °C shaking water bath, using collagenase II (500 U ml^{-1}, Invitrogen) solution in Ham's F10 medium (Sigma) supplemented with 10% horse serum (Invitrogen). We washed the fragmented myofibers and further digested them for 30 min in 37 °C shaking water bath with collagenase II (100 U ml^{-1}, Invitrogen) and dispase (2 U ml^{-1}, Invitrogen). We triturated the digested cell/fragmented fiber suspensions and washed them to yield mononucleated cell suspensions. We filtered the dissociated suspensions through 70- and 30-µm filters and labeled mononucleated cells with VCAM-biotin (1:100, 429), CD31-APC (1:100, MEC 13.3), CD45-APC (1:100, 30-F11) (all BD Bioscience) and Sca-1-Pacific-Blue (1:100, D7, Biolegend). We used streptavidin-PE-cy7 (1:100, BD Biosciences) to amplify the VCAM signal. Where indicated, single-cell preparations were labeled with anti-mouse CD31 FITC (1:100, 11-0311), anti-mouse CD45 FITC (1:100, 11-0451), anti-mouse Sca-1 FITC (1:100, 11-5981) (all eBioscence) and biotin-anti-SM/C-2.6 (1:100, a gift from S. Fukada[40]). We used streptavidin-PerCP-Cy5.5 (1:100, BD Biosciences) to amplify the SM/C-2.6 signal. We carefully optimized cell sorting for purity and viability and subjected SM/C-2.6$^+$CD45$^-$CD31$^-$Sca1$^-$ or VCAM$^+$CD31$^-$CD45$^-$Sca-1$^-$ cells to FACS analysis right after sorting to ensure SC purity. For culture experiments, 10^4 sorted SCs were plated on dishes coated with matrigel alone (ECM gel, Sigma) or with matrigel supplemented with purified collagen VI (5 µg cm^{-2}), or on biomimetic structures coated with matrigel alone (ECM gel, Sigma). We cultured sorted SCs for 48 h or 7 days at 37 °C in cell incubator, using DMEM supplemented with 20% horse serum, 10% fetal bovine serum (Gibco), 1% chicken embryo extract (Sera Laboratories International) and, where indicated, 10 nM EdU (Invitrogen).

Isolation and culture of muscle fibroblasts. We used hindlimb muscles for preparing primary muscle fibroblasts by enzymatic digestion with collagenase II (100 U ml^{-1}, Invitrogen) and dispase (2 U ml^{-1}, Invitrogen) for 30 min at 37 °C. We filtered the dissociated suspensions through 70- and 30-µm filters and plated them for 10 min on gelatin-coated dishes. After removal of floating cells, we maintained the attached cells in culture until confluence. In order to enrich for fibroblasts, we expanded primary cultures for one further passage until confluence, and prepared them for cell type characterization and grafting.

© 2013 Macmillan Publishers Limited. All rights reserved.

***In vivo* muscle stiffness.** We carefully dissected TA muscles from mice and subjected them to stress–strain tests with a Zwick/Roell Z005 device (Zwick, Germany). We anchored muscles to the jaws of the device using a suture thread, and subjected them to two consecutive compressive load–unload cycles with the following settings: 0.01 mm s^{-1}, strain rate; 10% strain, end of loading phase (compared with the initial sample length); no load, end of load–unload cycle. We calculated the elastic modulus from the first linear portion of the stress–strain curve for each cycle.

Biomimetic structures. For the generation of biomimetic structures, we prepared a solution of 3% (*w*/*v*) gelatin (Sigma) in PBS or of 5% (*w*/*v*) gelatin in PBS. Genipin (Challenge Bioproducts Co., Ltd) was added to the solutions at 0.2% (*w*/*w*). Each mixture was kept at 40 °C under moderate stirring, until polymerization was completed as indicated by turning into blue color. Samples were left drying at room temperature for 48 h, rinsed in water to remove genipin residues, sterilized under UV light and then kept in PBS until use at 4 °C. The mechanical properties of genipin-crosslinked biomimetic structures were measured with a Zwick/Roell Z005 device. Samples were subjected to compressive load–unload cycles with the following settings parameters: 0.01 mm s^{-1}, strain rate; 10% strain, end of loading phase; no load, end of load–unload cycle. The Young's modulus of each sample was evaluated from the slope of the initial linear portion of the stress–strain curve. Biomimetic structures composed by 3% gelatin were characterized by an elastic modulus of ~7 kPa, whereas those composed by 5% gelatin displayed an elastic modulus of ~12 kPa. At least three specimens for each composition were tested. Biomimetic structures were maintained in culture medium at 37 °C overnight, before SC plating.

Statistical analyses. We expressed data as means ± s.e.m. or, where indicated, as means ± s.d. We determined statistical significance by unequal variance Student's *t*-test. A P-value < 0.05 was considered statistically significant.

Other methods. Additional information on methods is provided in Supplementary Methods.

References

1. Gillies, A. R. & Lieber, R. L. Structure and function of the skeletal muscle extracellular matrix. *Muscle Nerve* **44,** 318–331 (2011).
2. Bönnemann, C. G. The collagen VI-related myopathies: muscle meets its matrix. *Nat. Rev. Neurol.* **21,** 379–390 (2011).
3. Lampe, A. K. & Bushby, K. M. Collagen VI related muscle disorders. *J. Med. Genet.* **42,** 673–685 (2005).
4. Zou, Y., Zhang, R. Z., Sabatelli, P., Chu, M. L. & Bönnemann, C. G. Muscle interstitial fibroblasts are the main source of collagen VI synthesis in skeletal muscle: implications for congenital muscular dystrophy types Ullrich and Bethlem. *J. Neuropathol. Exp. Neurol.* **67,** 144–154 (2008).
5. Braghetta, P. *et al.* An enhancer required for transcription of the Col6a1 gene in muscle connective tissue is induced by signals released from muscle cells. *Exp. Cell Res.* **314,** 3508–3518 (2008).
6. Bonaldo, P. *et al.* Collagen VI deficiency induces early onset myopathy in the mouse: an animal model for Bethlem myopathy. *Hum. Mol. Genet.* **7,** 2135–2140 (1998).
7. Irwin, W. A. *et al.* Mitochondrial dysfunction and apoptosis in myopathic mice with collagen VI deficiency. *Nat. Genet.* **35,** 367–371 (2003).
8. Grumati, P. *et al.* Autophagy is defective in collagen VI muscular dystrophies, and its reactivation rescues myofiber degeneration. *Nat. Med.* **16,** 1313–1320 (2010).
9. Mauro, A. Satellite cell of skeletal muscle fibers. *J. Biophys. Biochem. Cytol.* **9,** 493–495 (1961).
10. Cosgrove, B. D., Sacco, A., Gilbert, P. M. & Blau, H. M. A home away from home: challenges and opportunities in engineering in vitro muscle satellite cell niches. *Differentiation* **78,** 185–194 (2009).
11. Lepper, C., Partrigde, T. A. & Fan, C. M. An absolute requirement for Pax7-positive satellite cells in acute injury skeletal muscle regeneration. *Development* **138,** 3639–3646 (2011).
12. Sambasivan, R. *et al.* Pax7-expressing satellite cells are indispensable for adult skeletal muscle regeneration. *Development* **138,** 3647–3656 (2011).
13. Zammit, P. S., Partridge, T. A. & Yablonka-Reuveni, Z. The skeletal muscle satellite cell: the stem cell that came in from the cold. *J. Histochem. Cytochem.* **54,** 1177–1191 (2006).
14. Yablonka-Reuveni, Z., Day, K., Vine, A. & Shefer, G. Defining the transcriptional signature of skeletal muscle stem cells. *J. Anim. Sci.* **86,** E207–E216 (2008).
15. Ono, Y. *et al.* BMP signalling permits population expansion by preventing premature myogenic differentiation in muscle satellite cells. *Cell Death Differ.* **18,** 222–234 (2011).
16. Tedesco, F. S., Dellavalle, A., Diaz-Manera, J., Messina, G. & Cossu, G. Repairing skeletal muscle: regenerative potential of skeletal muscle stem cells. *J. Clin. Invest.* **120,** 11–19 (2010).
17. Brack, A. S., Conboy, I. M., Conboy, M. J., Shen, J. & Rando, T. A. A temporal switch from Notch to Wnt signaling in muscle stem cells is necessary for normal adult myogenesis. *Cell Stem Cell* **2,** 50–59 (2008).
18. Cornelison, D. D. *et al.* Essential and separable roles for Syndecan-3 and Syndecan-4 in skeletal muscle development and regeneration. *Genes Dev.* **18,** 2231–2236 (2004).
19. Kuang, S., Gillespie, M. A. & Rudnicki, M. A. Niche regulation of muscle satellite cell self-renewal and differentiation. *Cell Stem Cell* **2,** 22–31 (2008).
20. Le Grand, F., Jones, A. E., Seale, V., Scime, A. & Rudnicki, M. A. Wnt7a activates the planar cell polarity pathway to drive the symmetric expansion of satellite stem cells. *Cell Stem Cell* **4,** 535–547 (2009).
21. Pisconti, A., Cornelison, D. D., Olguín, H. C., Antwine, T. L. & Olwin, B. B. Syndecan-3 and Notch cooperate in regulating adult myogenesis. *J. Cell Biol.* **190,** 427–441 (2010).
22. Shea, K. L. *et al.* Sprouty1 regulates reversible quiescence of a self-renewing adult muscle stem cell pool during regeneration. *Cell Stem Cell* **6,** 117–129 (2010).
23. Conboy, I. M. & Rando, T. A. The regulation of Notch signaling controls satellite cell activation and cell fate determination in postnatal myogenesis. *Dev. Cell* **3,** 397–409 (2002).
24. Calve, S., Odelberg, S. J. & Simon, H. G. A transitional extracellular matrix instructs cell behavior during muscle regeneration. *Dev. Biol.* **344,** 259–271 (2010).
25. Gilbert, P. M. *et al.* Substrate elasticity regulates skeletal muscle stem cell self-renewal in culture. *Science* **329,** 1078–1081 (2010).
26. Guilak, F. *et al.* Control of stem cell fate by physical interactions with the extracellular matrix. *Cell Stem Cell* **5,** 17–26 (2009).
27. Couteaux, R., Mira, J. C. & d'Albis, A. Regeneration of muscles after cardiotoxin injury. I. Cytological aspects. *Biol. Cell* **62,** 171–182 (1988).
28. Zammit, P. S. *et al.* Muscle satellite cells adopt divergent fates: a mechanism for self-renewal? *J. Cell Biol.* **166,** 347–357 (2004).
29. Kuo, H. J., Maslen, C. L., Keene, D. R. & Glanville, R. W. Type VI collagen anchors endothelial basement membranes by interacting with type IV collagen. *J. Biol. Chem.* **272,** 26522–26529 (1997).
30. Engler, A. J., Sen, S., Sweeney, H. L. & Discher, D. E. Matrix elasticity directs stem cell lineage specification. *Cell.* **126,** 677–689 (2006).
31. Andersson, G. *et al.* Engraftment of retroviral EGFP-transduced bone marrow in mice prevents rejection of EGFP-transgenic skin grafts. *Mol. Ther.* **8,** 385–391 (2003).
32. Mann, C. J. *et al.* Aberrant repair and fibrosis development in skeletal muscle. *Skelet. Muscle* **1,** 21 (2011).
33. Bentzinger, C. F. *et al.* Fibronectin regulates wnt7a signaling and satellite cell expansion. *Cell Stem Cell* **12,** 75–87 (2013).
34. Bröhl, D. *et al.* Colonization of the satellite cell niche by skeletal muscle progenitor cells depends on Notch signals. *Dev. Cell* **23,** 469–481 (2012).
35. Alexopoulos, L. G., Youn, I., Bonaldo, P. & Guilak, F. Development of osteoarthritic changes in Col6a1-knocnout mice: biomechanics of type VI collagen in cartilage pericellular matrix. *Arthritis Rheum.* **60,** 771–779 (2009).
36. Iyengar, P. *et al.* Adipocyte-derived collagen VI affects early mammary tumor progression *in vivo*, demonstrating a critical interaction in the tumor/stroma microenvironment. *J. Clin. Invest.* **115,** 1163–1176 (2005).
37. Levental, K. R. *et al.* Matrix crosslinking forces tumor progression by enhancing integrin signaling. *Cell* **139,** 891–906 (2009).
38. Lopez, J. I., Kang, I., You, W. K., McDonald, D. M. & Weaver, V. M. In situ force mapping of mammary gland transformation. *Integr. Biol. (Camb.)* **3,** 910–921 (2011).
39. Mizushima, N., Yamamoto, A., Matsui, M., Yoshimori, T. & Ohsumi, Y. *In vivo* analysis of autophagy in response to nutrient starvation using transgenic mice expressing a fluorescent autophagosome marker. *Mol. Biol. Cell* **15,** 1101–1111 (2004).
40. Fukada, S. *et al.* Purification and cell-surface marker characterization of quiescent satellite cells from murine skeletal muscle by a novel monoclonal antibody. *Exp. Cell Res.* **296,** 245–255 (2004).

Acknowledgements

We thank S. Dupont and M. Montagner for helpful discussion, L. Vitiello and A. Cabrelle for advices and technical help, and S. Piccolo for critical reading of the manuscript. We are grateful to N. Mizushima for the GFP-LC3 mice, S. Fukada for the SM/C-2.6 antibody and R. Wagener for the α3(VI) antibody. This work was financially supported by Telethon-Italy Grants GGP10225 and GGP11082, Italian Ministry of Education, University and Research Grant RBAP11Z3YA_003, and University of Padova Strategic Projects (to P.B.); Glenn Foundation for Medical Research, NIH Grants P01 AG036695, R01 AR56849, DP1 OD000392 (an NIH Director's Pioneer Award), Department of Veterans Affairs (Merit Review) (to T.A.R.).

© 2013 Macmillan Publishers Limited. All rights reserved.

Author contributions

A.U. planned and performed most *in vivo* and *in vitro* experiments and wrote the paper. M.Q. carried out the analysis of collagen VI production by SCs. V.M. performed *in vivo* SC quantification. F.G. generated and characterized biomimetic structures and performed myofiber studies. S.M. performed histological analysis and myofiber studies. P.G. and B.B. performed mouse genotyping and treatments. F.M. and G.V. provided the mechanical analysis. F.S.T. was involved in muscle injury experiments. G.C. provided conceptual advice and was involved in data analysis. T.A.R. oversaw the results and was involved in data analysis. P.B. coordinated the study, oversaw the results and wrote the paper. All authors discussed the results and commented on the manuscript.

Additional information

Supplementary Information accompanies this paper at http://www.nature.com/naturecommunications

Competing financial interests: The authors declare no competing financial interests.

Reprints and permission information is available online at http://npg.nature.com/reprintsandpermissions/

How to cite this article: Urciuolo, A. *et al.* Collagen VI regulates satellite cell self-renewal and muscle regeneration. *Nat. Commun.* 4:1964 doi: 10.1038/ncomms2964 (2013).

© 2013 Macmillan Publishers Limited. All rights reserved.

frontiers in
AGING NEUROSCIENCE

ORIGINAL RESEARCH ARTICLE
published: 15 September 2014
doi: 10.3389/fnagi.2014.00244

Cyclosporin A promotes *in vivo* myogenic response in collagen VI-deficient myopathic mice

Francesca Gattazzo[1,2], Sibilla Molon[1], Valeria Morbidoni[1], Paola Braghetta[1], Bert Blaauw[3], Anna Urciuolo[1]*† and Paolo Bonaldo[1]*

[1] Department of Molecular Medicine, University of Padova, Padova, Italy
[2] Interdepartmental Research Center E. Piaggio, University of Pisa, Pisa, Italy
[3] Department of Biomedical Sciences, University of Padova, Padova, Italy

Edited by:
Emanuele Marzetti, Catholic University of the Sacred Heart, Italy

Reviewed by:
Urs Ruegg, University of Geneva, Switzerland
Antonio Musarò, Sapienza University of Rome, Italy

***Correspondence:**
Anna Urciuolo and Paolo Bonaldo, Department of Molecular Medicine, University of Padova, Via U. Bassi 58/B, Padova I-35131, Italy
e-mail: a.urciuolo@ucl.ac.uk; bonaldo@bio.unipd.it

†Present address:
Anna Urciuolo, Stem Cells and Regenerative Medicine, University College London Institute of Child Health, London, UK

Mutations of genes encoding for collagen VI cause various muscle diseases in humans, including Bethlem myopathy and Ullrich congenital muscular dystrophy. Collagen VI null (*Col6a1*$^{-/-}$) mice are affected by a myopathic phenotype with mitochondrial dysfunction, spontaneous apoptosis of muscle fibers, and defective autophagy. Moreover, *Col6a1*$^{-/-}$ mice display impaired muscle regeneration and defective self-renewal of satellite cells after injury. Treatment with cyclosporin A (CsA) is effective in normalizing the mitochondrial, apoptotic, and autophagic defects of myofibers in *Col6a1*$^{-/-}$ mice. A pilot clinical trial with CsA in Ullrich patients suggested that CsA may increase the number of regenerating myofibers. Here, we report the effects of CsA administration at 5 mg/kg body weight every 12 h in *Col6a1*$^{-/-}$ mice on muscle regeneration under physiological conditions and after cardiotoxin (CdTx)-induced muscle injury. Our findings indicate that CsA influences satellite cell activity and triggers the formation of regenerating fibers in *Col6a1*$^{-/-}$ mice. Data obtained on injured muscles show that under appropriate administration, regimens CsA is able to stimulate myogenesis in *Col6a1*$^{-/-}$ mice by significantly increasing the number of myogenin (MyoG)-positive cells and of regenerating myofibers at the early stages of muscle regeneration. CsA is also able to ameliorate muscle regeneration of *Col6a1*$^{-/-}$ mice subjected to multiple CdTx injuries, with a concurrent maintenance of the satellite cell pool. Our data show that CsA is beneficial for muscle regeneration in *Col6a1*$^{-/-}$ mice.

Keywords: collagen VI, skeletal muscle, congenital muscular dystrophy, animal model, cyclosporin A, muscle regeneration

INTRODUCTION

Collagen VI is an extracellular matrix protein that forms a microfibrillar network in the endomysium of skeletal muscle. The critical role played by this protein in muscle is clearly shown by collagen VI null (*Col6a1*$^{-/-}$) mice, which display an early onset myopathic phenotype characterized by mitochondrial dysfunction, defective autophagy, and spontaneous apoptosis of muscle fibers (Bonaldo et al., 1998; Irwin et al., 2003; Grumati et al., 2010). Cyclosporin A (CsA) is a well-known immunosuppressant drug that was found to have multiple beneficial effects on the myopathic phenotype of *Col6a1*$^{-/-}$ mice, including (i) decreased opening of the mitochondrial permeability transition pore; (ii) rescue of myofiber apoptosis; (iii) stimulation of autophagy in muscle fibers; and (iv) recovery of muscle strength (Irwin et al., 2003; Grumati et al., 2010). Mutations of *COL6* genes in humans cause several muscle disorders, including Bethlem myopathy and Ullrich congenital muscular dystrophy (Lampe and Bushby, 2005). A pilot clinical trial in Ullrich and Bethlem patients showed that CsA favorably affects mitochondrial function and dramatically decreases the incidence of apoptosis in muscle fibers. Notably, a significant increase in the number of regenerating myofibers was observed in younger patients undergoing CsA treatment, suggesting that CsA may also increase the overall efficiency of muscle regeneration in patients (Merlini et al., 2008, 2011).

Muscle regeneration relies on the presence of satellite cells, which are quiescent under physiological conditions but become activated upon damage, thus undergoing proliferation and terminal differentiation. At the same time, a subset of activated satellite cells returns to the quiescent state in their original niche under the basal lamina, through a self-renewal process (Tedesco et al., 2010). The differentiation of satellite cells is regulated by a number of transcription factors, where Pax7 is required for satellite cell specification and survival, whereas MyoD, myogenin (MyoG), and MRF4 are essential for satellite cell proliferation and differentiation (Buckingham and Rigby, 2014). Terminal differentiation coincides with the abundant synthesis of myosin heavy chain (MHC). The cardiotoxin (CdTx) injury model is widely used to investigate skeletal muscle regeneration (Chargé and Rudnicki, 2004; Shi and Garry, 2006). We recently demonstrated that collagen VI is a critical component of satellite cell *niche* and that ablation of collagen VI leads to impaired muscle regeneration and reduced satellite cell self-renewal after injury (Urciuolo et al., 2013). Studies performed in tibialis anterior (TA) muscle showed that *Col6a1*$^{-/-}$ mice undergo a marked depletion of the satellite cell pool 7 days after CdTx injection, and this defect

becomes much more dramatic after multiple rounds of CdTx injury (Urciuolo et al., 2013). Given the effects displayed by CsA in collagen VI-deficient mice and Ullrich/Bethlem patients (Irwin et al., 2003; Merlini et al., 2008), here we analyzed in detail the outcomes of CsA administration on muscle regeneration and satellite cells in *Col6a1*$^{-/-}$ mice under physiological conditions and after CdTx-induced injury.

MATERIALS AND METHODS

MICE

We performed experiments in wild-type mice of the inbred C57BL/6NCrl strain and in *Col6a1*$^{-/-}$ mice that were backcrossed in the C57BL/6NCrl strain for eight generations (Irwin et al., 2003). All data were obtained from 6-month-old mice. Mice were housed in individual cages in an environmentally controlled room (23°C, 12 h light/12 h dark cycle) and provided food and water *ad libitum*. Mouse procedures were approved by the Ethics Committee of the University of Padova and authorized by the Italian Ministry of Health.

IN VIVO TREATMENTS

Cyclosporin A (Sandimmun 50 mg/ml, Novartis) was dissolved in olive oil and a stock solution at a concentration of 10 mg/ml was prepared. For CsA administration under physiological conditions, mice were subjected to intraperitoneal (i.p.) injection of vehicle (olive oil) or CsA at 5 mg/kg body weight every 12 h for 10 days. In experiments with higher dosage CsA, mice were subjected to i.p. injection of vehicle or CsA at 25 mg/kg body weight every 24 h for 10 days. Animals were sacrificed 12 h after the last administration of CsA or vehicle. For single CdTx injury (Couteaux et al., 1988), mice were treated by i.p. injection with vehicle or CsA at 5 mg/kg body weight every 12 h for 10 days. At day 4 from the first administration of vehicle or CsA, mice were anesthetized with isoflurane (Merial) and TA muscles injected with 30 μl CdTx (Naja mossambica mossambica, 10 μM; Sigma). Analgesia (Rimadyl) was administered subcutaneously for 3 days and mice were sacrificed 7 days after muscle damage (i.e., 10 days after the first injection of vehicle or CsA). For multiple injury experiments, TA muscles were subjected to three distinct injections of CdTx, each one every 30 days. Four days before the third CdTx injection, mice were treated by i.p. injection with vehicle or CsA at 5 mg/kg body weight every 12 h for 10 days. Mice were sacrificed 30 days after the third CdTx injury (i.e., 24 days after the last injection of vehicle or CsA).

HISTOLOGICAL ANALYSIS

Tibialis anterior muscles were isolated from mice, frozen in liquid nitrogen, weighted on a precision balance, and kept at −80°C until use. Cross-sections (10 μm thick) were used and processed for hematoxylin–eosin or Azan-Mallory staining following standard protocols. Samples were analyzed with a Zeiss Axioplan light microscope equipped with Leica DC500 digital camera. Myofiber cross-sectional area and the area of fibrosis were evaluated with the IM1000 software (Leica).

ISOLATION OF EXTENSOR DIGITORUM LONGUS SINGLE MYOFIBERS

We carefully dissected extensor digitorum longus (EDL) muscles from 6-month-old mice and subjected them to enzymatic digestion with collagenase I (2 mg/ml, Gibco) for 80 min at 37°C. We blocked the digestion with Dulbecco's Modified Eagle Medium (DMEM, Sigma), supplemented with 0.2 M L-glutamine (Invitrogen), 1:100 penicillin-streptomycin (Invitrogen), 1:100 fungizone (Invitrogen), and 10% horse serum (Gibco), and gently released single myofibers from muscles. Every 15–25 min, undamaged and non-contracted fibers were transferred in a new dish containing fresh medium, and this procedure was repeated five times in order to remove debris and interstitial cells. Freshly isolated fibers were finally fixed in 4% paraformaldehyde in PBS for 15 min and maintained at 4°C in PBS until use.

IMMUNOFLUORESCENCE

For immunofluorescence on muscle sections, frozen TA sections (7 μm) were fixed for 20 min with 4% paraformaldehyde in PBS and permeabilized for 6 min with cold methanol. For the unmasking of Pax7 and MyoG, slides were treated twice with 0.01 M citric acid (pH 6) at 90°C for 5 min. For mouse antibodies staining, samples were first incubated for 2.5 h with 4% bovine serum albumin (BSA IgG-Free, Jackson Immunoresearch) in PBS and then treated for 30 min with a blocking solution containing 0.05 mg/ml Fab fragment anti-mouse IgG (Jackson Immunoresearch). When mouse antibodies were not used, samples were only incubated for 1 h at room temperature with 4% bovine serum albumin in PBS. After the blocking step, samples were incubated with primary antibodies at 4°C overnight. The following primary antibodies were used: mouse anti-Pax7 (1:20; Developmental Studies Hybridoma Bank); mouse anti-MyoG (F5D, 1:15; Developmental Studies Hybridoma Bank); mouse anti-embryonic MHC (eMHC) (F1.652, 1:20; Developmental Studies Hybridoma Bank); rabbit anti-laminin (L9393, 1:800; Sigma). After washing, samples were incubated with the appropriate secondary antibody for 1 h at room temperature. Secondary antibodies used were biotinylated anti-mouse (115-007-003, 1:1000), Cy2 or Cy3 anti-mouse (115-226-062, 1:500, or 115-165-006, 1:1000), Cy2 or Cy3 anti-rabbit (111-225-144, 1:500, or 115-165-006, 1:1000) (all Jackson Immunoresearch). To reveal the biotinylated antibody, Cy2 or Cy3 streptavidin (016-220-084, 1:1500, or 016-160-084, 1:2500; Jackson Immunoresearch) was used. For immunofluorescence of EDL single myofibers, cells were permeabilized with 0.5% Triton X-100 in PBS, treated with 20% goat serum (Invitrogen) in PBS for 1 h, and incubated at 37°C for 1 h or at 4°C overnight with mouse anti-Pax7 antibody (1:20; Developmental Studies Hybridoma Bank). After washing, samples were incubated with the appropriate secondary antibody as described above. Nuclei were stained with Hoechst 33258 (Sigma). Samples were analyzed with a Zeiss Axioplan Leica DC500 epifluorescence microscope or with a Leica SP5 confocal microscope.

TUNEL

For apoptosis analysis on TA cryosections, the DeadEnd™ Fluorometric TUNEL assay (Promega) was used. Samples were fixed for 15 min with 4% paraformaldehyde, permeabilized for 5 min with 0.5% Triton X-100, and processed following manufacturer instructions.

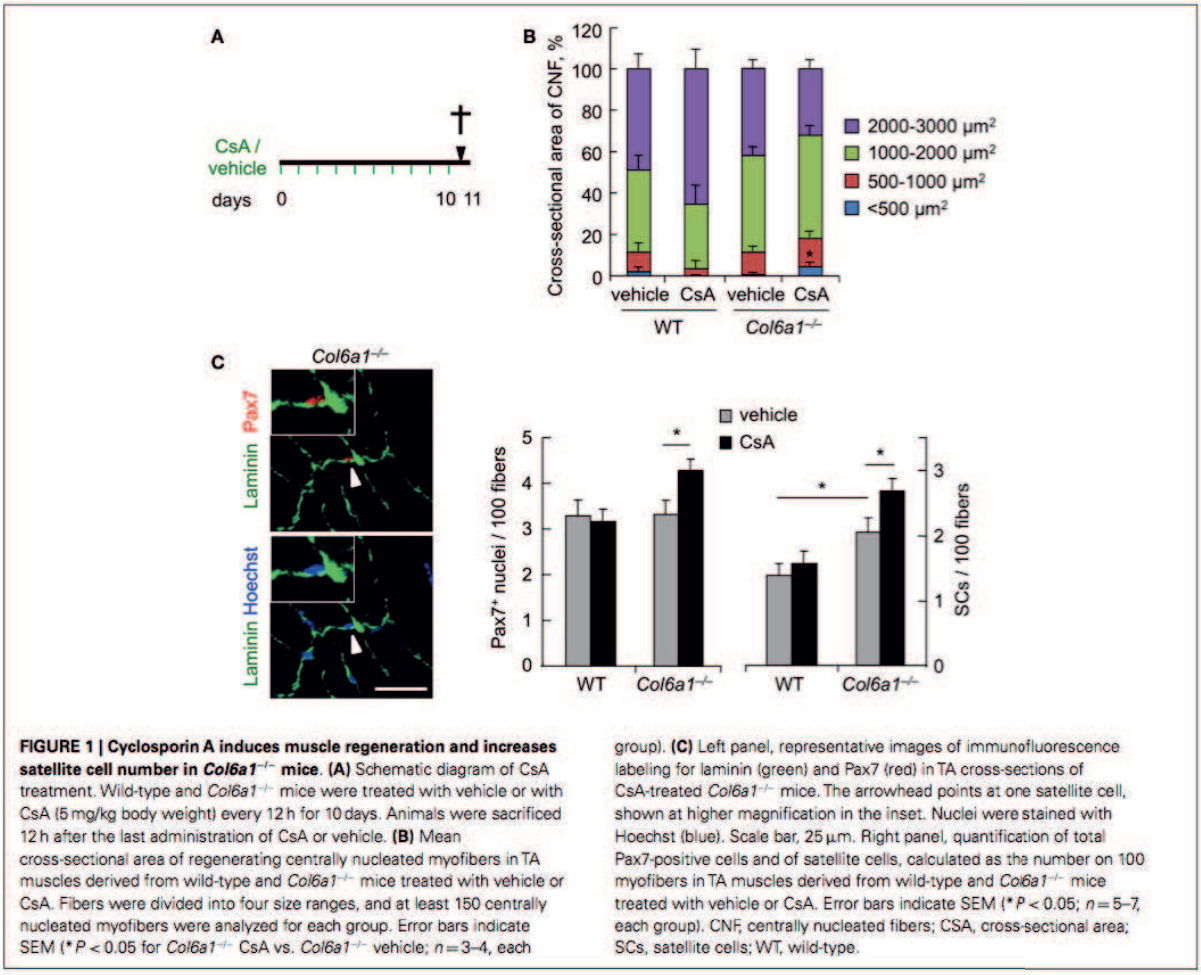


FIGURE 1 | Cyclosporin A induces muscle regeneration and increases satellite cell number in *Col6a1*$^{-/-}$ mice. **(A)** Schematic diagram of CsA treatment. Wild-type and *Col6a1*$^{-/-}$ mice were treated with vehicle or with CsA (5 mg/kg body weight) every 12 h for 10 days. Animals were sacrificed 12 h after the last administration of CsA or vehicle. **(B)** Mean cross-sectional area of regenerating centrally nucleated myofibers in TA muscles derived from wild-type and *Col6a1*$^{-/-}$ mice treated with vehicle or CsA. Fibers were divided into four size ranges, and at least 150 centrally nucleated myofibers were analyzed for each group. Error bars indicate SEM (* $P < 0.05$ for *Col6a1*$^{-/-}$ CsA vs. *Col6a1*$^{-/-}$ vehicle; $n = 3$–4, each group). **(C)** Left panel, representative images of immunofluorescence labeling for laminin (green) and Pax7 (red) in TA cross-sections of CsA-treated *Col6a1*$^{-/-}$ mice. The arrowhead points at one satellite cell, shown at higher magnification in the inset. Nuclei were stained with Hoechst (blue). Scale bar, 25 µm. Right panel, quantification of total Pax7-positive cells and of satellite cells, calculated as the number on 100 myofibers in TA muscles derived from wild-type and *Col6a1*$^{-/-}$ mice treated with vehicle or CsA. Error bars indicate SEM (* $P < 0.05$; $n = 5$–7, each group). CNF, centrally nucleated fibers; CSA, cross-sectional area; SCs, satellite cells; WT, wild-type.

STATISTICAL ANALYSES

Data are expressed as means ± SEM. We determined statistical significance by unequal variance Student's *t*-test, and a *P* value of <0.05 was considered statistically significant.

RESULTS

CsA INDUCES MUSCLE REGENERATION IN *Col6a1*$^{-/-}$ MICE UNDER PHYSIOLOGICAL CONDITIONS

To investigate the effects of CsA administration in *Col6a1*$^{-/-}$ mice under physiological conditions, we subjected animals to i.p. injection of vehicle or CsA at 5 mg/kg body weight every 12 h and analyzed muscles after 10 days of treatment (**Figure 1A**). This dosage of CsA was previously found to trigger a marked amelioration of the myopathic phenotype of *Col6a1*$^{-/-}$ mice, with rescue from mitochondrial depolarization and apoptosis and reactivation of the autophagic flux in muscle fibers (Irwin et al., 2003; Grumati et al., 2010). To evaluate whether this CsA treatment triggered *de novo* formation of myofibers in *Col6a1*$^{-/-}$ mice, we first analyzed the cross-sectional area of regenerating, centrally nucleated fibers in TA muscle, by dividing regenerating myofibers into four different size ranges. Unlike wild-type animals, CsA treatment led to a significant increase of the percentage of regenerating myofibers with small area (<500 µm^2) in *Col6a1*$^{-/-}$ mice when compared to vehicle-treated *Col6a1*$^{-/-}$ animals (**Figure 1B**). These data were also confirmed by immunofluorescence analysis for eMHC, an established marker of newly forming fibers (Ciciliot and Schiaffino, 2010). Immature myofibers expressing eMHC were present in TA muscles of *Col6a1*$^{-/-}$ mice treated with CsA, but not in those treated with vehicle (Figure S1A in Supplementary Material). Based on these results, we evaluated the number of myogenic cells by performing immunostaining for Pax7. CsA administration increased the total number of Pax7-positive cells and also the number of satellite cells (i.e., Pax7-positive cells located underneath the basal lamina) in *Col6a1*$^{-/-}$ TA but not in wild-type TA (**Figure 1C**). These data were confirmed by analyzing freshly isolated EDL myofibers, which showed a significant increase in the number of Pax7-positive cells on myofibers derived from CsA-treated *Col6a1*$^{-/-}$ mice when compared to vehicle-treated animals (Figure S1B in Supplementary Material). To assess whether the increased number of Pax7-positive cells in *Col6a1*$^{-/-}$ animals was

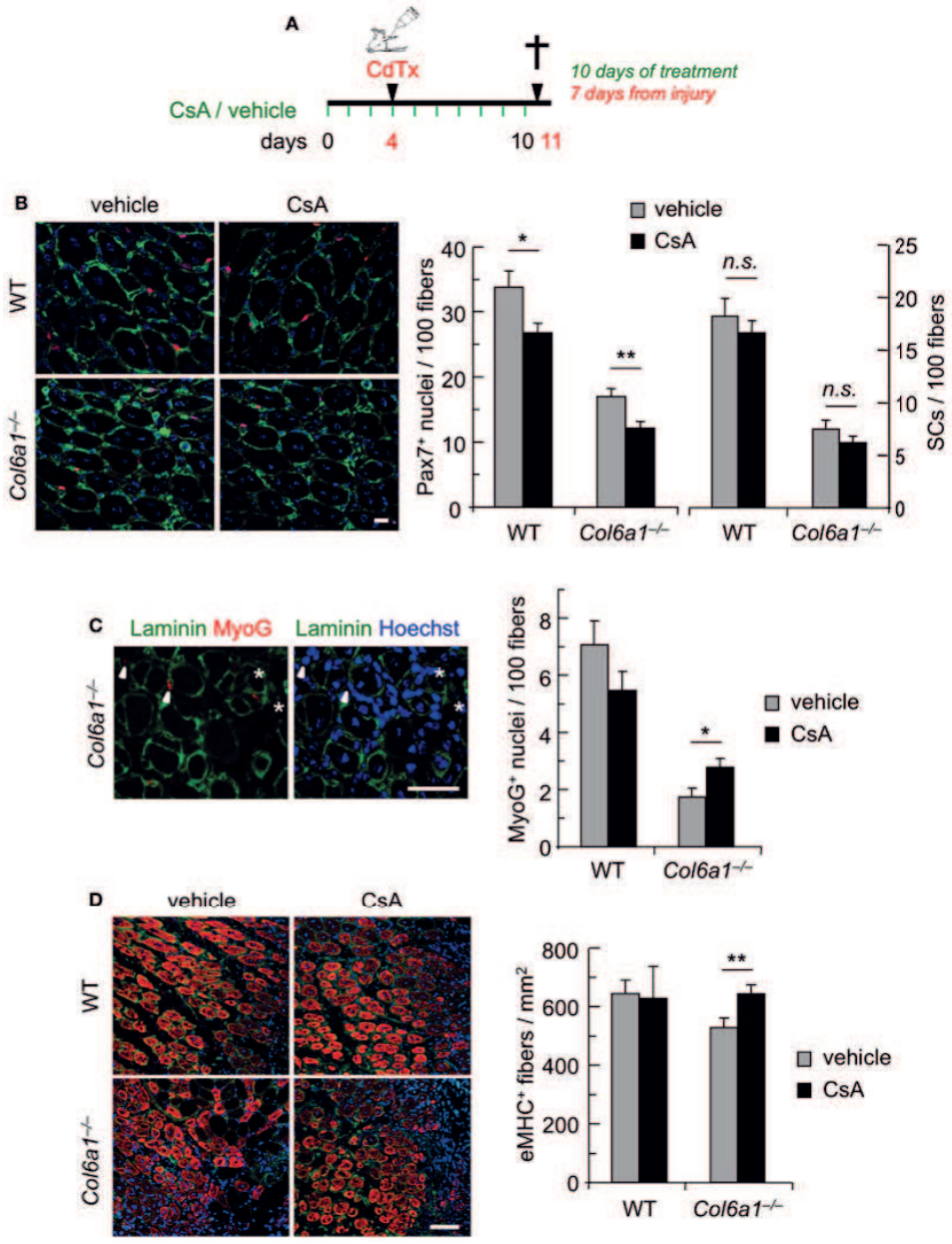


FIGURE 2 | Continuous administration of CsA during a single CdTx injury stimulates muscle differentiation in *Col6a1*$^{-/-}$ mice. **(A)** Schematic diagram of CsA treatment and CdTx injury. Wild-type and *Col6a1*$^{-/-}$ mice were treated with vehicle or CsA (5 mg/kg body weight) every 12 h for 10 days. Four days after the first injection of vehicle or CsA, TA muscles were injured with CdTx and drug treatment continued for other 7 days. Animals were sacrificed 12 h from the last administration of CsA or vehicle. **(B)** Left panels, representative images of immunofluorescence labeling for laminin (green) and Pax7 (red) in 7-day-post-injury TA cross-sections of wild-type and *Col6a1*$^{-/-}$ mice treated with vehicle or CsA. Scale bar, 25 μm. Right panel, quantification of total Pax7-positive cells and of satellite cells, calculated as the number on 100 myofibers in 7-day-post-injury TA muscles of wild-type and *Col6a1*$^{-/-}$ mice treated with vehicle or CsA. Error bars indicate SEM (**$P < 0.01$; *$P < 0.05$; n.s. not significant; $n = 3$–5, each group). **(C)** Left panels, representative images of immunofluorescence labeling for laminin (green) and MyoG (red) in 7-day-post-injury TA cross-sections of *Col6a1*$^{-/-}$ mice treated with vehicle or CsA. Nuclei were stained with Hoechst (blue). The arrowheads point at MyoG-positive cells outside the basal lamina, and the asterisks mark MyoG-positive cells located underneath the basal lamina (corresponding to myogenic cells that are undergoing fusion).

(Continued)

FIGURE 2 | Continued
Scale bar, 50 μm. Right panel, quantification of total MyoG-positive cells, calculated as the number on 100 myofibers in 7-day-post-injury TA muscles of wild-type and *Col6a1*$^{-/-}$ mice treated with vehicle or CsA. Error bars indicate SEM (*$P < 0.05$; $n = 3$–5, each group). **(D)** Left panels, representative images of immunofluorescence for laminin (green) and eMHC (red) in 7-day-post-injury TA cross-sections of wild-type and *Col6a1*$^{-/-}$ mice treated with vehicle or CsA. Nuclei were stained with Hoechst (blue). Scale bar, 50 μm. Right panel, quantification of the number of eMHC-positive myofibers per regenerating area in 7-day-post-injury TA cross-sections of wild-type and *Col6a1*$^{-/-}$ mice treated with vehicle or CsA. Error bars indicate SEM (**$P < 0.01$; $n = 3$–5, each group). SCs, satellite cells; WT, wild-type.

only provided by this drug dosage or could be also elicited by higher CsA concentrations known to cause strong immunosuppressive effects (Homan et al., 1980), we subjected mice to i.p. injection of CsA at 25 mg/kg body weight every 24 h for 10 days. Interestingly, at this higher dosage, CsA led to a dramatic decrease in the number of total Pax7-positive cells and of satellite cells both in wild-type and in *Col6a1*$^{-/-}$ mice when compared to vehicle-treated animals (Figure S1C in Supplementary Material). These results highlight the relevance of CsA dosage in inducing beneficial effects in *Col6a1*$^{-/-}$ muscles and accordingly with previous studies carried out with the immunosuppressive drug FK506 (Irwin et al., 2003), they suggest that immunosuppression exacerbates the phenotype of *Col6a1*$^{-/-}$ mice.

CONTINUOUS ADMINISTRATION OF CsA DURING CdTx INJURY STIMULATES THE EARLY PHASES OF MUSCLE DIFFERENTIATION IN *Col6a1*$^{-/-}$ MICE

To further assess the capability of CsA to ameliorate the muscle regenerative defects of *Col6a1*$^{-/-}$ mice, we carried out CsA treatment under experimentally induced muscle injury. Toward this aim, wild-type and *Col6a1*$^{-/-}$ mice were treated for 10 days with vehicle or CsA at 5 mg/kg body weight every 12 h; 4 days after the start of treatment, TA muscles were subjected to CdTx damage and mice were sacrificed 7 days after injury (**Figure 2A**). TUNEL assay showed that the incidence of apoptotic nuclei 7 days after CdTx injection was very low in wild-type TA, in agreement with the concept that myofiber demise is almost completed at this stage from injury (Hawke et al., 2003). Conversely, *Col6a1*$^{-/-}$ TA showed a higher number of TUNEL-positive myonuclei 7 days after injury, and CsA administration was able to significantly decrease the incidence of apoptotic myofibers triggered by CdTx injury in *Col6a1*$^{-/-}$ TA muscles (Figure S2 in Supplementary Material). We next evaluated the number of myogenic cells by immunofluorescence for the Pax7 and MyoG markers. CsA administration led to a significant decrease in the number of total Pax7-positive cells in both wild-type and *Col6a1*$^{-/-}$ injured TA, without any significant change in the number of satellite cells (i.e., Pax7-positive cells located underneath basal lamina) (**Figure 2B**). This response was paralleled by a significant increase of the total number of MyoG-positive cells in injured TA muscles of CsA-treated *Col6a1*$^{-/-}$ mice when compared to vehicle-treated *Col6a1*$^{-/-}$ mice, whereas wild-type injured TA muscles did not show any significant difference in MyoG positivity between vehicle and CsA-treated animals (**Figure 2C**). Additionally, *Col6a1*$^{-/-}$ mice treated with CsA showed an increased number of regenerating myofibers expressing eMHC, whereas no differences in eMHC-positive regenerating myofibers were found in wild-type animals (**Figure 2D**). As the defective satellite self-renewal of *Col6a1*$^{-/-}$ mice is strictly dependent on the lack of extracellular collagen VI and on the lower muscle stiffness (Urciuolo et al., 2013), it was not surprising to observe that in this experimental condition CsA does not display any overt effect on satellite cell maintenance. On the other hand, the remarkable increase in the number of differentiated (i.e., MyoG-positive) myogenic cells, together with the higher number of newly forming (i.e., eMHC-positive) myofibers, indicates that CsA administration is able to improve muscle differentiation upon damage in the *Col6a1*$^{-/-}$ myopathic mouse model.

ADMINISTRATION OF CsA DURING REPEATED MUSCLE INJURY COUNTERACTS MUSCLE LOSS AND FIBROSIS AND PRESERVES THE SATELLITE CELL POOL IN *Col6a1*$^{-/-}$ MICE

Although muscles of *Col6a1*$^{-/-}$ animals display a delayed regeneration after injury, we have previously shown that at 30 days after CdTx injury they are still able to complete the regeneration process (Urciuolo et al., 2013). However, and at difference from wild-type mice, the capability of *Col6a1*$^{-/-}$ animals to undergo muscle regeneration and preserve the satellite cell pool is lost after multiple muscle injuries, leading to a severe loss of muscle mass (Urciuolo et al., 2013). Therefore, we investigated whether CsA is able to counteract the defective muscle regeneration and the depletion of the satellite cell pool triggered by multiple injuries in *Col6a1*$^{-/-}$ mice. Toward this aim, we subjected TA muscles of wild-type and *Col6a1*$^{-/-}$ mice to three rounds of CdTx injury. Animals were treated for 10 days with vehicle or CsA at 5 mg/kg body weight every 12 h during the third injury and sacrificed 30 days after the last injury (**Figure 3A**). Interestingly, CsA administration was highly effective in reducing the extensive muscle fibrosis triggered by triple injury in *Col6a1*$^{-/-}$ mice (**Figure 3B**). The beneficial effects of CsA in *Col6a1*$^{-/-}$ muscles undergoing multiple injuries were also confirmed by the increased myofiber cross-sectional area and by the improvement of the muscle mass in CsA-treated *Col6a1*$^{-/-}$ mice when compared to vehicle-treated *Col6a1*$^{-/-}$ mice (Figure S3 in Supplementary Material). Notably, CsA administration led to marked increase of both total Pax7-positive cell number and satellite cell number in *Col6a1*$^{-/-}$ TA muscles subjected to multiple injuries (**Figures 3C,D**). Altogether, these results show that at this regimen CsA is capable to preserve not only muscle fibers but also the satellite cell pool of collagen VI-deficient mice.

DISCUSSION

In the present study, we evaluated the potential beneficial effects exerted by CsA on skeletal muscle regeneration in *Col6a1*$^{-/-}$ mice, both under physiological condition and after muscle damage. The rationale for this study was based on previous findings in patients affected by collagen VI myopathies, suggesting that besides counteracting myofiber apoptosis and mitochondrial dysfunction, CsA treatment may also increase muscle regeneration (Merlini et al., 2008, 2011). In addition, our recent findings

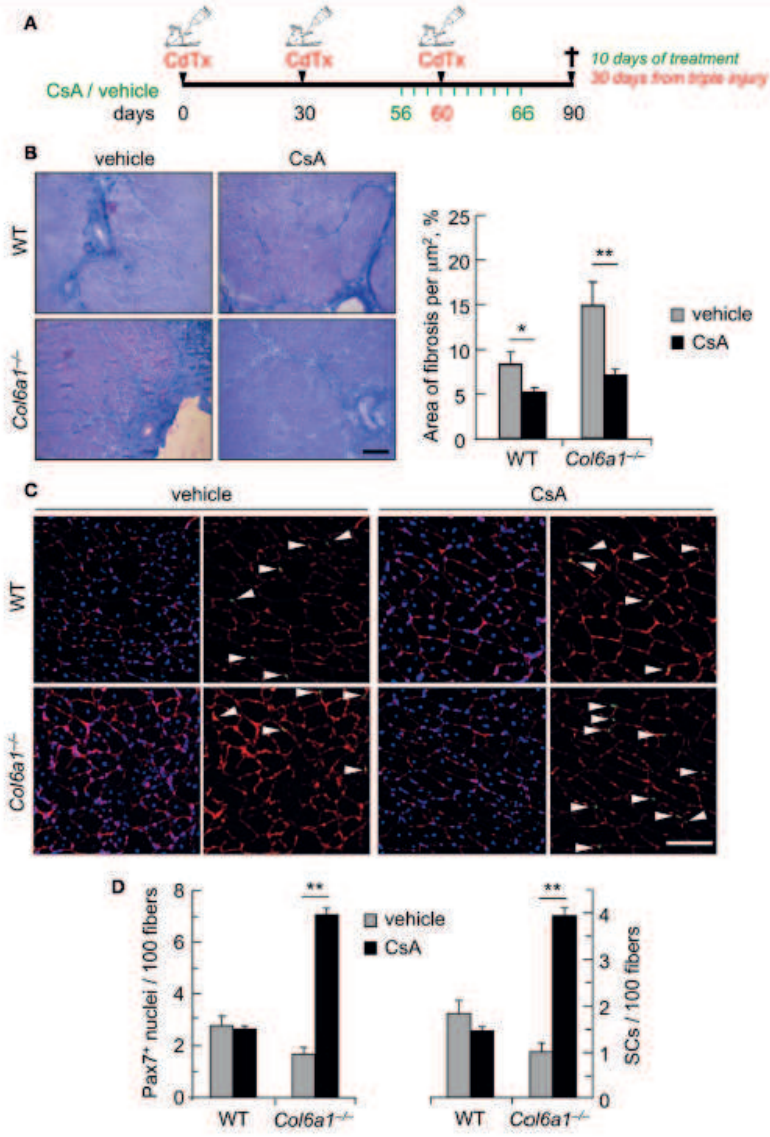


FIGURE 3 | Administration of CsA during a triple muscle injury counteracts muscle loss and fibrosis and preserves the satellite cell pool in *Col6a1*$^{-/-}$ mice. **(A)** Schematic diagram of CsA treatment and CdTx injuries. TA muscles of wild-type and *Col6a1*$^{-/-}$ mice were given three repeated injections of CdTx every 30 days. Four days before the last injury, *Col6a1*$^{-/-}$ mice were treated with vehicle or CsA (5 mg/kg body weight) every 12 h for 10 days. Mice were sacrificed 30 days after the third injury (i.e., 24 days from the last administration of vehicle or CsA). **(B)** Left panels, Azan-Mallory staining of triple injured TA cross-sections from wild-type and *Col6a1*$^{-/-}$ mice treated with vehicle or CsA. Scale bar, 50 µm. Right panel, quantification of the fibrotic area in triple-injured TA cross-sections from wild-type and *Col6a1*$^{-/-}$ mice treated with vehicle or CsA. Error bars indicate SEM (**$P < 0.01$; *$P < 0.05$; $n = 4$–8, each group). **(C)** Representative images of immunofluorescence labeling for laminin (red) and Pax7 (green) in triple-injured TA cross-sections from wild-type and *Col6a1*$^{-/-}$ treated with vehicle or CsA. Arrows point at Pax7-positive nuclei. Nuclei were stained with Hoechst (blue). Scale bar, 100 µm. **(D)** Quantification of total Pax7-positive cells and of satellite cells, calculated as the number on 100 myofibers in triple-injured TA cross-sections from wild-type and *Col6a1*$^{-/-}$ mice treated with vehicle or CsA. Error bars indicate SEM (**$P < 0.01$; $n = 4$–8, each group). SC, satellite cells; WT, wild-type.

showed impaired regeneration and defective satellite cell self-renewal in collagen VI-deficient muscles (Urciuolo et al., 2013). Therefore, we investigated how CsA treatment impacts on the regeneration of collagen VI-deficient mice. Under physiological conditions, CsA was capable to amplify the pool of total Pax7-positive cells and of satellite cells and increased the amount of

newly formed centrally nucleated myofibers, thus suggesting a new role for CsA in stimulating myogenesis in *Col6a1*$^{-/-}$ muscles. Notably, these beneficial effects were dose-dependent, as they were observed at 10 mg/kg/day but not at a higher immunosuppressant dose (25 mg/kg/day), which conversely had a negative impact on the satellite cell pool. These data are in agreement with previous results in which the same protocol of CsA administration was found to desensitize the mitochondrial permeability transition pore and reduce myofiber apoptosis in *Col6a1*$^{-/-}$ mice (Irwin et al., 2003). Although we previously demonstrated that CsA stimulates autophagy in skeletal myofibers (Grumati et al., 2010), the increased number of satellite cells in muscles of CsA-treated *Col6a1*$^{-/-}$ animals is not a direct consequence of a stimulatory effect on autophagy. Indeed, reactivation of the autophagic flux in *Col6a1*$^{-/-}$ mice by different pharmacological or dietary treatments does not exert any significant effect on satellite cells (Urciuolo et al., 2013). Our present findings are consistent with the strong amelioration of the myophatic phenotype in *Col6a1*$^{-/-}$ mice following CsA administration and indicate that besides decreasing mitochondrial dysfunction and apoptosis and reactivating autophagy in muscle fibers (Irwin et al., 2003; Grumati et al., 2010), the drug is also able to increase the pool of functional Pax7-positive cells and stimulate the formation of newly formed fibers.

The beneficial effects exerted by CsA on the regeneration capabilities of *Col6a1*$^{-/-}$ mice become very evident under experimentally induced single and multiple muscle injuries. Our data indicate that CsA is capable to induce myogenesis in *Col6a1*$^{-/-}$ mice after muscle damage. In fact, when TA muscles were damaged during a continuous CsA administration, analysis at 7 days post-injury showed that CsA elicits a significant increase in the number of MyoG-positive cells and of regenerating myofibers in *Col6a1*$^{-/-}$ muscles. Interestingly, this response is not associated with an improvement of the number of satellite cells, suggesting that under these conditions CsA is unable to ameliorate satellite cell self-renewal. The effect of CsA on muscle regeneration was even more remarkable when we exacerbated the muscle phenotype of *Col6a1*$^{-/-}$ mice through triple CdTx damage. Our findings indicate that CsA is protective against fibrotic tissue formation, maybe exerting this effect through an indirect regulation of the inflammatory state that occurs during muscle regeneration (Serrano et al., 2011). A similar beneficial effect of CsA in reducing muscle fibrosis was reported for *mdx* mice undergoing exercise (De Luca et al., 2005). Furthermore, CsA administration was able to counteract the loss of satellite cells elicited by repeated muscle injuries in *Col6a1*$^{-/-}$ animals, concurrently guaranteeing myogenic differentiation, as confirmed by the increase of myofiber cross-sectional area and muscle mass. Although it was beyond the scope of this study to dissect the mechanism(s) through which CsA leads to increased satellite cell number in *Col6a1*$^{-/-}$ mice after repeated injuries, it can be hypothesized that CsA administration may not directly influence the self-renewal capability of satellite cells and that the preservation of satellite cell pool may be mediated by an increase of their survival. This assumption is supported by the fact that the defective satellite cell self-renewal of *Col6a1*$^{-/-}$ mice is strictly dependent on the lack of collagen VI itself and its consequences on muscle stiffness (Urciuolo et al., 2013) and that CsA treatment is able to reduce apoptosis in *Col6a1*$^{-/-}$ muscles (Irwin et al., 2003). To our knowledge, no literature work has investigated in detail the effects of *in vivo* CsA administration on stem cell homeostasis in skeletal muscles. A recent study reported some beneficial effects of CsA on neuronal stem cells, showing that *in vivo* CsA administration increases the number of neurospheres due to enhanced neuronal stem cell survival, rather than increased proliferation (Hunt et al., 2010).

The pharmacology of CsA is complex, and the drug binds a family of cellular peptidyl-prolyl *cis–trans* isomerases known as cyclophilins. Binding of CsA with the abundant cyclophilin A leads to inhibition of calcineurin, a cytosolic phosphatase found in many cell types, thus preventing dephosphorylation of its substrates (Liu et al., 1991). A number of studies have shown that calcineurin signals are involved in the control of myofiber size, myofiber type, and skeletal muscle regeneration (Schiaffino and Serrano, 2002; Sakuma and Yamaguchi, 2010; Hudson and Price, 2013). Although inhibition of calcineurin was shown to delay muscle regeneration (Sakuma et al., 2003, 2005), literature studies investigating the outcomes of calcineurin inhibition by genetic approaches or by CsA administration in animal models of muscle diseases have produced contrasting results (Stupka et al., 2004; De Luca et al., 2005; Parsons et al., 2007). The reasons for these discrepancies rely upon multiple factors, including the genetic model studied, the dose of the drug, the type of muscle, the duration of treatment, and the route of treatment. For instance, the efficacy of CsA in the *mdx* mice, an animal model of Duchenne muscular dystrophy, was reported to be dependent on the dosage and length of the treatment (Stupka et al., 2004; De Luca et al., 2005). Notably, the protective effects of CsA in *Col6a1*$^{-/-}$ mice do not rely upon calcineurin inhibition, as the same beneficial effects are also displayed by non-immunosuppressive CsA analogs that do not bind calcineurin, such as Debio 025 and NIM811 (Angelin et al., 2007; Zulian et al., 2014), whereas they cannot be mimicked by the calcineurin inhibitor FK506 (Irwin et al., 2003). Although our interest was far from the study of calcineurin activity, in this work we used a definite CsA dosage (5 mg/kg every 12 h, i.e., the same dose shown to be effective in rescuing different aspects of the muscle pathology of *Col6a1*$^{-/-}$ mice), and this dosage is known to only partially reduce the activity of calcineurin (Dunn et al., 2002; Michel et al., 2004).

In conclusion, our results indicate that besides the already known beneficial effects of CsA administration in ameliorating the myophatic phenotype of *Col6a1*$^{-/-}$ mice through the rescue from mitochondrial and autophagic dysfunction of muscle fibers, CsA is also capable to stimulate muscle regeneration and preserve the satellite cell pool in this disease model. These findings support and strengthen the increased muscle regeneration observed in Ullrich patients undergoing clinical trial with CsA, pointing at CsA and its non-immunosuppressive derivatives as a promising therapeutic route for this group of inherited muscle diseases.

AUTHOR CONTRIBUTIONS

Francesca Gattazzo planned and performed *in vivo* and *ex vivo* experiments and wrote the paper. Sibilla Molon performed cardiotoxin damage, immunofluorescence, and histology. Valeria Morbidoni performed *in vivo* satellite cell quantification. Bert

Blaauw carried out part of the *in vivo* studies. Paola Braghetta was involved in CsA administration. Anna Urciuolo oversaw the results and interpreted the data. Paolo Bonaldo oversaw the results and wrote the paper. All the authors discussed the results, revised the work, commented on the manuscript, and agreed on the final draft.

ACKNOWLEDGMENTS

This work was supported by grants from Telethon-Italy (GGP10225 and GGP11082), the Italian Ministry of Education, University and Research (FIRB Strategic Project RBAP11Z3YA_003), and the University of Padova.

SUPPLEMENTARY MATERIAL

The Supplementary Material for this article can be found online at http://www.frontiersin.org/Journal/10.3389/fnagi.2014.00244/abstract

REFERENCES

Angelin, A., Tiepolo, T., Sabatelli, P., Grumati, P., Bergamin, N., Golfieri, C., et al. (2007). Mitochondrial dysfunction in the pathogenesis of Ullrich congenital muscular dystrophy and prospective therapy with cyclosporins. *Proc. Natl. Acad. Sci. U.S.A.* 104, 991–996. doi:10.1073/pnas.0610270104

Bonaldo, P., Braghetta, P., Zanetti, M., Piccolo, S., Volpin, D., and Bressan, G. M. (1998). Collagen VI deficiency induces early onset myopathy in the mouse: an animal model for Bethlem myopathy. *Hum. Mol. Genet.* 7, 2135–2140. doi:10.1093/hmg/7.13.2135

Buckingham, M., and Rigby, P. W. J. (2014). Gene regulatory networks and transcriptional mechanisms that control myogenesis. *Dev. Cell* 28, 225–238. doi:10.1016/j.devcel.2013.12.020

Chargé, S. B. P., and Rudnicki, M. (2004). Cellular and molecular regulation of muscle regeneration. *Physiol. Rev.* 84, 209–238. doi:10.1152/physrev.00019.2003

Ciciliot, S., and Schiaffino, S. (2010). Regeneration of mammalian skeletal muscle: basic mechanisms and clinical implications. *Curr. Pharm. Des.* 16, 906–914. doi:10.2174/138161210790883453

Couteaux, R., Mira, J. C., and D'Albis, A. (1988). Regeneration of muscles after cardiotoxin injury. I. Cytological aspects. *Biol. Cell* 62, 171–182. doi:10.1111/j.1768-322X.1988.tb00719.x

De Luca, A., Nico, B., Liantonio, A., Didonna, M. P., Fraysse, B., Pierno, S., et al. (2005). A multidisciplinary evaluation of the effectiveness of cyclosporine a in dystrophic mdx mice. *Am. J. Pathol.* 166, 477–489. doi:10.1016/S0002-9440(10)62270-5

Dunn, S. E., Simard, A. R., Prud'homme, R. A., and Michel, R. N. (2002). Calcineurin and skeletal muscle growth. *Nat. Cell Biol.* 4, E46. doi:10.1038/ncb0302-e46a author reply E46–47,

Grumati, P., Coletto, L., Sabatelli, P., Cescon, M., Angelin, A., Bertaggia, E., et al. (2010). Autophagy is defective in collagen VI muscular dystrophies, and its reactivation rescues myofiber degeneration. *Nat. Med.* 16, 1313–1320. doi:10.1038/nm.2247

Hawke, T. J., Meeson, A. P., Jiang, N., Graham, S., Hutcheson, K., DiMaio, J. M., et al. (2003). p21 is essential for normal myogenic progenitor cell function in regenerating skeletal muscle. *Am. J. Physiol. Cell Physiol.* 285, C1019–C1027. doi:10.1152/ajpcell.00055.2003

Homan, W. P., Fabre, J. W., Williams, K. A., Millard, P. R., and Morris, P. J. (1980). Studies on the immunosuppressive properties of cyclosporin A in rats receiving renal allografts. *Transplantation* 29, 361–366. doi:10.1097/00007890-198005000-00003

Hudson, M. B., and Price, S. R. (2013). Calcineurin: a poorly understood regulator of muscle mass. *Int. J. Biochem. Cell Biol.* 45, 2173–2178. doi:10.1016/j.biocel.2013.06.029

Hunt, J., Cheng, A., Hoyles, A., Jervis, E., and Morshead, C. M. (2010). Cyclosporin A has direct effects on adult neural precursor cells. *J. Neurosci.* 30, 2888–2896. doi:10.1523/JNEUROSCI.5991-09.2010

Irwin, W. A., Bergamin, N., Sabatelli, P., Reggiani, C., Megighian, A., Merlini, L., et al. (2003). Mitochondrial dysfunction and apoptosis in myopathic mice with collagen VI deficiency. *Nat. Genet.* 35, 367–371. doi:10.1038/ng1270

Lampe, A. K., and Bushby, K. M. D. (2005). Collagen VI related muscle disorders. *J. Med. Genet.* 42, 673–685. doi:10.1136/jmg.2002.002311

Liu, J., Farmer, J. D., Lane, W. S., Friedman, J., Weissman, I., and Schreiber, S. L. (1991). Calcineurin is a common target of cyclophilin-cyclosporin A and FKBP-FK506 complexes. *Cell* 66, 807–815. doi:10.1016/0092-8674(91)90124-H

Merlini, L., Angelin, A., Tiepolo, T., Braghetta, P., Sabatelli, P., Zamparelli, A., et al. (2008). Cyclosporin A corrects mitochondrial dysfunction and muscle apoptosis in patients with collagen VI myopathies. *Proc. Natl. Acad. Sci. U.S.A.* 105, 5225–5229. doi:10.1073/pnas.0800962105

Merlini, L., Sabatelli, P., Armaroli, A., Gnudi, S., Angelin, A., Grumati, P., et al. (2011). Cyclosporine A in Ullrich congenital muscular dystrophy: long-term results. *Oxid. Med. Cell. Longev.* 2011, 139194. doi:10.1155/2011/139194

Michel, R. N., Dunn, S. E., and Chin, E. R. (2004). Calcineurin and skeletal muscle growth. *Proc. Nutr. Soc.* 63, 341–349. doi:10.1079/PNS2004362

Parsons, S. A., Millay, D. P., Sargent, M. A., Naya, F. J., McNally, E. M., Sweeney, H. L., et al. (2007). Genetic disruption of calcineurin improves skeletal muscle pathology and cardiac disease in a mouse model of limb-girdle muscular dystrophy. *J. Biol. Chem.* 282, 10068–10078. doi:10.1074/jbc.M609368200

Sakuma, K., Nakao, R., Aoi, W., Inashima, S., Fujikawa, T., Hirata, M., et al. (2005). Cyclosporin A treatment upregulates Id1 and Smad3 expression and delays skeletal muscle regeneration. *Acta Neuropathol.* 110, 269–280. doi:10.1007/s00401-005-1049-x

Sakuma, K., Nishikawa, J., Nakao, R., Watanabe, K., Totsuka, T., Nakano, H., et al. (2003). Calcineurin is a potent regulator for skeletal muscle regeneration by association with NFATc1 and GATA-2. *Acta Neuropathol.* 105, 271–280. doi:10.1007/s00401-002-0647-0

Sakuma, K., and Yamaguchi, A. (2010). The functional role of calcineurin in hypertrophy, regeneration, and disorders of skeletal muscle. *J. Biomed. Biotechnol.* 2010, 721219. doi:10.1155/2010/721219

Schiaffino, S., and Serrano, A. L. (2002). Calcineurin signaling and neural control of skeletal muscle fiber type and size. *Trends Pharmacol. Sci.* 6147, 569–575. doi:10.1016/S0165-6147(02)02111-9

Serrano, A. L., Mann, C. J., Vidal, B., Ardite, E., Perdiguero, E., and Muñoz-Cánoves, P. (2011). Cellular and molecular mechanisms regulating fibrosis in skeletal muscle repair and disease. *Curr. Top. Dev. Biol.* 96, 167–201. doi:10.1016/B978-0-12-385940-2.00007-3

Shi, X., and Garry, D. J. (2006). Muscle stem cells in development, regeneration, and disease. *Genes Dev.* 20, 1692–1708. doi:10.1101/gad.1419406

Stupka, N., Gregorevic, P., Plant, D. R., and Lynch, G. S. (2004). The calcineurin signal transduction pathway is essential for successful muscle regeneration in mdx dystrophic mice. *Acta Neuropathol.* 107, 299–310. doi:10.1007/s00401-003-0807-x

Tedesco, F. S., Dellavalle, A., Diaz-Manera, J., Messina, G., and Cossu, G. (2010). Repairing skeletal muscle: regenerative potential of skeletal muscle stem cells. *J. Clin. Invest.* 120, 11–19. doi:10.1172/JCI40373

Urciuolo, A., Quarta, M., Morbidoni, V., Gattazzo, F., Molon, S., Grumati, P., et al. (2013). Collagen VI regulates satellite cell self-renewal and muscle regeneration. *Nat. Commun.* 4, 1964. doi:10.1038/ncomms2964

Zulian, A., Rizzo, E., Schiavone, M., Palma, E., Tagliavini, F., Blaauw, B., et al. (2014). NIM811, a cyclophilin inhibitor without immunosuppressive activity, is beneficial in collagen VI congenital muscular dystrophy models. *Hum. Mol. Genet.* doi:10.1093/hmg/ddu254

Conflict of Interest Statement: The authors declare that the research was conducted in the absence of any commercial or financial relationships that could be construed as a potential conflict of interest.

Received: 27 June 2014; accepted: 29 August 2014; published online: 15 September 2014.
Citation: Gattazzo F, Molon S, Morbidoni V, Braghetta P, Blaauw B, Urciuolo A and Bonaldo P (2014) Cyclosporin A promotes in vivo myogenic response in collagen VI-deficient myopathic mice. Front. Aging Neurosci. 6:244. doi: 10.3389/fnagi.2014.00244
This article was submitted to the journal Frontiers in Aging Neuroscience.
Copyright © 2014 Gattazzo, Molon, Morbidoni, Braghetta, Blaauw, Urciuolo and Bonaldo. This is an open-access article distributed under the terms of the Creative Commons Attribution License (CC BY). The use, distribution or reproduction in other forums is permitted, provided the original author(s) or licensor are credited and that the original publication in this journal is cited, in accordance with accepted academic practice. No use, distribution or reproduction is permitted which does not comply with these terms.

References

Angelin A et al., 2007. Mitochondrial dysfunction in the pathogenesis of Ullrich congenital muscular dystrophy and prospective therapy with cyclosporins. *Proc Natl Acad Sci USA*, 104(3): 991-6.

Bentzinger CF et al., 2013. Cellular dynamics in the muscle satellite cell niche. *EMBO reports*, 14(12): 1062–72. *Review.*

Bernardi P and Bonaldo P, 2008. Dysfunction of mitochondria and sarcoplasmic reticulum in the pathogenensis of collagen VI muscular dystrophies. *Ann YN Acad Sci*, 1147: 303-311. *Review*.

Bertini E and Pepe G, 2002. Collagen type VI and related disorders: Bethlem myopathy and Ullrich scleroatonic muscular dystrophy. *Eur J Paediatr Neurol*, 6: 193-198. *Review*.

Bonaldo P et al., 1989. Alpha 1 chain of chick type VI collagen. The complete cDNA sequence reveals a hybrid molecule made of one short collagen and three von Willebrand factor type A–like domains. *J Biol Chem*, 264: 5575–5580.

Bonaldo P and Colombatti A, 1989. The carboxyl terminus of the chicken α3 chain of collagen VI is a unique mosaic structure with glycoprotein Ib-like, fibronectin type III, and Kunitz modules. *J Biol Chem*, 264: 20235-20239.

Bonaldo P et al. 1990. Structural and functional features of the alpha 3 chain indicate a bridging role for chicken collagen VI in connective tissues. *Biochemistry* 29: 1245–1254.

Bonaldo P et al., 1998. Collagen VI deficiency induces early onset myopathy in the mouse: an animal model for Bethlem myopathy. *Hum Mol Genet*, 7: 2135-2140.

Bönnemann CG, 2011. The collagen VI-related myopathies: muscle meets its matrix. *Nat Rev Neurol*, 7(7): 379-90. *Review.*

Braghetta P et al., 2008. An enhancer required for transcription of the *Col6a1*gene in muscle connective tissue is induced by signals released from muscle cells. *Exp Cell Research*, 314(19): 3508-3518.

Broek TRW, Grefte S and von den Hoff JW, 2010. Regulatory factors and cell populations involved in skeletal muscle regeneration. *J Cell Physiol,* 224: 7-16. *Review.*

Buckingham M 2001. Skeletal muscle formation in vertebrates. *Curr Opin Genet Dev*, 11(4): 573-80. *Review.*

Burg MA et al., 1996. Binding of the NG2 proteoglycan to type VI collagen and other extracellular matrix molecules. *J Biol Chem*, 271: 26110–26116.

Campbell KP and Stull JT, 2003. Skeletal muscle basement membrane-sarcolemma-cytoskeleton interaction minireview series. *J Biol Chem*, 278(15):12599-600. *Review.*

Cescon M et al., 2015. Collagen VI at a glance. *J Cell Sci*, 128(19):3525-31.

Chargé SB and Rudnicki MA, 2004. Cellular and molecular regulation of muscle regeneration. *Physiol Rev*, 84(1):209-38. *Review.*

Chu ML et al., 1990. Mosaic structure of globular domains in the human type VI collagen α3 chain: similarity to von Willebrand Factor, fibronectin, actin, salivatory proteins and aprotinin type protease inhibitors. *The EMBO Journal*, 9(2): 385-393.

Ciciliot S and Schiaffino S, 2010. Regeneration of mammalian skeletal muscle: basic mechanisms and clinical implications. *Curr Pharmaceut Design,* 16: 906-914. *Review.*

Colombatti A et al., 1987. Biosynthesis of chick type VI collagen (I. Intracellular assembly and molecular structure). *J Bio Chem*, 262: 14454-14460.

Colombatti A and Bonaldo P, 1987. Biosynthesis of chick type VI collagen (II. Processing and secretion in fibroblast and smooth muscle cells). *J Biol Chem*, 262: 14461-14466.

Colombatti A and Bonaldo P, 1991. The superfamily of proteins with von Willebrand factor type A-linked domains: one theme common to components of extracellular matrix, homeostasis, cellular adhesion, and defense mechanisms. *Blood*, 77: 2305-2315.

Cosgrove BD et al, 2009. A home away from home: challenges and opportunities in engineering in vitro muscle satellite cell niches. *Differentiation*, 78(2-3): 185-94. *Review.*

Couteaux R, Mira JC and d'Albis A, 1988. Regeneration of muscles after cardiotoxin injury. I. Cytological aspects. *Biol Cell,* 62(2): 171-82.

Daley WP, Peters SB and Larsen M, 2008. Extracellular matrix dynamics in development and regenerative medicine. *J Cell Sci*, 121(Pt3): 255-64. *Review.*

Dziadek, M et al., 2002. Alternative splicing of transcripts for the alpha3 chain of mouse collagen VI: identification of an abundant isoform lacking domains N7–N10 in mouse and human. Matrix Biol, 21: 227-241.

Doliana R, Bonaldo P and Colombatti A (1990). Multiple forms of chicken alpha 3(VI) collagen chain generated by alternative splicing in type A repeated domains. *J Cell Biol*, 111: 2197–2205.

Dumont NA, Wang YX and Rudnicki MA, 2015. Intrinsic and extrinsic mechanisms regulating satellite cell function. *Development*, 142: 1572-1581. *Review.*

Hessle H, Engvall E. Type VI collagen. Studies on its localization, structure, and biosynthetic form with monoclonal antibodies. *J Biol Chem*, 259(6):3955-61.

Engvall E, Hessle H and Klier G, 1986. Molecular assembly, secretion, and matrix deposition of type VI collagen. *J Cell Biol*, 102(3): 703-10.

Ferraro E, Molinari F and Berghella L, 2012. Molecular control of neuromuscular junction development. J Cachexia Sarcopenia Muscle, 3(1):13-23. *Review.*

Fitzgerald J et al., 2008. Three novel collagen VI chains, α4(VI), α5(VI), and α6(VI). *J Biol Chem*, 283(29): 20170–20180.

Frontera WR and Ochala J, 2015. Skeletal muscle: a brief review of structure and function. *Calcif Tissue Int*, 96:183–195. *Review.*

Gara SK et al., 2008. Three novel collagen VI chains with high homology to the α3 chain. *J Biol Chem*, 283(16): 10658-10670.

Gara SK et al., 2011. Differential and restricted expression of novel collagen VI chains in mouse. *Matrix Biol*, 30: 248-257.

Gattazzo F et al., 2014. Cyclosporin A promotes in vivo myogenic response in collagen VI-deficient myopathic mice. *Front Aging Neurosci*, 6: 244.

Gilbert PM et al., 2010. Substrate elasticity regulates skeletal muscle stem cell self-renewal in culture. *Science*, 329(5995): 1078–81.

Grumati P et al., 2010. Autophagy is detective in collagen VI muscular dystrophies, and its reactivation rescues myofiber degeneration. *Nat Med*, 16(11): 1313-1320.

Grumati P et al., 2011. Physical exercise stimulates autophagy in normal skeletal muscles but is detrimental for collagen VI-deficient muscles. *Autophagy*, 7(12): 1415-23.

Gualandi F et al., 2009. Autosomal recessive Bethlem Myopathy. *Neurology*, 3(22): 1883-91.

Guilak F et al., 2009. Control of stem cell fate by physical interactions with the extracellular matrix. *Cell stem cell*, 5(1): 17–26.

Hopkins PM, 2006. Skeletal muscle physiology. *Contin Educ Anaesth Crit Care Pain*, 6(1): 1-6. *Review.*

Irwin WA et al., 2003. Mitochondrial dysfunction and apoptosis in myopathic mice with collagen VI deficiency. *Nature Genetics*, 35: 367-371.

Karalaki M et al., 2009. Muscle regeneration: cellular and molecular events. *In vivo,* 23(5): 779–96. *Review.*

Keene DR, Engvall E and Glanville RW, 1988. Ultrastructure of type VI collagen in skin and cartilage suggests an anchoring function for this filamentous network. *J Cell Biol*, 107: 1995-2006.

Kuang S, Gillespie MA and Rudnicki MA, 2008. Niche regulation of muscle satellite cell self-renewal and differentiation. *Cell Stem Cell,* 2(1): 22-31. *Review.*

Kuo HJ et al., 1997. Type VI collagen anchors endothelial basement membranes by interacting with type IV collagen. *J Biol Chem*, 272(42): 26522–9.

Lampe AK and Bushby KM, 2005. Collagen VI related muscle disorders. *J Med Genet*,

42(9): 673-85. *Review*.

Mauro A, 1961. Satellite cell of skeletal muscle fibers. *J Biophys Biochem Cytol*, 9: 493-495.

Merlini L and Bernardi P, 2008. Therapy of collagen VI-related myopathies (Bethlem and Ullrich). *Neurotherapeutics*, 5: 613-618. *Review*.

Merlini L et al., 2008a. Autosomal recessive myosclerosis myopathy is a collagen VI disorder. *Neurology*, 71(16): 1245-1253.

Merlini L et al., 2008b. Cyclosporin A corrects mitochondrial dysfunction and muscle apoptosis in patients with collagen VI myopathies. *Proc Natl Acad Sci USA*, 105 (13): 5225-5229.

Merlini L et al., 2011. Cyclosporin A in Ullrich congenital muscular dystrophy: long-term results. *Oxid Med Cell Longev*, 2011: 139194.

Mizushima N et al., 2008. Autophagy fights disease through cellular self-digestion. *Nature*, 451(7182): 1069–75. *Review.*

Motohashi N and Asakura A, 2014. Muscle satellite cell heterogeneity and self-renewal. *Front Cell Dev Biol*, 2: 1. *Review.*

Musarò A, 2014. The basis of muscle regeneration. *Adv Biol,* 2014: 612471. *Review.*

Palma E et al., 2009. Genetic ablation of cyclophilin D rescues mitochondrial defects and prevents muscle apoptosis in collagen VI myophatic mice. *Hum Mol Genet*, 18(11): 2024-2031.

Pfaff M et al., 1993. Integrin and Arg-Gly-Asp dependence of cell adhesion to the native and unfolded triple helix of collagen type VI. *Exp Cell Res*, 206: 167-176.

Saitta B et al., 1990. Alternative splicing of the human alpha 2(VI) collagen gene generates multiple mRNA transcripts which predict three protein variants with distinct carboxyl termini. *J Biol Chem,* 265: 6473–80.

Sanes JR. The Basement Membrane/Basal Lamina of skeletal muscle. *J Biol Chem*, 278: 601-12604. *Minireview*.

Snijders T et al., 2015. Satellite cells in human skeletal muscle plasticity. *Front Physiol*, 6: 283. *Review.*

Tedesco FS et al., 2010. Repairing skeletal muscle: regenerative potential of skeletal muscle stem cells. *J C Invest*, 120(1): 11-19. *Review.*

Thomas K, Engler AJ and Meyer GA, 2015. Extracellular matrix regulation in the muscle satellite cell niche. *Connect Tissue Res*, 56(1): 1–8. *Review.*

Tidball JG and Villalta AS, 2010. Regulatory interactions between muscle and the immune system during muscle regeneration. *Am J Physiol Regul Integr Comp Physiol,* 298: 1173-1187. *Review.*

Timpl R, 1996. Macromolecular organization of basement membranes. *Curr Opin Cell Biol*, 8(5): 618-24. *Review.*

Urciuolo, A. et al., 2013. Collagen VI regulates satellite cell self-renewal and muscle regeneration. *Nature communications*, 4(May): 1964.

Wiberg C et al., 2002. Biglycan organizes collagen VI into hexagonal-like networks resembling tissue structures. J Biol Chem, 277(51): 49120-6.

Weil D et al., 1998. Cloning and chromosomal localization of human genes encoding the three chains of type VI collagen. *Am J Hum Genet*, 2: 435–45.

Zanussi S et al., 1992. The human type VI collagen gene, mRNA and protein variants of the alpha 3 chain generated by alternative splicing of an additional 5-end exon. *J Biol Chem*, 267: 24082-9.

Zhang RZ et al., Cloning and sequence analysis of cDNAs encoding the alpha 1, alpha 2 and alpha 3 chains of mouse collagen VI. Biochem J, 291 (Pt 3): 787-92.

Zou Y et al., 2008. Muscle interstitial fibroblasts are the main source of collagen VI synthesis in skeletal muscle: implications for congenital muscular dystrophy types Ullrich and Bethlem. *J Neuropathol Exp Neurol*, 67(2): 144-154.

1. Introduction

1.1 The gastrointestinal system

The gastrointestinal (GI) tract consists of a hollow muscular tube starting from the oral cavity, continuing through the pharynx, oesophagus, stomach and small and large intestine. The small intestine is further subdivided into the duodenum, jejunum and ileum, while the large intestine is subdivided into the cecum, colon, rectum, and anal canal. The human whole digestive tract is about 4.5 metres long. The digestive system includes also accessories organs, such as salivary glands, pancreas, gallbladder and liver, that produce exocrine secretions containing enzymes and mucus and regulates metabolism. The GI tract releases hormones from enzymes to help regulating the digestive process (Ross and Pawlina, 2010).

The GI system has a number of sophisticated and autonomous functions coordinated over a range of length and time scales. The primary functions of the GI tract are *i)* digestion, *i.e.* the mechanical and enzymatic breakdown of food into smaller components; *ii)* absorption, from the lumen into the blood or lymphoid vessels; *iii)* motility, *i.e.* the contractions and relaxation of the gastrointestinal smooth muscle necessary for the food transport; *iv)* secretion of hormones, to help regulate the digestive process, and enzyme and mucus, that regulate metabolism; *v)* excretion of faeces; and *vi)* protection, *i.e.* against pathogens by secreting enzymes and activating the immune system, or by triggering reflexes, such as diarrhea or vomit. These functions are achieved through a series of organs with distinct roles from mouth to anus. The stomach and small intestine are principally responsible for digestion and absorption, a process incorporating both physical (*e.g.*, retropulsion in the stomach) and chemical (*e.g.*, bile and enzymes in the small intestine) mechanisms. The large intestine is primarily devoted to absorption of water and some minerals and compaction of faeces, with storage in the sigmoid colon and rectum prior to elimination (Cheng et al., 2010).
From the histological point of view, the GI tract can be divided into four different concentric layers in the following order: *i)* mucosa, the innermost layer, composed by the epithelium, the lamina propria (*i.e.* a layer of connective tissue) and muscularis mucosae (*i.e.* a thin smooth muscle layer); *ii)* submucosa, consisting of a dense irregular layer of connective tissue with blood and lymphatic vessels, and nerve branches; *iii)*

muscularis externa, which is made of two different concentric smooth muscle layers, an inner circular and an outer longitudinal one, which regulate through the peristalsis (*i.e.* the coordinated contractions of these layers) the propulsion of the food through the tract; and *iv)* serosa and adventitia, the outermost layers consisting in several layers of connective tissue, covering the intraperitoneal and the retroperitoneal parts of the GI, respectively (Ross and Pawlina, 2010).

The entire GI tract, the associated glands (salivary glands and pancreas) and the gallbladder are innervated by the enteric nervous system (ENS), a part of the autonomic nervous system that integrates motility, secretions, blood flow, and immune and inflammatory responses into organised patterns of behaviour through neural reflexes. The ENS is commonly described as a "second brain" for its capability to function autonomously from the central nervous system, even if normal digestive function requires communication links between each other. Neurons of the ENS are collected into two types of ganglia (*i.e.* a group of efferent nerve cell bodies). Ganglia are connected each other by amielinic nervous fibers and with the effector system (muscle cells, glands, blood vessels, and immune cells) forming a so-called plexus. The ENS has two major ganglionated plexuses: *i)* the submucous (or Meissner's) plexus, located between the submucosa and the circular muscular layer; and *ii)* the myenteric (or Auerbach's) plexus, located between the circular and longitudinal muscular layers. The density of neurons is higher in the myenteric plexus compared to submucous one and they are connected each other (Hansen, 2003). Submucous plexus sense the lumen environment and is involved in regulating the gastrointestinal blood flow as well as controlling the epithelial cell functions and secretions, whereas myenteric plexus regulates mainly the relaxation and contraction of the intestinal wall (*i.e.* the peristalsis). Enteric neurons can be divided into three classes: the primary afferent neurons, the interneurons, and the motor neurons. Based on the function of the neurotransmitters they secrete, motor neurons can be divided in excitatory (acetylcholine, serotonin and neuropeptides, such as substance P, that stimulates contraction and increase secretions) and inhibitory (norepinephrine and nitric oxide) (Nezami and Srinivasan, 2010). Besides ENS activity, peristalsis is also regulated by interstitial cells of Cajal, which are spontaneously active pacemaker cells widely distributed within the submucosal, intra-muscular and inter-muscular layers, driving the spontaneous electrical and mechanical activities of smooth muscle cells (Takaki, 2003).

The mucosa of the GI is responsible for most digestion and absorption of nutrients, electrolytes and water, and for secretory processes (the latter mainly carried out by glands that secrete hormones and digestive enzymes). The absorptive surface area of the small intestinal mucosa is dramatically increased by numerous finger-like protrusions that point toward the lumen, the so-called villi, and invaginations into the submucosa known as the crypts of Lieberkühn. On the contrary, the mucosa of the large intestine contains only crypts, that invaginate deeply into the submucosa. Four differentiated cell types mediate the functions of the intestinal epithelium: *i)* enterocytes, whose primary function is absorption of nutrients and water, in addition to provide a selective permeable barrier, achieved by intercellular tight junctions structures, that limits the permeation of luminal noxious molecules; *ii)* goblet cells, that produce mucus and whose number increase from proximal (small intestine) to distal (colon and rectum) as the stool becomes increasingly compacted; *iii)* enteroendocrine cells, that control gut physiology by secreting a variety of hormones; and *iv)* Paneth cells, that reside at the bottom-most positions of the crypts of the small intestine and secrete antimicrobial agents such as cryptidins (termed defensins in humans) and lysozyme, which play an essential role in the control of the microbial environment of the intestine. The intestinal epithelium is renewed every three to five days by vigorous proliferation of crypt progenitors that reside in the crypt (Barker et al., 2008; Suzuki, 2013).

1.2 Inflammatory bowel diseases

Inflammatory Bowel Diseases (IBDs) are complex, multifactorial disorders characterized by chronic relapsing intestinal inflammation. The two major subtypes of IBD are Ulcerative Colitis (UC) and Crohn's Disease (CD). IBDs represent a worldwide health-care problem with a continually increasing incidence in areas where the disease was previously infrequent (Gómez-Gómez et al., 2015).

UC is characterized by mucosal inflammation and limited to a part or extended to the entire colon in a uninterrupted pattern and it is superficial, affecting only the mucosal layer of the intestinal wall. In contrast, CD can cause transmural inflammation and may affect any part of the GI tract (most commonly, the terminal ileum or the perianal region) in a non-continuous type. Unlike UC, CD is commonly associated with complications such as granulomas, abscesses, fistulas and strictures (Abraham and Cho, 2009; Loddo and Romano, 2015). However, in the most severe forms of UC, the intestine

can get distended, presenting deep ulceration and possibly intestinal perforation (de Mattos et al., 2015).

Although the etiology of IBD remains largely unknown, it is now clear that CD and UC represent two distinct forms of chronic inflammation of the gastrointestinal tract and, as such, have different causes and different pathogenic mechanisms. Still, the factors underlying the appearance of both CD and UC are roughly the same, and include a temporal association with progressive changes in the environment (*i.e.* smoking, diet, drugs, geography, social stress, and psychological element), an intrinsic genetic predisposition, the existence of a rich enteric flora, and an abnormal immune reactivity which is ultimately responsible for damaging the gut and causing clinical manifestations (Danese and Fiocchi 2006; Zhang and Li, 2014).

The most common type of reaction that the body mounts against external or internal offending agents is inflammation and the gut is particularly susceptible to inflammation as indicated by the fact that, and even under normal circumstances, there is a baseline degree of "physiological inflammation" in the mucosa, elicited by the abundant number of leukocytes in the lamina propria. Under normal circumstances there is an intimate interaction between commensal intestinal bacteria (*i.e.* the so-called enteric microbiota, that is a complex ecosystem of approximately 300-500 bacterial species) and the immune system (both innate, *i.e.* macrophages and dendritic cells, and adaptive, *i.e.* T and B lymphocytes), and this complex crosstalk is tightly regulated under the control of the so-called immune tolerance. When this interaction is disrupted, the loss of tolerance towards the autologous enteric microbiota is lost, resulting in an inappropriate immune response in the mucosa. If inflammation persists and becomes chronic, it represents an excessive response that almost invariably leads to lingering injurious effects resulting in anatomical and functional abnormalities, typical of IBD. Why tolerance is lost and an abnormal response to otherwise normal gut bacteria develops in IBD is still not entirely clear (Danese and Fiocchi 2006; Abraham and Cho, 2009).

Over the past decades, there have been huge advances in understanding of genetic contributions to IBD. Until now several genome wide associations studies (GWAS), followed by meta analysis of both principal forms of IBD (CD and UC) identified a total of 201 IBD associated loci, of which 37 and 27 loci contribute specifically to the development of CD and UC, respectively (Bianco et al., 2015). Single-nucleotide polymorphisms (SNPs) associated with increased risk of developing IBDs were identified in genes involving microbial sensing (NOD2, IRF5, NFKB1, RELA, REL, RIPK2,

CARD9, and PTPN22), autophagy and clearance (ATG16L1, IRGM, and NCF4), and integrating antimicrobial adaptive immune responses (IL23R, IL10, IL12, IL18RAP/IL1R1, IFNGR/IFNAR1, JAK2, STAT3, and TYK2), pointing out the importance of the crosstalk between host innate and adaptive immune responses against microbes in the pathogenesis of IBD (Steinbach and Plevy, 2014).

The localized release of certain cytokines, such as IL-12 and IL-17, by antigen-presenting cells (APC) and macrophages, was found to be implicated in the chronic intestinal manifestations of CD patients. In turn, these cytokines trigger a polarized differentiation towards Th1 lymphocyte, leading to an increased release of pro-inflammatory cytokines, including TNF-α and INF-γ. Additionally, Th1 lymphocyte cytokines stimulate APCs and macrophages to secrete a wider spectrum of inflammatory cytokines such as IL-1, IL-6, IL-8, IL-12, and IL-18, resulting in a self-sustained cycle. In UC, the main interleukin responsible for the inflammation and chronicity of the disease is IL-13 and, despite the Th1 involvement, patients also present a Th2 response with increased secretion of IL-4, IL-5, and IL-9, in addition to an IL-17 increase (de Mattos et al., 2015).

1.3 Intestinal macrophages

In the healthy organism, the innate immune system provides the first line of defence against external or internal danger signals, by initiating a protective inflammatory response that develops during time through different phases, from initiation and full inflammation, to resolution and re-establishment of tissue integrity. The first phase of an inflammatory response is aimed at destroying pathogens, followed by a phase in which dead and dying cells, damaged ECM material and cellular debris are removed, to end up with a recovery phase in which the tissue is repaired and restored to a healthy fully functional condition. In this perspective, inflammation presumably evolved as an adaptive response to tissue malfunction or homeostatic imbalance, which need to be tightly controlled to avoid excessive tissue damage leading to disease (Italiani and Boraschi, 2014).

In the gut, the innate immune system consists of the intestinal epithelium, which functions as a barrier, and the cells of the innate immune system, such as neutrophils, dendritic cells, monocytes/macrophages, innate lymphoid cells (ILCs) and natural killer cells (Haag and Siegmund, 2015). This form of immunity is initiated by pattern

recognition receptors (PRRs), including toll-like receptors (TLRs) on the cell surface and nucleotide-binding oligomerization domain receptors (NLRs) in the cytoplasm, that recognize foreign carbohydrate, lipid, and nucleic acid ligands (*i.e.*, pathogen-associated molecular patterns, PAMPs, and danger-associated molecular pattern, DAMPs) essential for microbe survival (Zhang and Li, 2014).

Mononuclear phagocytes, comprising both macrophages and dendritic cells, play a key role in discriminating between pathogenic organisms and innocuous antigens such as food proteins and resident commensal flora, helping to determine whether protective immunity or tolerance occurs (Bain and Mowat, 2011). Intestinal macrophages represent the largest pool of tissue macrophages in the human body and are the most abundant monocular phagocytes in the gut, especially in the large intestine, where they comprise approximately one-fifth of all leukocytes and greatly outnumber dendritic cells. Most of the intestinal macrophages are in the lamina propria below the epithelial monolayer, although some can extend transepithelial dendrites into the intestinal lumen to sample antigens, playing essential roles in maintaining intestinal homeostasis, but are also central drivers of the pathology associated with IBD (Bain and Mowat, 2011). A discrete population of macrophages is also present in the smooth muscle layers of the gut wall where they interact with enteric neurons, thereby regulating GI motility (Muller et al., 2014).

Macrophages are generally classified into two major functional groups, based on the their surface receptors and on the mediators they produce (Table 1). Basically, "inflammatory" M1 macrophages are polarized by IFN-γ produced by NK and Th1 lymphocytes, and produce pro-inflammatory cytokines and reactive oxygen and nitrogen species, that promote the differentiation and activation of the Th1 and Th17 lymphocytes, and are essential for the eradication of intracellular infections. Th1 response in turn helps macrophages by enhancing their ability to clear intracellular pathogens. Upregulation of M1 macrophage activity can induce tissue damage and predispose the host to developing neoplastic lesions. On the contrary, "wound-healing" M2 macrophages are polarized by IL-4 produced by granulocytes or Th2 lymphocytes in response to injury or activation by some fungi and parasites. M2 macrophages produce matrix metalloproteinases and growth factors, and demonstrate efficient phagocytosis of debris without production of pro-inflammatory cytokines. In addition, M2

macrophages are also efficient at recruiting Foxp3-positive regulatory T cells (Treg), which further downregulate local immune responses (Steinbach and Plevy, 2014).
Based on more recent data, this view is going to being replaced by a novel one taking into account the considerable plasticity of macrophages, where they acquire distinct functions of host defence, wound healing, and immune regulation based on environmental cues they encounter. Therefore macrophages are now considered a highly heterogeneous population of cells with a continuum of activation states (Dave et al., 2014)

	M1	M2	Resident intestinal Mφ
Phenotypic markers			
F4/80	+++	+++	+++
CD11b	+++	+++	+++
CD11c	++	–	++
CD14	++	?	++
CD68	++	++	++
CD115 (M-CSFR)	++	++	++
CD163 (Scavenger R)	–	+	?
CD206 (Mannose R)	–	++	+
CD210 (IL-10R)	–	–	+
CX_3CR1	–	–	+++
MHC class II	++	+	+++
IL-4R	–	+	–
Functions			
Phagocytosis	+++	+/–	+++
Costimulatory molecules	++	+/–	+/–
TLR-responsiveness	++	+	–
Factor produced			
TNF-α	+++	–	+/–
iNOS	+++	–	–
Reactive oxygen intermediates	+++	–	–
Arginase	–	++	–
IL-10	–	++	++
COX-2	++	+/–	++

Table 1. Features of M1, M2 and resident intestinal macrophages (Mφ) in the mouse (from Bain and Mowat, 2011).

1.3.1 Origins and functions of intestinal resident macrophages in intestine homeostasis

Like other tissue macrophages, intestinal resident macrophages of the lamina propria are first established before birth from precursors originating in the yolk sac and/or foetal liver. However, unlike other tissue macrophages that are maintained in adult life

by self-renewal *in situ*, intestinal murine macrophages pool requires continuous replenishment by Ly6C-positive blood monocytes (Gross et al., 2015). The majority of blood monocytes, so-called Ly6C^{hi} monocytes, expresses high levels of Ly6C/Gr-1, CCR2 and CD62L, but low levels of CX_3CR1. The entry of Ly6C^{hi} monocytes into the circulation from the bone marrow is dependent on the CCL2(MCP-1)-CCR2 axis. A smaller population of murine monocytes, called Ly6C^{lo} monocytes, expressing lower levels of Ly6C and CCR2 but higher amounts of CX_3CR1, were initially proposed to be precursors of steady state tissue macrophage (Bain and Mowat, 2014a). However, more recently it has become clear that the primary functions of these Ly6C^{lo} monocytes is to act as phagocytes in the blood-stream, patrolling and maintaining the vasculature, and they might be considered as terminally differentiated blood-resident macrophages (Italiani and Boraschi, 2014). Ly6C-positive murine monocytes constantly enter the normal colonic mucosa and begin to undergo a process of local differentiation through a series of short-lived intermediates (CX_3CR1^{int}), resulting within 4-5 days into mature F4/80^{hi}CD64^{+}MHCII^{+}CD11c^{+}CX_3CR1^{hi} resident macrophages. The phenotypic differentiation of monocytes is paralleled by the progressive acquisition of the typical functions of resident intestinal macrophages, characterized by *i)* increased production of IL-10, lysosomal and hydrolytic enzymes, and an increase in the number and size of mitochondria; *ii)* enhanced phagocytic activity; *iii)* acquisition of scavenger receptors (such as CD206 and CD163); and *iv)* development of unresponsiveness to TLR ligation, downregulating key TLR signalling molecules [*e.g.* TNF receptor associated factor 6 (TRAF6)], and upregulating negative regulators of TLR and NF-κB signalling [*e.g.* IL-1 receptor-associated kinase (IRAK)-M and A20)](Smith et al., 2011; Bain and Mowat, 2014a; Cerovic et al., 2014). Intestinal resident macrophages exhibit greater phagocytic activity for enteric bacteria, inert material, senescent enterocytes and leukocytes, and stronger bactericidal activity than autologous blood monocytes. However, in contrast to blood monocytes and other tissue macrophages, intestinal resident macrophage phagocytosis and bactericidal activity is not accompanied by the release of pro-inflammatory cytokines nor results in respiratory burst (Smith et al., 2011). This tolerant anergic phenotype of intestinal resident macrophages is likely conditioned by the constitutive production of the anti-inflammatory cytokine IL-10, one of the major factors ensuring macrophages quiescence in response to environmental stimuli, TGF-β, CXCL1 and PPARγ ligands (Bain and Mowat, 2014b; Cerovic et al., 2014). Thus the

environment in the gut influences newly recruited monocytes to acquire an anti-inflammatory phenotype.

Autophagy and phagolysosomal function have emerged as a central components of the macrophage machinery to eradicate intracellular bacteria or clear apoptotic and necrotic cells, internalized by phagocytosis. Several studies demonstrated that TLR signalling enhances the phagosome formation and also increase the entrapment of *Mycobacterium* in autophagosomes, whose contents can be degraded by the fusion with late endosomes and/or lysosomes. Moreover, defective autophagy could also modulate phagocytosis, as suggested by the impaired eradication of intracellular bacteria in macrophages of CD patients with mutations in autophagy genes (Sheikh and Plevy, 2010; Vural and Kehrl, 2014).

After a period of weeks to possibly several months, tissue macrophages undergo programmed cell death and are replaced by newly recruited blood monocytes (Smith et al., 2011). Intestinal resident macrophages are also involved in wound-healing processes. Macrophages associated with colonic crypts of Lieberkühn promote MyD88-dependent survival and proliferation of epithelial progenitor cell during colonic wound healing. Macrophages also appear to be able to influence the permeability of the epithelium barrier via the secretion of IL-6 and nitric oxide, thereby potentially increasing the invasion of pathogens. Moreover, the expression of CX_3CL1 by enterocytes is crucial for the anatomical position of intestinal macrophages under the epithelial layer (Bain and Mowat, 2014a; Zigmond and Jung, 2013).

In contrast to their progenitor cells, intestinal resident macrophages do not serve as professional antigen-presenting cells (APC), such as dendritic cells, due to their low, or even absent, cell surface expression of CD40, CD80 and CD86 (*i.e.* T cell activating co-stimulatory signals). As a consequence, they have a lower capability to prime naïve T cells (Gross et al., 2015). On the other hand, IL-10 produced by intestinal resident macrophages is responsible for the final differentiation and maintenance of Treg lymphocytes in the intestinal lamina propria, thereby maintaining immune tolerance (Bain and Mowat, 2011).

1.4 Mouse model of colitis

Much of the recent progress in the understanding the pathogenesis of IBD has been achieved by the study of experimental animal models. Animal models of IBD have been

used for over fifty years and although these models do not represent the complexity of human disease and do not replace studies with patient material, they are valuable tools for studying many important disease aspects that are difficult to address in humans, such as the pathophysiological mechanisms in early phases of colitis and the effects of emerging therapeutic strategies (Perše and Cerar, 2012).

Early models resulted from the observation that a variety of laboratory animals fed with extracts from certain species of seaweed display similar symptoms to human IBD. Subsequent refinement and development of this model led to a variety of other experimental models that can be classified into four main categories: *i)* chemically induced models, *i.e.* administration of specific chemical agents such as dextran sodium sulphate (DSS) and 2,4,6-trinitrobenzene sulfonic acid (TNBS) that induce intestinal inflammation and tissue damage; *ii)* spontaneous colitis model, *i.e.* naturally occurring mutant strains that spontaneously develop colitis (*e.g.* C3H/HeBir and SAMP1/Yit); *iii)* gene knockouts and transgenic strains for specific gene (*e.g.* IL-2 null, IL-10 null and Nod2^{2939iC} mice); and *iv)* adoptive cell transfer models, *i.e.* reconstitution of immunodeficient mice with T cells or immune tissue (Boismenu and Chen, 2000).

Animal models of IBD have significant advantages. One can investigate not only factors implicated in the pathogenesis, but also the secondary effects of ulceration (*e.g.* liver changes, effects on protein metabolism, electrolytic changes in the cellular and extracellular spaces) and other systemic complications. They may also be used to study the influence of drugs or other potential therapies on the pathogenesis and course of the disease process. However, none of the current IBD models represent a faithful equivalent of the human diseases (Barnett and Fraser, 2011)

Chemically induced murine models of intestinal inflammation are the most commonly used models because of they are simple to induce and the onset, duration, and severity of inflammation are immediate and controllable. A variety of agents have been used as inducers of colitis in animal models, including carragenin, acetic acid, oxazolone and very recently, sodium hydroxide. While predominantly used in rodents, compounds such as these have also been used to develop colitis models also in dogs and rabbits. The two most widely used chemicals used to induce IBD in such models are DSS and TNBS. Both agents recapitulate many of the events proposed to initiate and sustain the human IBD, although DSS more closely mimics UC, whereas TNBS CD (Barnett and Fraser, 2011). TNBS is delivered intrarectally with ethanol, that is required to break the mucosal barrier, where it is believed to haptenize colonic autologous or microbiota proteins

rendering them immunogenic to the host immune system. As $CD4^+$ T cells have been shown to play a central role in chronic TNBS colitis, this model is useful to study T helper cell-dependent mucosal immune responses (Wirtz and Neurath, 2007).

1.4.1 DSS-induced colitis mouse model

DSS $(C_6H_7Na_3O_{14}S_3)_n$ is a sulphated polysaccharide with highly variable molecular weight, ranging from 5 kDa to up to 1400 kDa. It is a polyanionic derivative of dextran and the first report of its use dates back in the year 1985, when Ohkusa et al. published their investigation on DSS-induced colitis in hamsters. The most severe murine colitis, resulting from administration of 40-50kDa and most closely resembles human UC, was characterized by Okayasu et al. in 1990. Nowadays DSS colitis model is very popular in IBD research due to its rapidity, simplicity, reproducibility and controllability, as demonstrated by the numerous studies of colitis in mice, rats, hamsters and guinea pigs (Chassaing et al., 2014).

DSS is most commonly administered in drinking water, often as a 3% solution, although it can also be administered rectally. Depending on the concentration, the duration, and the frequency of DSS administration, the animals may develop acute or chronic colitis or even colitis-induced dysplastic lesions. Mice show differential susceptibilities and responsiveness to DSS-induced colitis. In particular, colitis onset and severity depends on many factors: not only DSS (*i.e.* concentration, molecular weight, duration of DSS exposure, manufacturer, and batch) but also genetic (*i.e.* strain and substrain, gender) and microbiological (*i.e.* microbiota and intestinal flora) factors of animal, in addition to stress. Differences in the DSS susceptibility do not correlate with differences in the consumption of DSS-supplemented water. However, there is a need to monitor DSS consumption, especially when animals are exposed to different therapeutic strategies that may vary DSS consumption (Perše and Cerar, 2012).

It has emerged that the molecular weight of DSS plays a crucial role in the induction of colitis or colitis-induced dysplastic lesions (carcinogenicity) and that the severity and location differs with the administration of DSS at different molecular weight. In particular, it was found that mice treated with 40 kDa DSS developed more severe colitis, diffused in the middle and distal third of colon, compared to 5 kDa DSS, instead diffused mainly in the cecum and upper colon. In contrast, higher molecular weight (500 kDa) failed to induce colitis because the passage through the mucosal membrane is

prevented (Kitajima et al., 2000). In addition, carcinogenic activity in colon was found to be induced by DSS of 54 kDa, whereas larger or smaller molecular weights did not (Hirono et al., 1983).

The mechanism by which DSS triggers intestinal inflammation is unclear but it is widely accepted that it is toxic to colonic epithelial cells and induces defects in the epithelial barrier integrity causing increased colonic mucosal permeability, allowing bacteria to penetrate, and consequently macrophage activation (Boismenu and Chen, 2000). Further, its anticoagulant property aggravates intestinal bleeding. The mechanism by which DSS passes through mucosal epithelial cells (transcellularly or paracellularly, *i.e.* via tight junctions) remains unclear. However it has been found that DSS causes quick alterations in the inner colon mucus layer, making it permeable to bacteria, which reach the epithelial cells thus triggering an inflammatory reaction (Johansson et al., 2010). More recently, it has been published that DSS could induce colitis in mice by forming nano-lipocomplexes with medium-chain-length fatty acids (MCFAs) present in the colonic lumen, which fuse with colonocyte membrane (Laroui et al., 2012). The specificity of DSS for the colon could be a function of water and electrolyte absorption in the presence of numerous bacteria (Chassaing et al., 2014).

One day after DSS treatment, small amounts of this compound were found in colonic macrophages and mesenteric lymph nodes, one of the components of tight junction complex zonula occludens-1 (ZO-1) was lost and pro-inflammatory cytokines (TNF-α, IL-1-β, IFN-γ, IL-10, and IL-12) expression was significantly upregulated in the colon. The production of these pro-inflammatory cytokines increases progressively during DSS treatment. By day 3, significant increase in permeability to Evans blue was observed and at this time first histological changes in the colonic mucosa in the form of basal crypts loss and increased inflammatory cell infiltration can be seen. The impairment of epithelial barrier function is associated with loss and redistribution of the tight junction proteins such as occludin, ZO-1, claudin-1, -3, -4, and -5 and an increased epithelial apoptotic ratio, typical signs also reported also in human IBD. It was proposed that imbalance between apoptosis and proliferation causes relevant leaks in the epithelial barrier, allowing the entrance of luminal antigens and microorganisms (Perše and Cerar, 2012).

Intestinal microflora and their products have been implicated in the pathogenesis of human IBD, and in DSS-induced colitis in mice as well, as evidenced by the amelioration

of inflammation in germ-free animals and in mice treated with antibiotics. The first who suggested the contribution of colonic bacteria or their products in the development of colitis in this model were Okayasu et al. that observed an increased numbers of Enterobacteriaceae, Bacteroidaceae, and Clostridium spp. in the colons of mice treated with DSS. Interestingly, mice reared in germ-free conditions (lacking any intestinal microflora) develop only minor signs of mucosal inflammation, indicating that intestinal microflora may play an important modifying role in the susceptibility and responsiveness to DSS-induced damage of epithelial cells (Perše and Cerar, 2012).
Similar to IBD in humans, genetic factors play an important role in DSS-induced lesions, as demonstrated by differences in susceptibility and responsiveness to DSS among inbred strains and substrains of mice, that could be related to genetic differences in the ability of the mucosa to withstand inflammatory damage or in the capability to limit the inflammatory response, or both (Mähler et al., 1998).

The clinical and histological features induced by DSS mirror those seen in human IBD, particularly UC. Mice with high susceptibility to DSS show severe rectal bleeding and weight loss within 3-4 days of DSS administration. Other signs of illness displayed by treated mice include hunched back, raised fur, symptoms of sepsis and reduced mobility as a result of diarrhea and anaemia. Usually, mice on DSS will lose 20-30% of body weight depending on the concentration and duration of DSS (Perše and Cerar, 2012).
Acute and chronic models of intestinal inflammation can be achieved by modifying the concentration of DSS and the frequency of administration. Acute colitis is usually induced by continuous administration of 2-5% DSS for short period (4-9 days). Clinical manifestation of DSS colitis in acute phase may include weight loss, diarrhea, occult blood in stools, anaemia, and eventually death. Typical histological changes induced by DSS include mucin and goblet cell depletion, epithelial necrosis and ulceration (*i.e.* disappearance of colonic epithelium). Further, DSS induces an influx of neutrophils into the lamina propria and submucosa. Transepithelial migration of neutrophils (*i.e.* cryptitis) and extensive migration of neutrophils through the mucosal epithelium and into the crypt lumen (*i.e.* crypt abscess) are commonly associated with human IBD but occasionally reported in DSS-induced pathology. Chronic (advanced) lesions can be induced by continuous treatment with low concentrations of DSS or cycling administration of DSS (*e.g.*, 4 cycles of DSS for 7 days followed by 10 days of water). Chronic DSS colitis results in mononuclear leukocyte infiltration, crypt architecture

disarray and increasing distance (*i.e.*, widening of the gap) between crypt bases and muscularis mucosa, deep mucosal lymphocytosis and possible transmural inflammation (Perše and Cerar, 2012).

Similarly to IBD, DSS-induced colitis models displayed upregulation of different cytokines, chemokines, nitric oxide, and inducible nitric oxide synthase (iNOS). Increased expression of different Th1-mediated inflammatory mediators (TNF-α, IL-1β, IFN-γ, IL-10 and IL-12) was observed as early as the first day of DSS treatment, whose production increased progressively during DSS treatment. On the contrary, Th2-mediated inflammatory response predominates in the chronic DSS-colitis, characterized by lower levels of TNF-α, IL-17 and KC/CXCL1, and elevated levels of IL-6, IFN-γ, IL-4 and IL-10. Progressive upregulation in the transcripts for Th1 cytokines (IL-12, IFN-γ, IL-1 and TNF-α) was observed with increasing dosage of DSS. Different cytokine profile was also observed between strains (Perše and Cerar, 2012).

Interestingly, unlike IBD, the adaptive immunity (T and B cells) is not required for the development of DSS-induced colitis. Studies have shown that DSS administration causes colitis in NK-deficient and in T- and B-cell deficient mice, suggesting that these cells may not be critical in the induction of the colitis (Chassaing et al., 2015). However, some studies showed that lymphocytes contribute to colitis progression, suggesting that adaptive immunity may act as an aggravating factor in DSS-induced colitis (Kim et al., 2006).
Hence, the DSS-induced colitis model is particularly useful to study the contribution of the innate immune system to the development of intestinal inflammation, besides various aspects of IBD such as pathogenesis, genetic predisposition, and the role of microflora, as well as bowel malignancy secondary to IBD and epithelial repair mechanisms.

1.5 Role of macrophages in intestinal inflammation

The composition of the macrophage pool in the intestinal mucosa markedly changes during disruption of tissue homeostasis by infection and/or inflammation. During sterile inflammation, such as that induced by feeding mice with DSS, the normal balance between the proportion of CX_3CR1^{hi} (resident) and CX_3CR1^{int} macrophages is reversed,

with intense recruitment and accumulation of blood Ly6C^{hi} monocytes and their CX_3CR1^{int} progeny, becoming the dominant cell type during acute colitis. These CX_3CR1^{int} cells display a pro-inflammatory phenotype, retaining their enhanced production of pro-inflammatory cytokines (*e.g.* TNF-α, IL1-β, IL-6, IL-12 and IL-23), iNOS and displaying enhanced TLR responsiveness. The entry of pro-inflammatory cells into the inflamed colon mucosa is driven mainly by the CCL2(MCP-1)-CCR2, but also by CCL3-CCR1 chemokine axes (Bain and Mowat, 2014b; Cerovic et al., 2014). The chemokine CCL2 is produced at high levels in the inflamed tissues by fibroblasts, epithelial and endothelial cells in response to inflammatory cytokines or microbial molecules (Italiani and Boraschi, 2014).

Additionally, activated macrophages secrete TGF-β, which is a potent chemoattractant for other macrophages and neutrophils and, hence, increases the recruitment of these cells to sites of inflammation. Cytokine secretion not only augments the phagocytic intracellular killing but also serves as a critical link between the innate and adaptive arms of the immune system, thus playing an important role in gut homeostasis and inflammation (Dave et al., 2014).

It has been observed that the number of resident intestinal macrophages changes very little during inflammation, possibly because Ly6C^{+} recruited monocytes adopt a pro-inflammatory phenotype shaped by the inflamed environment, instead the anti-inflammatory one of resident macrophages. Moreover, they continue to produce high levels of IL-10 and are TLR hyporesponsive, suggesting that resident macrophages do not turn, or little, into pro-inflammatory phenotype under these conditions (Bain and Mowat, 2014b).

There are multiple lines of evidence, mainly using the DSS-induced colitis model, showing that Ly6C^{hi} monocytes and their CX_3CR1^{int} pro-inflammatory derivatives are directly involved in intestinal inflammation. Firstly, CCR2-deficient mice are less susceptible to DSS-induced colitis, due to defective monocytes recruitment. Second, the administration of an anti-CCR2 depleting antibody, that targets Ly6C^{hi} monocytes selectively, ameliorates colitis and correlates with lower levels of IL-6 and IL1-β in colonic tissue. Third, TNF-α production by macrophages appears to be central in disease progression, as the severity of DSS-induced colitis is reduced in TNF-α-deficient Ly6C^{hi} monocytes. Fourth, macrophages lacking STAT3, a transcription factor within the signal transduction pathway of IL-10 receptor, develop a spontaneous enterocolitis

characterized by histological features similar to IBD and increased pro-inflammatory cytokines. Fifth, Rag 1 deficient or SCID (both lacking lymphocytes) mice develop severe DSS-induced colitis, suggesting that the adaptive system does not play a primary role (at least in the acute phase) in this IBD model. Sixth, colonic macrophages of IL-10 deficient mice display exaggerated pro-inflammatory responses to bacterial products and spontaneously develop severe colitis, similar to that seen in CD patients, in consequence of the absence of this anti-inflammatory cue that drives $Ly6C^{hi}$ monocytes to preferentially differentiate into a pro-inflammatory subset producing large amounts of IL-12 and IL-23. Remarkably, the depletion of all macrophages in IL-10 deficient mice prevents the development of colitis. Moreover, IL-10 receptor deficiency is also associated with an early onset form of severe IBD in humans (Mahida, 2000; Wirtz and Neurath, 2007; Weber et al., 2009; Zigmond et al., 2013; Bain and Mowat, 2014a; Cerovic et al., 2014;)

During the resolution of colitis in mice, the expanded population of CX_3CR1^{int} pool contracts to homeostatic level, which is paralleled to a reduction of neutrophils number. The exact mechanisms for the contractions of the inflammatory cells is unclear, although it seems likely that most elicited CX_3CR1^{int} cells are cleared by apoptosis or may convert into anti-inflammatory resident macrophages that contribute to physiological tissue remodelling (Bain and Mowat, 2014b). Importantly, the contribution of intestinal macrophages to the restoration of homeostasis is dependent on the TGF-β/TGF-β receptor axis, as demonstrated by the delayed resolution of DSS-induced colitis in mice whose intestinal macrophages are unresponsive to this cytokine (Bain and Mowat, 2014a).

1.6 Intestinal macrophages in human gut homeostasis and disease

Under steady state conditions, human resident intestinal macrophages display a similar phenotype to that described in mice, characterized by profound inflammatory anergy despite avid phagocytic and bactericidal activity. As for the murine counterpart, precursors of intestinal macrophages are bone marrow-derived monocytes, which circulate through the blood before being recruited into the intestinal mucosa by IL-8 and TGF-β. These freshly recruited monocytes exhibit an inflammatory phenotype, but are immediately polarized into anti-inflammation anergic macrophages by signals from the intestinal mucosa (Kühl et al., 2015). A phenotypic monocyte differentiation process,

analogous to that displayed by mice, seems to exist in human intestine. It has been found that $CD14^{hi}CD16^{-}$ blood monocytes (equivalent of $Ly6C^{+}$ murine monocytes) appear to differentiate into resident intestinal macrophages though a series of intermediates which involves downregulation of CD14 and upregulation of CD64, CD68, MHCII, CD209 and CD163 (Weber et al., 2009; Bain and Mowat, 2011; Bain and Mowat, 2014a).

Macrophages represent one cell population contributing to the pathogenesis of IBD. Indeed, inflammatory lesions in IBD display an increased accumulations of infiltrating $CD14^{+}$ macrophages, characterized by *i)* enhanced expression of T cell costimulatory molecules (CD80 and CD86); *ii)* activated NF-κB; *ii)* production of pro-inflammatory cytokines (*e.g.* TNF, IL1-β, IL-6, IL-8, IL-23 and IFNγ), nitric oxide and CCL2/MCP-1, attracting further monocytes; and *iv)* responsiveness to exogenous stimulation (by *e.g.* TLR ligands) (Steinbach and Plevy, 2014). This macrophage phenotype might result from polarization cue derived from the pro-inflammatory environment of the inflamed intestinal mucosa that shapes the fate of newly recruited monocytes. These findings suggest a scenario where polarization toward the anergic, anti-inflammatory resident macrophages might be disturbed in IBD patients due to defective TGF-β signaling (Kühl et al., 2015)

In IBD, large numbers of $CD14^{+}CD68^{+}$ macrophages massively infiltrate the intestinal mucosa and diffusely spread throughout the thickened mucosa and submucosa and, in CD patients, they infiltrate also the muscular layer and the mesenteric fat. Even if overall macrophage numbers are comparable, the composition (M1 and M2 phenotype) and functions of intestinal macrophages differ in the inflamed gut of UC and CD patients. This might explain the overall different outcome in CD and UC (Kühl et al., 2015).

1.7 The role of extracellular matrix in inflammation

The ECM is a three-dimensional, non-cellular structure present in all tissues, composed by water, proteins and polysaccharides, and it is a fundamental component of multicellular organisms (Bonnans et al., 2014). The ECM is composed by two main macromolecules: *i)* proteoglycans, which are made of glycosaminoglycan (GAG) chains covalently linked to a specific protein core; and *ii)* fibrous proteins (*i.e.* collagens, elastin, fibronectin and laminin). It is a highly dynamic structure that provides not only essential physical scaffolding for the cellular constituents but also initiates crucial biochemical

and biomechanical cues that are required for tissue morphogenesis, differentiation and homeostasis. Each tissue has a unique ECM composition and topology that is generated during tissue development through a dynamic and reciprocal, biochemical and biophysical dialogue between the various cellular components (*e.g.* epithelial, fibroblast, adipocyte, endothelial cells) and the evolving cellular and protein microenvironment (Frantz et al., 2010).

A growing number of experimental data point out a role of several ECM proteins (*e.g.* collagens, laminins, proteoglycans and glycoproteins) in regulating the inflammatory process. ECM molecules bind via adhesins pathogens, which use the ECM as a site for propagation and spreding, causing breakdown of the ECM. Larger ECM components, that are relatively inert when bound within an uninjured matrix, may be broken down within the inflammatory environment to smaller, biologically active fragments which can also influence infiltrating inflammatory cells. In response to signals from an inflammatory environment, leukocytes leave the circulatory system and migrate through the ECM to the site of insult. During this process, interactions with the matrix serve to regulate immune cell action in both a positive and negative fashion, tailoring cell function to one that is appropriate for the type and magnitude of insult. For example, adhesion of phagocytes to various ECM components promotes phagocytic functions (*i.e.* ingestion and oxidative burst), thereby enhancing the host defence against infections. Moreover, *in vitro* studies showed that ECM can also modulate gene expression of inflammatory cells. In addition to this, cells of the immune response may transiently secrete ECM proteins in response to specific signals, and these can then act in an autocrine or paracrine fashion (Morwood and Nicholson, 2006; Adair-Kirk and Senior, 2007; Sorokin, 2010). This indicate that ECM molecules can affects many aspects of immune cell behaviours, including infiltration/recruitment, differentiation, and functional activation, both in a pro- or anti-inflammatory manner (Lu et al., 2012). Indeed, several ECM proteins have also anti-inflammatory functions contributing to the downregulation of inflammation, thereby enhancing tissue repair(Morwood and Nicholson, 2006).

In chronically inflamed tissues the ECM is modified by cytokines and proteases [in particular, matrix metalloproteinases (MMPs)] that are produced by infiltrating immune cells or by activated tissue-resident cells. There is strong evidence suggesting that several cytokines (*e.g.* TNF, IFN-γ and TFG-β), which are upregulated at sites of inflammation, can alter both the synthesis and turnover of various ECM molecules, typically those of the interstitial matrix, as well as the secretion and/or activation of

proteases in particular the MMPs, thereby leading to tissue remodelling and release of chemokines/cytokines from ECM (Sorokin, 2014). Indeed, excessive ECM production and deposition without reciprocally balanced degradation can result in fibrosis, which can lead to organ failure, besides increasing the risk of cancer (Bonnans et al., 2014).

Tissue damage and fibrosis, a consequence of local chronic inflammation and impaired tissue repair, are a hallmark of progression and severity of several chronic inflammatory diseases, including IBD. It is known, for instance, that CD progression can advance towards two seemingly opposing phenomena: *i)* excessive deposition of ECM components by myofibroblast leading to fibrosis, and *ii)* ECM destruction that eliminates boundaries between tissues, causing fistulae. Microscopic colitis, a less common form of IBD, has an ECM component as well, the thickening of the collagenous layer in the subepithelium, which is thought to be the cause of diarrhea in this condition. These examples demonstrate that ECM build-up and/or destruction play a central role in IBD (Shimshoni et al., 2015). Furthermore, MMPs are known to be upregulated in inflammatory conditions, including IBD, whose susceptibility was found to be linked to several SNPs in MMP-encoding genes. Distinct roles for different MMPs have been recently described in intestinal inflammation regulation, beyond ECM degradation, angiogenesis, fibrosis, immune cell infiltration and wound healing (O'Sullivan et al., 2015). Evidences pointed out also that the fine balance between MMPs and tissue inhibitors of metalloproteinases (TIMPs) appears to be disturbed in IBD, but how these proteins are regulated is not known (Speca et al., 2012).

Intestinal fibrosis is related to the abnormal function of several cell types, mainly fibroblasts and myofibroblasts. These cells could be activated by both autocrine factors and paracrine signals, derived from immune and non-immune cells, and by pathogen-associated molecular patterns (PAMPs) derived from microorganisms that interact with pattern recognition receptors such TLRs. Among soluble factors that regulate the activation of the ECM-producing cells, there are cytokines (*e.g.*, IL-6, Il-13; IL-17, IL-21, and TNF-α), chemokines (*e.g.*, CCL2/MCP-1 and MIP-1), growth factors (*e.g.*, TGF-β1, CTGF, IGF) and products of the oxidative stress (Wynn, 2008).

Both in UC and CD, fibrosis follows the distribution and location of inflammation, with collagens and fibronectins being the major components. In UC, the deposition of ECM is restricted to the mucosal and submucosal layers of the large bowel, whereas in CD it can involve the entire bowel wall of the GI tract including the mucosa, submucosa, muscularis mucosae, muscular and serosa layers. Injury to intestine is not an uncommon

phenomenon, even in otherwise healthy individuals. However, acute inflammatory response is usually followed by physiological healing of the damaged tissue and restoration of the normal structure and function of the intestine. If this does not occur chronic inflammation can develop, characterized by continuous events of injury and repair that may lead to the development of fibrosis. It is still unclear which factors triggers the road to chronicity in IBD, but various findings suggest that innate and adaptive immune mechanisms acting in chronic inflammation may divert the healing process towards fibrogenesis (Speca et al., 2012). Although several lines of evidence suggest that inflammation is necessary to prompt the onset of the fibrotic process, subsequently it plays a minor role in progression of the disease. Furthermore, this process does not occur in all patients, suggesting that distinct mechanisms exist for inflammation and restitution/fibrosis (Speca et al., 2012).

2. Methods

2.1 Animals

Specific pathogen free wild-type C57BL/6N and *Col6a1*$^{-/-}$, previously backcrossed in the C57BL/6N strain for eight generations (Bonaldo et al., 1998), were used. Mice were kept in filtered cages in a level B clean room under controlled temperature and light-dark cycle (23 °C, 12 h light/12 h dark cycle). All mice had *ad libitum* access to food and water before and during the study. Male mice of 3-months-old were used for intestine characterization in physiological condition, experimental DSS-induced acute colitis and recovery male mice, whereas both male and female of 2/3-months-old mice were used for FACS analysis of macrophage polarization and phagocytosis in physiological condition and after 3 days of DSS-induced colitis. Mouse procedures were approved by the Ethics Committee of the University of Padova and authorized by the Italian Ministry of Health.

2.2 DSS experimental colitis

Mice were administered 3% Dextran Sulfate Sodium (DSS; molecular weight 40 kDa, TdB Consultancy), a sulfated polysaccharide that is toxic to colonic epithelial cells and induces mucosal inflammation (Perše and Cerar, 2012), dissolved in drinking water. Three DSS models were used to study the effect of the absence of collagen VI on different phase of intestinal inflammation: *i)* 3 days DSS to assess mild inflammation to investigate macrophage polarization and phagocytosis; *ii)* 5 days DSS to induce acute colitis and *iii)* 4 days DSS followed by 10 days of recovery with tap water, to study the impact on the severity and on the healing/resolution of inflammation, respectively. Body weight of mice treated with DSS to induce both acute colitis and recovery was recorded daily and the body weight loss has been expressed as percentage of body weight treated/body weight untreated ration. At the end of the treatment mice were sacrificed by cervical dislocation, colons were carefully removed and luminal content was eliminated by flushing PBS. Colons for analysis of macrophage polarization and phagocytosis were put on RPMI on ice until manipulation. Instead, colons of mice untreated and treated with DSS to study the severity of inflammation and the resolution phase were divided in different pieces and specimens were either fixed in 10% buffered

neutral formalin and embedded in paraffin for histological analysis, or snap frozen in liquid nitrogen for further analysis (immunofluorescence, real time qPCR, and MPO assay). DSS-induced acute colitis severity was assessed with the disease activity index (DAI), that is a score frequently used on experimental colitis and it is based on three criteria: body weight, stool consistency and bleeding (Table 1). These clinical parameters are functional measurements that are somewhat analogous to clinical symptoms observed in human IBD (Murthy et al., 1993). These experiments were assessed in collaboration with Prof. Castagliuolo and Dr Brun (Department of Molecular Medicine, University of Padova).

Table 1. Criteria for scoring Disease Activity Index*

Score	***Weight loss (%)***	***Stool consistency***†	***Occult blood/gross bleeding***
0	0	normal	negative
1	1-5	loose stools	-
2	5-10	-	few blood
3	10-15	no stools	bood with loose stools
4	>15	diarrhea	blood without stools/ bleeding more than score 3

* Disease Activity Index= (combined score of weight loss, stoll consistency, and bleeding)/3.
† Normal stools = well formed pellets; loose stools = pasty stool that does not stick to the anus; no stools = no stool inside colon; and diarrhea = liquid stools that stick to the anus.
(From Murthy et al., 1993)

2.3 Histological analysis

Cross-sections (8 μm thick) of paraffin embedded specimens were processed by Prof. Porzionato laboratory (Department of Molecular Medicine, University of Padova) following standard protocols with hematoxylin–eosin to examine morphology and changes in the intestinal architecture and, after DSS-treatment, to investigate the epithelial cell erosion, the extent of inflammation and healing. Examination of the sections was performed under a Leica DM4500B microscope (Leica Microsystems) connected with a Leica DFC320 high-resolution digital camera (Leica Microsystems) and a computer equipped with Leica Application Suite Version 2.8.1 software for image acquisition (Leica Microsystems).

2.4 Real time quantitative PCR (real time qPCR)

Total RNA was extracted using TRIzol Reagent (Life Technologies) following the manufacturer's protocol. For mouse tissues 1 mL of reagent was used. Colonic RNA extracted from DSS-treated mice was further purified via precipitation with lithium chloride as previously described (Viennois et al., 2013), to efficiently remove DSS that inhibits PCR. RNA was then quantified using a Nanodrop ND-1000 instrument (Nanodrop Technologies) and 1 µg total colonic tissue RNA was retrotranscribed using the SuperScript III First-Strand Synthesis System for RT-PCR (Life Technologies), following manufacturer's instructions. Resulting cDNAs were used to perform real time qPCR using Rotor-Gene SYBR Green PCR Kit mastermix (Qiagen) with the RotorGeneQ instrument (Qiagen). The mRNA expression level of each gene was calculated by comparing with *s-16* housekeeping gene. All results are expressed as fold induction compared to wild-type in physiological condition. Primer sequences used in this study are listed in Table 2.

Table 2. List of primers for real time qPCR used.

	Forward primer (5' > 3')	**Reverse primer (5' > 3')**
s-16	GCAGTACAAGTTACTGGAGCC	CGGTAGGATTTCTGGTATCG
Col1a1	GAGCGGAGAGTACTGGATCG	GCTTCTTTTCCTTGGGGTTC
Col6a1	TGCCCTGTGGATCTATTCTTCG	CTGTCTCTCAGGTTGTCAATG
Col6a2	CATCTCACCCCAGGAGCAGGAA	TACACGTTGACTGGGCAGTCGG
Col6a3	AACCCTCCACATACTGCTAATTC	TCGTTGTCACTGGCTTCATT
Col6a4	ATGACAAGTGCCGACCAGCC	ACTAGCCGCAAAGCCCCAAG
Col6a5	TGCTCTGTTGGTGGTGTCCC	TGCCCAGGTCTAGCATCCCA
Col6a6	TTCAGTGCACAGAGGGGCAG	GACAGCTGCCTTGGTCACGT
Cxcl1	CTGCACCCAAACCGAAGTC	AGCTTCAGGGTCAAGGCAAG
Cxcl2	ATCCAGAGCTTGAGTGTGACGC	AAGGCAAACTTTTTGACCGCC
Cxcl10	ATGACGGGCCAGTGAGAATG	TCAACACGTGGGCAGGATAG
Il-1β	GCCACCTTTTGACAGTGATGAG	TGATGTGCTGCTGCGAGATT
Il-6	GAGGATACCACTCCCAACAGA	AAGTGCATCATCGTTGTTCATACA
Il-10	GACTTTAAGGGTTACTTGGGTTGC	CAGCTTCTCACCCAGGGAAT
F4/80	CTTTGGCTATGGGCTTCCAGTC	GCAAGGAGGACAGAGTTTATCGTG
Mcp-1	CTTCTGGGCCTGCTGTTCA	CCAGCCTACTCATTGGGATCA
Tnf-α	AGCCCACGTCGTAGCAAACC	CATCGGCTGGCACCACTAGT

2.5 Immunofluorescence staining

Immunofluorescence analysis were performed in both murine and human samples to detect collagen VI and macrophage immunoreactivity. In addition immunofluorescence whole mount of myenteric plexuses of the distal ileum longitudinal smooth muscle for collagen VI and peripherin was performed.

Immunofluorescence on murine specimens. Tissue cryosections (8 μm thick) were permeabilized with methanol-acetone for 10 min at -20 °C, let dry at room temperature, washed in PBS, and incubated for 30 min with a blocking solution containing 10% goat serum (Sigma) in PBS. Sections were incubated over night at 4 °C with primary antibodies diluted in 5% goat serum in PBS. The following antibodies were used: guinea pig anti-α3 collagen VI chain (1:500; kindly supplied by Prof. Raimund Wagener, Cologne) and rat anti-F4/80 (1:500; AbD Serotec). After three washing in PBS, slides were incubated for 1 h with anti-guinea pig Cy2 (1:500, Jackson Immunoresearch) and anti-rat Cy3 (1:1000, Jackson Immunoresearch) diluted in 5% goat serum in PBS solution. Nuclei were stained with Hoechst 33258 (Sigma). After washing three times in PBS, slides were mounted in 80% glycerol-PBS and analyzed by confocal microscopy (Leica SP5), supporting LAS software (Leica Microsystem).

Immunofluorescence on human specimens. The following human ileal specimens were kindly provided by Dr Angriman (Department of Surgery Oncology and Gastroenterology, University of Padova): subjects undergoing surgery for colonic carcinoma (control), macroscopically normal and diseased portion of a Chron's disease patient. Human tissue cryosections (8 μm thick) were permeabilized with methanol-acetone for 10 min at -20 °C, let dry at room temperature, washed in PBS, and incubated for 30 min with a blocking solution containing 10% goat serum (Sigma) in PBS. Sections were incubated over night at 4 °C with primary antibodies diluted in 5% goat serum in PBS. The following antibodies were used: rabbit anti- collagen VI (1:500; Fitzgerald) and mouse anti-CD163 (1:500; Santa Cruz). After three washing in PBS, slides were incubated for 1 h with anti-rabbit Cy2 (1:500, Jackson Immunoresearch) and anti-mouse Cy3 (1:1000, Jackson Immunoresearch) diluted in 5% goat serum in PBS solution. Nuclei were stained with TOTO-3 iodide (Life Technologies). After washing three times in PBS, slides were mounted in 80% glycerol-PBS and analyzed by confocal microscopy (Leica SP2), supporting LAS software (Leica Microsystem).

Whole mount immunofluorescence of murine myenteric plexuses . Distal ileal 10 cm-segments of 3-months-old mice in physiological condition were filled with fixative solution (4% paraformaldehyde, 0.2% saturated picric acid in PBS) for 1 h at room temperature and then washed with PBS for at least 1 h. Using a stereoscopic microscope longitudinal muscle layer (containing longitudinal muscle-myenteric plexus, LMMP) was gently stripped by circular muscle layer/mucosa (containing the submucosal plexus, SMP). Both layers were pinned down on a silicon support, washed with PBS/0.2% Triton X-100 (PBS-T) and then incubated for 30 min with a blocking solution containing 2% BSA-IgG free (Jackson) in PBS-T. Specimens were incubated over night. at room temperature with the following antibodies diluted in PBS-T/BSA 2%: guinea pig anti-α3 collagen VI (1:500; kindly supplied by Prof. Raimund Wagener, Cologne); rabbit anti-peripherin (1:500, Novus Biologicals). After three washing in PBS-T, specimens were incubated for 1 h with anti-guinea pig Cy2 (1:500, Jackson Immunoresearch) and anti-rabbit Cy3 (1:500, Jackson Immunoresearch) or anti-mouse Cy2 (1:500, Jackson Immunoresearch). diluted in PBS-T/BSA 2%. Nuclei were stained with Hoechst 33258 (Sigma). After washing three times in PBS, slides were mounted in 80% glycerol-PBS and analyzed by confocal microscopy (Leica SP5), supporting LAS software (Leica Microsystem) Low magnification images were acquired by optical and epifluorescence microscopy Leica DC500 ZEISS Axioplan, using the IM2000 software.

2.6 Gastrointestinal functionality assays

Functionality assays were used to analyse both GI motility and *ex vivo* contractility of the distal ileum. Gastrointestinal transit and intestinal permeability were assessed in collaboration with Prof. Castagliuolo (Department of Molecular Medicine, University of Padova), whereas ex vivo contractility were performed by Prof. Giron (Department of Pharmaceutical and Pharmacological Sciences, University of Padova).

Gastrointestinal transit. Mice were administered 70 µL FITC(fluorescein isothiocyanate)-dextran (70 kDa, MP Biomedicals LLC) in PBS (6.25 mg/mL) via oral gavage, with minimum animal handling. Mice were sacrificed after 1 h. The entire GI system, from stomach to colon, was carefully removed. Stomach, caecum and colon were examined separately, whereas the small intestine was divided equally into 8 segments. Luminal contents from each segment were collected, by flushing PBS, and clarified by centrifugation (10,000 rpm for 15 min at 4°C). Fluorescence analysis was assessed with

fluorescence spectroscopy at 494/521 nm (LS 50 B, Perkin Elmer). Data were expressed as percentage of fluorescence per each segment. GI transit was calculated as the geometric center (GC) of the distribution of the fluorescent probe along the whole tract.

Fecal output and water content analysis. Fecal excretion was assessed placing mice individually in cages and left there 1 hour. All the mice were analysed at the same time, in the morning. During this period, food was withdrawn, and fecal pellet output was then monitored. Pellets were collected, counted and weighed immediately (wet weight) and after drying (over night at 70 °C) (dry weight). Water content was expressed as percentage of (wet weight-dry weight)/wet pellet weight.

Ex vivo distal ileum contractility. Full-thickness distal ileum was isolated and gently flushed with oxygenated Krebs solution to remove luminal content. One cm ileal segments were mounted vertically by 5-0 silk ligated at each end in organ baths containing 10 mL of Krebs solution, maintained at 37°C and under aerated conditions (95% O_2 and 5% CO_2). Changes in muscle tension were recorded by isometric transducers (World Precision Instruments) connected to a quad bridge amplifier and PowerLab 4/30 data acquisition system using LabChart6 software (ADInstruments). Acetylcholine receptor-mediated contractions were evaluated in the presence of the cholinergic receptor agonist carbachol (CCh) at different concentrations (0.001-100 μM). For Electrical Field Stimulation (EFS), to evoke myenteric neuron-mediated contractions, ileal preparations were positioned between a pair of parallel electrodes connected to a Grass S88 stimulator (Grass Instrument Co.). Frequency-response curves to EFS (2-5 Hz, 1 ms pulse duration; 10-50 Hz, 10 s pulse trains, 40 V) were evaluated. In particular, EFS within 20 Hz determines a nervous response mediated by the release of acetylcholine, whereas beyond 20 Hz also muscle influence is recorded. At the end of the experiment isoprenaline was added, a β_1 and β2 adrenoreceptor agonists that provoks the relaxation of intestinal smooth muscle. Data were normalized on dry weight and both smooth muscle and myenteric neuron responsiveness were expressed ad g tension/g tissue dry weight.

Intestinal permeability. Segments of duodenum, ileum, and proximal colon were collected, rinsed free of luminal contents, and opened along the mesenteric border. Samples were mounted in Ussing chambers connected to a voltage-clamp apparatus apparatus (EVC 4009, World Precision Instruments, Saratosa, FL). Each half chamber was filled with 5 ml Krebs solution, bathing both the mucosal and serosal side of the specimen and left to equilibrate for 20 min, to achieve steady-state conditions. The

Krebs solution was continuously kept under aerated conditions (95% O_2 and 5% CO_2)and stirred by gas flow in the chambers. pH was kept at 7.4 at a temperature of 37°C with a heater block system. After equilibration, the Krebs solution in the mucosal compartment 50 μL was added of horseradish peroxidase (HRP, 10 μM; Sigma) and 50 μL of FITC–dextran (4kDa, 3 mg/mL; MolecularProbe). HRP served as marker for transcellular permeability, whereas FITC-dextran 4 kDa served as marker for paracellular permeability. After 30 minutes, a sample of 250 μL was taken from the serosal side and replaced with 250 μl mL Krebs solution. Collected samples were stored in the dark at 4°C until analysis. To determine the HRP content, 50 μL of each sample were transferred to 96-wells plate. To each well, 50 μL TMB (3,3',5,5'-tetramethylbenzidine) substrate (Thermo Scientific) was added. TMB is a cromogen that yield a blue colour when oxidazed typically as a result of oxygen radicals produced by hydrolysis of hydrogen peroxide HRP. The plate was incubated at room temperature until a pale blue colour developed (few seconds). The reaction was stopped adding 100 μL of phosphoric acid, that changes the colour to yellow and the absorbance of the coloured reaction product was measured at 450 nm using a microplate reader (Sunrise; Tecan). To determine the content of FITC–dextran, 50 μL of each sample were transferred to a Victor plate and then analyzed using a fluorescence multi-well plate reader (Victor, PerkinElmer) with excitation and emission wavelengths of 490 nm and 520 nm, respectively.

2.7 Intestinal macrophage isolation

Intestinal macrophages were isolated from colonic mucosa of both untreated and 3% DSS treated mice to analyse their polarization and phagocytosis activity.

After sacrifice, colons were carefully removed and put in RPMI media on ice. Luminal content was discarded by PBS wash, then colons were open longitudinally and incubated with DTT (10 mM, Applichem) to remove mucous for 20 min in vigorous agitation. Colonic mucosa was then scratched away from muscular layers with the help of two slides and digested for 20 min at 37°C with collagenase II (0.2 mg/mL, Sigma-Aldrich) and DNAse I (2 μg/mL, Applichem) in 5 mL of RPMI, followed by a mechanical digestion through a filter to dissociate undigested tissue. Conic material was then centrifuged in RPMI at 1,800 rpm for 8 min at 20°C. Cell pellet was resuspended in 4 mL of RPMI and layered onto 3 mL Ficoll™ Paque Plus (GE Healthcare Life Sciences) and centrifuged at

2,000 rpm for 20 min at 20°C without brake to separate mononucleated cells of the mucosa. Interphase, containing both fibroblasts ad immune cells, between Ficoll and RPMI was harvested and washed once with RPMI at 1,800 rpm for 8 min at 20°C. Then two different approaches were applied to study M1 and M2 polarization and phagocytic activity of $CD11b^+$ macrophages, both by flow cytometric analysis.

Macrophage polarization. To investigate macrophage polarization, colonic mucosa cells were analyzed by flow cytometry incubating with CD11b, a specific monocyte/macrophage marker, and M1 or M2 specific antibodies. Colonic mucosal cells of the interphase of Ficoll gradient, were once washed in RPMI and then plated a 12-well plate with 500 µL DMEM 10% FBS at 37°C for 2 h to separate infiltrating from resident $CD11b^+$ macrophages, based on their ability to adhere or not to plastic, respectively (Smith et al., 1997). Later, both infiltrating and resident cells were harvested, put in different tubes, and washed with 1 mL of BSA buffer (2% BSA in PBS) at 1,600 for 6 min at 20°C. Cell were then dispersed in 100 µL of ice cold BSA buffer and incubated with PE-coniugated CD11b (DB Biosciences) for 30 min on ice. Each samples were equally divided in two tubes and washed with 1 mL ice cold BSA buffer at 1,600 for 6 min at 20°C. Then one tube was incubated with rabbit anti-iNOS (1:100, Santa Cruz), in permeabilization buffer (eBioscience) at room temperature; one with rabbit anti-CD206 (1:100, Abcam) in BSA buffer on ice, for 30 min. Tubes were washed with ice cold BSA buffer at 1,600 for 6 min at 20°C and then incubated with anti-rabbit Cy2 in permeabilization buffer (1:200, Jackson Immunoresearch) at room temperature, or in BSA buffer on ice, for 30 min. Samples were analysed with FACScalibur (BD Biosciences) based on a CellQuest software (BD Biosciences) acquiring at least 10,000 events. Data were analyzed using the WinMDI 2.9 (Windows). One experimental replicate consisted on the sum of mucosal cells isolated from two independent colons.

Macrophage phagocytosis. To investigate phagocytic ability, colonic mucosal macrophages were sorted with MACS (magnetic cell sorting) CD11b microbeads (Miltenyi Biotec). Colonic mucosal cells of the interphase of Ficoll™ Paque Plus gradient, were once washed in RPMI and then resuspended in 400 µL of buffer (0.5% BSA, 2 mM EDTA in PBS, pH 7.2) and then incubated with with 50 µL of anti-CD11b antibody (CD11b Microbeads, Miltenyi Biotec), coniugated with metal beads for 30 min on ice. Then cells were resuspended with 1mL of buffer and centrifuged to discard unbound antibody. Cells were resuspended with 500 µL of buffer and sorted with a MS column, placed on the magnetic field of a MACS separator, that hold CD11b-bound cells. CD11b-

bound cells were then eluited by washing column with 1 mL of buffer after being removed from MACS separator. Cells were then centrifuged at 1,800 rpm for 8 min at 20°C and then plated in a 12-well plate with 500 µL DMEM 10% FBS at 37°C for 2 h to separate infiltrating from resident $CD11b^+$ macrophages. Later, infiltrating macrophages were separated from resident cells, exploiting their adherence ability, and both cell populations were incubated for 30 min at 37°C with FITC-labelled microparticles (Sigma-Aldrich). Cells were harvested, washed with ice cold buffer (2% BSA in PBS) at 1,600 for 6 min at 20°C to remove unphagocyted microparticles, and then dispersed in 100 µL of ice cold buffer and incubated with PE-coniugated MHC class II (1:100, BD Biosciences), a macrophage marker, for 30 min on ice. Cells were washed with ice cold buffer at 1,600 for 6 min at 20°C, the dispersed in 100 µL of ice cold buffer and conserved at 4°C until analysis. Flow cytometric analysis was performed with FACScalibur flow cytometer (BD Biosciences) based on a CellQuest software (BD Biosciences) acquiring at least 10,000 events. Data were analyzed using the WinMDI 2.9 (Windows). One experimental replicate consisted on the sum of mucosal cells isolated from two independent colons.

2.8 Myeloperoxidase activity assay

The determination of myeloperoxidase (MPO) activity is an index of inflammation. MPO is the most abundant pro-inflammatory enzyme stored in the azurophilic granules of neutrophils, and its determination is an index of neutrophils activity. Full thickness of colon segments were weighted and then mechanically homogenized in 5% CTAB buffer [50 mM cetyltrimethylammonium bromide (Sigma-Aldrich) in 50 mM potassium phosphate buffer, pH=6]. Homogenates were then centrifuged at 10,000 rpm for 10 minutes at 4°C. Seven µL of the supernatant was added to 100 µL of working buffer containing 0.167 mg/ml *O*-dianisidine dihydrochloride (Sigma-Aldrich) and 0.0005% hydrogen peroxide. MPO activity assays were performed in duplicates on 96 well microtiter plates and analyzed with a microplate reader (Sunrise, Tecan; Switzerland). Absorbance was recorded at 450 nm for 3 minutes at regular intervals of 1 min. MPO activity was expressed as units per milligram of tissue.

2.9 Statistical analysis

All data are expressed as means ± s.e.m. Statistical analysis of data was performed with Student's t test for unpaired data and a $P < 0.05$ was considered statistically significant (*, $P < 0.05$; **, $P < 0.01$).

3. Results

3.1 Collagen VI is expressed in ileum and colon, and around longitudinal muscle myenteric plexus

At first I analysed collagen VI deposition in both small and large intestine of 3-month-old wild-type mice (Fig. 1). Similarly to previously reported studies (Gara et al., 2011), immunofluorescence analysis with an antibody against α3(VI) chain showed that collagen VI is widely expressed along the villus/crypt axis of distal ileum, in the crypts of colon, and in the muscular layer of longitudinal and circular smooth muscle of wild-type adult intestine (Fig. 1A). I further analysed collagen VI localization by whole mount confocal immunofluorescence of longitudinal muscle myenteric plexus of distal ileum and I found that this ECM protein is also abundantly deposited in tight contact with the myenteric ganglia and the nerve fibers below longitudinal muscle (Fig. 1B).

3.2 Histological analysis does not reveal any gross abnormality in the intestine of collagen VI deficient mice

Since collagen VI has a wide distribution in murine intestine, we next investigated the impact of collagen VI ablation on the overall morphology of distal ileum and colon by histological analysis with haematoxylin-eosin staining (Fig. 2). Towards this aim, we analysed 3-month-old wild-type and *Col6a1*$^{-/-}$ mice, in which absence of the α1(VI) chain leads to a complete loss of collagen VI deposition in the ECM. When compared to wild-type, *Col6a1*$^{-/-}$ mice displayed a similar tissue morphology, and no gross macroscopic abnormalities in the architecture of ileal villus/crypt axis or of the colonic crypts were detected (Fig. 2A-B). Also smooth muscle layers appeared normal in *Col6a1*$^{-/-}$ intestine, suggesting that lack of collagen VI does not influence the general mucosal structure nor alters the muscle layer pattern.

3.3 Myenteric plexus of collagen VI null distal ileum displays a normal pattern of peripherin organization and distribution

I analyzed longitudinal muscle myenteric plexus of distal ileum from 3-month-old wild-type and *Col6a1*$^{-/-}$ mice, using whole mount immunofluorescence for the neuronal marker peripherin, a type III intermediate filament protein (Fig 3). At lower magnification, *Col6a1*$^{-/-}$ ganglia appeared to have smaller area compared to wild-type (Fig. 3A). However the number of ganglia per field seemed to be equal between wild-type and *Col6a1*$^{-/-}$ mice. Confocal high magnification maximum projection displayed a normal distribution and organization of peripherin (Fig 3B). These data suggest that the global architecture of myenteric ganglia is not grossly affected by lack of collagen VI, however further analysis are needed to understand whether collagen VI ablation has any impact on neuron number and subtype.

3.4 Collagen VI deficient mice display increased gastrointestinal motility

One of the primary functions of the GI system is motility, which refers to the contraction and relaxation of smooth muscles to allow for food transport along the whole tract. We investigated whether lack of collagen VI causes alterations in GI physiology, using different assays (Fig. 4). First, we analyzed the whole GI transit of a fluorescent probe, a FITC-dextran whose molecular weight hampers its absorption by mucosa, for 1 hour in 3-month-old wild-type and *Col6a1*$^{-/-}$ mice. This method gives a direct parameter of motility, which is expressed as the mean geometric center of the distribution of the probe fluorescence. Interestingly, *Col6a1*$^{-/-}$ mice displayed an increased FITC-dextran transit compared to wild-type (Fig 4A). I also performed further analysis of GI motility by other methods. I collected the pellet excreted in 1 hour by individually caged wild-type and *Col6a1*$^{-/-}$ mice, and I measured the water content. During pellet harvest, I did not observe differences in the appearance of stools, such as liquid or pasty, or presence of blood. The number of collected pellet resulted increased in *Col6a1*$^{-/-}$ mice compared to wild-type (Fig. 4B). Next, I weighted pellet and let them dry over night at 70°C, to measure the content of water, expressed as percentage of (wet weight – dry weight)/wet weight. I found that *Col6a1*$^{-/-}$ mice had an increased number of excreted pellet compared to wild-type, with an increased percentage of water content (Fig. 4C). Collectively, these data suggest that the GI motility is increased in *Col6a1*$^{-/-}$ mice.

We further deepened this aspect and, in collaboration with Prof. Maria Cecilia Giron (Department of Pharmaceutical and Pharmacological Sciences, University of Padova), we analysed the neuromuscular features of GI motility, by performing *ex vivo* contractility studies of distal ileum segments of 3-month-old mice (Fig. 5). We analyzed acetylcholine receptor-mediated contractions by means of cumulative doses of a cholinergic agonist, carbachol (Fig. 5A). Acetylcholine receptor is mainly expressed by smooth muscle cells and in this way only contractions originated by smooth muscle responsiveness to carbachol were recorded. The strength of carbachol-induced contractions detected in the two genotypes were comparable, suggesting that both the expression of acetylcholine receptors and their sensibility are not affected by collage VI ablation. We also recorded contractions mediated by enteric neurons applying Electric Field Stimulation (EFS) (Fig. 5B). Wild-type and *Col6a1*$^{-/-}$ mice displayed a similar neuronal responsiveness, suggesting that also the activity of enteric neuronal compartment is not affected by collagen VI deficiency.

3.5 Ablation of collagen VI affects intestinal paracellular permeability

Along the whole GI tract, a single layer of epithelial cells separates the inside of the body from the external environment, thus representing the first component of the barrier function against luminal noxious agents and molecules. Another primary function of the intestinal epithelial cells is the absorption of nutrients and water. Intestinal permeability is an intrinsic property of the intestine and is defined as the "facility with which intestinal epithelium allows molecules to pass through by non-mediated passive diffusion" (Ménard et al., 2010). We used FITC-dextran and horseradish peroxidase for 30 minutes for testing the permeability of different intestinal segments (duodenum, ileum and proximal colon) in 3-month-old wild-type and *Col6a1*$^{-/-}$ mice by using Ussing chambers. (Fig. 6). FITC-dextran is a probe with a molecular weight that allows the measurement of the paracellular permeability, *i.e.* between epithelial cells (Fig. 6A). We found that the FITC-dextran permeability was reduced in *Col6a1*$^{-/-}$ mice in each intestinal segments, compared to wild-type. We also tested transcellular permeability, *i.e.* the endocytosis process of epithelial cells (Fig. 6B). We found that the capability of intestinal epithelium to endocytosis is not affected in *Col6a1*$^{-/-}$ mice compared to wild-type. These data suggest that cell junctions, which ensure paracellular permeability, are

affected by the lack of collagen VI, thus causing an impairment in the paracellular permeability.

3.6 Lack of collagen VI influences the severity of DSS-induced colitis

The above findings indicate that in physiological conditions, despite the high expression and wide distribution of collagen VI in the intestine, lack of this ECM component does not lead to gross changes in intestinal morphology but it impacts on GI physiology leading to increased motility. While this phenotype does not seem to have any consequence on the survival rate of collagen VI deficient mice, we wondered whether it may have a role during colonic mucosa injury. Towards this aim, we administered wild-type and *Col6a1*$^{-/-}$ mice Dextran Sodium Sulphate (DSS), dissolved in drinking water at a final concentration of 3% (Fig. 7). DSS is a sulphated polymer toxic for colonic mucosa and widely used in experimental colitis. We sacrificed mice after 5 days to study the effect of collagen VI ablation on acute colitis (Fig. 7A).

Some of the visible symptoms that mice experience during experimental colitis is body weight loss, reduced motility and, in some cases, haemorrhagic diarrhea. We monitored body weight daily, whose eventual loss is the major symptom of GI inflammation, and we recorded any sign of illness. The effects of DSS treatment began to be visible at day 3 after the beginning of the experiment, when both genotypes displayed a slight decreased of the body weight. During the first days of experimental colitis, we did not observed any difference in body weight loss between the two genotypes. A small difference began to arise at day 4 after the beginning of the experiment, becoming overt and statistically significant during the last day (day 5), when wild-type mice displayed a marked body weight loss when compared to *Col6a1*$^{-/-}$ mice (Fig. 7B,C). Mice started to exhibit signs of illness, such as reduced motility, between day 3 and day 4 from the beginning of DSS treatment, and appearance of blood in stools became evident at day 4, being more frequent in wild-type than *Col6a1*$^{-/-}$ mice. Soon after the sacrifice, we performed a macroscopic examination of stool consistency and bleeding. These, together with the percentage of body weight loss at day 5, provided an evaluation of the severity of experimental colitis, whose combined score is the so-called DAI (Disease Activity Index) (Murthy et al., 1993). *Col6a1*$^{-/-}$ mice had a decreased DAI score when compared to wild-type, suggesting that the severity of DSS-induced acute colitis was lower in the absence of collagen VI (Fig. 7D). Histological analysis of paraffin embedded colons revealed the

presence of areas of inflammation, characterized by increased leucocyte infiltration, ulceration (*i.e.* disappearance of colonic crypts), and mucin-producing goblet cell depletion, typical changes described in this kind of experimental colitis model. These lesion areas were more extensive in wild-type colons, being instead more circumscribed in *Col6a1*$^{-/-}$ colons. We then analysed by real time qPCR the mRNA expression of the most upregulated pro-inflammatory (TNF-α, IL-1β, and IL-6) and anti-inflammatory (IL-10) cytokines during colitis (Fig. 8). mRNA levels of both pro-inflammatory and anti-inflammatory cytokines were upregulated in DSS-treated colons compared to physiological condition, and interestingly the levels were less increased in *Col6a1*$^{-/-}$ mice compared to wild-type following DSS treatment (Fig. 8A-D). These results, together with the DAI score and histological examination, revealed that the in absence of collagen VI mice experience a decreased susceptibility to DSS-induced acute colitis.

3.7 Collagen VI deficient mice are unable to efficiently turn off inflammation during recovery from acute DSS-induced colitis

During DSS treatment, *Col6a1*$^{-/-}$ mice displayed a decreased susceptibility to DSS-induced acute colitis, opening the question whether this was related to a delay in the onset of the inflammatory process. To assess this aspect, we carried out further experiments where DSS-induced acute colitis was followed by a recovery phase (Fig. 9). We decreased the number of days of acute experimental colitis in order to avoid the precocious death of animals, possibly due to excessive body weight loss and inflammation, particularly experienced by wild-type mice. Considering that the fourth day of acute colitis is the time point at which illness signs became evident and the difference in body weight loss between wild-type and *Col6a1*$^{-/-}$ began to be appreciated, then becoming significant at the fifth day with rectal bleeding and reduced motility, we administered 3% DSS for 4 days, followed by tap water for 10 days (Fig. 9A). We recorded body weight daily and found that, while neither wild-type nor *Col6a1*$^{-/-}$ mice were able to completely rescue the body weight loss during the recovery phase (R1-R10), *Col6a1*$^{-/-}$ mice displayed a remarkable difference in their body weight trend when compared to wild-type (Fig. 9B). At the first day of recovery (R1), wild-type mice displayed a rapid increase of body weight loss that tended to diminish during the next days (R2-R4), followed by a rescue of the body weight. This rescue was not linear, and after the sixth day (R6) wild-type mice showed a relapse, followed by a further rescue

phase of the body weight loss starting from the eighth day (R8). On the contrary, in *Col6a1*$^{-/-}$ mice body weight loss dramatically worsened compared to wild-type from the first day (R1) until the seventh day (R7), followed by a rescue from the eighth day (R8) until the tenth day (R10). Notably, the trend of body weight loss in *Col6a1*$^{-/-}$ mice remained significantly increased starting from the second day (R2) of recovery until the last day (R10), when compared to wild-type.

Histological analysis of paraffin embedded colons revealed that the amelioration of body weight loss in wild-type mice correlated with a reduction in inflammation areas and ulceration (Fig.9C). Indeed, after 10 days of recovery most wild-type mice showed an increased epithelial regeneration, and only in few cases some small areas of inflammatory cell infiltration were still present in the tissue. Conversely, *Col6a1*$^{-/-}$ colons exhibited persistent inflammatory areas, and in some cases transmural inflammatory cell infiltration in the muscle layer.

We analysed in more detail the inflammatory response during the recovery phase by real time qPCR (Fig. 10A-D). As expected, mRNA expression levels of pro- (TNF-α, IL-1β, and IL-6) and anti-inflammatory (IL-10) cytokines strongly decreased in wild-type mice after 10 days of recovery. Together with the rescue of body weight loss and histological analysis, this further evidence suggests that inflammation is going to be completely resolved in wild-type mice. Not surprisingly, in *Col6a1*$^{-/-}$ mice the mRNA expression levels of pro- and anti-inflammatory cytokines were still high during recovery when compared to acute DSS-induced colitis, and additionally they were also higher when compared to the corresponding wild-type samples. These data, supported by the increased loss of body weight and the histological analysis, strongly suggest that in the absence of collagen VI inflammation is still ongoing following acute colitis.

3.8 Collagen VI expression is highly regulated during inflammation

We wondered whether collagen VI expression is affected during colitis and how is it regulated both in the inflammatory and in resolution phase. The major form of collagen VI is made of three chains encoded by separate genes (*Col6a1, Col6a2, Col6a3*), but in some tissues three other collagen VI genes (*Col6a4, Col6a5, Col6a6*) display a restricted expression. Previous studies showed that among these three non canonical collagen VI-related genes, *Col6a6* is not expressed in the intestine (Gara et al., 2011). We analyzed the mRNA expression of *Col6a1*, *Col6a2, Col6a3, Col6a4* and *Col6a5* by real time qPCR,

together with the expression of another unrelated ECM gene, *Col1a1*, in wild-type colons (Fig. 11). Compared to physiological conditions, the expression of *Col1a1* gene was upregulated during acute colitis, but returned to basal level during recovery (Fig. 11A). Conversely, the expression of collagen VI–related genes was dynamically regulated. In fact, during acute colitis *Col6a1, Col6a2, Col6a3* and *Col6a4* were upregulated, whereas *Col6a5* did not changed, compared to physiological conditions (Fig. 11B-F). During recovery *Col6a1, Col6a2, Col6a3* and *Col6a5* expression level decreased when compared to DSS-induced acute colitis, and the expression levels of these genes were also decreased when compared to physiological conditions. The expression of *Col6a4*, instead, returned to basal levels during recovery. This peculiar pattern of expression of collagen VI related genes during acute inflammation and the subsequent resolution phase suggests a tissue- and/or environment-specific regulation for collagen VI and its different isoforms, which could mediate distinct functions.

3.9 During DSS-induced acute colitis, collagen VI deficient mice display a decreased expression of chemokine genes that is maintained during recovery

Since real time qPCR analysis in colonic specimens during recovery revealed that *Col6a1*$^{-/-}$ mice had still high pro-inflammatory gene expression levels compared to physiological conditions, we investigated the recruitment of inflammatory cells. Towards this aim, we performed real time qPCR for chemokines that act as chemotactic factors for macrophages, the most involved innate immune cell types in experimental colitis induced by DSS, and neutrophils, whose role is beneficial to resolution of inflammation by eliminating invading microbes (Fournier and Parkos, 2012) (Fig. 12). We analyzed the mRNA expression of the following chemokines: *i)* MCP-1, one of the key chemokines that regulate migration and infiltration of monocytes/macrophages; *ii)* CXCL1 and CXCL2, major neutrophil chemokines; and *iii)* CXCL10, involved in the recruitment of both monocytes/macrophages and T cells (Fig. 12A-D). Compared to physiological conditions, the expression level of these chemokines was upregulated during acute colitis in both wild-type and *Col6a1*$^{-/-}$ colons. However, their expression levels were reduced in *Col6a1*$^{-/-}$ colons when compared to wild-type. After 10 days of recovery, expression levels of all these chemokines decreased significantly in wild-type colons

compared to acute colitis, and no differences between wild-type and *Col6a1*$^{-/-}$ colons were detected. In *Col6a1*$^{-/-}$ colons, the mRNA levels of all cytokines decreased, except for CXCL10. Nevertheless, while in wild-type mice chemokine expression decreased to physiological condition levels, in *Col6a1*$^{-/-}$ mice the expression of CXCL1 was still higher compared to physiological conditions, while CXCL10 decreased to physiological condition levels. These results suggest that, except for CXCL10 in *Col6a1*$^{-/-}$ colons, the chemotaxis of inflammatory cell, which is elevated in acute inflammation induced by DSS treatment, is turned off after 10 days recovery. These data could explain the reduced cytokine expression levels displayed by wild-type mice during recovery. On the contrary, the partial decrease of chemoattractant proteins in *Col6a1*$^{-/-}$ mice could explain why they still have high cytokine levels compared to physiological conditions.

3.10 Collagen VI deficient mice display higher macrophage number, more polarized towards M1, and neutrophil activity during recovery from DSS-induced colitis

Since in the absence of collagen VI mRNA levels of chemokines and inflammatory genes are not completely abolished during 10 days of colitis, we analyzed macrophages and neutrophils during acute colitis and after 10 days of recovery. We analyzed the macrophage number in colonic mucosa by immunofluorescence for a commonly used marker, F4/80, and we also analyzed the distribution of collagen VI with respect to macrophages (Fig. 13). As highlighted by real time qPCR data, collagen VI was increased during DSS-induced acute colitis in wild-type colonic cryosections, compared to physiological conditions. Immunofluorescence showed that collagen VI was often found in contact with F4/80^{+} macrophages of the colonic mucosa, whose number was found dramatically increased in this condition. Instead, after 10 days of recovery, expression the collagen VI decreased to physiological level.

We next counted the number of F4/80^{+} macrophages in colonic mucosa (Fig. 14A). In physiological conditions, the number of F4/80^{+} cells in the colonic mucosa was decreased in *Col6a1*$^{-/-}$ compared to wild-type mice. It is well known that the number of macrophages increases both in IBD patients and in experimental models of DSS colitis, since these cells are the main players in the intestinal inflammatory process (Steinbach and Plevy, 2014). In agreement with this, the number of F4/80^{+} cells increased in both

genotypes after DSS-induced acute colitis, as also highlighted by immunofluorescence. However the macrophage number in wild-type colons was higher compared to *Col6a1*$^{-/-}$ and this difference could explain the increased expression levels for cytokines and chemokines displayed by wild-type mice during DSS-induced acute colitis. During recovery, the recruitment of inflammatory cells is turned off to allow regenerative processes to occur. In agreement with this, wild-type colons displayed a decreased number of F4/80^{+} cells, which however remained significantly higher when compared to physiological conditions. On the contrary, F4/80^{+} macrophages in *Col6a1*$^{-/-}$ colons displayed a further increase of their number during recovery. This could be related to a dysregulation of macrophage behaviour due to the absence of collagen VI.

We assessed neutrophil activity with MPO assay, which allows to determine the activity of myeloperoxidase, an enzyme contained mainly in neutrophils but also in a lesser extent in monocytes/macrophages (Fig. 14B). In physiological conditions, MPO activity, expressed as unit number on mg of tissue, was similar in wild-type and *Col6a1*$^{-/-}$ colons. After DSS-induced acute colitis, wild-type colons displayed an increased MPO activity compared to physiological conditions and to DSS-treated *Col6a1*$^{-/-}$ colons. However, in *Col6a1*$^{-/-}$ colon MPO activity remained unchanged when compared to physiological conditions. During recovery, wild-type MPO activity was reduced to physiological levels, whereas *Col6a1*$^{-/-}$ colons displayed a dramatically increase compared to physiological conditions and to DSS-acute induce colitis. These data suggest that the absence of collagen VI also affects neutrophil activity.

To gain insight on macrophage behaviour, we analyzed polarization by flow cytometry and we determined the percentage of pro-inflammatory M1 (CD11b^{+}iNOS^{+}) and anti-inflammatory M2 (CD11b^{+}CD206^{+}) colonic mucosa macrophages from wild-type and *Col6a1*$^{-/-}$ mice maintained under physiological conditions or during recovery phase. Based on their capacity to adhere or not to plastic, we also discriminated intestinal macrophages between infiltrating (*i.e.* recruited from the vascular compartment) and resident, respectively (Fig. 14C,D). The percentages of M1 and M2 macrophages, expressed as fold change, were normalized to wild-type in physiological conditions. In physiological conditions, resident macrophages had an equal distribution between M1 and M2 in wild-type colons, whereas they displayed a more pronounced M1 polarization *in Col6a1*$^{-/-}$ colons. Intriguingly, infiltrating macrophages showed similar M1 and M2 levels both in wild type and in *Col6a1*$^{-/-}$ colonic mucosa. During the recovery phase, resident and infiltrating macrophages of both genotypes displayed a higher M1 level

compared to M2 level, that was more pronounced in *Col6a1*$^{-/-}$ resident macrophages. In addition, while M1 level in wild-type resident macrophages was higher compared to physiological conditions, whereas M2 level was reduced, both M1 and M2 levels of infiltrating macrophages were reduced compared to physiological conditions. Interestingly, *Col6a1*$^{-/-}$ resident macrophages displayed an increased M1 level compared to wild-type during recovery phase, but the level did not changed compared to physiological conditions. Infiltrating macrophages of both genotypes displayed both a reduced M1 and M2 levels compared to physiological conditions. When comparing wild-type and *Col6a1*$^{-/-}$ during recovery, no difference in infiltrating macrophages emerged. These data reveal that the absence of collagen VI alters macrophage behaviour, stimulating their polarization towards pro-inflammatory M1, both in physiological conditions and during the recovery phase, when inflammation is progressively turned off.

3.11 Collagen VI deficiency affects macrophage polarization and phagocytosis in physiological conditions and during mild inflammation

Although inflammation severity in acute experimental colitis was reduced in *Col6a1*$^{-/-}$ mice, recovery experiments revealed that the inflammatory process was still ongoing and that the number of macrophages increased in *Col6a1*$^{-/-}$ mice. So we decided to study macrophage behaviour during the first steps of the inflammatory process, by treating mice with 3%DSS for 3 days, *i.e.* in mild inflammation condition, during which macrophages are strongly recruited from the vascular compartment by chemokines produced by fibroblast and epithelial cells (Fig. 15). First, we analyzed macrophage polarization by flow cytometry and we determined the percentage of pro-inflammatory M1 ($CD11b^{+}iNOS^{+}$) and anti-inflammatory M2 ($CD11b^{+}CD206^{+}$) colonic mucosa macrophages from wild-type and *Col6a1*$^{-/-}$ mice maintained under physiological conditions or during mild intestinal inflammation, discriminating between infiltrating (*i.e.* recruited from the vascular compartment) and resident, respectively (Fig. 15A,B). The percentages of M1 and M2 macrophages, expressed as fold change, were normalized to wild-type in physiological conditions. During mild inflammation, M1 and M2 levels of wild-type resident macrophages increased compared to physiological conditions, whereas they remained stable in *Col6a1*$^{-/-}$ colonic mucosa. In addition, wild-type infiltrating macrophages showed an increased M1 polarization, whereas M2 level

remained unaffected. In contrast, in *Col6a1*$^{-/-}$ colonic mucosa both M1 and M2 levels remained unchanged compared to physiological conditions. These data reveal that, besides under physiological conditions the absence of collagen VI induces a polarization of resident macrophages towards the M1 phenotype, after mild inflammation with 3% DSS for 3 days, during which resident macrophages tune their polarization and infiltrating macrophages are strongly recruited from the vascular compartment displaying a M1 phenotype in wild-type colons, the absence of collagen VI seems to alter their behaviour.

One of the functions of colonic macrophages is their ability to phagocyte pathogens or dangerous agents, which is easily testable *ex vivo* using FITC-microparticles. Colonic mucosa macrophages, magnetically sorted with CD11b^{+}, were discriminated between resident and infiltrating and the phagocytic ability of MHC type II^{+} cells was assessed by flow cytometry, and expressed as mean fluorescence of phagocyted FITC-microparticles (Fig. 15 C,D). Macrophage activity was studied both in physiological and under mild inflammation conditions. In normal conditions, wild-type resident colonic macrophages displayed a decreased phagocytosis compared to *Col6a1*$^{-/-}$ cells. This capability changed during mild inflammation, since both in wild-type and *Col6a1*$^{-/-}$ mice resident macrophages showed a reduced capability compared to physiological conditions. Notably, this decrease was much higher in *Col6a1*$^{-/-}$ mice, which showed even a reduced capability compared to wild-type mice. When comparing infiltrating macrophage activity in wild-type and *Col6a1*$^{-/-}$ mice, no difference emerged neither in physiological conditions nor under inflammation.

These data indicate that the absence of collagen VI influences the phagocytic activity of colonic macrophages in physiological conditions, which is strongly affected during mild inflammation.

3.12 Collagen VI expression and the number of CD163^{+} macrophages are increased in ileal mucosa and muscle layers of Crohn's disease patients

Altogether, our data suggest that collagen VI influences macrophage behaviour both in physiological conditions and during inflammation. Since these cells are thought to be one of the cell populations that contribute to wasting in Inflammatory Bowel Diseases, we determined whether expression of collagen VI is deregulated in samples from patients affected by Crohn disease. With this aim, we analyzed by confocal

immunofluorescence of human cryosections the distribution of collagen VI together with the macrophage marker CD163 (Fig. 16). Collagen VI immunoreactivity was found in both ileal mucosa and around smooth muscle fibers in control (*i.e.* subjects undergoing surgery for colonic carcinoma) and Crohn's disease patient specimens. Intestinal macrophages, stained for CD163, were found both in the mucosa and in the lamina propria of villi, and a high number was also present in the muscle layer of human control (Fig. 16A). Interestingly, strong immunoreactivity for collagen VI was found in macroscopically normal mucosa and muscle layer, and in diseased ileal tissue of a Crohn's disease patient (Fig. 16B). When compared to control, the number of $CD163^+$ macrophages appeared higher in macroscopically normal ileal mucosa of Crohn's disease patient, whereas they were fewer in the muscle layer. On the contrary, the macroscopically diseased ileal tissue of patient displayed a larger number of $CD163^+$ macrophages, which were found in contact with larger amounts of collagen VI. Moreover, some $CD163^+$ macrophages appeared to co-localize with collagen VI. These data suggest that collagen VI deposition could be deregulated during the onset and inflammation of Crohn's disease.

4. Discussion

The extracellular matrix (ECM) is a complex meshwork of secreted molecules that constitute the cell microenvironment, composed of a dynamic and complex array of glycoproteins, collagens, glycosaminoglycans and proteoglycans (Kim et al., 2011). The ECM is well known for its ability to provide structural support for organs and tissues, for cell layers in the form of basement membranes, and for individual cells as substrates for cell motility (Hynes 2009). Besides its original concept as an inert, space-filling material that provides only mechanical strength to tissue and organ, the ECM is now considered as a dynamic structure that interacts with cells and generates biochemical signals through feedback loops that orchestrate their behavior. Indeed, ECM macromolecules modulate a plethora of cellular events, spanning from proliferation, migration, growth, differentiation, to survival (Daley et al., 2008). The importance of ECM is evident by the increasing number of diseases associated with mutations of genes coding for ECM components and affecting tissue homeostasis, ranging from musculoskeletal, cardio-vascular, renal, ocular and skin defects. In addition, excessive deposition or, conversely, destruction of the ECM can also lead to pathologies such as fibrosis or osteoarthritis (Naba et al., 2015).

Among the complex network of ECM proteins, collagen VI has been emerged in the last decade as a multifunctional component, whose dysregulation is related to numerous diseases.

Collagen VI is a glycoprotein with a widespread distribution in tissues of multicellular organisms, and particularly abundant in the basement membrane of skin and skeletal muscle. It is mainly composed by three different chains encoded by separate genes and organized in a supermolecular assembly, leading to the formation of a extended microfilamentous network that links cells and other ECM components (Bonaldo et al., 1989). The complexity of collagen VI is further increased by the recent discovery of three additional genes encoding for collagen VI chains, whose homology with α3(VI) chain suggests that they are able to form alternative α1α2α4, α1α2α5 or α1α2α6 triple helical assemblies (Fitzgerald et al., 2008; Gara et al., 2008). Mutations in gene encoding collagen VI cause the so-called collagen VI-related myopathies, which comprised principally Bethlem myopathy and Ullrich congenital muscle dystrophy (Bönnemann,

2011). However, altered expression or mutations of the collagen VI genes have been linked to the central and peripheral nervous system, articular cartilage, bone and also to cancer (Cescon et al., 2015).

The collagen VI knockout mouse generated by the team of Prof. Bonaldo in 1996 has provided a valuable model for the dissection of the pathomolecular defects caused by the lack of collagen VI and for the identification of novel therapeutic opportunities in the treatment of the corresponding human diseases (Bonaldo et al., 1998). The initial characterization of collagen VI null (*Col6a1*$^{-/-}$) mice revealed that ablation of this ECM protein has a major impact in skeletal muscles, causeing myofiber apoptosis and degeneration and leading to muscle weakness and wasting (Irwin et al. 2003; Grumati et al. 2010). Detailed investigations of the pathomolecular mechanisms underlying these defects revealed the presence of dysfunctional mitochondria and altered organelles, whose accumulation is caused by a defective regulation of the autophagic process associated with oxidative stress and increased production of reactive oxygen species (Irwin et al. 2003; Grumati et al. 2010; Menazza et al. 2010). Collagen VI knockout mice also display decreased muscle strength and lower resistance to physical exercise (Irwin et al. 2003; Grumati et al. 2011). Besides these studies focused on skeletal muscles, the *Col6a1*$^{-/-}$ mouse model was also used to investigate the effects of the absence of this protein in the homeostasis of other tissues. Altogether, these studies revealed that collagen VI regulates a plethora of different cellular and tissue events, including mechanical support, cytoprotection, cell differentiation, and tissue regeneration.

Despite its broad distribution in the intestinal compartment, the role of collagen VI in this district was never investigated before. The aim of this part of my PhD work was to investigate the role of collagen VI in intestine homeostasis and during inflammation in an experimental model of colitis.

Collagen VI is widely distributed in both distal ileum and colon. In particular, it appears concentrated throughout the lamina propria along the villus/crypt axis of distal ileum, in the crypts of colon and in the muscular layer of smooth muscle of wild-type mice, in agreement with previous studies (Gara et al., 2011). In the intestine, collagen VI can be synthesized and secreted not only by interstitial fibroblasts, the main ECM-producing cells in the body, but also by smooth muscle cells (Colombatti and Bonaldo, 1987). In addition, it has been found that collagen VI is also produced by intestinal epithelial cells as a basal lamina component (Groulx et al., 2011). Studies concerning the differential

expression of the additional three chains of collagen VI highlighted a peculiar distribution pattern in intestine: α4(VI) chain is abundant in the sub-mucosal and mucosal layers but completely absent in the muscular layer, α5(VI) is present in the mucosal layer, and α6(VI) is completely absent (Gara et al., 2011). Furthermore, we found that collagen VI is abundantly deposited in tight contact with the myenteric ganglia and nerve fibers below longitudinal muscle of distal ileum. However, it seems that collagen VI does not co-localize with peripherin, a neuronal marker, and it is not preset inside nerve fibers, strongly suggesting that it is not produced by neurons. Previous immunohistochemical studies on of the distribution of various ECM components in rat and guinea pig colon showed that also laminin, fibronectin and collagen IV are present in or nearby the basement membrane that surrounds enteric ganglia, whereas nidogen and heparin sulphate proteoglycan were demonstrated in the basement membrane of both enteric ganglia and Schwann cells (Bannerman et al., 1986). Our group showed that collagen VI is produced by Schwann cells and has a role in regulating myelination and function of peripheral nerve (Vitale et al., 2001; Chen et al., 2014). This opens the possibility that in the enteric compartment collagen VI may be also produced by enteric glial cells, that are actively involved in the control of gastrointestinal functions, such as motility, mucosal secretion, host defence, epithelial permeability and support for neurons and epithelial cells (Gulbransen and Sharkey, 2012). A putative role for collagen VI in myelination in this compartment is however unlikely, since enteric glial cells envelop neuronal cell bodies and axon bundles without producing myelin (Rühl, 2006).

The ECM plays a crucial role during development and absence of one of its components may lead to profound changes in the overall tissue architecture, even causing premature death. For example, laminin α5 deficient mice die embryonically due to smooth muscle defects in the small intestine, although overt alterations in villus organization was also reported, whereas lack of laminin α5 chain specifically in the subepithelial basement membrane of small intestine leads to a compensatory deposition of colonic laminins, resulting in a tissue transformation from small intestinal to colonic mucosal architecture (Bolcato-Bellemin et al., 2003; Mahoney et al., 2008). The mouse knockout model of collagen VI does not display any abnormality during embryonic development and mice are viable at birth, without any overt anatomical defect (Bonaldo et al., 1998). The macroscopic architecture and morphology of organs is not altered in collagen VI null

mice, except for skeletal muscle which shows an early onset myopathic phenotype. Therefore, it is not surprising that, despite its wide distribution in murine intestine, lack of collagen VI does lead to any gross abnormality in the overall intestinal architecture. Considering the primary functions played by the gastrointestinal system, from digestion and absorption of nutrients to protection against pathogens, collagen VI deficient mice are able to grow and feed and no visible alteration is seen under physiological conditions. By investigating the morphology of myenteric plexuses of distal ileum, we found that ganglia are smaller in collagen VI null mice, despite the regular organization and expression of peripherin. Enteric ganglia are composed by several neuronal subtypes, classified on the basis of the neurotransmitter they secrete, and glial cells. It may be interesting to deepen this studies in the future to assess whether collagen VI may influence the survival, number and subtypes of enteric neurons, besides glial cells. The impact of ECM on the differentiation of specific neuronal subtypes was recently investigated by *in vitro* cultures of enteric neurons in smooth muscle engineered sheets, with different combinations of collagen I, collagen IV, laminin and/or heparan sulphate (Raghavan and Bitar, 2014). It was found that enteric neuronal progenitor cells differentiate to functionally innervate smooth muscle, capable to mediate contraction/relaxation pattern by neuronal stimuli, in different ways based on the influence of ECM composition. Thus, a specific microenvironment could influence neuronal differentiation and may also facilitate adequate trophic support and phenotype maintenance of differentiated neurons.

Past studies on collagen VI deficient mice revealed that the functionality is impaired or reduced in several tissues. The first evidence emerged in skeletal muscle, in which the lack of this ECM component causes a loss of contractile strength (Irwin et al., 2003). Furthermore, the absence of collagen VI affects peripheral nerve conduction velocity, motor coordination and delays the response to acute pain stimuli (Chen et al., 2014). A decreased tensile strength and stiffness was also found in collagen VI deficient tendons (Izu et al., 2011). We carried out several studies aimed at assessing the effects of the absence of collagen VI in intestinal functionality. We first measured gastrointestinal motility and found that collagen VI deficient mice have an increased transit of the dextran fluorescent probe compared to wild-type. This data was corroborated by the increased number of fecal output, which can be considered an index of colonic propulsion, and the increased water content, indicating that that the increased motility

exhibited by collagen VI deficient mice leads to a higher number of excreted pellet impairing the efficiency of water absorption. An intact enteric nervous system with the preservation of myenteric ganglia is required for intestinal motility and function, which is achieved by contractions and relaxations of the smooth muscle. Surprisingly, at difference from previous studies on skeletal muscle (Irwin et al., 2003) and peripheral nerves (Chen et al., 2014), *ex vivo* contractility performed on distal ileum segments showed that lack of collagen VI does not affect the neuromuscular features of gastrointestinal motility, *i.e.* neither smooth muscle nor neuronal responsiveness. It remains to be explored whether the increased gastrointestinal motility observed in the absence of collagen VI is due to a differential pattern of secreted neurotransmitters, *i.e.* increased number of excitatory enteric neurons or decreased inhibitory neurons, or if the release or uptake of neurotransmitters is affected. Besides the activity of the enteric nervous system, gastrointestinal motility is also regulated by spontaneously active pacemaker cells, namely interstitial cells of Cajal. A hypothesis that could be explored in the future is whether the number of interstitial cells of Cajal is affected by lack of collagen VI.

Several studies shed light on the importance of the ECM in the gut colonization by neural crest cells, the progenitors of the vast majority of both enteric neurons and glial cells. Lack of a defined ECM pattern impairs the migration of neural crest cells, thereby leading to severe enteric nervous system related disease, such as Hirschsprung's disease, characterized by the absence of neural ganglia along variable length of the distal intestine, resulting in a functional obstruction (Tam, 2016). ECM molecules function as substrates for locomotion, guidance and signalling during enteric neural crest migration and enteric nervous system formation, and several proteins were found to coordinate this process, including fibronectin, tenascin-C, laminins, collagen IV and proteoglycans (Newgreen et al., 2013). Also a role for cell-ECM adhesion receptors, especially β1 integrin, was proposed, since ablation of β1 integrin leads to lack of ganglia in the descending colon and to abnormal enteric nervous formation, due to progenitor impairment in interacting with migration-promoting fibronectin (Breau et al., 2009). Recently, also collagen VI emerged as a new player in the scenario. A novel insertional mutant mouse line as Hirschsprung's disease model has been identified, in which enteric neural crest cells specifically overexpress *Col6a4.* Increased cell-autonomous deposition of collagen VI around enteric neural crest cells during development resulted in slower

migration of these cells, most likely due to interference with fibronectin, and thereby leading to an aganglionic megacolon phenotype resembling Hirschsprung's disease (Soret et al., 2015).

The relationship between gastrointestinal motility disorders and muscular dystrophies has been reported in literature since long time. Gastrointestinal symptoms are frequent in patients with myotonic dystrophy type 1 and may be associated with reduced gastrointestinal motility caused by smooth muscle dysfunction (Tanaka et al., 2013). The dystrophin deficient *mdx* mouse model displays alterations in the gastrointestinal propulsion, with a significant delay in the small intestinal transit and a decreased amount of excreted stools, possibly due to impairment of nitric oxide function (Mulè et al., 2010). However, to date, no evidence of gastrointestinal disorders in patients affected by collagen VI-related myopathies has been reported.

Intestinal permeability, an intrinsic property of the intestinal epithelium, refers to the transport of molecules from the intestinal lumen to the lamina propria. It can occur through two distinct mechanisms, *i.e.* paracellular and transcellular permeability. The epithelium is composed by a single cell epithelial layer, whose cohesion and polarity is guaranteed by the apical junctional complex, characterized by tight and adherens junctions, and by the subjacent desmosomes (Ménard et al., 2010). Among these, tight junctions are the rate-limiting factor for the epithelial paracellular permeation of molecules, controlling molecular penetration of ions, solutes, water and cells, besides their role as a fence dividing apical and basolateral domains to compartmentalize the plasma membrane (Ichikawa-Tomikawa et al., 2011). Literature work showed that ECM and tight junctions influence the expression and function of each other components. Alveolar epithelial cells cultured on three different ECM components display different outcomes: on fibronectin coat cells they form high-resistance barriers and show continuous claudin-3 and claudin-18 localization to the plasma membrane, as opposed to cells cultured on either collagen I or laminin, which form low resistance monolayers and display areas of cell-cell contact that are claudin deficient (Koval et al., 2010). In turn, claudins have identified to modulate the activation of ECM metalloproteinases, enzymes that are involved in the degradation of various ECM components and playing important roles in tumour invasion and spreading leading to metastasis (Hwang et al., 2014). In intestine, it has been recently found that syndecan-1 acts in synergy with tight junctions in the maintenance of regulation of the intestinal barrier, and that this

proteoglycan is able to modulates the expression of tight junction components ZO-1 and occludin (Wang et al., 2015). In our studies, it emerged that the paracellular permeability is decreased in the absence of collagen VI. This may be due to a differential expression and/or distribution of tight junction proteins, or to changes in the microenvironment of the basement membrane, due to lack of collagen VI. A recent *in vitro* study showed that intestinal epithelial cells cultured on a basement membrane-coated substrate display a columnar appearance of cells and a distribution of tight junctions that is closer to *in vivo* intestinal epithelium (Vllasaliu et al., 2014). Collagen VI knockdown in epithelial cells leads to striking cell spreading and is accompanied by a significant increase in the number of stress fibers and of adhesion structures in the central body of the cell (Groulx et al., 2011). Moreover, collagen VI is characterized by a microfilamentous network interacting with several other ECM components, and its absence affects *in vitro* fibronectin production, deposition and organization (Groulx et al., 2011; Sabatelli et al., 2001). As consequence, loss of collagen VI leads to a destabilization of its complex network thereby impairing biomechanical properties of tissue, as emerged in skeletal muscle and tendons (Izu et al., 2011; Urciuolo et al, 2013). Therefore it may be possible that both biochemical and mechanical cues affect intestinal permeability in the absence of collagen VI. On the contrary, transcellular permeability, which involves endocytosis at the epithelial luminal membrane followed by exocytosis at the basolateral membrane of large molecules, seems to be not affected in collagen VI null mice, suggesting that the epithelial function and/or the endocytosis mechanisms are not perturbed by the lack of this ECM protein.

Tissue regeneration is a process during which interactions between infiltrating inflammatory cells and resident cells must be finely coordinated in order to restore homeostasis and functionality. ECM components are other main actors in this scenario, as they can both control the way in which a tissue responds to injury and function as a scaffold where the regenerative process occurs. Based on the amplitude of the injury, ECM responses can be both positive or detrimental, leading for example to unfunctional fibrotic tissue substitution. Moreover, the ECM serves as a reservoir for several growth factors and cytokines that are released during ECM remodeling, and cell can respond to both mechanical and biomechanical changes in the ECM through crosstalk between integrins and the actin cytoskeleton (Kim et al., 2011). In this way, ECM bioactive molecules can modulate the inflammatory process, by promoting infiltration/migration,

activation, both in pro- and anti-inflammatory manner. Thus, the inflammatory process becomes the only way with which the body reacts against noxious agents to restore tissue homeostasis, but if this process persists inflammation become chronic resulting in anatomical and functional abnormalities. Collagen VI recently emerged as a key ECM component that plays active roles during tissue regeneration. Moreover, its involvement in an increasing number of diseases corroborates the concept that there is still much to unveil about the functions of this ECM molecule. Of note, collagen VI is needed for maintaining a proper skeletal muscle stiffness, which in turn regulates satellite cell activity during muscle regeneration (Urciuolo et al., 2013). Collagen VI was also implicated in peripheral nerve regeneration, where it plays a crucial role in macrophage recruitment and polarization (Chen et al., 2015a). In addition, a very recent study by our team highlighted a role for collagen VI in hair follicle regeneration (Chen et al., 2015b).

The best way to study tissue regeneration and inflammation in the intestine is to perform mucosal injury by experimental model of colitis. In the past years, several experimental models of colitis were proposed, using different approaches. Among them, one of the most used and well-established is Dextran Sodium Sulphate (DSS)-induced colitis, particularly useful to study the contribution of the innate immune system to the development of intestinal inflammation. Studies about the role of ECM in experimental models revealed that it influences in different manner the severity of colitis and the inflammatory response. Most of these studies concerned proteoglycans. Lumican, a keratin sulphate proteoglycan present in large amounts in connective tissues rich in fibrillary collagen such as the intestinal submucosa, was shown to affect the outcome of colitis, with low innate immune and inflammatory responses, and a more severe body weight loss and tissue damage (Lohr et al., 2012). Also syndecan-1 has protective effects during experimental colitis, since its lack aggravates colitis by promoting increased leukocyte recruitment accompanied by up-regulation of inflammatory mediators, thus hampering efficient wound repair (Floer et al., 2010). Moreover, orally administration of proteoglycans in DSS-induced colitis in rats ameliorates the clinical symptoms of bloody stools and diarrhea, and reduces the degree of mucosal erosion and inflammatory cell infiltration into the erosive area (Ota et al., 2008). Among ECM glycoproteins, osteopontin deficiency accelerates the spontaneous development of colitis in IL-10 deficient mice, by affecting the gut microbiota and macrophage phagocytic activity (Toyonaga et al., 2015). Laminins seem to exert different effects: high expression of

laminin α1 and α5 decreases susceptibility to experimentally DSS-induced colitis, but in a pro-oncogenic context they favors colitis-associated cancer (Spenlé et al., 2014). To our knowledge, no extensive studies about the effects of the lack of collagens in experimental colitis have been reported in the literature until now. However, treatment with the synthetic collagen analogue $(Gly\text{-}Pro\text{-}Hyp)_{10}$ was found to ameliorate colitis, by interfering with collagen binding of proMMP-2 and proMMP-9, which in turn are involved in the recruitment of immune cells such as neutrophils and macrophages and shedding of biologically active proinflammatory cytokines (Heimesaat et al., 2012).

During DSS-acute colitis, lack of collagen VI seems to exerts a beneficial effect on the severity of the experimental colitis. In fact, in the absence of collagen VI mice display less signs of illness, displaying lower body weight loss and decreased DAI. Histological analysis, accompanied by real time qPCR data about inflammatory cytokines, confirmed these findings, indicating that in the absence of collagen VI the responsiveness to DSS is markedly reduced. In the literature it is well-known that DSS has differential susceptibilities based on different factors, where microbiological and genetic ones are the most important, but the way it works in inducing mucosal damage is still poorly known (Perše and Cerar, 2012). However, it is conceivable that, following the alterations in the mucous layers induced by DSS, bacteria are more able to reach the epithelial cells, triggering an inflammatory reaction (Johansson et al., 2010). Moreover, several studies pointed out that the proper integrity of the intestinal epithelium is essential to prevent the entrance of luminal microbes and their potentially toxic products, triggering mucosal inflammation. Besides this, physiological permeability, guaranteed by apical junctional complexes of tight junctions that form a physical barrier linking together cells, also plays a crucial role. During experimental colitis in rats, the permeability increases, as a consequence of the changes in the expression and distribution of claudins, increased intestinal epithelial cell apoptosis and the activation of the immune system (Yuan et al., 2015). Our data show that collagen VI deficient mice display a decreased intestine permeability in physiological conditions, and this may explain the different susceptibility to DSS with respect to wild-type mice, possibly impairing the entrance of luminal bacteria and consequently reducing the immune system activation. Further studies on the expression and distribution of tight junction proteins in the epithelial cells during colitis of wild-type and collagen VI null mice will be useful to get more insights on this aspect.

With the aim to investigate possible delay in the inflammatory process, we performed a recovery study following DSS-induced colitis. Notably, lack of collagen VI caused a marked body weight loss during the recovery phase. Although 10 days recovery were not sufficient to restore completely the body weight loss displayed by wild-type mice, the partial rescue of the body weight loss in wild-type mice was accompanied by amelioration of the histological signs, showing small inflammatory areas and increased epithelial regeneration, signs that were on the contrary exacerbated during acute colitis. These findings support the concept that collagen VI exerts a beneficial effect on tissue regeneration, as previously highlighted by our studies in other tissues, such as skeletal muscle and peripheral nerve system (Urciuolo et al., 2013; Chen et al., 2015a). On the contrary, in the absence of collagen VI, mice display a dramatical worsening of the body weight loss when compared to wild-type mice. In addition, histological analysis revealed persistent inflammatory areas, which became in some cases more severe leading to transmural inflammation. These data are corroborated by the persistently high expression of inflammatory cytokines in collagen VI null mice during recovery when compared to acute DSS-induced colitis, indicating that the inflammatory process is still ongoing in the absence of collagen VI. These findings suggest that collagen VI is required to efficiently break off inflammation, following noxious stimulus withdrawal, thereby enhancing tissue regeneration.

Several studied pointed out that the ECM influences macrophage modulation and function as a structural scaffold for immune cell infiltration. Biomaterials based on collagen I matrix containing high-sulfated hyaluran are able to modulate human pro-inflammatory M1 macrophages by decreasing inflammatory macrophages functions, including uptake of pathogens and release of pro-inflammatory cytokines, and by decreasing the activity of transcription factors controlling macrophage polarization towards M1 subset (Franz et al., 2013). *In vivo* implanted hydrogel coatings composed by dermal and urinary bladder ECM show a reduced pro-inflammatory M1 response and a resultant increase in M2:M1 ratio, with a decreased foreign body reaction (Wolf et al., 2014). Tenascin-C was shown to enhance inflammatory responses by accelerating macrophage migration and synthesis of proinflammatory/profibrotic cytokines via integrin $\alpha_V\beta_3$/FAK-Src/NF-κB, resulting in increased cardiac fibrosis (Shimojo et al., 2015).

ECM can also exerts several functions contributing to tumor progression, by releasing

proteolytic fragments that act as inflammatory stimuli for the recruitment of innate immune cells and the expression of pro-inflammatory genes, such as elastin fragments, denaturated and fragmented collagen I, fibronectin, soluble biglycan and tenascin-C (Chanmee et al., 2014). In addition, a tightly cross-talk exists between ECM and macrophages. ECM components can be secreted by macrophages, that conversely can also influence tissue remodeling by secreting metalloproteinases, thereby facilitating the recruitment of further inflammatory cells to the site of tissue injury (Murray and Wynn, 2011). A growing number of studies indicate that collagen VI, highly expressed in a variety of tumors, affects the tumor microenvironment by increasing the recruitment of macrophages, thus promoting tumor development and metastasis via modulation of the immune system. The synthesis and secretion of collagen VI by macrophages depends on their activation stage, stage of differentiation, and cell density. M2 macrophages were reported to produce more α3(VI) than M1 macrophages, suggesting tumor-associated macrophages, which are mainly skewed towards M2 phenotype, as one of the key providers for collagen VI in tumors, and collagen VI significantly enhances the *in vitro* adhesion of macrophages, suggesting a potential role in macrophage recruitment (Schnoor et al., 2008). This concept is supported by the evidence that the cleaved C5 domain of collagen VI (also called endotrophin) is able to promote tumor inflammation by increasing macrophage recruitment and upregulating the production of inflammatory factors (Park et al., 2012; Chen et al., 2013).

The role of collagen VI on *in vivo* macrophage function has been extensively demonstrated by our findings in peripheral nerve regeneration. We recently published that collagen VI is an essential component of peripheral nerves required for proper nerve myelination and function, and during nerve injury it plays an essential role in macrophage recruitment and polarization, whose activity is pivotal for debris clearance, growth factor production, ECM remodeling and tissue regeneration (Chen et al., 2014; Chen et al., 2015a). In particular, our studies showed that addition of purified native collagen VI *in vitro* functions as a chemoattractant for macrophages, increasing their migration, and promotes M2 polarization. Furthermore, collagen VI regulates both macrophage migration and polarization towards M2 *in vivo*, contributing to PNS regeneration (Chen et al., 2015a).

The major inflammatory cell types in the DSS model of colitis belong to the innate immune system, first macrophages, followed by neutrophils, which are recruited mainly

by the former. On the contrary, the adaptive immune system is not crucial in induction of DSS colitis in mice (Axelsson et al., 1996). Several lines of evidence point out that central to inflammatory responses are the integrin-mediated adhesive interactions of cells with their ECM-rich environment, highlighting the importance of ECM-monocyte interactions in the pathogenesis of experimental colitis, and the link with inflammatory bowel disease in humans. Of note, inhibition of the main collagen-binding integrin $\alpha_1\beta_1$ expressed on monocytes in two different experimental models of colitis is associated with significantly attenuated inflammation, decreased mucosal monocyte accumulation, activation, and pro-inflammatory cytokine production, demonstrating that the engagement of integrins by ECM plays a pivotal role in mediating intestinal inflammation via promotion of monocyte/macrophage movement and/or activation within the inflamed tissue (Fiorucci et al., 2002; Krieglstein et al., 2002). In addition to the pro-migratory role of integrins in the blood-to-tissue paradigm, it has been emerged that $\alpha_1\beta_1$ integrin adhesion specifically inhibits macrophage exit from a peripheral inflammatory lesions, thereby causing the persistence of macrophages in tissue, and the subsequent cytokine production feeding inflammatory responses until chronicity (Becker et al., 2013). Besides this, also blockade of either $\alpha_4\beta_1$/VCAM-1 and $\alpha_L\beta_2$/ICAM-1 was found to ameliorate experimental colitis, abrogating leukocyte invasion and adhesion (Soriano et al., 2000; Bendjelloul et al., 2000) In this scenario, it appears clear that a fine balance in ECM-inflammatory cell interactions is needed. To gain insight about the role of collagen VI in innate immune system involvement during intestinal inflammation, we analyzed the expression of chemokines, acting as chemotactic factors for macrophages and/or neutrophils, as well as macrophage polarization and neutrophil activity, in acute colitis and recovery conditions. During acute colitis, increased levels of chemokine expression were found in the presence of collagen VI, which progressively reduced during the recovery phase. This decrease could be related to the fact that inflammatory cell recruitment should be completed, following DSS withdrawal, to allow regeneration mechanisms to occur. Interestingly, the expression of collagen VI was also modulated during different phases of inflammation, showing an increase during acute colitis, and a decrease in the subsequent resolution phase. These findings suggest a putative role as chemoattractant for this ECM component, corroborating our previous findings in peripheral nerve injury (Chen et al., 2015a). Moreover, since collagen VI is known to interact with several integrins, including $\alpha_1\beta_1$, it may promote monocyte

migration via these receptors (Pfaff et al., 1993). Modulation of collagen VI deposition during the first stages of inflammation was also highlighted by our previous works in skeletal muscle and peripheral nerve (Urciuolo et al., 2013; Chen et al., 2015a). Moreover, collagen VI genes display a peculiar pattern of expression during the different phases of intestinal inflammation, suggesting that probably a tight tissue- and/or environment-specific regulation of its different isoforms may occur, thereby mediating distinct functions to ensure tissue homeostasis. In addition, further analysis revealed that collagen VI is important for intestinal macrophage number, polarization and activity, both in physiological condition and in different phase of inflammation. In fact, lack of collagen VI affects macrophages number in the colonic mucosa in physiological conditions, and macrophages are more polarized toward the pro-inflammatory M1 phenotype, whereas the presence of collagen VI ensure a balanced M1:M2 ratio. Based on our data, it emerges that during inflammation the number of macrophages in collagen VI deficient mice progressively increases during acute colitis and the subsequent recovery phase, in association with an increase of neutrophil activity, thus explaining why inflammation is still ongoing in the absence of this ECM component during the recovery phase. The aberrant microenvironment caused by lack of collagen VI probably affects a proper anti-inflammatory M2 activity of resident macrophages, unable to trigger efficiently tissue regeneration, considering the huge number of M1 still present in the tissue during the recovery phase. To gain more insight about the effects of collagen VI on macrophages behavior and activity, we analyzed macrophage polarization in the first steps of experimental induced colitis, when inflammation is still mild. In this context, when resident macrophages should tune their polarization toward M1 to respond to noxious stimuli, and infiltrating macrophages are strongly recruited by the blood compartment as an effect of the inflammatory process, lack of collagen VI does not efficiently increase resident and infiltrating M1 polarization, possibly because of an impaired chemoattractant activity. In addition, during mild colitis, lack of collagen VI also impairs the phagocytic activity of resident macrophages, suggesting a role for this ECM protein in regulating macrophage activity. Since it is known that autophagy is strictly related to phagocytosis, the defective autophagic regulation that occur in collagen VI deficient mice (Grumati et al., 2010) may be also occurring in intestinal macrophages, thereby explaining the decreased phagocytosis displayed by these cells under mild inflammation. Our findings suggest that collagen VI exerts a crucial role in

intestinal macrophage behavior, influencing M1:M2 ratio and activity, both in homeostatic conditions and during inflammation. Moreover, since collagen VI is produced by macrophages, it could be possible that this ECM protein exerts its modulation by both paracrine and autocrine manner. The hypothesis that collagen VI promotes macrophage recruitment and activity through integrins remains to be explored in the future.

The innate immune system is thought to be the main player in the pathogenesis of IBDs, complex multifactorial disorders characterized by chronic relapsing intestinal inflammation. Inflammatory lesions in IBD display increased accumulation of infiltrating macrophages, whose pro-inflammatory M1 phenotype worsens the course of the disease (Steinbach and Plevy, 2014). Analysis of collagen VI immunofluorescence revealed a strong deposition and expression of this ECM component in the ileal mucosa and muscular layer not only in macroscopically diseases, but also in apparently normal ileum of a CD patient, as compared to non-affected subjects. Moreover, the macroscopically diseased ileal tissue of patient displayed a high number of macrophages, which were in contact with larger amounts of collagen VI. The co-localization of collagen VI and macrophages in CD diseased ileum suggests that this ECM component is expressed by macrophages, in the light of previous findings about production of collagen VI by human macrophages (Schnoor et al., 2008). These data suggest the novel concept that dysregulation of this ECM component can precede tissue damage and play an active role in the onset and maintenance of inflammation in IBD, possibly by modulating inflammatory cell recruitment and facilitating their invasion through cell-matrix interactions. Moreover, by regulating macrophage function, collagen VI may be relevant to IBD pathophysiology, in the light of the primary macrophage intrinsic dysfunction described in CD patients, resulting in an impaired attraction of granulocytes and inappropriate ignition of defensive inflammatory responses toward intruding luminal bacteria (Casanova and Abel, 2009).

In conclusion, this part of my PhD work supports the concept that a defined ECM microenvironment composition is critical for triggering an appropriate inflammatory response to counteract toxic agents and a subsequent tissue regeneration to ensure homeostasis. Among the intestinal ECM components, collagen VI reveals to be a novel intriguingly actor, by actively contributing to the preservation of intestinal homeostasis

and tuning appropriate inflammatory response by modulating intestinal macrophage activity. Considering the increasing evidence about macrophage dysfunction in the onset and development of IBD, collagen VI may have broad implications as a potentially new biomarker for disease progression.

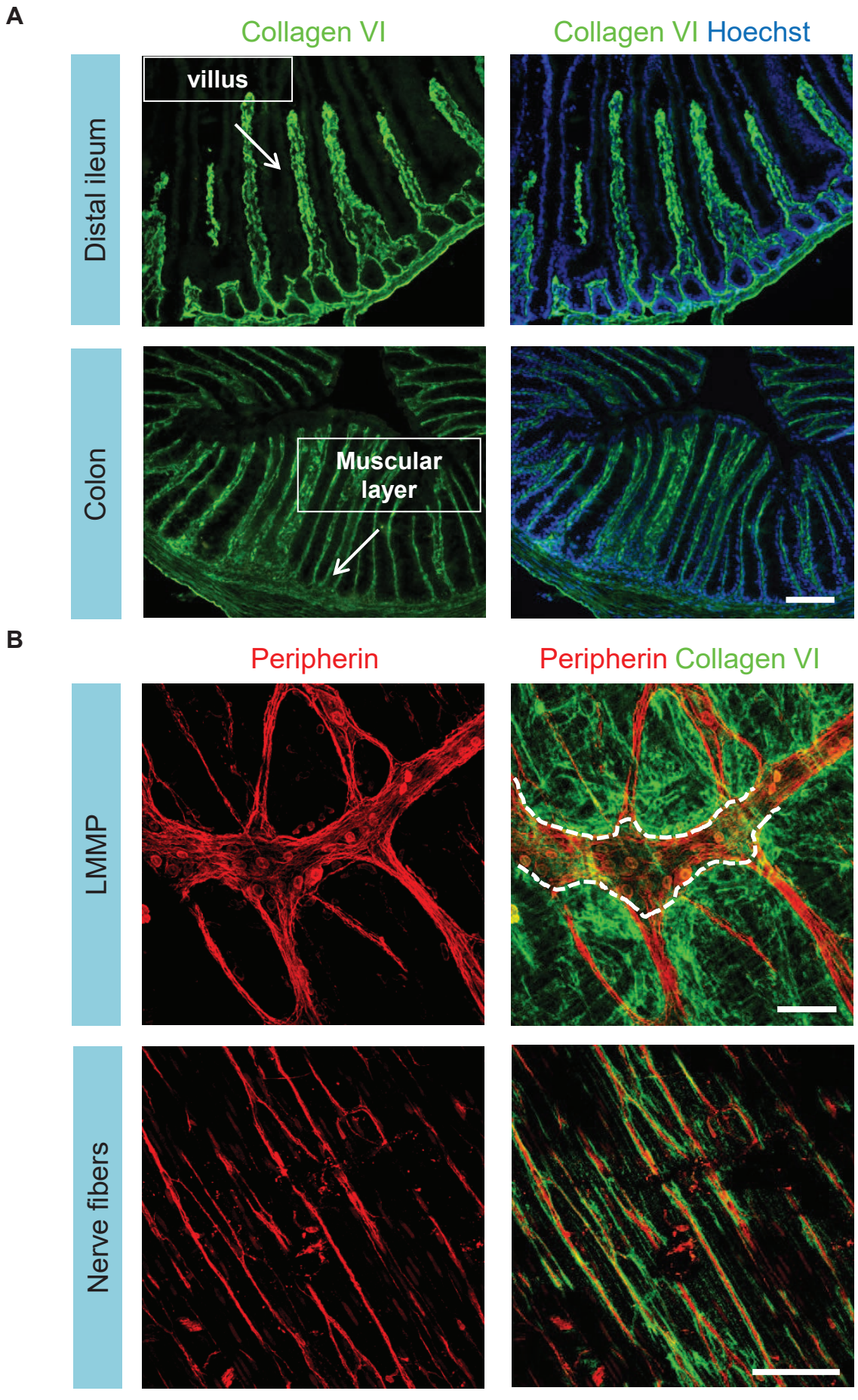

A
Collagen VI
Collagen VI Hoechst
Distal ileum
villus
Colon
Muscular layer
B
Peripherin
Peripherin Collagen VI
LMMP
Nerve fibers

Figure 1. Analysis of collagen VI localization in mouse intestine. A. Immunofluorescence staining for collagen VI on cryosections of wild-type distal ileum and colon. Nuclei were stained with Hoechst (blue). Scale bar, 100 µm. **B.** Whole mount confocal immunofluorescence for peripherin (red) and collagen VI (green) of wild-type longitudinal muscle myenteric plexus (LMMP, upper) and nerve fibers (below) of distal ileum. Dotted white line indicates a ganglium. Scale bar, 50 µm.

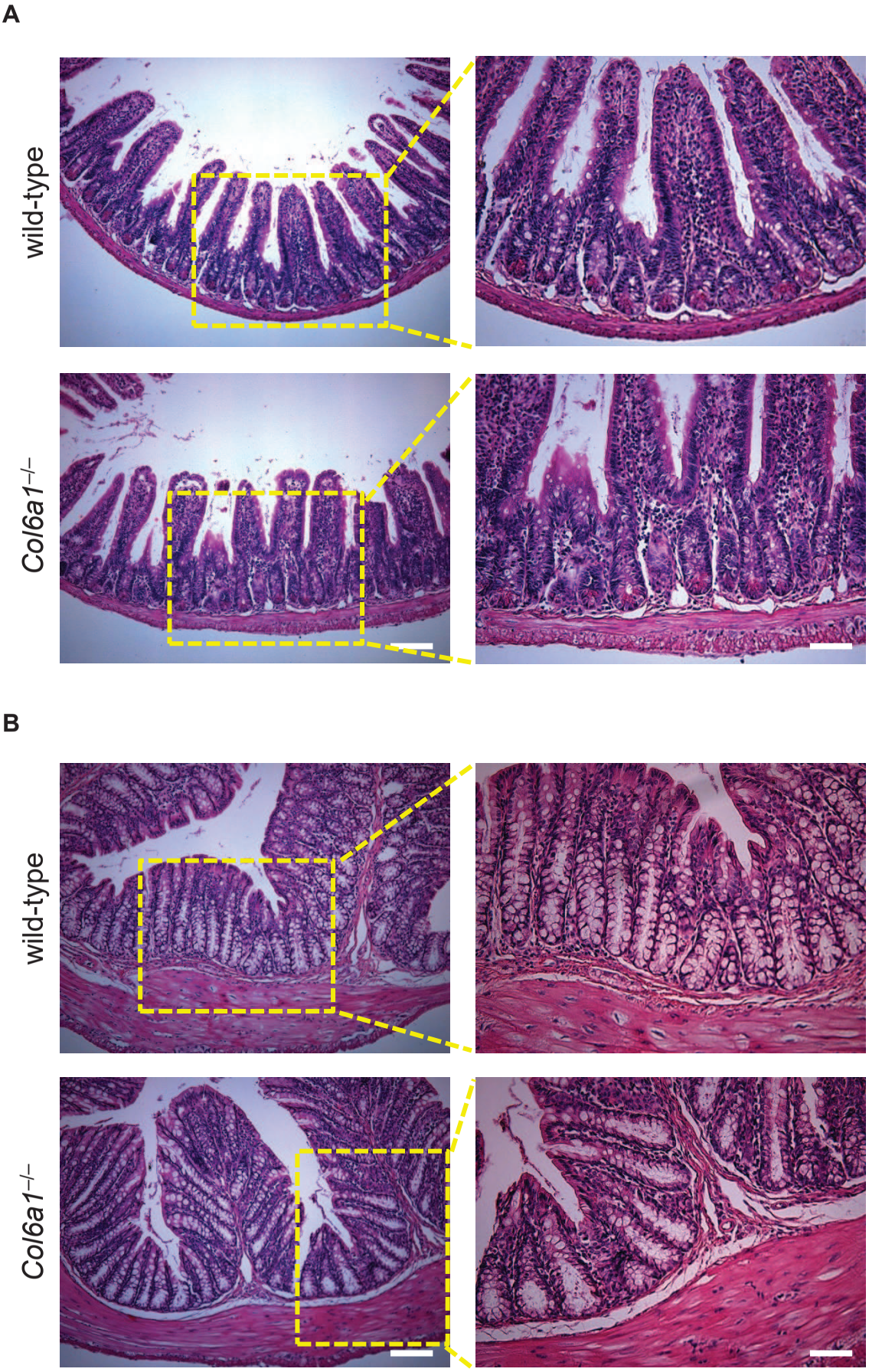

A
wild-type
Col6a1−/−
B
wild-type
Col6a1−/−

Figure 2. Histological analysis of adult distal ileum and colon from wild-type and collagen VI null mice. A-B. Hematoxilin-eosin staining on paraffinated sections of wild-type and *Col6a1*$^{-/-}$ distal ileum (A) and colon (B). Dotted yellow line indicate the area shown at higher magnification. Scale bar, 150 μm (left panels) or 75 μm (right panels).

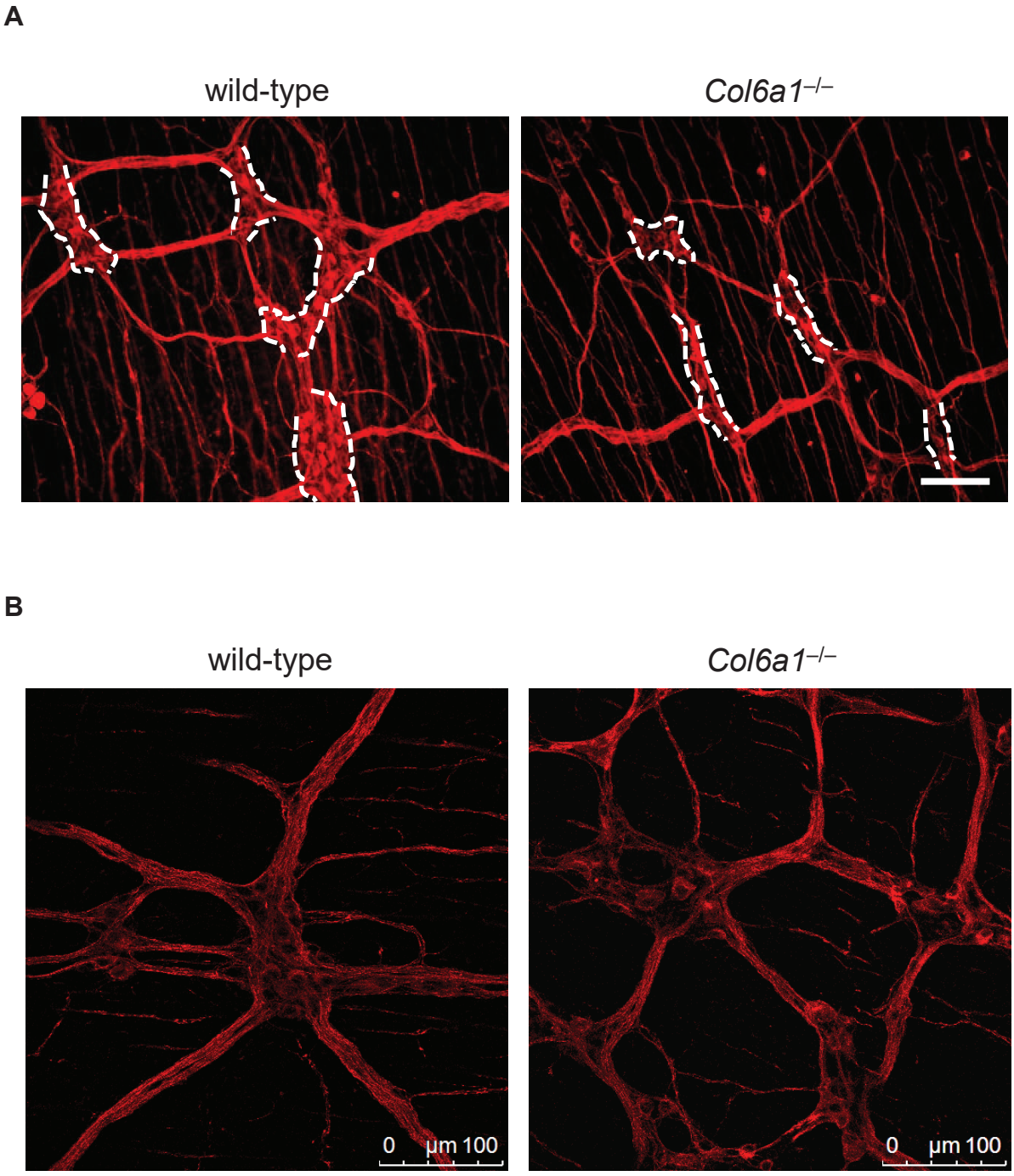


Figure 3. Whole mount immunofluorescence of longitudinal muscle myenteric plexus of distal ileum from wild-type and collagen VI null mice. A. Representative low magnifications of whole mount images of immunofluorescence for peripherin (red) in wild-type and *Col6a1*$^{-/-}$ longitudinal muscle myenteric plexus of distal ileum. Dotted white lines indicate ganglia. Scale bar, 100 µm. **B.** Whole mount maximum projection confocal immunofluorescence for peripherin (red) in wild-type and *Col6a1*$^{-/-}$ longitudinal muscle myenteric plexus of distal ileum. Scale bar, 100 µm.

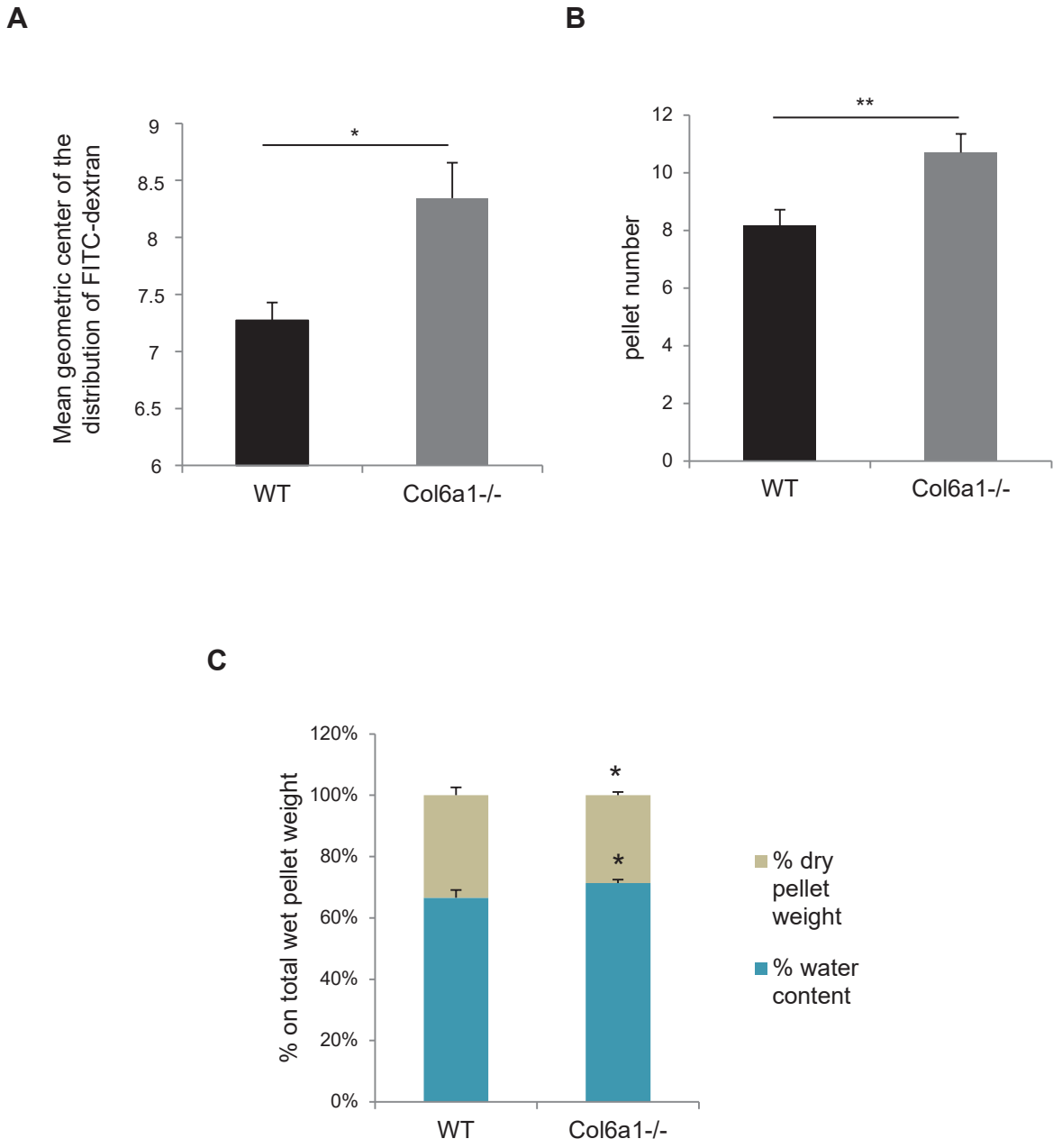


Figure 4. Analysis of gastrointestinal motility in wild-type and *Col6a1*$^{-/-}$ mice under physiological conditions. A. Gastrointestinal motility of wild-type and *Col6a1*$^{-/-}$ mice measured by fluorescent FITC-dextran transit and expressed as geometric center. **B.** Number of pellet collected in 1 hour in wild-type and *Col6a1*$^{-/-}$ mice caged individually. **C.** Percentage of water content in collected wild-type and *Col6a1*$^{-/-}$ pellet after heating over night at 70° C, expressed as the percentage of (wet weight – dry weight)/wet weight. WT, wild-type. *, $P < 0.05$; **, $P < 0.01$.

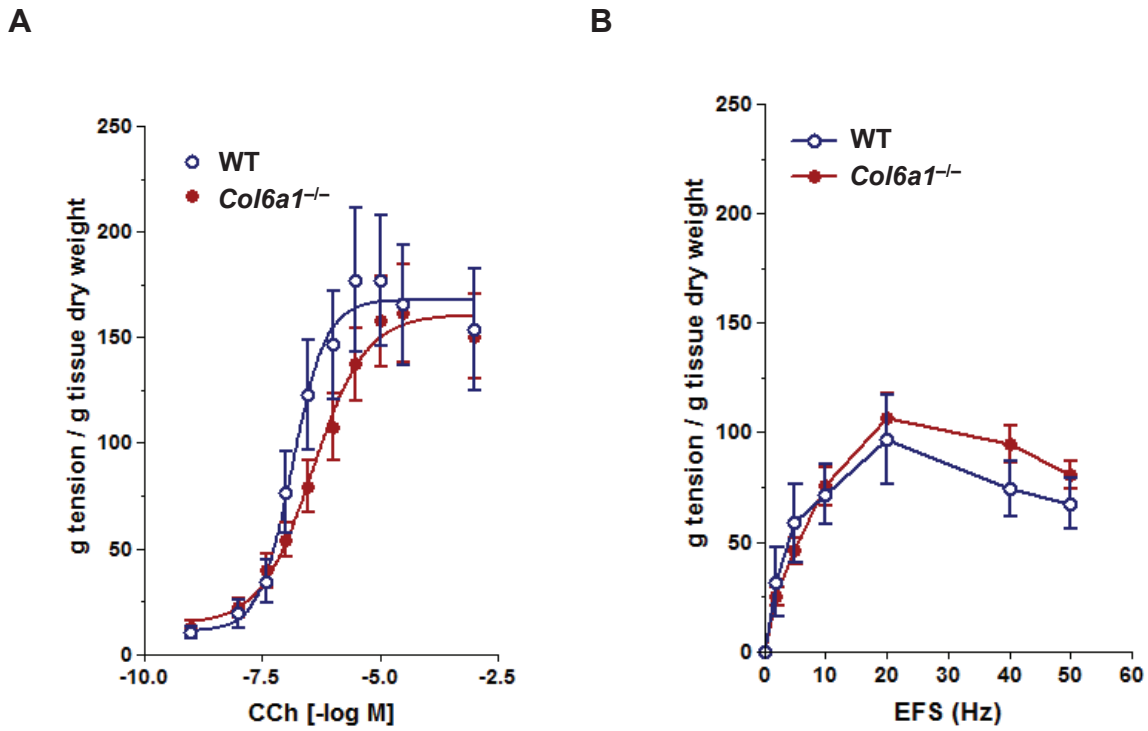


Figure 5. *Ex vivo* contractility of distal ileum of 3-month-old wild-type and *Col6a1*$^{-/-}$ mice under physiological conditions. A. Acetylcholine receptor-mediated contractions contractility of wild-type and *Col6a1*$^{-/-}$ isolated distal ileum segments, recorded by means of cumulative doses of carbachol (CCh) and expressed as g tension/g dry weight tissue. **B.** Myenteric neuron-mediated contractions of wild-type and *Col6a1*$^{-/-}$ isolated distal ileum segments recorded by means of Electric Field Stimulation (EFS) and expressed as g tension/g dry weight tissue. WT, wild-type.

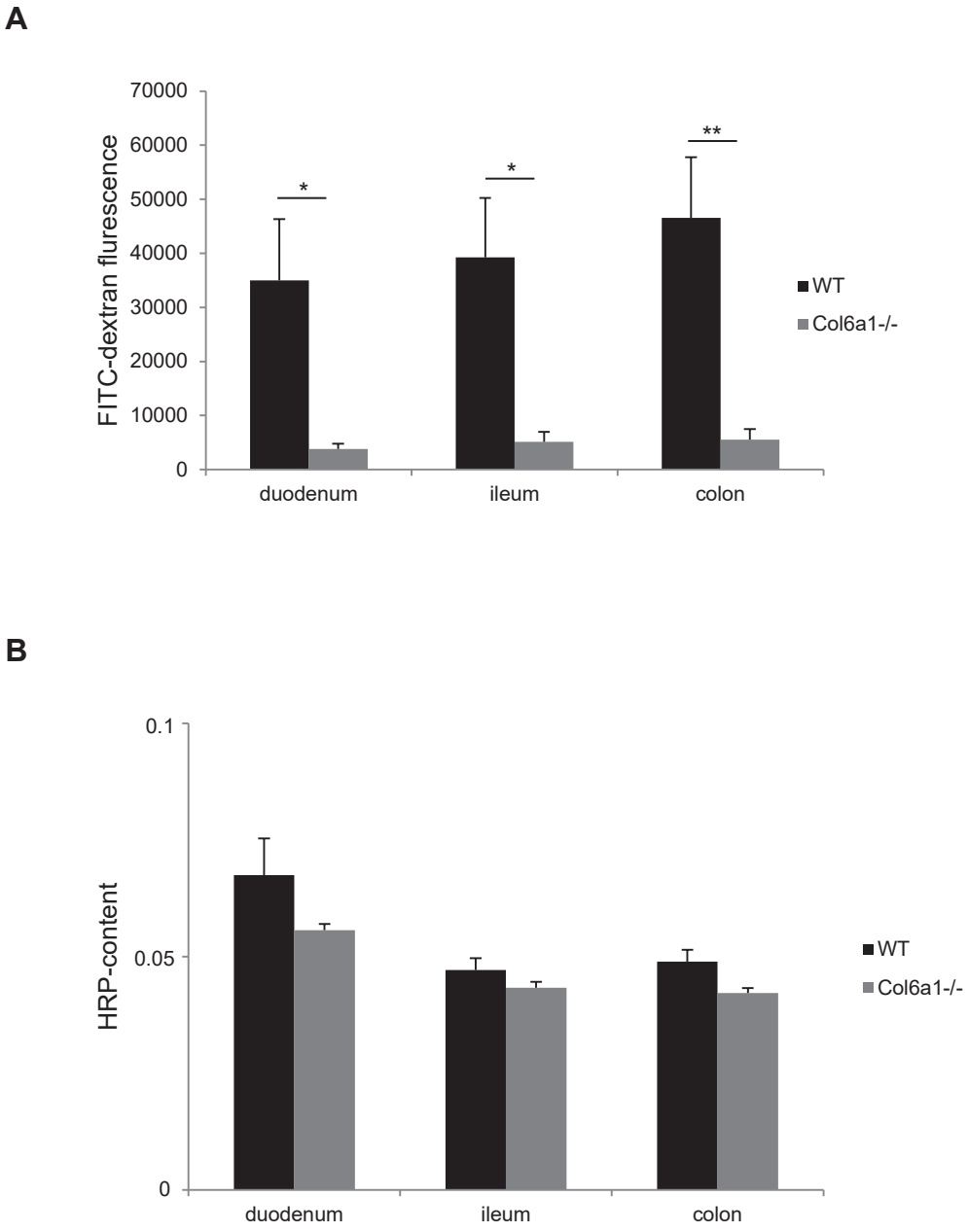
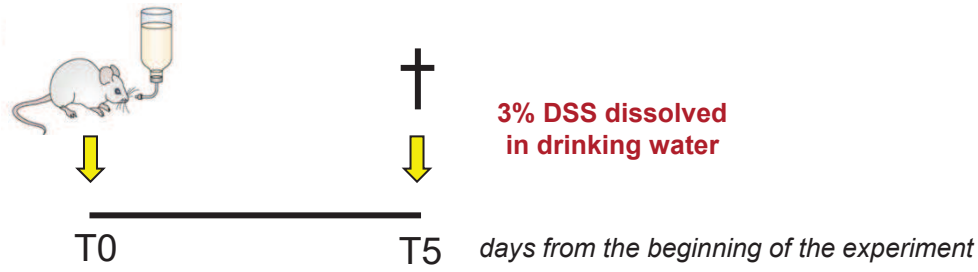
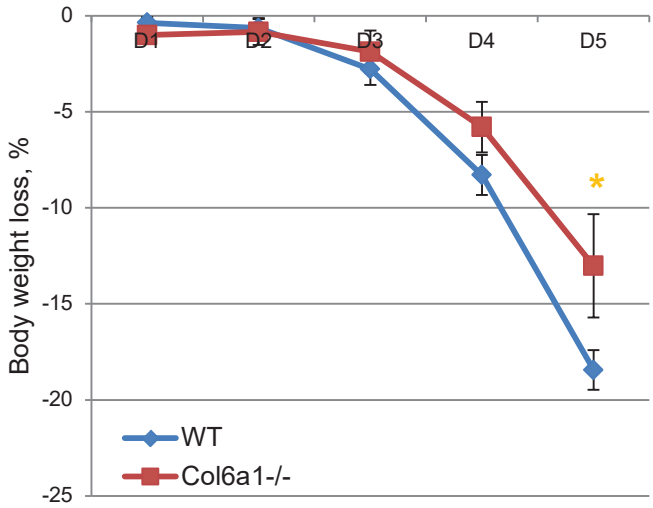


Figure 6. Analysis of gastrointestinal permeability in wild-type and *Col6a1*$^{-/-}$ mice. A. Analysis of transcellular permeability with FITC-dextran after 30 minutes. **B.** Analysis of transcellular permeability with horseradish peroxidase (HRP) after 30 minute. WT, wild-type. *, $P < 0.05$; **, $P < 0.01$.

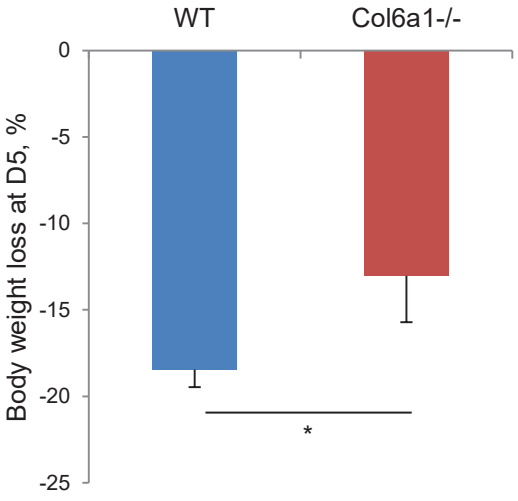
A


3% DSS dissolved
in drinking water
T0
T5
days from the beginning of the experiment

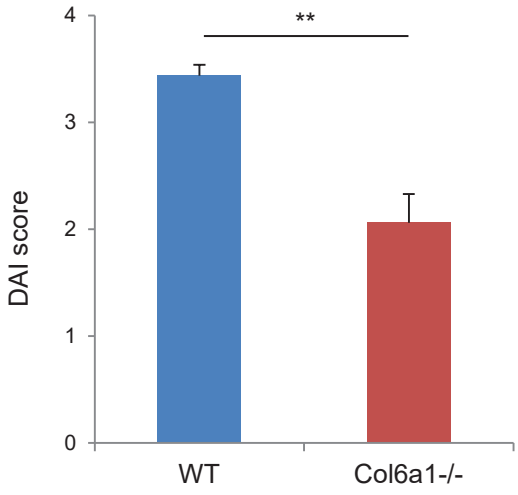
B


Body weight loss, %
0
-5
-10
-15
-20
-25
D1
D2
D3
D4
D5
*
WT
Col6a1-/-

C


WT
Col6a1-/-
Body weight loss at D5, %
0
-5
-10
-15
-20
-25
*

D


DAI score
4
3
2
1
0
**
WT
Col6a1-/-

E

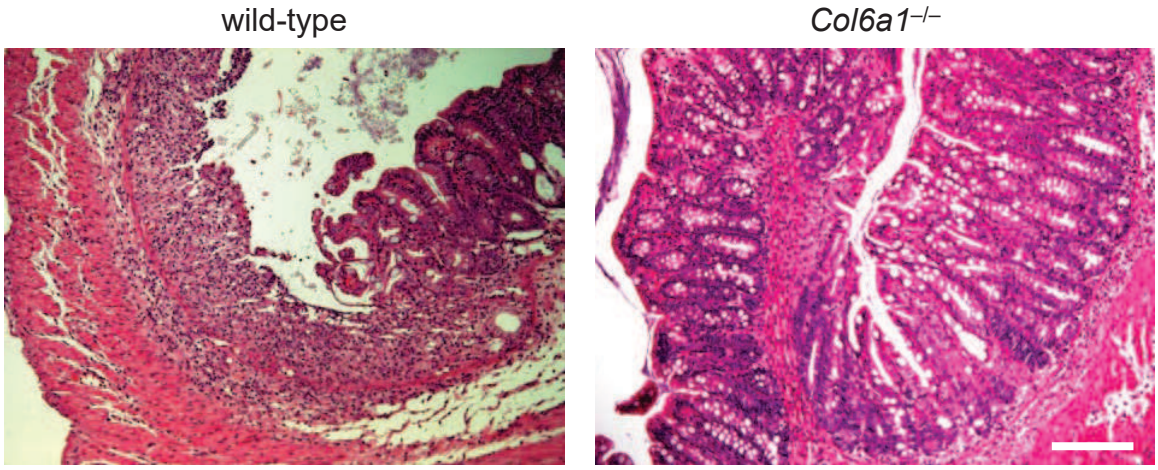


Figure 7. Body weight trend, DAI score and colon histological analysis of wild-type and *Col6a1*$^{-/-}$ mice during DSS-induced acute colitis. A. Schematic diagram of the experimental procedure to induce acute colitis with 3% Dextran Sodium Sulphate (DSS) for 5 days. **B.** Trend of the body weight loss displayed by wild-type and *Col6a1*$^{-/-}$ mice during 5 days of DSS treatment, expressed as percentage of body weight loss. **C.** Percentage of the loss of body weight at the end of treatment (D5). **D.** Evaluation of the disease activity index (DAI) in wild-type and *Col6a1*$^{-/-}$ mice. **E.** Hematoxylin-eosin staining on paraffinated sections of colon of wild-type and *Col6a1*$^{-/-}$ mice treated for 5 days with DSS. Scale bar, 100 μm. WT, wild-type. *, $P < 0.05$. **, $P < 0.01$.

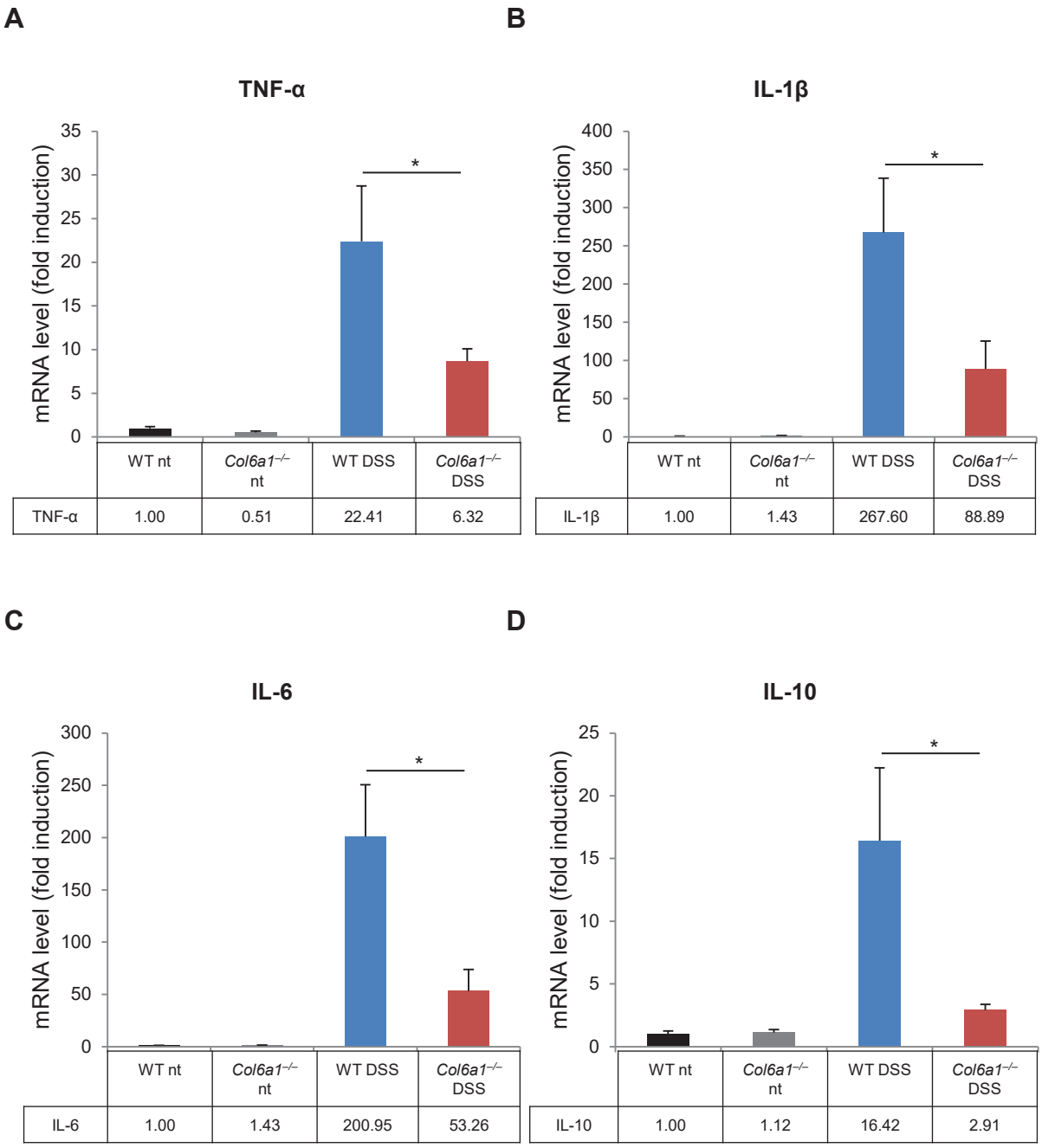
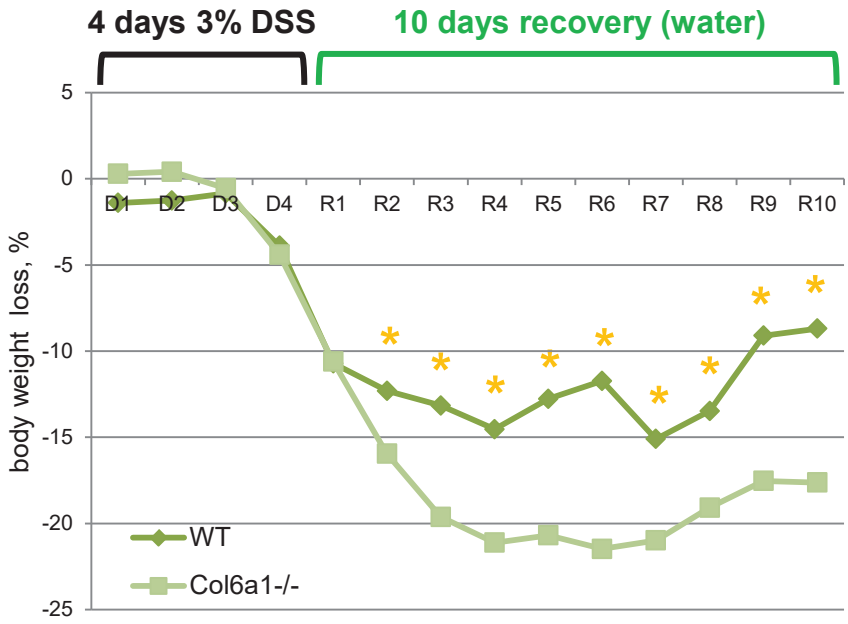


Figure 8. Expression of inflammatory cytokines in wild-type and *Col6a1*$^{-/-}$ mice subjected to DSS-induced acute colitis. A-D. Real-time qPCR analysis of pro-inflammatory (TNF-α, IL-1β, and IL-6) and anti-inflammatory (IL-10) cytokines in wild-type and *Col6a1*$^{-/-}$ mice under physiological conditions and in DSS-induced acute colitis. Data are expressed as fold induction compared to wild-type in physiological conditions. *, $P < 0.05$. All differences between DSS-treated and physiological conditions for each genotypes are statistically significant. DSS, acute colitis; nt, not treated; WT, wild-type.

A


3% DSS
dissolved
in drinking
water
T0
T4
T14
days from the beginning
of the experiment

B


4 days 3% DSS
10 days recovery (water)
body weight loss, %
5
0
-5
-10
-15
-20
-25
D1
D2
D3
D4
R1
R2
R3
R4
R5
R6
R7
R8
R9
R10
WT
Col6a1-/-

C

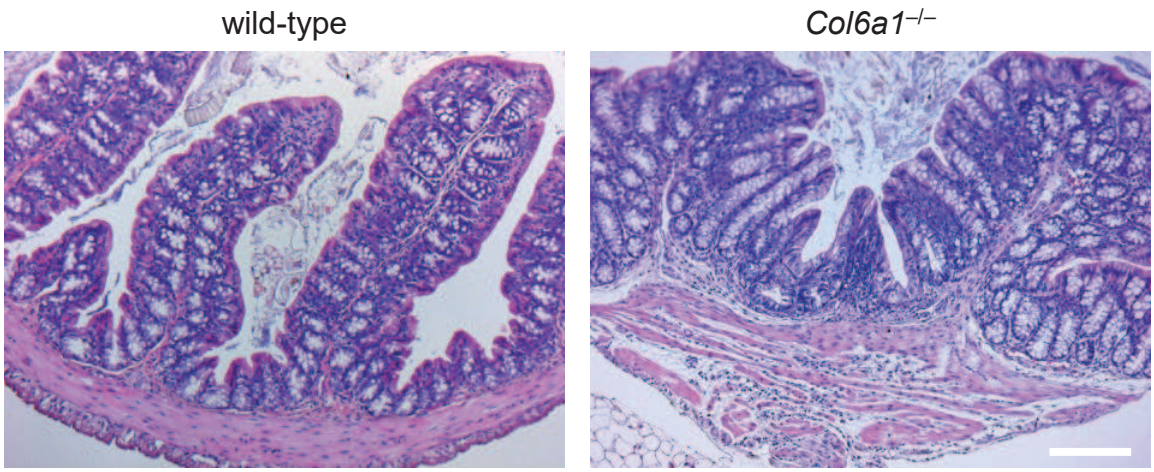

wild-type
Col6a1$^{-/-}$

Figure 9. Trend of body weight loss and colon histological analysis in wild-type and *Col6a1*$^{-/-}$ mice subjected to DSS-induced acute colitis followed by recovery. **A.** Schematic diagram of the experimental procedure to induce acute colitis by 4 day treatment with 3% DSS, followed by 10 days of recovery with tap water. **B.** Trend of the body weight loss displayed by wild-type and *Col6a1*$^{-/-}$ treated with 3% DSS for 4 days followed by recovery, expressed as percentage of body weight loss. **C.** Hematoxylin-eosin staining on paraffinated colon sections from wild-type and *Col6a1*$^{-/-}$ mice treated with 3% DSS for 4 days followed by recovery. Scale bar, 150 μm. *, $P < 0.05$.

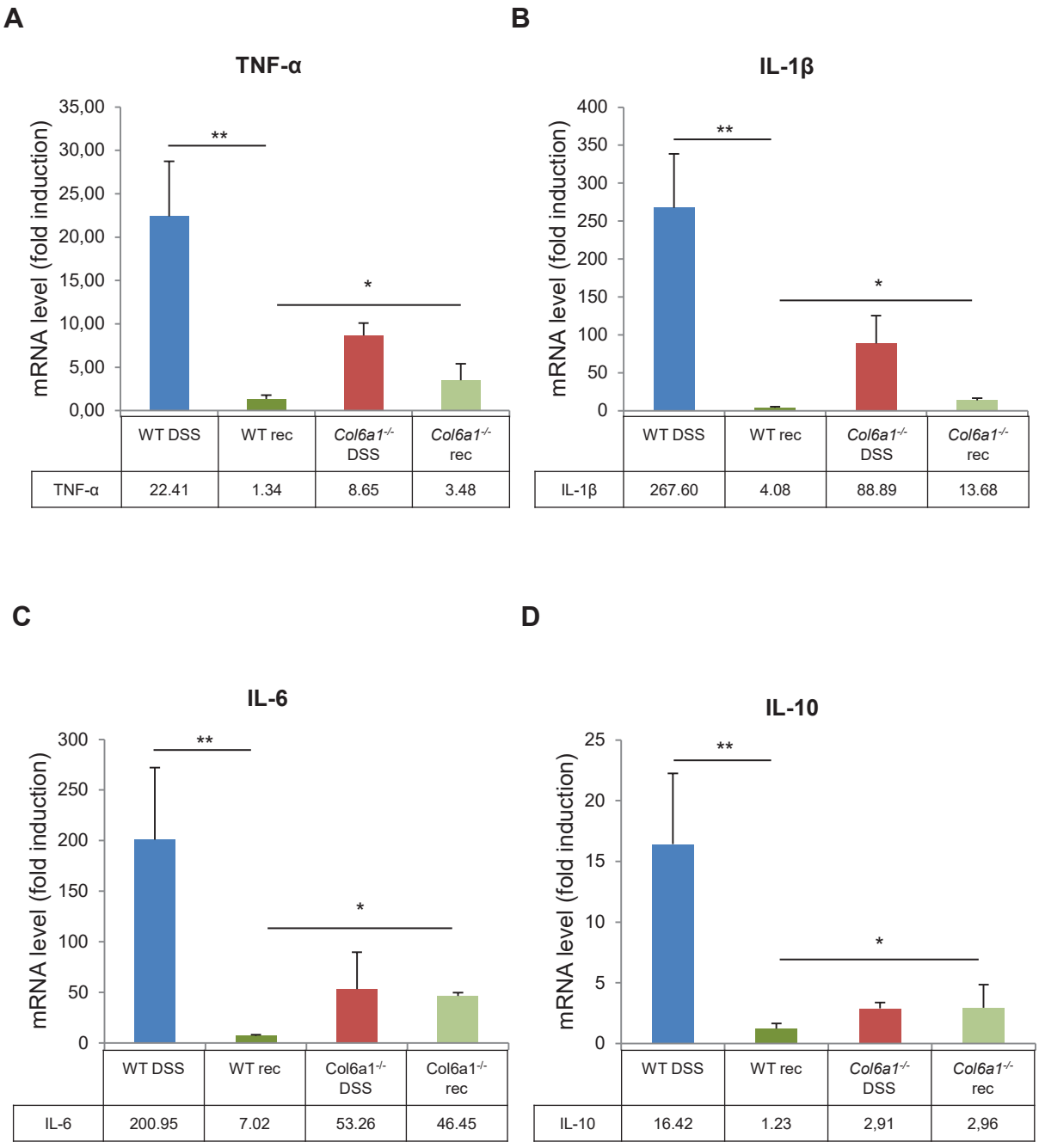


Figure 10. Expression of inflammatory cytokines in wild-type and *Col6a1*$^{-/-}$ mice treated with DSS followed by recovery. A-D. Real-time qPCR analysis of pro-inflammatory (TNF-α, IL-1β, and IL-6) and anti-inflammatory (IL-10) cytokines in wild-type and *Col6a1*$^{-/-}$ mice subjected to DSS-induced acute colitis and after 10-day recovery. Data are expressed as fold induction compared to wild-type in physiological conditions. DSS, acute colitis; rec, DSS-induced acute colitis followed by 10-day recovery. WT, wild-type. *, $P < 0.05$; **, $P < 0.01$.

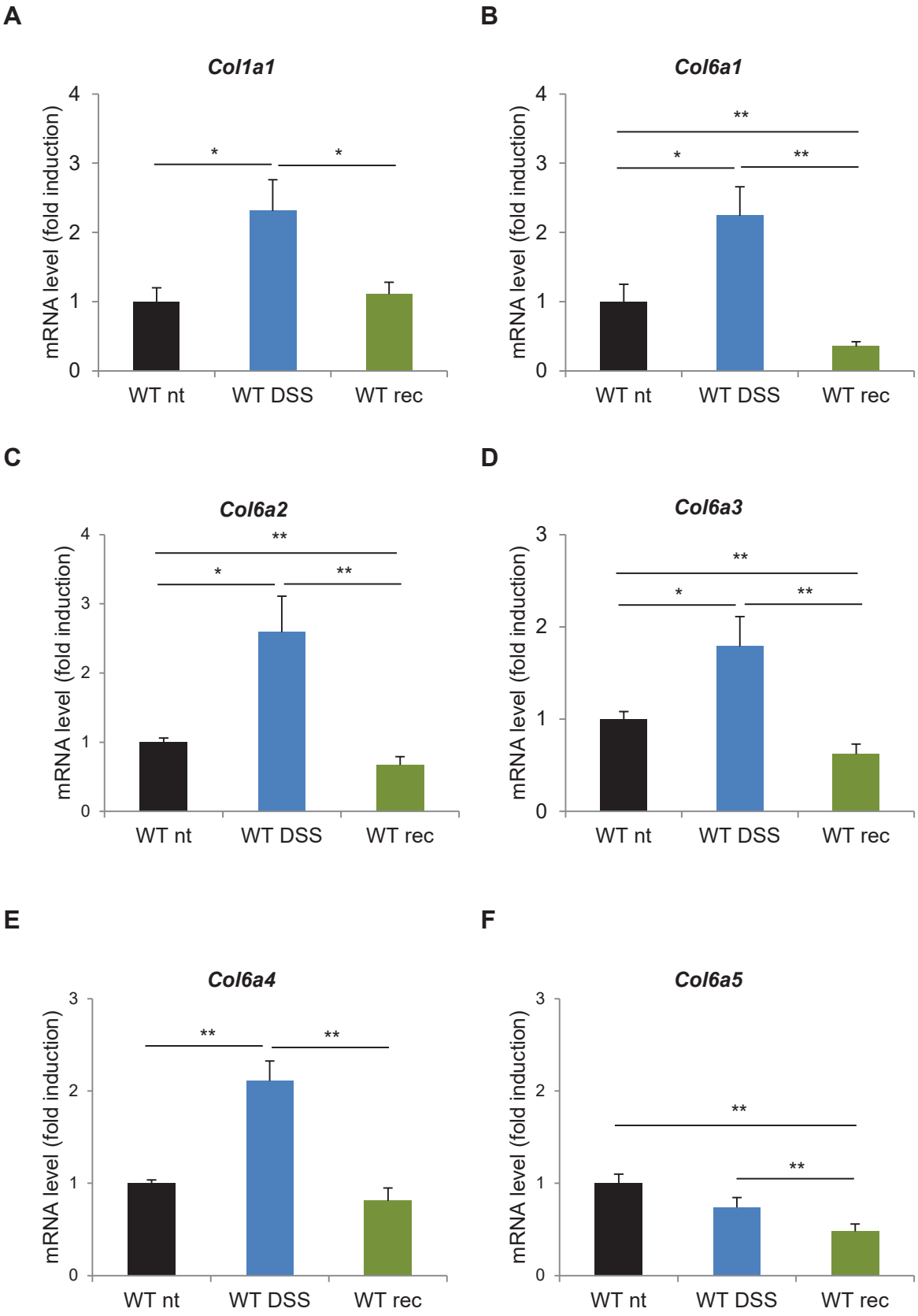
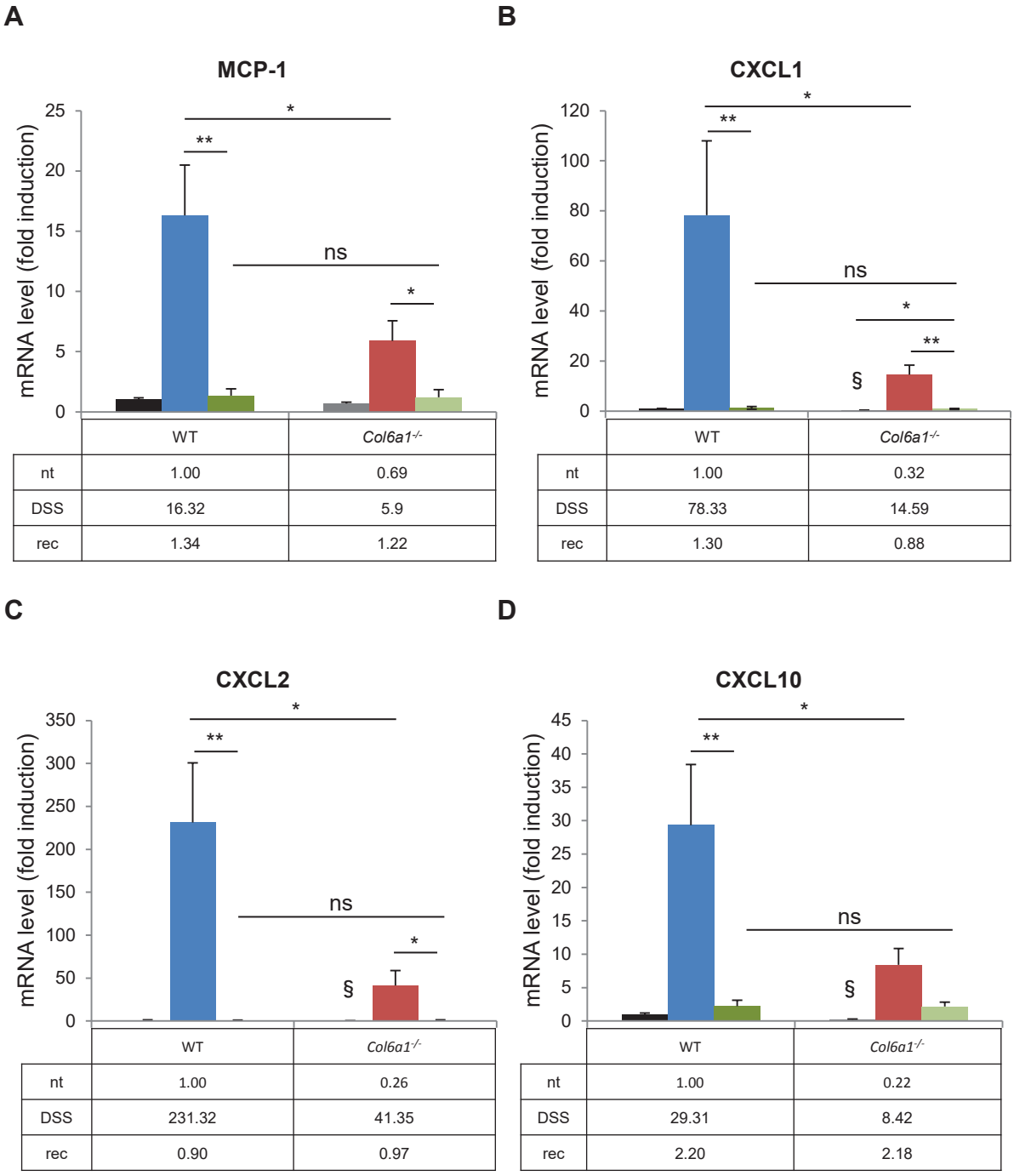

A
Col1a1
mRNA level (fold induction)
WT nt
WT DSS
WT rec
B
Col6a1
C
Col6a2
D
Col6a3
E
Col6a4
F
Col6a5

Figure 11. Expression of collagen VI genes in wild-type and *Col6a1*$^{-/-}$ mice under untreated conditions, DSS-induced acute colitis, and recovery. A-F. Real time qPCR data of *Col1a1* (used as a control ECM gene) and collagen VI genes (*Col6a1, Col6a2, Col6a3, Col6a4,* and *Col6a5)* in wild-type and *Col6a1*$^{-/-}$ mice under physiological condition, DSS-induced acute colitis, and DSS-induced colitis followed by 10-day recovery. Data are expressed as fold induction compared to wild-type in physiological conditions. DSS, acute colitis; nt, not treated; rec, DSS-induced acute colitis followed by 10-day recovery. WT, wild-type. *, $P < 0.05$; **, $P < 0.01$.



	WT	*Col6a1*$^{-/-}$
nt	1.00	0.69
DSS	16.32	5.9
rec	1.34	1.22

	WT	*Col6a1*$^{-/-}$
nt	1.00	0.32
DSS	78.33	14.59
rec	1.30	0.88

	WT	*Col6a1*$^{-/-}$
nt	1.00	0.26
DSS	231.32	41.35
rec	0.90	0.97

	WT	*Col6a1*$^{-/-}$
nt	1.00	0.22
DSS	29.31	8.42
rec	2.20	2.18

Figure 12. Expression of chemokines genes in wild-type and *Col6a1*$^{-/-}$ mice under untreated conditions, DSS-induced acute colitis, and recovery. A-D. Real time qPCR analysis of chemotactic cytokines for monocytes/macrophages and neutrophils (MCP-1, CXCL1, CXCL2 and CXCL10). Data are expressed as fold induction compared to wild-type mice under physiological condition. DSS, acute colitis; nt, not treated; rec, DSS-induced acute colitis followed by 10-day recovery; WT, wild-type. *, $P < 0.05$; **, $P < 0.01$; §, $P < 0.01$ for WT nt vs *Col6a1*$^{-/-}$ nt.

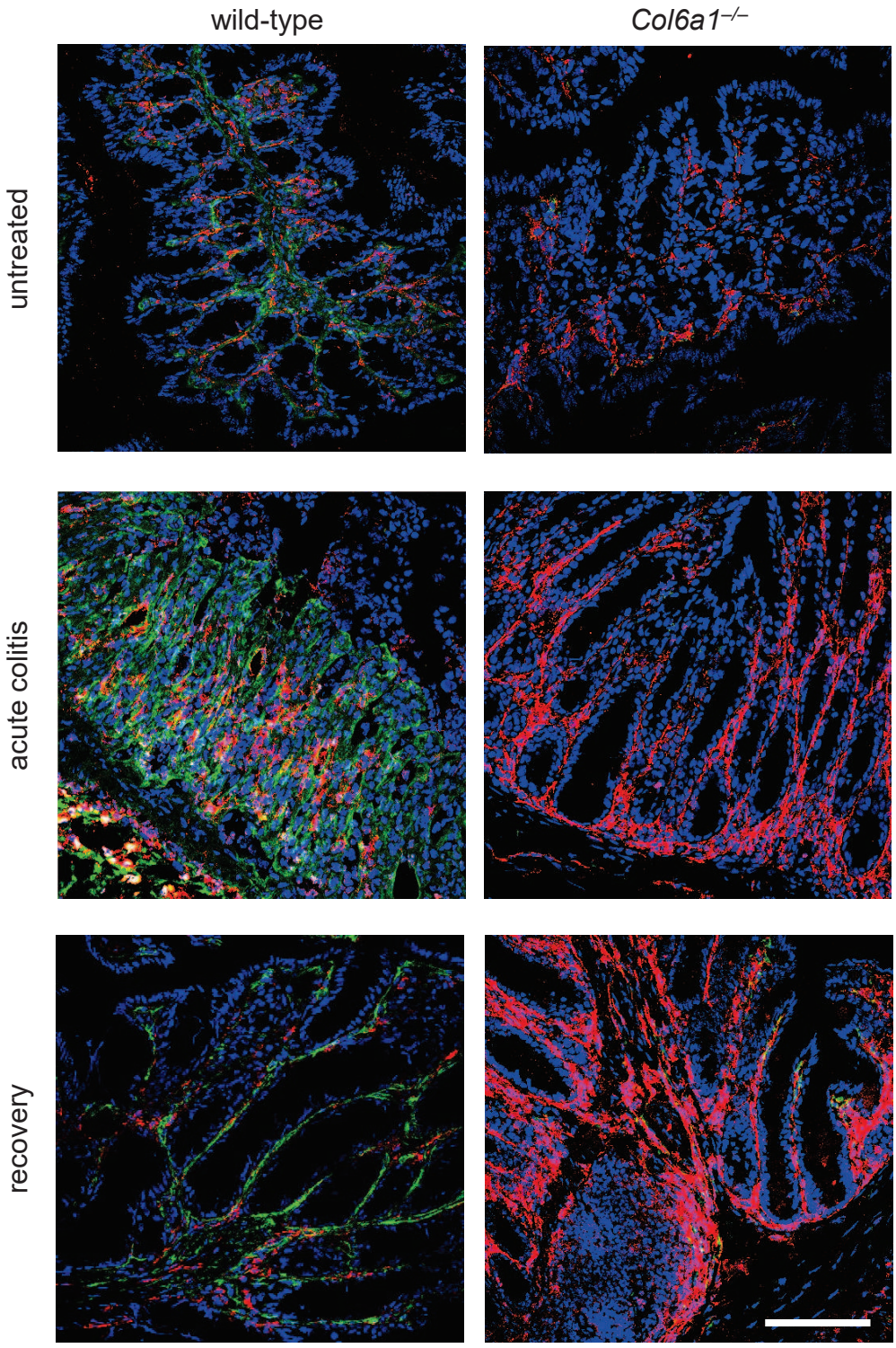
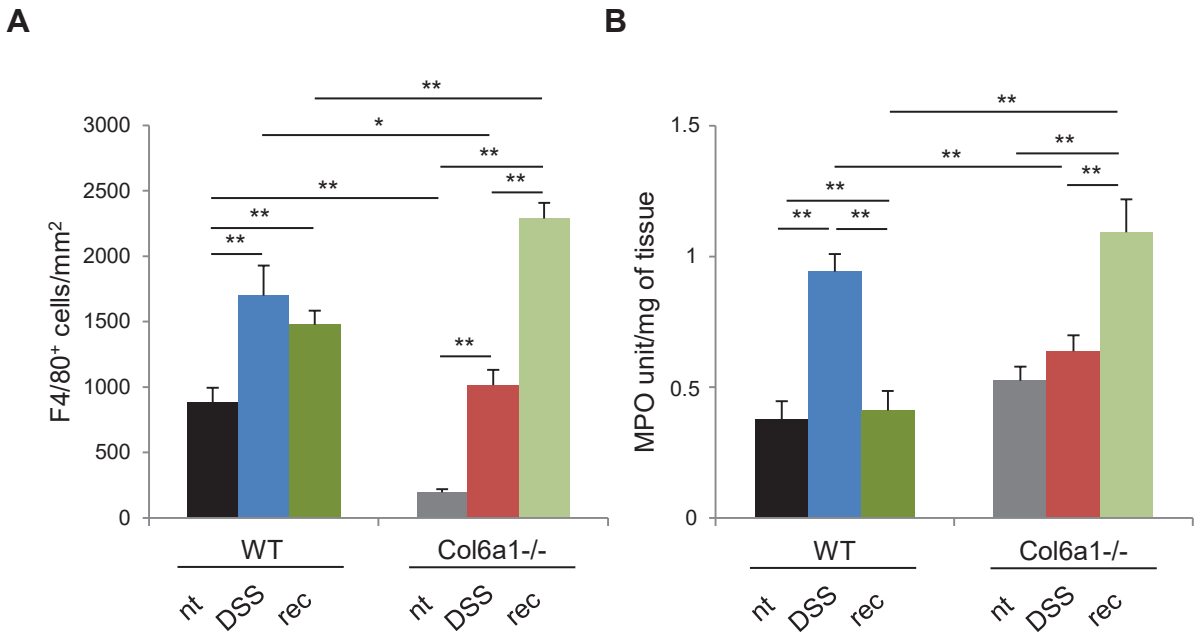
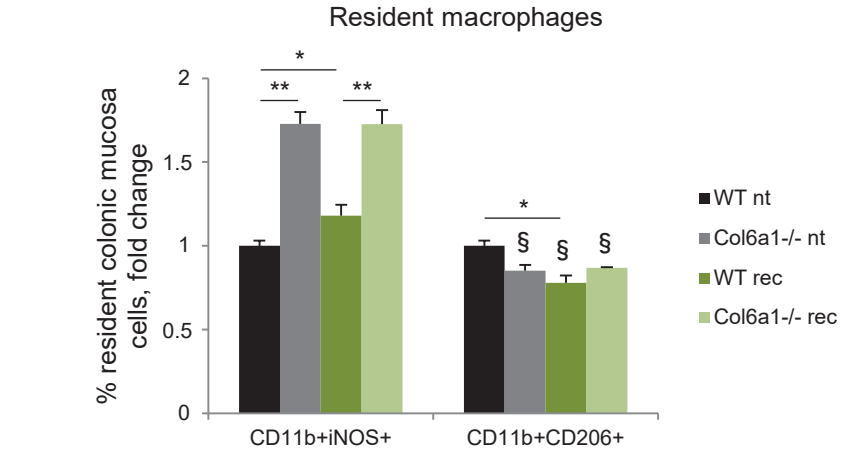


Figure 13. Immunofluorescence analysis for collagen VI and F4/80⁺ colonic mucosa macrophages. Confocal immunofluorescence for F4/80 (red) and collagen VI (green) in colon criosections from wild-type and *Col6a1*$^{-/-}$ under untreated conditions, DSS-induced acute colitis, and DSS-induced colitis followed by 10-day recovery. Scale bar, 100 μm.


A
B
F4/80+ cells/mm2
MPO unit/mg of tissue
WT
Col6a1-/-
nt
DSS
rec


C
Resident macrophages
% resident colonic mucosa cells, fold change
CD11b+iNOS+
CD11b+CD206+
WT nt
Col6a1-/- nt
WT rec
Col6a1-/- rec

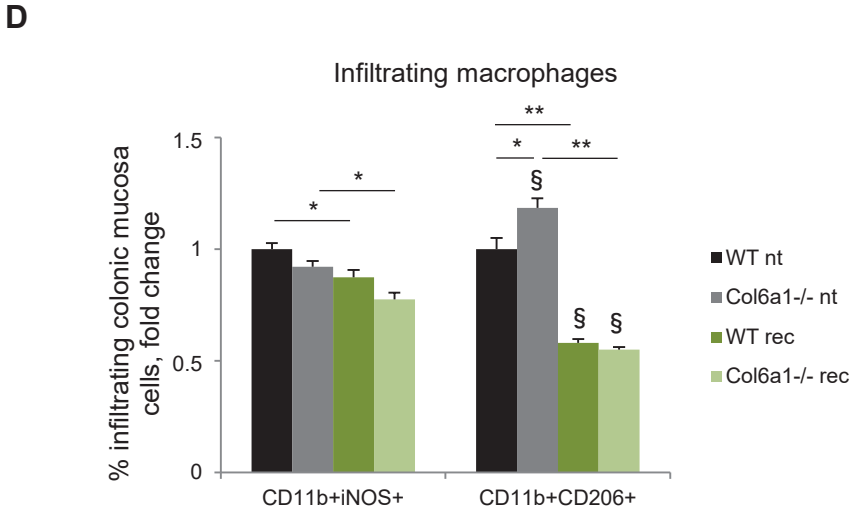
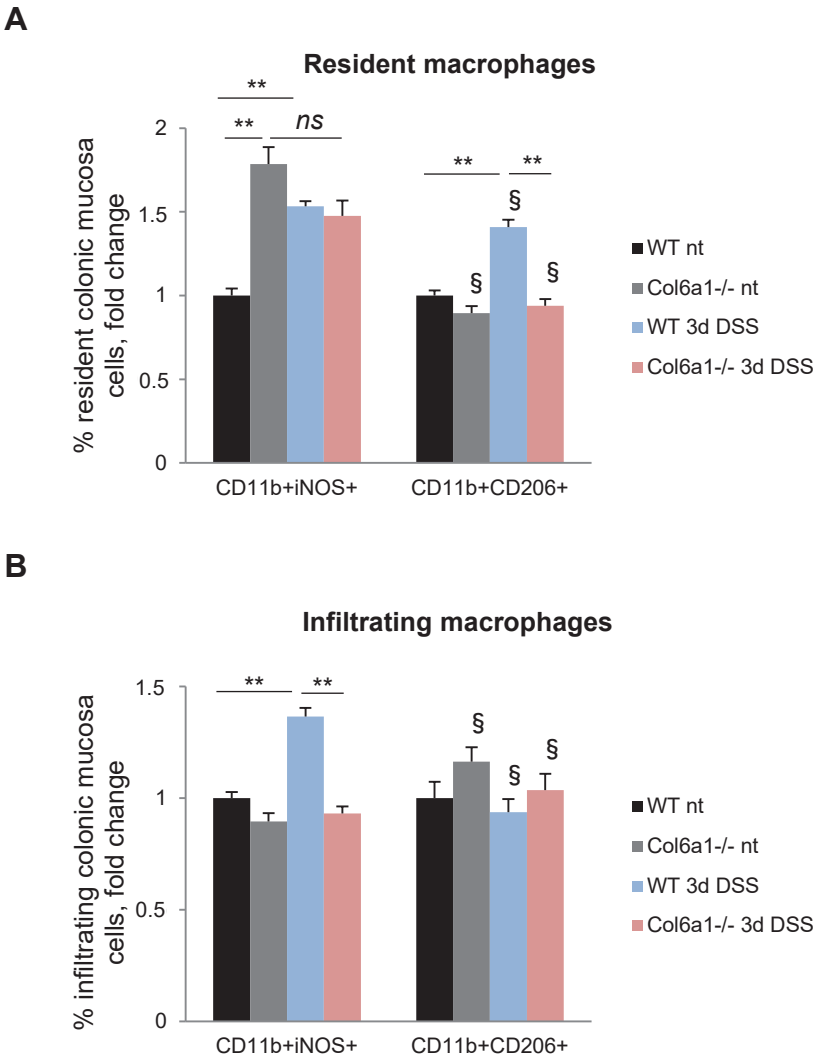

D
Infiltrating macrophages
% infiltrating colonic mucosa cells, fold change
CD11b+iNOS+
CD11b+CD206+
WT nt
Col6a1-/- nt
WT rec
Col6a1-/- rec

Figure 14. Analysis of the number of F4/80$^+$ macrophages and of neutrophil activity in wild-type and *Col6a1*$^{-/-}$ colons. A. Analysis of F4/80$^+$ colonic mucosal macrophages of wild-type and *Col6a1*$^{-/-}$ mice under physiological condition, DSS-induced acute colitis and DSS-induced colitis followed by 10-day recovery. **B.** MPO assay in colons of wild-type and *Col6a1*$^{-/-}$ mice under under physiological condition, DSS-induced acute colitis and DSS-induced colitis followed by 10-day recovery. **C, D.** Analysis of M1 (CD11b$^+$iNOS$^+$) and M2 (CD11b$^+$CD206$^+$) phenotype of resident and infiltrating colonic mucosa macrophages of wild-type and *Col6a1*$^{-/-}$ mice under physiological condition and DSS-induced colitis followed by 10-day recovery, expressed as fold change with respect to untreated wild-type for each condition. DSS, acute colitis; nt, not treated; rec, DSS-induced acute colitis followed by 10-day recovery; WT, wild-type. *, $P < 0.05$; **, $P < 0.01$.


A
Resident macrophages
% resident colonic mucosa cells, fold change
2
1.5
1
0.5
0
**
**
ns
**
**
§
§
§
CD11b+iNOS+
CD11b+CD206+
WT nt
Col6a1-/- nt
WT 3d DSS
Col6a1-/- 3d DSS
B
Infiltrating macrophages
% infiltrating colonic mucosa cells, fold change
1.5
1
0.5
0
**
**
§
§
§
CD11b+iNOS+
CD11b+CD206+
WT nt
Col6a1-/- nt
WT 3d DSS
Col6a1-/- 3d DSS

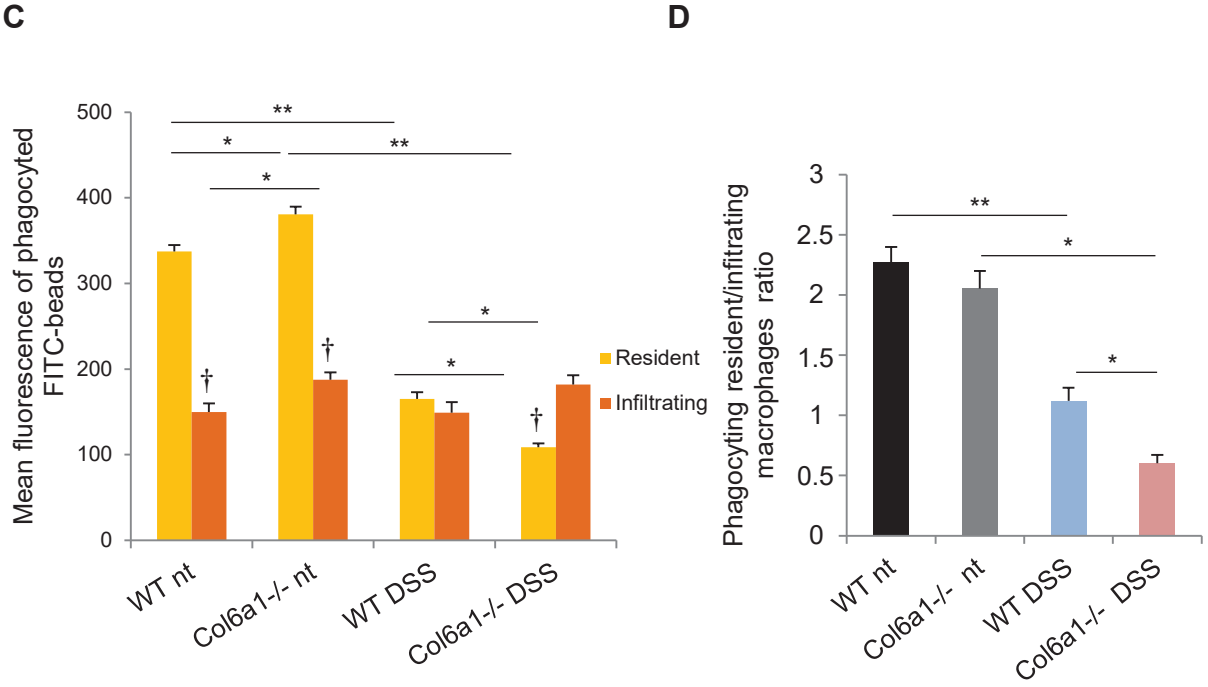
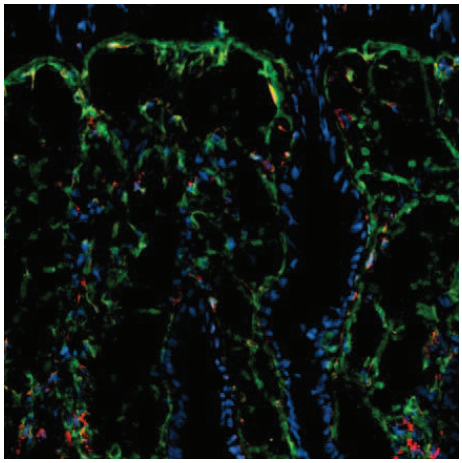

C
Mean fluorescence of phagocyted FITC-beads
500
400
300
200
100
0
**
*
*
**
*
*
†
†
†
Resident
Infiltrating
WT nt
Col6a1-/- nt
WT DSS
Col6a1-/- DSS
D
Phagocyting resident/infiltrating macrophages ratio
3
2.5
2
1.5
1
0.5
0
**
*
*
WT nt
Col6a1-/- nt
WT DSS
Col6a1-/- DSS

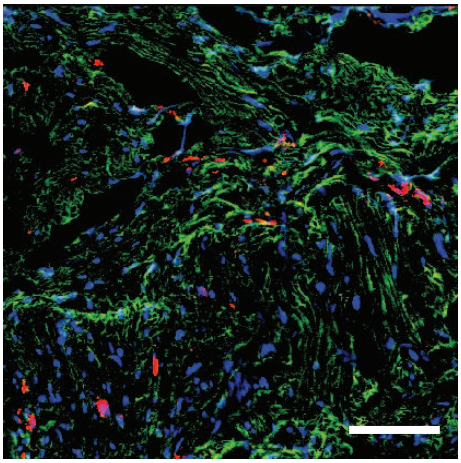
Figure 15. Analysis of polarization and phagocytic activity of colonic mucosal macrophages of wild-type and *Col6a1*$^{-/-}$ mice under physiological conditions and after mild inflammation with 3% DSS for 3 days. A, B. Analysis of M1 ($CD11b^+iNOS^+$) and M2 ($CD11b^+CD206^+$) phenotype of resident and infiltrating colonic mucosa macrophages of wild-type and *Col6a1*$^{-/-}$ mice in physiological conditions and during mild inflammation, expressed as fold change with respect to untreated wild-type for each condition. **C, D.** Analysis of FITC-microparticle phagocytosis of resident and infiltrating $CD11b^+$ MCH-II^+ colonic mucosal macrophages of wild-type and *Col6a1*$^{-/-}$ mice in physiological conditions and during mild inflammation, expressed as absolute number (C) and as the ratio of resident macrophages vs infiltrating macrophages (D). DSS, acute colitis; nt, not treated; WT, wild-type. *, $P < 0.05$; **, $P < 0.01$. §, indicates statistic difference between M1 and M2 macrophages for each condition, $P < 0.01$. †, indicates statistic difference between resident and infiltrating phagocytic capability for each condition, $P < 0.01$.

A

Macroscopically normal ileal mucosa

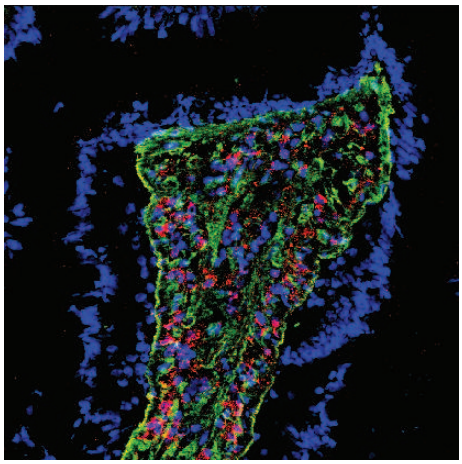


Macroscopically normal ileal muscle layer

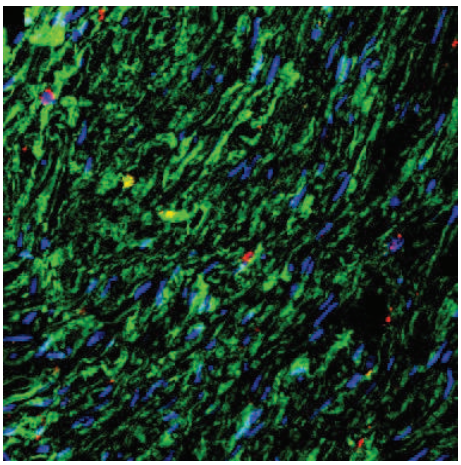


B

Macroscopically normal ileal mucosa



Macroscopically normal ileal muscle layer



Macroscopically diseased ileal muscle layer

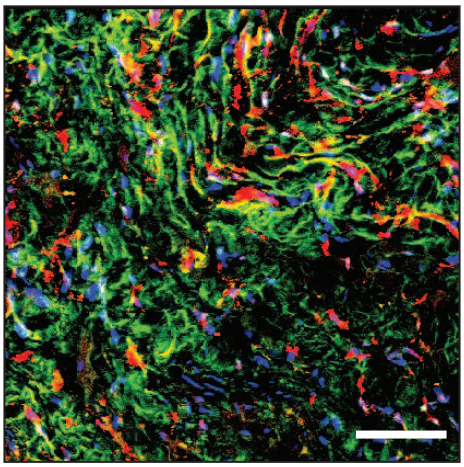


Figure 16. Immunofluorescence analysis of collagen VI deposition and of CD163$^+$ macrophages in human specimens from Crohn's disease patients. A. Analysis of CD163$^+$ macrophages (red) and collagen VI (green) by confocal immunofluorescence in cryosections of ileal mucosa and muscle layers from a control subject undergoing surgery for colonic carcinoma. **B.** Analysis of CD163$^+$ macrophages (red) and collagen VI (green) by confocal immunofluorescence in cryosections of ileal macroscopically normal mucosa and normal muscle layers and of diseased tissue from a patient undergoing surgery for Crohn's disease localized to the distal ileum. Nuclei were stained with TOTO-3. Scale bar, 75 μm.

References

Abraham C and Cho JH, 2009. Inflammatory bowel disease. *N Engl J Med*, 361(21): 2066-78. *Review.*

Adair-Kirk TL and Senior RM, 2008. Fragments of extracellular matrix as mediators of inflammation. *Int J Biochem Cell Biol*, 40(6-7): 1101-10. *Review.*

Axelsson LG et al., 1996. Dextran sulfate sodium (DSS) induced experimental colitis in immunodeficient mice: effects in CD4(+) -cell depleted, athymic and NK-cell depleted SCID mice. *Inflamm Res*, 45(4): 181-91.

Bain CC and Mowat AMcI, 2011. Intestinal macrophages – specialized adaptation to a unique environment. *Eur J Immunol*, 41(9): 2494-8. *Review.*

Bain CC and Mowat AMcI, 2014a. The monocyte-macrophage axis in the intestine. *Cell Immunol*, 291(1-2): 41-8. *Review.*

Bain CC and Mowat AMcI, 2014b. Macrophages in intestinal homeostasis and inflammation. *Immuno Revl*, 260(1): 102-17. *Review*

Bannerman PG et al., 1986. Light microscopic immunolocalization of laminin, type IV collagen, nidogen, heparan sulphate proteoglycan and fibronectin in the enteric nervous system of rat and guinea pig. *J Neurocytol*, 15(6):733-43.

Barker N, van de Wetering M and Clevers H, 2008. The intestinal stem cell. *Genes & Dev, 22: 1856-1864. Review.*

Barnett M and Fraser A, 2011. Animal model of colitis: lessons learned, and their relevance to the clinic. Ulcerative Colitis – treatments, special populations and the future. Dr. Mortimer O'Connor (Ed.), ISBN: 978-953-307-739-0, in tech.

Becker HM et al., 2013. α1β1 integrin-mediated adhesion inhibits macrophage exit from a peripheral inflammatory lesion. *J Immunol*, 190(8): 4305-14

Bendjelloul F et al., 2000. Intercellular adhesion molecule-1 (ICAM-1) deficiency protects mice against severe forms of experimentally induced colitis. *Clin Exp Immunol*, 119(1): 57-63.

Bonaldo P et al., 1998. Collagen VI deficiency induces early onset myopathy in the mouse: an animal model for Bethlem myopathy. *Hum Mol Genet*, 7: 2135-2140.

Bönnemann CG, 2011. The collagen VI-related myopathies: muscle meets its matrix. *Nat Rev Neurol*, 7(7): 379-90. *Review.*

Bianco AM, Girardelli M and Tommasini A, 2015. Genetics of inflammatory bowel disease from multifactorial to monogenic forms. *World J Gastroenterol*, 21(43): 12296-310. *Review.*

Boismenu R and Chen Y, 2000. Insights from mouse models of colitis. *J Leukoc Biol*, 67(3): 267-78. *Review.*

Bolcato-Bellemin AL et al., 2003. Laminin alpha5 chain is required for intestinal smooth muscle development. *Dev Biol*, 260(2):376-90.

Bonaldo P et al., 1989. Alpha 1 chain of chick type VI collagen. The complete cDNA sequence reveals a hybrid molecule made of one short collagen and three von Willebrand factor type A–like domains. *J Biol Chem*, 264: 5575–5580.

Bonnans C, Chou J and Werb Z, 2014. Remodelling the extracellular matrix in development and disease. *Nat Rev Mol Cell Biol*, 15(12): 786-801. *Review.*

Breau MA et al., 2009. Beta1 integrins are required for the invasion of the caecum and proximal hindgut by enteric neural crest cells. *Development*, 136(16): 2791-801.

Casanova JL and Abel L, 2009. Revisiting Crohn's disease as a primary immunodeficiency of macrophages. *J Exp Med*, 206(9): 1839-43.

Cerovic V et al., 2014.Intesitnal macrophages and dendritic cells: what's the difference?. *Trends Immunol*, 35(6): 270-7. *Review.*

Cescon M et al., 2015. Collagen VI at a glance. *J Cell Sci*, 128(19):3525-31.

Chanmee T et al., 2014. Tumor-associated macrophages as major players in the tumor microenvironment. *Cancers (Basel)*, 6(3): 1670-90. *Review.*

Chassaing B et al., 2014. Dextran sulfate sodium (DSS)-induced colitis in mice. *Curr Protoc Immunol*, 104: Unit 15.25.

Chen P, Cescon M and Bonaldo P, 2013. Collagen VI in cancer and its biological mechanisms. *Trends Mol Med*, 19(7): 410-7. *Review.*

Chen P et al., 2014. Collagen VI regulates peripheral nerve myelination and function. *FASEB J*, 28(3): 1145-56.

Chen P et al., 2015a. Collagen VI regulates peripheral nerve regeneration by modulating macrophage recruitment and polarization. *Acta Neuropathol*, 129(1): 97-113.

Chen P et al., 2015b. Lack of collagen VI promotes wound-induced hair growth. *J Invest Dermatol*, 135(10): 2358-67.

Cheng LK et al., 2010. Gastrointestinal system. *Wiley Interdiscip Rev Syst Biol Med*, 2(1): 65-79. *Review.*

Colombatti A and Bonaldo P, 1987. Biosynthesis of chick type VI collagen (II. Processing and secretion in fibroblast and smooth muscle cells). *J Biol Chem*, 262: 14461-14466.

Daley WP, Peters SB and Larsen M, 2008. Extracellular matrix dynamics in development and regenerative medicine. *J Cell Sci.* 121(Pt 3): 255-64. *Review.*

Danese S and Fiocchi C, 2006. Etiopathogenesis of inflammatory bowel diseases. *World J Gastroenterol*, 12(30): 4807-12. *Review.*

Dave MD et al., 2014. Immunology of inflammatory bowel disease and molecular targets for biologics. *Gastroenterol Clin North Am*, 43(3): 405–424. *Review.*

de Mattos BR et al., 2015. Inflammatory bowel disease: an overview of immune mechanisms and biologicals treatments. *Mediators Inflamm*, 2015: 493012. *Review.*

Fiorucci S et al., 2002. Immunity. Importance of innate immunity and collagen binding integrin alpha1beta1 in TNBS-induced colitis. *Immunity*, 17(6): 769-80.

Fitzgerald J et al., 2008. Three novel collagen VI chains, α4(VI), α5(VI), and α6(VI). *J Biol Chem*, 283(29): 20170–20180.

Floer M et al., 2012. Enoxaparin improves the course of dextran sodium sulfate-induced colitis in syndecan-1-deficient mice*. Am J Pathol*, 176(1): 146-57.

Fournier BM and Parkos CA, 2012. The role of neutrophils during intestinal inflammation. *Mucosal Immunol*, 5(4): 354-66. *Review.*

Frantz C, Stewart KM and Weaver VM, 2010. The extracellular matrix at a glance. J Cell Sci, 123(Pt 24): 4195-200. *Review.*

Franz S et al., 2013. Artificial extracellular matrices composed of collagen I and high-sulfated hyaluronan promote phenotypic and functional modulation of human pro-inflammatory M1 macrophages. *Acta Biomater*, 9(3): 5621-9.

Gara SK et al., 2008. Three novel collagen VI chains with high homology to the α3 chain. *J Biol Chem*, 283(16): 10658-10670.

Gara SK et al., 2011. Differential and restricted expression of novel collagen VI chains in mouse. *Matrix Biol*, 30: 248-257.

Gross M, Salame TM and Jung S, 2015. Guardians of the gut – murine intestinal macrophages and dendritic cells. *Front Immunol*, 6: 254. *Review.*

Groulx JF et al., 2011. Collagen VI is a basement membrane component that regulates epithelial cell-fibronectin interactions. *Matrix Biol*, 30(3): 195-206.

Grumati P et al., 2010. Autophagy is detective in collagen VI muscular dystrophies, and its reactivation rescues myofiber degeneration. *Nat Med*, 16(11): 1313-1320.

Grumati P et al., 2011. Physical exercise stimulates autophagy in normal skeletal muscles but is detrimental for collagen VI-deficient muscles. *Autophagy*, 7(12): 1415-23.

Gómez-Gómez GJ et al., 2015. Current stage in inflammatory bowel disease: What is next?. *World J Gastroenterol*, 21(40): 11282-303. *Review.*

Gulbransen BD and Sharkey KA, 2012. Novel functional roles for enteric glia in the gastrointestinal tract. *Nat Rev Gastroenterol Hepatol*, 9(11): 625-32. *Review.*

Haag LM and Siegmund B, 2015. Intestinal microbiota and the innate immune system - a crosstalk in Chron's disease pathogenesis. *Front Immunol*, 6: 489. *Review.*

Hansen MB, 2003. The enteric nervous system I: organisation and classification. *Pharmacol Toxicol*, 92(3): 105-13. *Review.*

Heimesaat MM et al., The synthetic hydroxyproline-containing collagen analogue (Gly-Pro-Hyp)10 ameliorates acute DSS colitis*. Eur J Microbiol Immunol*, 2(3): 192-200.

Hirono I et al., 1983. Carcinogenicity of dextran sulfate sodium in relation to its molecular weight. *Cancer Lett*, 18(1): 29-34.

Hwang TL et al., 2014. Claudin-4 expression in gastric cancer cells enhances the invasion and is associated with the increased level of matrix metalloproteinase-2 and -9 expression. *Oncol Lett*, 8(3): 1367-1371.

Hynes RO, 2009. The extracellular matrix: not just pretty fibrils. *Science*, 326(5957): 1216-9. *Review.*

Ichikawa-Tomikawa N et al., 2011. Possible involvement of tight junctions, extracellular matrix and nuclear receptors in epithelial differentiation. *J Biomed Biotechnol*, 2011: 253048. *Review.*

Irwin WA et al., 2003. Mitochondrial dysfunction and apoptosis in myopathic mice with collagen VI deficiency. *Nature Genetics*, 35: 367-371.

Italiani P and Boraschi D, 2014. From monocytes to M1/M2 macrophages: phenotypical vs. functional differentiation. *Front Immunol*, 5: 514. *Review.*

Izu Y et al., 2011. Dysfunctional tendon collagen fibrillogenesis in collagen VI null mice. *Matrix Biol*, 30(1):53-61.

Johansson ME et al., 2010. Bacteria penetrate the inner mucus layer before inflammation in the dextran sulfate colitis model. *PLoS One*, 5(8): e12238.

Kim SH, Turnbull J and Guimond S, 2011. Extracellular matrix and cell signalling: the dynamic cooperation of integrin, proteoglycan and growth factor receptor. *J Endocrinol*, 209(2): 139-51. *Review.*

Kim TW et al., 2006. Involvement of lymphocytes in dextran sulfate sodium-induced experimental colitis. *World J Gastroenterol*, 12(2): 302-5.

Koval M et al., 2010. Extracellular matrix influences alveolar epithelial claudin expression and barrier function. *Am J Respir Cell Mol Biol*, 42(2): 172-80.

Krieglstein CF et al., 2002. Collagen-binding integrin alpha1beta1 regulates intestinal inflammation in experimental colitis*. J Clin Invest*, 110(12): 1773-82.

Kühl AA et al., 2015. Diversity of intestinal macrophages in inflammatory bowel diseases. *Front Immunol,* 6: 613. *Review.*

Laroui H et al., 2012. Dextran sodium sulfate (DSS) induces colitis in mice by forming nano-lipocomplexes with medium-chain-length fatty acids in the colon. *PLoS One*, 7(3): e32084.

Loddo I and Romano C, 2015. Inflammatory bowel disease: genetics, epigenetics, and pathogenesis*. Front Immunol*, 6: 551. *Review.*

Lohr K et al., 2012. Extracellular matrix protein lumican regulates inflammation in a mouse model of colitis. *Inflamm Bowel Dis*, 18(1): 143-51.

Lu P, Weaver VM and Werb Z, 2012. The extracellular matrix: a dynamic niche in cancer progression. *J Cell Biol*, 196(4): 395-406. *Review.*

Mähler M et al., 1998. Differential susceptibility of inbred mouse strains to dextran sulfate sodium-induced colitis. *Am J Physiol*, 274(3 Pt 1): G544-51.

Kitajima S, Takuma S and Morimoto M, 1999. Changes in colonic mucosal permeability in mouse colitis induced with dextran sulfate sodium. *Exp Anim*, 48(3): 137-43.

Mahida YR, 2000. The key role of macrophages in the immunopathogenesis of inflammatory bowel disease. *Inflamm Bowel Dis,* 6(1): 21-33. Review.

Mahoney ZX et al., 2008. Laminin α5 influences the architecture of the mouse small intestinal mucosa. *J Cell Sci*, 121(Pt 15): 2493–2502.

Melgar S, Karlsson A and Michaëlsson E, 2005. Acute colitis induced by dextran sulfate sodium progresses to chronicity in C57BL/6 but not in BALB/c mice: correlation between symptoms and inflammation. *Am J Physiol Gastrointest Liver Physiol*, 288(6): G1328-38.

Ménard S, Cerf-Bensussan N and Heyman M, 2010. Multiple facets of intestinal permeability and epithelial handling of dietary antigens. *Mucosal Immunol*, 3(3): 247-59.

Menazza S et al., 2010. Oxidative stress by monoamine oxidases is causally involved in myofiber damage in muscular dystrophy. *Hum Mol Genet*, 19(21): 4207-15.

Morwood SR and Nicholson LB, 2006. Modulation of the immune response by extracellular matrix proteins. *Arch Immunol Ther Exp (Warsz),* 54(6): 367-74. *Review.*

Mulè F, Amato A and Serio R,2010. Gastric emptying, small intestinal transit and fecal output in dystrophic (mdx) mice*. J Physiol Sci*, 60(1): 75-9.

Muller PA et al., 2014. Crosstalk between muscularis macrophages and enteric neurons regulates gastrointestinal motility. *Cell*, 158(2): 30-313.

Murray PJ and Wynn TA, 2011. Protective and pathogenic functions of macrophage subsets. *Nat Rev Immunol*, 11(11): 723-37. *Review.*

Murthy SN et al., 1993. Treatment of dextran sulfate sodium-induced murine colitis by intracolonic cyclosporin. *Dig Dis Sci*, 38(9): 1722-34.

Naba A et al., 2015. The extracellular matrix: Tools and insights for the "omics" era. *Matrix Biol*, S0945-053X(15)00121-3. *Review.*

Newgreen DF et al., 2013. Simple rules for a "simple" nervous system? Molecular and biomathematical approaches to enteric nervous system formation and malformation. *Dev Biol*, 382(1):305-19. *Review.*

Nezami BG and Srinivasan S, 2010. Enteric nervous system in the small intestine: pathophysiology and clinical implications. *Curr Gastroenterol Rep*, 12(5): 358-65. *Review.*

O'Sullivan S, Gilmer JF and Medina C, 2015. Matrix metalloproteinases in inflammatory bowel disease: an update. *Mediators Inflamm, 2015*: 964131. *Review.*

Ota S et al., 2008. Effects of proteoglycan on dextran sulfate sodium-induced experimental colitis in rats. *Dig Dis Sci*, 53(12): 3176-83.

Park J et al., 2012. Adipocyte-derived endotrophin promotes malignant tumor progression. *J Clin Invest*, 122: 4243-4256.

Pfaff M et al., 1993. Integrin and Arg-Gly-Asp dependence of cell adhesion to the native and unfolded triple helix of collagen type VI. *Exp Cell Res*, 206: 167-176.

Perše M and Cerar A, 2012. Dextran sodium sulphate colitis mouse model: traps and tricks. *J Biomed Biotechnol*, 2012: 718617. *Review.*

Ross MH and Pawlina W, 2010. Istologia. Testo e atlante con elementi di biologia cellulare molecolare. C.E.A. Casa Editrice Ambrosiana.

Raghavan S and Bitar KN, 2014. The influence of extracellular matrix composition on the differentiation of neuronal subtypes in tissue engineered innervated intestinal smooth muscle sheets. *Biomaterials*, 35(26):7429-40.

Rühl A, 2006. Glial regulation of neuronal plasticity in the gut: implications for clinicians. *Gut*, 55(5): 600-602. *Review.*

Sabatelli P et al., 2001. Collagen VI deficiency affects the organization of fibronectin in the extracellular matrix of cultured fibroblasts. *Matrix Biol*, 20(7): 475-86.

Schnoor M et al., 2008. Production of type VI collagen by human macrophages: a new dimension in macrophage functional heterogeneity. *J Immunol*, 180(8): 5707-19.

Sheikh SZ and Plevy SE, 2010. The role of the macrophage in sentinel responses in intestinal immunity. *Curr Opin Gastroenterol*, 26(6): 578–582. *Review.*

Shimojo N et al., 2015. Tenascin-C may accelerate cardiac fibrosis by activating macrophages via the integrin αVβ3/nuclear factor-κB/interleukin-6 axis. *Hypertension*, 66(4): 757-66.

Shimshoni E et al., 2015. ECM remodelling in IBD: innocent bystander or partner in crime? The emerging role of extracellular molecular events in sustaining intestinal inflammation. *Gut*, 64(3): 367-72. *Review.*

Smith PD et al., 1997. Isolation and purification of CD14-negative mucosal macrophages from normal human small intestine. *J Immunol Methods*, 202(1): 1-11.

Smith PD et al., 2010. Intestinal macrophages and response to microbial encroachment. *Mucosal Immunol*, 4(1): 31-42. *Review.*

Soret R et al., 2015. A collagen VI-dependent pathogenic mechanism for Hirschsprung's disease. *J Clin Invest*, 125(12): 4483-96.

Soriano A et al.,2000. VCAM-1, but not ICAM-1 or MAdCAM-1, immunoblockade ameliorates DSS-induced colitis in mice. *Lab Invest*, 80(10): 1541-51.

Sorokin L, 2010. The impact of the extracellular matrix on inflammation. *Nat Rev Immunol*, 10(10):712-23. Review.

Speca S et al., 2012. Cellular and molecular mechanisms of intestinal fibrosis. *World J Gastroenterol*, 18(28): 3635-3661. *Review.*

Spenlé C et al., 2014. The laminin response in inflammatory bowel disease: protection or malignancy? PLoS One, 9(10): e111336.

Steinbach EC and Plevy SE, 2014. The role of macrophages and dendritic cells in the initiation of inflammation in IBD. *Inflamm Bowel Dis*, 20: 166-175. *Review.*

Suzuki T, 2013. Regulation of intestinal epithelial permeability by tight junctions. *Cell Mol Life Sci*, 70 (4): 631-59. *Review.*

Takaki M, 2003. Gut pacemaker cells: the interstitial cells of Cajal (ICC). *J Smooth Muscle Res*, 5: 137-161. *Review.*

Tam PK, 2016. Hirschsprung's disease: a bridge for science and surgery. *J Pediatr Surg*, 51(1): 18-22. *Review.*

Tanaka Y et al., 2013. Is there a difference in gastric emptying between myotonic dystrophy type 1 patients with and without gastrointestinal symptoms? *J Neurol*, 260(6): 1611-6.

Toyonaga T et al., 2015. Osteopontin Deficiency Accelerates Spontaneous Colitis in Mice with Disrupted Gut Microbiota and Macrophage Phagocytic Activity. *PLoS One*, 10(8): e0135552.

Urciuolo, A. et al., 2013. Collagen VI regulates satellite cell self-renewal and muscle regeneration. *Nature communications*, 4(May): 1964.

Viennois E et al., 2013. Dextran sodium sulfate inhibits the activities of both polymerase and reverse transcriptase: lithium chloride purification, a rapid and efficient technique to purify RNA. *BMC Res Notes*, 6: 360.

Vitale P et al., 2001. Mechanisms of transcriptional activation of the col6a1 gene during Schwann cell differentiation. *Mech Dev*,102(1-2): 145-56.

Vllasaliu D et al., 2014. Basement membrane influences intestinal epithelial cell growth and presents a barrier to the movement of macromolecules. *Exp Cell Res*, 323(1): 218-31.

Vural A and Kehrl JH, 2014. Autophagy in macrophages: impacting inflammation and bacterial infection. *Scientifica (Cairo), 2*014: 825463. *Review.*

Wang Z et al., 2015. Syndecan-1 acts in synergy with tight junction through Stat3 signaling to maintain intestinal mucosal barrier and prevent bacterial translocation. *Inflamm Bowel Dis*, 21(8): 1894-907.

Weber B, Saurer L and Mueller, 2009. Intestinal macrophages: differentiation and involvement in intestinal immunopathologies. *Semin Immunopathol*, 31(2): 171-84. *Review.*

Wirtz S and Neurath MF, 2007. Mouse models of inflammatory bowel disease. *Adv Drug Deliv Rev*, 59(11): 1073-83. *Review.*

Wolf MT et al., 2014. Macrophage polarization in response to ECM coated polypropylene mesh. *Biomaterials*, 35(25): 6838-49.

Wynn TA, 2008. Cellular and molecular mechanisms of fibrosis. *J Pathol*, 214(2): 199–210. *Review.*

Yuan B et al., 2015. Changes in the expression and distribution of claudins, increased epithelial apoptosis, and a mannan-binding lectin-associated immune response lead to barrier dysfunction in dextran sodium sulfate-induced rat colitis. *Gut Liver*, 9(6): 734-40.

Zhang YZ and Li YY, 2014.Inflammatory bowel disease: pathogenesis. *World J Gastroenterol,* 20(1): 91-99. *Review.*

Zigmond E and Jung S, 2013. Intestinal macrophages: well educated exceptions from the rule. *Trends Immunol*, 34(4): 162-8. *Review.*